

National Aeronautics and Space Administration

**Technology Evaluation for Environmental Risk
Mitigation Principal Center**

NASA-DoD Lead-Free Electronics Project

Joint Test Report - Final

December 2011

NASA-DoD Lead-Free Electronics Project – Joint Test Report

This document is intended to summarize the test data generated from the NASA-DoD Lead-Free Electronics Project.

This document is disseminated under the sponsorship of the National Aeronautics and Space Administration (NASA) in the interest of information exchange. The United States Government assumes no liability for its contents or use thereof.

This report does not constitute a standard, specification, or regulation. The United States Government does not endorse products or manufacturers. Trade or manufacturers' names appear herein only because they are considered essential to the object of this document. The report may not be used for advertising or product endorsement purposes.

Table of Contents

1	Introduction	1
2	Test Vehicle	2
2.1	Test Vehicle Design	2
2.2	Board Material	2
2.3	Board Finish	2
2.4	Solder Alloys	3
2.4.1	SAC305	3
2.4.2	SN100C	4
2.5	Flux	4
2.6	Components	6
2.6.1	Component Characterization	7
3	Assembly	9
3.1	NSWC Crane Assembly and Rework Effort	12
3.2	Test Vehicle Assembly Irregularities	16
3.2.1	Chip Scale Package (CSP)	16
3.2.2	Quad Flat No leads (QFN), Location U15	18
3.2.3	TSOP-50 Components Missing Internal Wire Bonds	20
4	Test Methods	21
5	Test Results	22
5.1	Vibration Test	22
5.1.1	Vibration Test Method	22
5.1.2	NASA-DoD Test Vehicle Vibration Testing Results Summary	26
5.1.3	NSWC Crane Test Vehicle Vibration Testing Results Summary	29
5.2	Mechanical Shock Test	47
5.2.1	Mechanical Shock Test Method	47
5.2.2	Mechanical Shock Testing Results Summary	49
5.3	Combined Environments Test	67
5.3.1	Combined Environments Test Method	67
5.3.2	Combined Environments Test Results Summary	68
5.3.3	Combined Environments Failure Analysis	74
5.3.4	Combined Environments Test Summary Tables	111
5.4	Thermal Cycle -55°C to +125°C Test	118
5.4.1	Thermal Cycle -55°C to +125°C Test Method	118
5.4.2	Thermal Cycle -55°C to +125°C Testing Results Summary	118
5.4.3	NSWC Crane Test Vehicle Thermal Cycle -55°C to 125°C Results Summary	163
5.4.4	Thermal Cycle -55°C to +125°C Testing Summary Tables	176
5.4.5	Thermal Cycle -55°C to +125°C Testing Results Discussion	183
5.5	Thermal Cycle -20°C to +80°C Test	184
5.5.1	Thermal Cycle -20°C to +80°C Test Method	184
5.5.2	Thermal Cycle -20°C to +80°C Testing Results Summary	184
5.6	Drop Testing	185
5.6.1	Drop Test Method	185
5.6.2	NASA-DoD Test Vehicle Drop Testing Results Summary	187
5.6.3	NASA-DoD Test Vehicle Drop Test Failure Analysis	188

5.6.4	NSWC Crane Test Vehicle Drop Testing Results Summary.....	192
5.6.5	NSWC Crane Test Vehicle Drop Test Failure Analysis.....	193
6	Assembly Observations.....	196
6.1	Combined Environments Test Vehicles – Raytheon.....	196
6.2	Combined Environments Test Vehicles – COM DEV International.....	196
6.3	Combined Environments Test Vehicles – Lockheed Martin.....	211
7	Copper Dissolution Testing.....	217
7.1	SAC305 & SN100C Copper Dissolution Testing.....	217
7.1.1	Introduction.....	217
7.1.2	Test Vehicle.....	217
7.1.3	Test Machine & Solder Alloy.....	217
7.1.4	Experimental setup.....	218
7.1.5	Copper Dissolution Measurements.....	223
7.1.6	Results.....	224
7.1.7	Data and discussion for SMT pattern.....	232
7.1.8	Inspection Criteria – Visual Indicators of Copper Dissolution.....	236
7.1.9	Kinetics of Copper Dissolution.....	236
7.1.10	Sn-Pb and Sn-Ag-Copper and Sn-Copper Based Alloys.....	237
7.1.11	Copper Dissolution Impact on Assembly Practices.....	238
7.1.12	Conclusions/Summary.....	240
8	Thermal Aging Discussion.....	241
9	Joint Test Report Summary.....	242
9.1	Joint Test Report Data Comparison.....	242
9.2	Joint Test Report Conclusions.....	243
10	Recommendations.....	244
11	Phase III.....	245
11.1	Overview.....	245
12	System-Level Demonstration.....	246
12.1	Flight Test Pb-free Solders.....	246
12.1.1	Objective.....	246
12.1.2	Concept.....	247
12.2	Field Test Pb-Free Solders in Harsh Environments.....	249
12.2.1	Objective.....	249
12.2.2	Concept.....	249
12.3	Electronic assemblies designed for operation in harsh aerospace environments {Lead-free Technology Experiment in a Space Environment (LTESE)} II.....	250
12.3.1	Objective.....	250
12.3.2	Concept.....	251
13	Bibliography.....	253

Tables

Table 1 - Test Vehicle Assembly Details	3
Table 2 - Solder Alloys and Associated Flux	5
Table 3 - Components Table.....	6
Table 4 – Test Vehicle Assembly Details.....	11
Table 5 – NSWC Crane Rework Effort; Vibration Test Boards	13
Table 6 - NSWC Crane Rework Effort; Drop Test Boards	14
Table 7 - NSWC Crane Rework Effort; Thermal Cycle Test Boards.....	15
Table 8 - Test Vehicle Performance Requirements	22
Table 9 - Vibration Profile.....	25
Table 10 - Percentage of Components Failed (Includes Mixed Solders)	26
Table 11 - Ranking of Solder Alloy/Component Finish Combinations	29
Table 12 - Component Percentage Failure by Force Level	30
Table 13 - Component Detachments.....	30
Table 14 - Results of Testing on As-Manufactured and Reworked Components	31
Table 15 - Results of Tests on Components Reworked Once vs. Twice	36
Table 16 - Mechanical Shock Test Methodology – Test Procedure.....	49
Table 17 - Shock Testing; Relative Ranking (Solder/Component Finish)	50
Table 18 - Combined Environments Test Methodology.....	67
Table 19 - Combined Environments Testing Vibration Level and Cycle Correlation	68
Table 20 - Number of Failed Components by Board Finish, Component, Component Finish and Solder Alloy on Manufactured Test Vehicles.....	70
Table 21 - Number of Failed Components by Board Finish, Component, Component Finish and Solder Alloy on Manufactured Test Vehicles.....	71
Table 22 - Number of Failed Components by Board Finish, Component, Component Finish, Solder Alloy, New Component Finish and Rework Solder on Rework Test Vehicles	72
Table 23 - Number of Failed Components by Board Finish, Component, Component Finish, Solder Alloy, New Component Finish and Rework Solder on Rework Test Vehicles	73
Table 24 - Components selected for failure analysis based on when a failure was recorded during Combined Environments Testing	74
Table 25 - Combined Environments Test; Summary of Manufactured Test Vehicle Test Results	112
Table 26 - Combined Environments Test; Relative Solder Performance, Manufactured Test Vehicles.....	114
Table 27 - Combined Environments Test; Summary of Rework Test Vehicle Test Results	115
Table 28 - Combined Environments Test; Relative Solder Performance, Rework Test Vehicles	117
Table 29 - Thermal Cycling Test Methodology; -55°C to +125°C.....	118
Table 30 - Manufactured Test Vehicle Component Population Failure Rates after 4068 Thermal Cycles.....	118
Table 31 - Reworked Test Vehicle Component Population Failure Rates after 4068 Thermal Cycles.....	119
Table 32 - Comparison of Test Vehicles With and Without Fabrication Defect: *Note - one failure at 1 cycle excluded from data analysis	155
Table 33 - Number of samples and percent failures per Crane rework condition thermally cycled between -55°C and 125°C. All test vehicles had an immersion Ag finish	163

Table 34 - As-manufactured (O), 1 st rework (1), and 2 nd rework (2) thermal cycles to failure and p-values for reworked CLCC's, PDIP's, TQFP's, and TSOP's. A p-value of <0.05 is considered statistically significant. All test vehicles had an immersion Ag finish.....	164
Table 35 - Failure percentage for all PDIP's from a specific batch. The percentage of PDIP's reworked and the percentage of PDIP's that were reworked and failed are also listed.....	169
Table 36 - N1/N10/N63 Solder Performance for -55C to +125 C Thermal Cycle Testing.....	177
Table 37 - N1/N10/N63 Solder Performance for -55C to +125 C Thermal Cycle Testing.....	178
Table 38 - Solder Performance Comparison for -55C to +125 C Thermal Cycle Testing.....	179
Table 39 - N1/N10/N63 Solder Performance for -55C to +125 C Thermal Cycle Testing.....	180
Table 40 - N1/N10/N63 Solder Rework Performance for -55C to +125 C Thermal Cycle Testing.....	181
Table 41 - Solder Rework Performance Comparison for -55C to +125 C Thermal Cycle Testing.....	182
Table 42 - Solder Rework Performance Comparison for -55C to +125 C Thermal Cycle Testing.....	183
Table 43 - Thermal Cycling Test Methodology; -20°C to +80°C.....	184
Table 44 - NASA-DoD Lead-Free Electronics Test Vehicle Drop Test Methodology.....	187
Table 45 - NSWC Crane Test Vehicle Drop Test Methodology.....	187
Table 46 - Components that Celestica Performed Failure Analysis On.....	189
Table 47 - Solder Alloy Test Information.....	218
Table 48 - Test Coupon Exposure Parameters; Celestica.....	221
Table 49 - Test Coupon Exposure Parameters; Rockwell Collins.....	222
Table 50 - N63 Solder Performance Comparison.....	242
Table 51 - On-Orbit Commercial (non-NASA) Satellite Failures(22).....	251

Figures

Figure 1 – QFN-20 Component Bottom Side Showing Die Thermal Pad.....	7
Figure 2 – NASA-DoD Lead-Free Electronics Project Test Vehicle Pre-Assembly.....	8
Figure 3 - NASA-DoD Lead-Free Electronics Project Test Vehicle Post-Assembly.....	9
Figure 4 - Test Vehicle Drawing, Chip Scale Package (CSP).....	17
Figure 5 - Chip Scale Package (CSP) Continuity Loop.....	18
Figure 6 - Quad Flat No leads (QFN), Component Location U15.....	19
Figure 7 - Missing Trace, QFN – U15.....	19
Figure 8 - Jumper Wire Attached to U15 Location to Permit Collection of Test Data.....	20
Figure 9 – TSOP Component Jumper.....	21
Figure 10 - Vibration Spectrum.....	24
Figure 11 - Test Minutes Required for Components to Fail (Test Vehicle 74 Data).....	27
Figure 12 - Full Field Peak Strains at 65 Hz (1G Sine Dwell, Test Vehicle 74).....	28
Figure 13 - The difference in average time to failure for each component type when comparing as-manufactured parts to reworked parts. A positive change indicates an increased time to failure after rework.....	32
Figure 14 - Test results for U61, in the As-Manufactured Condition and after Rework.....	33
Figure 15 - Results of PDIP-20, U38 in As-Manufactured Condition and after Rework.....	34
Figure 16 - The difference in average time to failure for each component type when comparing the 1 st SnPb rework to the 2 nd SnPb rework. A positive change indicates an increased time to failure after the 2 nd rework.....	35

Figure 17 - SN63 U52, Left Side Pad	37
Figure 18 - SN67 U52, Left Side Pad	37
Figure 19 - SN63 U54, Left Side Pad	38
Figure 20 - SN68 U28, Right Side Pad	39
Figure 21 - SN63 U41, Left Lead	40
Figure 22 - SN61 U20 Right Lead	40
Figure 23 - SN67 U31 Left Lead	41
Figure 24 - SN68 U31, Right Lead	42
Figure 25 - SN79 U12, Left Lead	43
Figure 26 - SN66 U62, Right Lead	43
Figure 27 - SN65 U62, Left Lead	44
Figure 28 - SN63 U61, Right Lead	45
Figure 29 - SN63 U16, Left Lead	45
Figure 30 - SN68 U29, Right Lead	46
Figure 31 - Mechanical Shock SRS Test Levels	48
Figure 32 - Test Vehicle 34 - Four Corner Balls of BGA U6 (SnPb Solder/SnPb Balls)	51
Figure 33 - Test Vehicle 89 - Four Corner Balls of BGA U2 (SAC305 Solder/SAC405 Balls)	52
Figure 34 - Test Vehicle 30 BGA U2 with Missing Pads (SnPb Solder/SnPb Balls)	53
Figure 35 - Test Vehicle 30 BGA U4 with Missing Pads (SnPb Solder/SnPb Balls)	53
Figure 36 - Test Vehicle 193 BGA U21 with Missing Pads (Flux Only/SAC405 Balls)	54
Figure 37 - Test Vehicle 193 BGA U21 with Missing Pads (Flux Only/SAC405 Balls)	55
Figure 38 - Combined Data from CLCC's U13 and U14	56
Figure 39 - Test Vehicle 191 CLCC U10 (Cracked SAC305/SnPb Solder Joint)	56
Figure 40 - X-Ray of a CSP-100 (Showing that only the outer balls form a daisy-chain (Red Lines).)	57
Figure 41 - Test Vehicle 34 - CSP U33	58
Figure 42 - Test Vehicle 89 - CSP U33	58
Figure 43 - Test Vehicle 34 - PDIPs U8 and U49 (a) Corner Lead, (b) Lead Adjacent to	59
Figure 44 - Test Vehicle 89 - PDIPs U8 and U49 (a) Corner Lead, (b) Lead Adjacent to	60
Figure 45 - Test Vehicle 89 PDIP U30 (Cracked Trace, SN100C)	61
Figure 46 - Test Vehicle 89 PDIP U38 (Cracked Trace, SN100C)	61
Figure 47 - Test Vehicle 89 PDIP U51 (SN100C)	62
Figure 48 - Test Vehicle 89 TQFP U3 (Cracked Leads, Missing Lead)	63
Figure 49 - Combined Data from TQFP's U20 and U58	64
Figure 50 - TSOP U25 Data	65
Figure 51 - TSOP U24 Data	65
Figure 52 - Test Vehicle 34 TSOP U61 (Cracked SnPb/SnPb Solder Joint)	66
Figure 53 - TV21 U34; Optical Micrograph of Insufficient Solder Observed on Lead 72 at 49X Magnification	75
Figure 54 - TV21 U57; Optical Micrograph, Residue between Leads	75
Figure 55 - TV21 U57; Optical Micrograph, Residue between Leads	76
Figure 56 - TV21 U57; Optical Micrograph, Component Lead 1	76
Figure 57 - TV23 U30; Optical Micrograph, PDIP-20	77
Figure 58 - TV23 U30; Cross-Sectional Micrographs of PDIP-20 Leads	78
Figure 59 - TV23 U30; Micrographs, Lead 9 of PDIP-20	79
Figure 60 - TV23 U43; FA Results, BGA-225, Location U43	80
Figure 61 - TV23 U43; Cross-Sectional Micrographs	80

Figure 62 - TV23 U43; Cross-Sectional Micrographs.....	81
Figure 63 - TV23 U43; SEM Mapping.....	82
Figure 64 - TV23 U43; Cross-Sectional Micrographs Show Warping.....	83
Figure 65 - TV72 U29; Visual Inspection Showing Cracked Solder Joints.....	83
Figure 66 - TV72 U29; Cross-Section Micrographs Showing Open Solder Joints.....	84
Figure 67 - TV72 U29; SEM Mapping, Pb was Found Around Upper Part of the Both Leads...	85
Figure 68 - TV117 U4; Orientation of the Corner Solder Balls	85
Figure 69 - TV117 U4; Cross-Sectional Micrographs of Corner Solder Balls.....	86
Figure 70 - TV117 U4; Diagram Showing Progression of Cracking in Component.....	86
Figure 71 - TV119 U36; X-Ray Image, CSP-100	87
Figure 72 - TV119 U36; X-Ray Image for Reference of the Cross-Section Analysis	87
Figure 73 - TV119 U36; Cross-Sectional Micrographs of Solder Balls A1, A2, A9 and A10	88
Figure 74 - TV119 U39; Optical Micrograph at 49X Magnification	89
Figure 75 - TV119 U39; SEM Image of Leads 19-25 at 22X Magnification.....	89
Figure 76 - TV119 U39; SEM Image, Lead 25	90
Figure 77 - TV119 U39; Cross-Sectional Micrograph, Lead 1	90
Figure 78 - TV119 U39; Cross-Sectional Micrograph, Lead 50	90
Figure 79 - TV140 U11; Optical Micrograph.....	91
Figure 80 - TV140 U11; Cross-Sectional Micrographs, Suspect PDIP-20 Lead	91
Figure 81 - TV142 U13; Optical Micrograph, CLCC Package Lead	92
Figure 82 - TV142 U13 Optical Micrographs of CLCC-20 Leads at 24X Magnification	92
Figure 83 - TV142 U13 X-Ray Inspection of CLCC-20 Component.	92
Figure 84 - TV142 U13 SEM Images of Component at 25X Magnification	93
Figure 85 - TV142 U13 SEM Images of Selected Leads at 55X Magnification.....	93
Figure 86 - TV142 U13; CLCC-20 Component	94
Figure 87 - TV142 U13; Cross-Sectional Micrographs of Lead 1 and Lead 5.....	94
Figure 88 - TV142 U13; Cross-Sectional Micrograph	95
Figure 89 - TV142 U13; SEM Image	95
Figure 90 - TV158 U6; FA Results.....	96
Figure 91 - TV158 U6; Cross-Sectional Micrographs.....	96
Figure 92 - TV158 U6; Cross-Sectional Micrographs.....	97
Figure 93 - TV158 U6; Cross-Sectional Micrographs.....	98
Figure 94 - TV158 U6; SEM Mapping.....	99
Figure 95 - TV158 U6; SEM Mapping.....	100
Figure 96 - TV158 U6; Cross-Sectional Micrographs Show Warping on BGA-225.....	100
Figure 97 - TV180 U21; FA Results.....	101
Figure 98 - TV180 U21; Cross-Sectional Micrographs.....	102
Figure 99 - TV180 U21; Cross-Sectional Micrographs.....	103
Figure 100 - TV180 U21; SEM Mapping.....	104
Figure 101 - X-Ray Inspection of TV181 U56 BGA-225	104
Figure 102 - TV181 U56; X-Ray Image Showing the Grinding Levels.....	105
Figure 103 - TV181 U56; Cross-Sectional Micrographs of Via Hole Connected to Ball A1	105
Figure 104 - TV181 U56; Cross-Sectional Micrographs of Solder Balls.....	106
Figure 105 - TV181 U56; SEM Image of Solder Ball A9 Cross-Section	106
Figure 106 - TV181 U25; Optical Micrographs	107
Figure 107 - TV181 U25; X-Ray Images of Component Leads.....	107
Figure 108 - TV181 U25; SEM Images.....	108

Figure 109 - TV181 U25; Optical Micrographs	108
Figure 110 - TV181 U25; Cross-Sectional Micrographs.....	108
Figure 111 - TV181 U25; SEM Image	109
Figure 112 - TV183 U 41; Optical Micrographs of Suspect Lead	109
Figure 113 - TV183 U 41; Cross-Sectional Micrographs.....	110
Figure 114 - CLCC-20 Weibull Plot for Immersion Silver Test Vehicle.....	120
Figure 115 - CLCC-20 Weibull Plot for Immersion Silver Test Vehicle.....	120
Figure 116 - NWSC Crane Reworked CLCC-20 Weibull Plot	121
Figure 117 - CLCC-20 Component on Test Vehicle after 4068 Thermal Cycles	122
Figure 118 - CLCC-20 Solder Joints; Left - Board 5, Component U14, SnPb/SnPb, Failed @ 2625 Cycles: Right - Board 43, Component U14, SAC305/SAC305, Failed @ 513 Cycles.....	122
Figure 119 - CLCC-20 Solder Joints; Left - Board 164, Component U14, SAC305/SnPb, Failed @ 1248 Cycles: Right - Board 126, Component U14, SnPb/SAC305, Failed @ 2064 Cycles .	123
Figure 120 - CLCC-20 Solder Joints, Board 103, Component U22, SN100C/SnPb, Failed @ 828 Cycles.....	123
Figure 121 - CLCC-20 Solder Joints, Board 104, Component U14, SN100C/SAC305, Failed @ 304 Cycles.....	123
Figure 122 - QFN-20 Weibull Plot for Immersion Silver and ENIG PWB Finishes	124
Figure 123 - NWSC Crane Reworked QFN-20 Weibull Plot.....	125
Figure 124 - QFN-20 Solder Joints, Board 6, Component U27, SnPb/Sn Dipped, Did Not Fail (DNF).....	126
Figure 125 - QFN-20 Solder Joints, Board 42, Component U54, SAC305/Sn, DNF	126
Figure 126 - QFN-20 Solder Joints, Board 104, Component U27, SN100C/Sn, DNF	126
Figure 127 - QFN-20 Solder Joints, Board 167, Component U15, SAC305/SnPb, DNF	127
Figure 128 - QFN-20 Solder Joints, Board 107, Component U28, SN100C/Sn, Reworked with SnPb Paste, 1 Rework Failed @ 277 Cycles	127
Figure 129 - QFN-20 Solder Joints, Board 108, Component U28, SN100C/Sn, Reworked with SnPb Paste, 2 Reworks, DNF	127
Figure 130 - QFN-20 Solder Joints, Board 109, Component U28, SN100C/Sn, Reworked with Stencil Quik, 1 Rework, DNF.....	128
Figure 131 - QFN-20 Solder Joints, Board 47, Component U15, SAC305/Sn, Reworked with Stencil Quik, 1 Rework, Failed @ 3660 Cycles	128
Figure 132 - TQFP-144 Weibull Plot for Immersion Silver PWB Finish	129
Figure 133 - TQFP-144 Weibull Plot for ENIG PWB Finish	129
Figure 134 - NSWSC Crane Reworked TQFP-144 Weibull Plot.....	130
Figure 135 - TQFP-144 Solder Joints, Board 9, Component U48, SnPb/SnPb Dipped, Failed @ 2648 Cycles.....	131
Figure 136 - TQFP-144 Solder Joints, Board 41, Component U20, SAC305/SnPb Dipped, Failed @ 3541 Cycles.....	131
Figure 137 - TQFP-144 Solder Joints, Board 106, Component U20, SN100C/SnPb Dipped, Failed @ 3258 Cycles	132
Figure 138 - TQFP-144 Solder Joints, Board 9, Component U1, SnPb/Sn, Failed @ 1 Cycle..	132
Figure 139 - TQFP-144 Solder Joints, Board 49, Component U57, SAC305/Sn, Failed @ 1430 Cycles.....	132
Figure 140 - TQFP-144 Solder Joints, Board 103, Component U48, SN100C/Sn, Failed @ 1712 Cycles.....	133

Figure 141 - TQFP-144 Solder Joints, Board 167, Component U57, SAC305/NiPdAu, Failed @ 3478 Cycles.....	133
Figure 142 - TQFP-144 Solder Joints, Board 127, Component U3, SnPb/NiPdAu, Failed @ 1744 Cycles.....	134
Figure 143 - TQFP-144 Solder Joints, Board 164, Component U7, SAC305/SAC305, Failed @ 2359 Cycles.....	134
Figure 144 - PBGA-225 Weibull Plot for Immersion Silver PWB Finish	135
Figure 145 - PBGA-225 Weibull Plot for ENIG PWB Finish.....	135
Figure 146 - Reworked PBGA-225 Weibull Plot for Immersion Silver Finish	136
Figure 147 - Reworked PBGA-225 Weibull Plot for ENIG PWB Finish	136
Figure 148 - PBGA-225 Solder Joints, Board 8, Component U5, SnPb/SnPb, Failed @ 2431 Cycles.....	137
Figure 149 - PBGA-225 Solder Joints, Board 127, Component U5, SnPb/SAC405, DNF	137
Figure 150 - PBGA-225 Solder Joints, Board 168, Component U5, SAC305/SnPb, Failed @ 1926 Cycles.....	138
Figure 151 - PBGA-225 Solder Joints, Board 49, Component U6, SAC305/SAC405, Failed @ 2763 Cycles.....	138
Figure 152 - PBGA-225 Solder Joints, Board 106, Component U55, SN100C/SnPb, Failed @ 1064 Cycles.....	139
Figure 153 - PBGA-225 Solder Joints, Board 104, Component U21, SN100C/SAC405, Failed @ 3812 Cycles.....	139
Figure 154 - Reworked PBGA-225 Solder Joints, Board 127, Component U56, Initially SnPb/SnPb, 1 rework Flux Only/SnPb, Failed @ 2349 Cycles.....	140
Figure 155 - Reworked PBGA-225 Solder Joints, Board 124, Component U6, Initially SnPb/SnPb, 1 rework SnPb/SAC405, Failed @ 2137 Cycles	140
Figure 156 - Reworked PBGA-225 Solder Joints, Board 127, Component U56, Initially SAC305/SAC405, 1 rework Flux Only/SAC405, Failed @ 2349 Cycles.....	140
Figure 157 - Reworked PBGA-225 Solder Joints, Board 164, Component U18, Initially SAC305/SAC405, 1 rework SnPb/SAC405, DNF	141
Figure 158 - CSP-100 Weibull Plot for Immersion Silver PWB Finish.....	142
Figure 159 - CSP-100 Weibull Plot for ENIG PWB Finish	142
Figure 160 - Reworked CSP-100 Weibull Plot for Immersion Silver PWB Finish	143
Figure 161 - Reworked CSP-100 Weibull Plot for ENIG PWB Finish.....	143
Figure 162 - CSP-100 Solder Joints, Board 7, Component U37, SnPb/SnPb, Failed @ 2837 Cycles.....	144
Figure 163 - CSP-100 Solder Joints, Board 124, Component U32, SnPb/SAC105, Failed @ 287 Cycles.....	144
Figure 164 - CSP-100 Solder Joints, Board 166, Component U32, SAC305/SnPb, Failed @ 3417 Cycles.....	145
Figure 165 - CSP-100 Solder Joints, Board 49, Component U60, SAC305/SAC105, Failed @ 3908 Cycles.....	145
Figure 166 - CSP-100 Solder Joints, Board 103, Component U33, SN100C/SnPb, Failed @ 2932 Cycles.....	145
Figure 167 - CSP-100 Solder Joints, Board 106, Component U36, SN100C/SAC105, Failed @ 3908 Cycles.....	146
Figure 168 - Reworked CSP-100 Solder Joints, Board 128, Component U19, Initially SnPb/SnPb, 1 rework Flux Only/SnPb, Failed @ 3012 Cycles.....	146

Figure 169 - Reworked CSP-100 Solder Joints, Board 126, Component U60, Initially SnPb/SnPb, 1 rework SnPb/SAC105, DNF.....	146
Figure 170 - Reworked CSP-100 Solder Joints, Board 168, Component U19, Initially SAC305/SAC105, 1 rework Flux Only/SAC105, DNF	147
Figure 171 - Reworked CSP-100 Solder Joints, Board 164, Component U33, Initially SAC305/SAC105, 1 rework SnPb/SAC105, DNF.....	147
Figure 172 - TSOP-50 Weibull Plot for Immersion Silver PWB Finish	148
Figure 173 - TSOP-50 Weibull Plot for ENIG PWB Finish	148
Figure 174 - TSOP-50 Rework Weibull Plot for 1 Rework	149
Figure 175 - TSOP-50 Rework Weibull Plot for 2 Rework	149
Figure 176 - TSOP-50 Solder Joints, Board 8, Component U40, SnPb/SnPb, Failed @ 1252 Cycles.....	150
Figure 177 - TSOP-50 Solder Joints, Board 44, Component U25, SAC305/SnPb, Failed @ 1787 Cycles.....	150
Figure 178 - TSOP-50 Solder Joints, Board 103, Component U39, SN100CSnPb, Failed @ 851 Cycles.....	151
Figure 179 - TSOP-50 Solder Joints, Board 8, Component U29, SnPb/SnBi, Failed @ 1424 Cycles.....	151
Figure 180 - TSOP-50 Solder Joints, Board 166, Component U39, SAC305/SnBi, Failed @ 1594 Cycles.....	152
Figure 181 - TSOP-50 Solder Joints, Board 102, Component U34, SN100C/SnBi, Failed @ 1985 Cycles.....	152
Figure 182 - TSOP-50 Solder Joints, Board 107, Component U61, SN100C/Sn, Failed @ 1258 Cycles.....	153
Figure 183 - Reworked TSOP-50 Solder Joints, Board 127, Component U12, Initially SnPb/SnPb, 1 rework SnPb/SnPb, Failed @ 1443 Cycles.....	153
Figure 184 - Reworked TSOP-50 Solder Joints, Board 47, Component U24, Initially SAC305/SnBi, 2 rework SnPb/SnBi, Failed @ 1810 Cycles	154
Figure 185 - Reworked TSOP-50 Solder Joints, Board 47, Component U29, Initially SAC305/Sn, 1 rework SnPb/Sn, Failed @ 1010 Cycles.....	154
Figure 186 - Cycles to failure for as-manufactured Sn finished PDIP's soldered with SN100C as a function of production batch showing a faster rate of failure for batches F, G, and I.	155
Figure 187 - Cycles to failure agglomerated for all as-manufactured PDIP's as a function of production batch showing a faster rate of failure for batches F, G, and I.....	156
Figure 188 - PDIP-20 Weibull Plot for Immersion Silver PWB Finish	157
Figure 189 - PDIP-20 Weibull Plot for ENIG PWB Finish.....	157
Figure 190 - Reworked PDIP-20 Weibull Plot.....	158
Figure 191 - Cross-sectional Views of the Fabrication Defect in the Test Vehicle at the PDIP-20 Locations (Left – Macro View, Right – Magnified View)	159
Figure 192 - Color X-ray Image of PDIP-20 Thermal Cycling Induced Cracked Trace	159
Figure 193 - PDIP-20 Thermal Cycling Induced Cracked Trace at Fabrication Defect Location	160
Figure 194 - PDIP-20 Solder Joints, Board 124, Component U23, SnPb/NiPdAu, DNF.....	161
Figure 195 - PDIP-20 Solder Joints, Board 43, Component U8, SN100C/NiPdAu, DNF.....	161
Figure 196 - PDIP-20 Solder Joints, Board 168, Component U49, SN100C/Sn, DNF	162
Figure 197 - Box and whisker plot comparing thermal cycles to failure for SAC305 finished CLCC's originally soldered with SAC305 and reworked 1 or 2 times with SAC305 finished	

CLCC's soldered with eutectic SnPb. No differences in cycles to failure were considered statistically significant. 165

Figure 198 - Box and whisker plot comparing thermal cycles to failure for SAC305 finished CLCC's originally soldered with SN100C and reworked 1 or 2 times with SAC305 finished CLCC's soldered with eutectic SnPb. No differences in cycles to failure were considered statistically significant. 165

Figure 199 - Box and whisker plot comparing thermal cycles to failure for Sn finished PDIP's originally soldered with SN100C and reworked 1 or 2 times with Sn finished PDIP's soldered with eutectic SnPb. The decrease in cycles to failure for both reworks was considered statistically significant. 166

Figure 200 - Box and whisker plot comparing thermal cycles to failure for NiPdAu finished PDIP's originally soldered with SN100C and reworked 1 or 2 times with Sn finished PDIP's soldered with eutectic SnPb. The decrease in cycles to failure for the second rework was considered statistically significant. 167

Figure 201 - Box and whisker plot comparing thermal cycles to failure for NiPdAu finished PDIP's originally soldered with SN100C and reworked 1 or 2 times with NiPdAu finished PDIP's soldered with eutectic SnPb. The decrease in cycles to failure for the second rework was considered statistically significant. 167

Figure 202 - Cumulative Percentage of failures for as-manufactured Sn finished PDIP's soldered with SN100C showing a faster rate of failure and higher overall rate of failure for PDIP's on Crane test vehicles vs. other test vehicles in the consortium. There were 20 Crane specific PDIPs vs. 63 general to the consortium. 168

Figure 203 - Cumulative Percentage of failures for as-manufactured NiPdAu finished PDIP's soldered with SN100C showing a faster rate of failure and higher overall rate of failure for PDIP's on Crane test vehicles vs. other test vehicles in the consortium. There were 6 Crane specific PDIPs vs. 37 general to the consortium. 169

Figure 204 - Recreated box and whisker plot comparing thermal cycles to failure for Sn finished PDIP's originally soldered with SN100C and reworked 1 or 2 times with Sn finished PDIP's soldered with eutectic SnPb showing the effect of only considering times to failure from batches F, G, and I. 170

Figure 205 - Recreated box and whisker plot comparing thermal cycles to failure for NiPdAu finished PDIP's originally soldered with SN100C and reworked 1 or 2 times with Sn finished PDIP's soldered with eutectic SnPb showing the effect of only considering times to failure from batches F, G, and I. 171

Figure 206 - Box and whisker plot comparing thermal cycles to failure for Sn finished TQFP's originally soldered with SAC305 and reworked 1 or 2 times with Sn finished TQFP's soldered with eutectic SnPb. The increase in cycles to failure for both reworks was considered statistically significant. 172

Figure 207 - Box and whisker plot comparing thermal cycles to failure for Sn finished TQFP's originally soldered with SN100C and reworked 1 or 2 times with Sn finished TQFP's soldered with eutectic SnPb. The increase in cycles to failure for both reworks was considered statistically significant. 172

Figure 208 - Box and whisker plot comparing thermal cycles to failure for Sn finished TSOP's originally soldered with SAC305 and reworked 1 or 2 times with Sn finished TSOP's soldered with eutectic SnPb. No differences in cycles to failure between the as-manufactured and reworked conditions were considered statistically significant, but the decrease in cycles to failure between the 1st and 2nd rework was considered significant. 174

Figure 209 - Box and whisker plot comparing thermal cycles to failure for Sn finished TSOP's originally soldered with SN100C and reworked 1 or 2 times with Sn finished TSOP's soldered with eutectic SnPb. The increase in cycles to failure for both reworks was considered statistically significant.....	174
Figure 210 - Box and whisker plot comparing thermal cycles to failure for SnBi finished TSOP's originally soldered with SAC305 and reworked 1 or 2 times with SnBi finished TSOP's soldered with eutectic SnPb. Only the increase in cycles to failure for the 2 nd rework was considered statistically significant.	175
Figure 211 - Box and whisker plot comparing thermal cycles to failure for SnBi finished TSOP's originally soldered with SN100C and reworked 1 or 2 times with SnBi finished TSOP's soldered with eutectic SnPb. No differences in cycles to failure between the as-manufactured and reworked conditions were considered statistically significant.....	176
Figure 212 - Interconnect Fracture Modes (Solder Ball Array Device) IPC 9702.....	185
Figure 213 - Typical Pad Cratering seen on BGA225 after Dye-and-Pry.....	190
Figure 214 - Typical Pad Cratering seen on BGA225 after cross-section.....	190
Figure 215 - SEM of Brittle Intermetallic Failure on BGA225.....	191
Figure 216 – Mechanical Failure Mapping.....	192
Figure 217 - Pad Cratering seen on CLCC-20.....	194
Figure 218 - Dye and Pry of a QFN-20 showing dye penetration through the bulk solder.....	194
Figure 219 – Fatigue Failure of TQFP-144 with 1x Rework as seen through cross sectioning.	195
Figure 220 - U34 TQFP, SEM Image, Solder Mask Crack near Lead 20 (X50).....	197
Figure 221 - U57 TQFP, SEM Image, Solder Mask Crack near Leads 73-81 (X25).....	197
Figure 222 - U34 TQFP, Lead 72 marked (X49); Open due to Non Coplanarity	198
Figure 223 - U57 TQFP, No Solder Contact to Lead 1 (X49); Open due to Non Coplanarity ..	198
Figure 224 – U39 TSOP, Cracks in Solder Joints and Solder Mask (X49).....	199
Figure 225 - U25 TSOP, SEM Image, Lead 2 in Center, Lead 1 Left (X70).....	200
Figure 226 - U39 TSOP, X-ray Image, Leads 1-3, Voids in Solder Joints	201
Figure 227 – U39 TSOP, Cross Sectional View of Lead 1, Solder (X49)	202
Figure 228 – U25 TSOP, Cross Sectional View of Lead 2, Solder (X136)	202
Figure 229 - U36 CSP, X-ray Image, Center Region, Solder Mask Cracks.....	203
Figure 230 – U36 CSP, Solder Ball A10, PCB Side, Cracks Developed at SnCu Phase.....	204
Figure 231 - U36 CSP, SEM image of Ball A2, Component Side (X800).....	205
Figure 232 – U13 CLCC, SEM Image, Lead 8, Solder Crack and Solder Mask Crack (X55) ..	206
Figure 233 – U13 CLCC, Cracks Developed Through Sn Phase, Lead 20	207
Figure 234 - U13 CCLC, X-ray Image, Voiding, Lead 20	208
Figure 235 – U56 BGA, Solder Ball A15, Cracks Developed at SnCu Phase	209
Figure 236 – U56 BGA, Cross Sectional View of Solder Ball A9, Void in Solder Joint (X682)	210
Figure 237 – U56 BGA, Cross Sectional View of Solder Ball A7, Crack on the Solder Joint at PCB Trace Interface.....	210
Figure 238 - Test Vehicle 183, Component U41 (TQFP-144); Unsoldered Lead from the Original Manufacturing Process.....	211
Figure 239 - Test Vehicle 183, Component U41 (TQFP-144); Unsoldered Lead from the Original Manufacturing Process.....	212
Figure 240 - Test Vehicle 183, Component U41 (TQFP-144); Solder Behind the Lead at the Heel is Irregular	213
Figure 241 - Test vehicle 117, Component U4 (BGA-225); Crack at the Component Pad	214

Figure 242 - Test vehicle 117, Component U4 (BGA-225); Crack at the PWB Pad	214
Figure 243 - Test Vehicle 140, Component U11 (PDIP-20); Lifted Pad	215
Figure 244 - Test Vehicle 140, Component U11 (PDIP-20); Partial Crack	216
Figure 245 – NASA-DoD Lead-Free Electronics Project, Copper Dissolution Test Coupon....	217
Figure 246 - Wave Solder Equipment Setup	218
Figure 247 - Thermocouple Placement.....	219
Figure 248 - Wave Solder Equipment with Test Coupon.....	220
Figure 249 - Rockwell Collins Dissolution Measurement Locations; SMT QFP	223
Figure 250 - Rockwell Collins Dissolution Measurement Locations; PTH DIP with Measurement Location Designators Shown	224
Figure 251 - SN100C Copper Dissolution Results; 0.036" PTH.....	225
Figure 252 - SN100C Copper Dissolution Results; 0.015" PTH.....	226
Figure 253 - Damage example – PTH trace disconnected from PTH barrel	227
Figure 254 - SN100C Cross-section of 0.036" PTH with 240 Seconds Exposure	227
Figure 255 - Copper Dissolution for SN100C Alloy Illustrating Impact of Location on Via Height.....	228
Figure 256 - SAC305 and SN100C Copper Dissolution Results for SMT QFP	229
Figure 257 - SAC305 and SN100C Copper Dissolution Results for PTH DIP at Middle Via Measurement Location.....	230
Figure 258 - SAC305 and SN100C Copper Dissolution Rate Comparison for 40 Second Exposure	230
Figure 259 - Mini Wave Soldering Processing Window Estimation.....	231
Figure 260 - Rework Temperature Profile.....	232
Figure 261 - Celestica Location A Cross-section Location and Pad Number	233
Figure 262 - Sequence of Pad Copper Dissolution by Exposure Time	234
Figure 263 - Illustration of Copper Dissolution Rate Variance for A Specific Exposure Time.	235
Figure 264 - SMT QFP Pad Thermal Profile.....	235
Figure 265 - Visual Indicators of Copper Dissolution(13): Knee- Pad- Barrel for Location of Copper Reduction Sequence	236
Figure 266 - Departure and Diffusion of Copper Atoms into Solder Melt (Kinetics of Copper Dissolution).....	237
Figure 267 - Impact of PWB Surface Finish on Copper Dissolution; ENIG.....	239
Figure 268 - Impact of PWB Surface Finish on Copper Dissolution; Immersion Tin	239
Figure 269 - F-15 Test Zones; Forward Fuselage, Cockpit, and Engine Bay	248
Figure 270 - F-15 Test Zones; Center Fuselage.....	248
Figure 271 - Cross-sectional View of Ni Cap Test Coupons for ISS Whisker Experiments	252

1 Introduction

The use of conventional tin-lead (SnPb) in circuit board manufacturing is under ever-increasing political scrutiny due to increasing regulations concerning lead. The “Restriction of Hazardous Substances” (RoHS) directive enacted by the European Union (EU) and a pact between the United States National Electronics Manufacturing Initiative (NEMI), Europe’s SolderTec at Tin Technology Ltd. and the Japan Electronics and Information Technology Industries Association (JEITA) are just two examples where worldwide legislative actions and partnerships/agreements are affecting the electronics industry. For the purposes of this document, lead-free (Pb-free) is defined as:

- Lead-Free is defined as less than 0.1% by weight of lead in accordance with Waste Electrical and Electronic Equipment (WEEE) Directive.
- Pb-free Tin is defined {GEIA-HB-0005-1 Program Management/Systems Engineering Guidelines for Managing the Transition to Lead-Free Electronics} to be pure tin or any tin alloy with <3% lead (Pb) content by weight. This means that some Pb-free finishes other than pure tin, such as tin-bismuth and tin-copper, are considered to be “tin” for the purposes of this standard. Many of these alloys have not been assessed for whiskering behavior.

As a result, many global commercial-grade electronic component suppliers are initiating efforts to transition to lead-free (Pb-free) in order to retain their worldwide market. Pb-free components are likely to find their way into the inventory of aerospace or military assembly processes under current government acquisition reform initiatives. Inventories “contaminated” by Pb-free result in increased risks associated with the manufacturing, product reliability, and subsequent repair of aerospace and military electronic systems.

Although electronics for military and aerospace applications are not included in the RoHS legislation, engineers are beginning to find that the commercial industry’s move towards RoHS compliance has affected their supply chain and changed their parts. Most parts suppliers plan to phase out their non-compliant, leaded production and many have already done so. As a result, the ability to find leaded components is getting harder and harder. Some buyers are now attempting to acquire the remaining SnPb inventory, if it’s not already obsolete.

Original Equipment Manufacturers (OEMs), depots, and support contractors have to be prepared to deal with an electronics supply chain that increasingly provides more and more parts with Pb-free finishes—some labeled no differently than their Pb counterparts—while at the same time providing the traditional Pb parts. The longer the transition period, the greater the likelihood of Pb-free parts inadvertently being mixed with Pb parts and ending up on what are supposed to be Pb systems. As a result, OEMs, depots, and support contractors need to take action now to either abate the influx of Pb-free parts, or accept it and deal with the likely interim consequences of reduced reliability due to a wide variety of matters, such as Pb contamination, high temperature incompatibility, and tin whiskering.

Allowance of Pb-free components produces one of the greatest risks to the reliability of a weapon system. This is due to new and poorly understood failure mechanisms, as well as unknown long-term reliability. When the decision is made to consciously allow Pb-free solder

and component finishes into SnPb electronics, additional effort (and cost) is required to make the significant number of changes to drawings and task order procedures.

This project is a follow-on effort to the Joint Council on Aging Aircraft/Joint Group on Pollution Prevention (JCAA/JG-PP) Pb-free Solder Project which was the first group to test the reliability of Pb-free solder joints against the requirements of the aerospace and military community.

2 Test Vehicle

2.1 Test Vehicle Design

The test vehicle for this project is a printed wiring assembly (PWA), designed to evaluate solder joint reliability.

Test vehicle size is 14.5 X 9 X 0.09 inches with six 0.5-ounce copper layers. The design incorporates components representative of the parts used for military and aerospace systems and was designed to reveal relative differences in solder alloy performance.

The test vehicle includes a variety of plated-through-hole (PTH) and surface mount technology (SMT) components. All components are “dummy” devices with pins internally daisy-chained and contain simulated die. The circuit board was designed with daisy-chained pads that are complementary to the components. Therefore, the solder joints on each component are part of a continuous electrical pathway that was monitored during testing by an event detector (Anatech or equivalent). Failure of a solder joint on a component breaks the continuous pathway and is recorded as an event. Each component has its own distinct pathway (channel).

2.2 Board Material

Project stakeholders selected FR4 per IPC-4101/26 (Specification for Base Materials for Rigid and Multilayer Printed Boards) with a minimum glass transition (T_g) of 170°C for the test vehicles. Test vehicle raw boards comply with IPC-6012 (Qualification and Performance Specification for Rigid Printed Boards), Class 3, Type 3. Pho-Tronics supplied the circuit cards and used Isola 370HR laminate.

2.3 Board Finish

Project stakeholders and participants selected immersion silver (0.2 - 0.4 microns; MacDermid Sterling) as the surface finish for the majority of the test vehicles (see Table 1). The consensus of the project team was that immersion silver has the best balance of desirable properties: good wetting by solders, good solder joint reliability, good long-term solderability upon storage, and retention of solderability after multiple reflow cycles. In addition, several major electronic manufacturing companies are currently using immersion silver in production. Circuit boards were processed per IPC-4553; Specification for Immersion Silver Plating for Printed Boards.

A limited number of test vehicles (see Table 1) were assembled using an Electroless Nickel Immersion Gold (ENIG) surface finish (Uyemura Kat 450 ENIG). The project stakeholders felt that ENIG would be a good secondary surface finish since it provides good planarity and solderability which can withstand multiple reflows. ENIG has also been shown to perform well

with regards to: substrate shelf-life, corrosion resistance, assembly process window, thermal resistance over several temperature excursions, and good reworkability. Circuit boards were processed per IPC-4552; Specification for Electroless Nickel/Immersion Gold (ENIG) Plating for Printed Circuit Boards.

Table 1 - Test Vehicle Assembly Details

Test Vehicle Type	Reflow Solder	Wave Solder	Serial Numbers (SN)	Board Finish
Lead-Free Rework All Test Vehicles	SAC305	SN100C	161-193	ImAg = All
SnPb Rework* All Test Vehicles	SnPb	SnPb	121-160	ImAg = Most ENIG SN154 through SN160
SnPb Manufactured Test Vehicles Thermal Cycle and Combined Environments	SnPb	SnPb	1, 3, 5-14, 20 - 24	ImAg = All
SnPb Manufactured Test Vehicles Vibration, Mechanical Shock and Drop	SnPb	SnPb	2, 4, 15-19, 25-34	ImAg = All
Lead-Free Manufactured Test Vehicles Thermal Cycle and Combined Environments	SAC305	SN100C	35, 39, 41-45, 50-54, 69-73, 93, 95, 97	ImAg = Most ENIG SN93, SN95, SN97
Lead-Free Manufactured Test Vehicles Vibration, Mechanical Shock and Drop	SAC305	SN100C	36-38, 40, 46-49, 55-68, 74-92, 94, 96	ImAg = Most ENIG SN94, SN96
Lead-Free Manufactured Test Vehicles Thermal Cycle and Combined Environments	SN100C	SN100C	100, 102-106, 116-120	ImAg = All
Lead-Free Manufactured Test Vehicles Vibration, Mechanical Shock and Drop	SN100C	SN100C	101, 111-115	ImAg = All
Lead-Free Manufactured Test Vehicles Crane Rework Effort	SN100C	SN100C	98-99, 107-110	ImAg = All
* Note - Lead-Free profiles used for reflow and wave soldering				

2.4 Solder Alloys

Selection criteria of prime importance included commercial availability, industry trends, and past reliability testing performance. Eutectic 63Sn37Pb (SnPb) alloy was used as the control for all testing.

2.4.1 SAC305

SnAgCu {Tin (Sn); Silver (Ag); Copper (Cu)} solder alloys are believed to be the leading choice of the commercial electronics industry for Pb-free solder. The Sn3.0Ag0.5Cu is recommended

by industry and research consortia as a prime candidate for replacing SnPb solder. Sn3.0Ag0.5Cu is commercially available and currently used in electronic applications. It has been determined that alloys with compositions within the range of Sn3.0-4.0Ag0.5-1.0Cu all have a liquidus temperature around 217°C and have similar microstructures and mechanical properties. Note;

This alloy was chosen for reflow soldering because this particular solder alloy has shown the most promise as a primary replacement for SnPb solder. The team decided that they wanted to select at least one “general purpose” alloy to be evaluated and it was determined that the SnAgCu solder alloy would best serve this purpose. Conclusions drawn from literature suggest that this alloy has good mechanical properties and may be as reliable as SnPb in some applications. BAE Systems reviewed several SAC305 solder alloys for printing, reflow, and cleaning characteristics before choosing EnviroMark™ 907 from Kester.

2.4.2 SN100C

This alloy {Sn-0.7Cu-0.05Ni + Ge = Tin (Sn); Copper (Cu); Nickel (Ni); Germanium (Ge)} is commercially available and the general trend in industry has been to switch to the nickel stabilized tin-copper alloy over standard tin-copper due to its superior performance. In addition, this nickel-stabilized alloy does not require special solder pots and has shown no joint failures in specimens with over four (4) years of service. The cost of this alloy in the form of bar solder is relatively low when compared to other Pb-free solder alloys in bar form.

The superior performance of the tin-copper-nickel alloy has been confirmed by university research which has found that the nickel addition works by facilitating solidification of the alloy as a fine uniform eutectic structure and suppressing the growth of primary tin dendrites that are the cause of shrinkage defects in the unmodified alloy. This mode of solidification enhances the fluidity of the alloy close to the melting point, a property that is important in a solder so that it is comparable with that of tin-lead solder at the same superheat. The tin-copper-nickel alloy is representative of a new class of modified tin-copper solders that are increasing in popularity as the limitations of the tin-silver-copper alloys in some applications become apparent. Nihon Superior SN100C was used for this project.

2.5 Flux

The flux systems used during soldering were "low residue" or no-clean fluxes and the group chose to clean the test vehicles after processing even though no-clean fluxes were used with some solders. Additionally, reflow was accomplished without nitrogen inerting, which might have created a smaller soldering process window (a credit to the BAE Systems crew for creating a quality test vehicle under such tough process conditions).

Table 2 - Solder Alloys and Associated Flux

Solder Alloy	Flux		
	Reflow Soldering	Wave Soldering	Manual Soldering
SAC305	ROL1	N/A	ROL0 Tacky Flux
SN100C	ROL0	ORL0	ROL0 Tacky Flux
SnPb baseline	ROL0	ORM0	ROL0 Tacky Flux

- Table provided by BAE Systems Irving, Texas
- N/A = Due to limitations on board numbers and components, these solder alloys were not used during the noted assembly processes
- RO = Rosin base
- {IPC J-STD-004B; Table 1-1, Flux Identification System}
 - ROL0 = Rosin, Low flux/flux residue activity, < 0.05% halide
 - ROL1 = Rosin, Low flux/flux residue activity, < 0.5% halide
 - ORL0 = Organic, Low flux/flux residue activity, < 0.05% halide
 - ORM0 = Organic, Moderate flux/flux residue activity, < 0.05% halide

2.6 Components

The project stakeholder's agreed to populate the test vehicles with the following components:

Table 3 - Components Table

Component Type	Component Finish	Part Number	Substrate
CLCC-20	SAC305	20LCC-1.27mm-8.90mm-DC-L-Au	Ceramic
	SnPb	Tinning for SAC305 & SnPb	
QFN-20	Sn	A-MLF20-5mm-.65mm-DC	Plastic
	SnPb		
QFP-144	Sn	A-TQFP144-20mm-.5mm-2.0-DC Tinning for SAC305 & SnPb	Plastic
	SnPb		
	NiPdAu		
	SAC305		
BGA-225	SnPb	PBGA225-1.5mm-27mm-DC	Plastic
	SAC405		
PDIP-20	Sn	A-PDIP20T-7.6mm-DC	Plastic
	NiPdAu		
	SnPb		
CSP-100	SnPb	A-CABGA100-.8mm-10mm-DC Reballed for SN100C	Plastic
	SAC105		
	SN100C		
TSOP-50	Sn	A-TII-TSOP50-10.16x20.95mm-.8mm-DC	Plastic
	SnBi		
	SnPb		

Note – The TSOP-50 components do not have a dummy die. For more information on the decision not to include dummy die, please see “NASA-DoD Lead-Free Electronics Project; Project Plan – December 2009”

Note – Tinning is defined as the process of removing and replacement of a component finish by immersion in a selected molten solder alloy

Note – A portion of the CSP-100 components were re-balled from SAC105 to SN100C for testing purposes

Note – QFN-20 components with the thermal die pad (see Figure 1) soldered to the board were the most reliable components under this test program

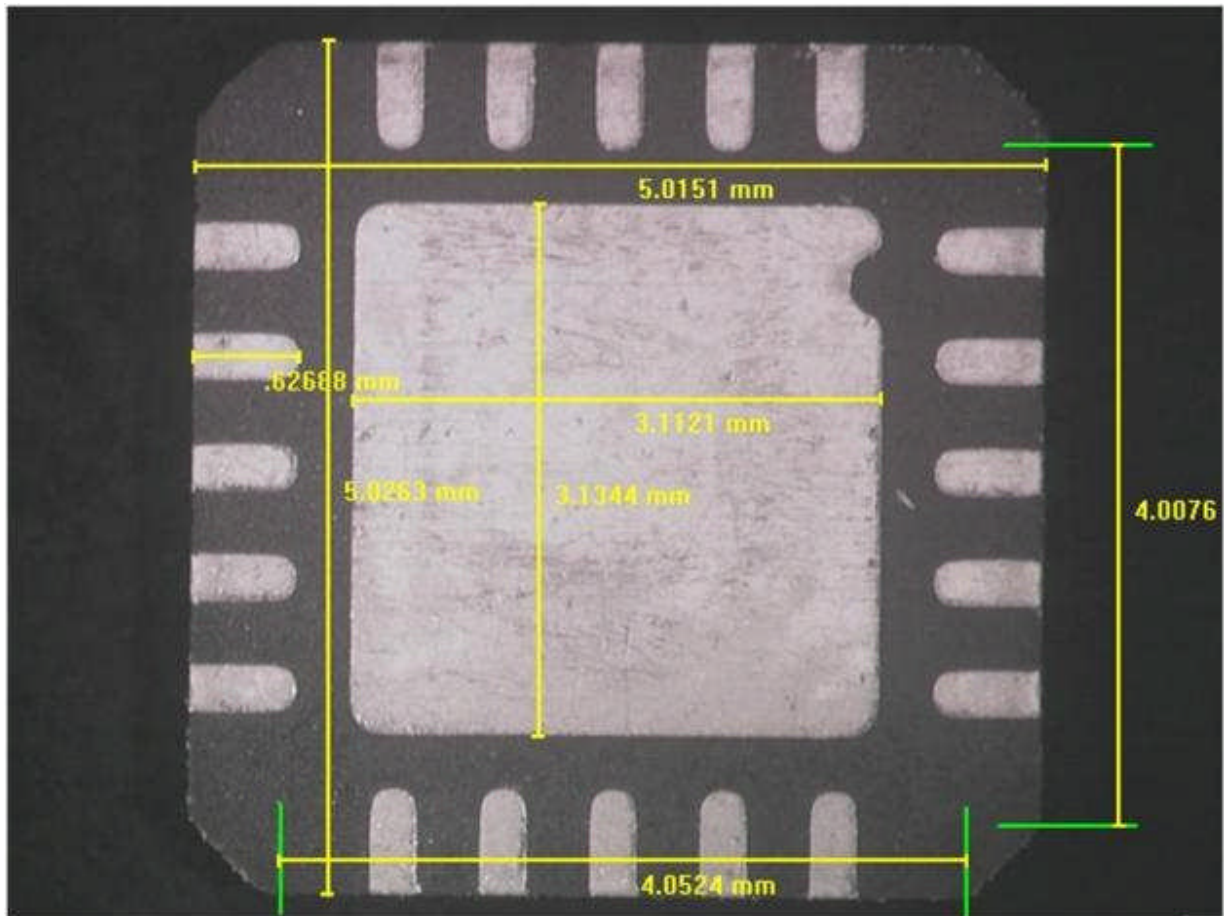


Figure 1 – QFN-20 Component Bottom Side Showing Die Thermal Pad

2.6.1 Component Characterization

Destructive physical analysis (DPA) was performed on samples from each of the component types that were placed onto the test vehicles. The DPA process was used to ensure that the components used for testing meet the consortia required standards and to evaluate the quality of construction. Results from destructive physical analysis are available on the NASA TEERM website; <http://teerm.nasa.gov>.

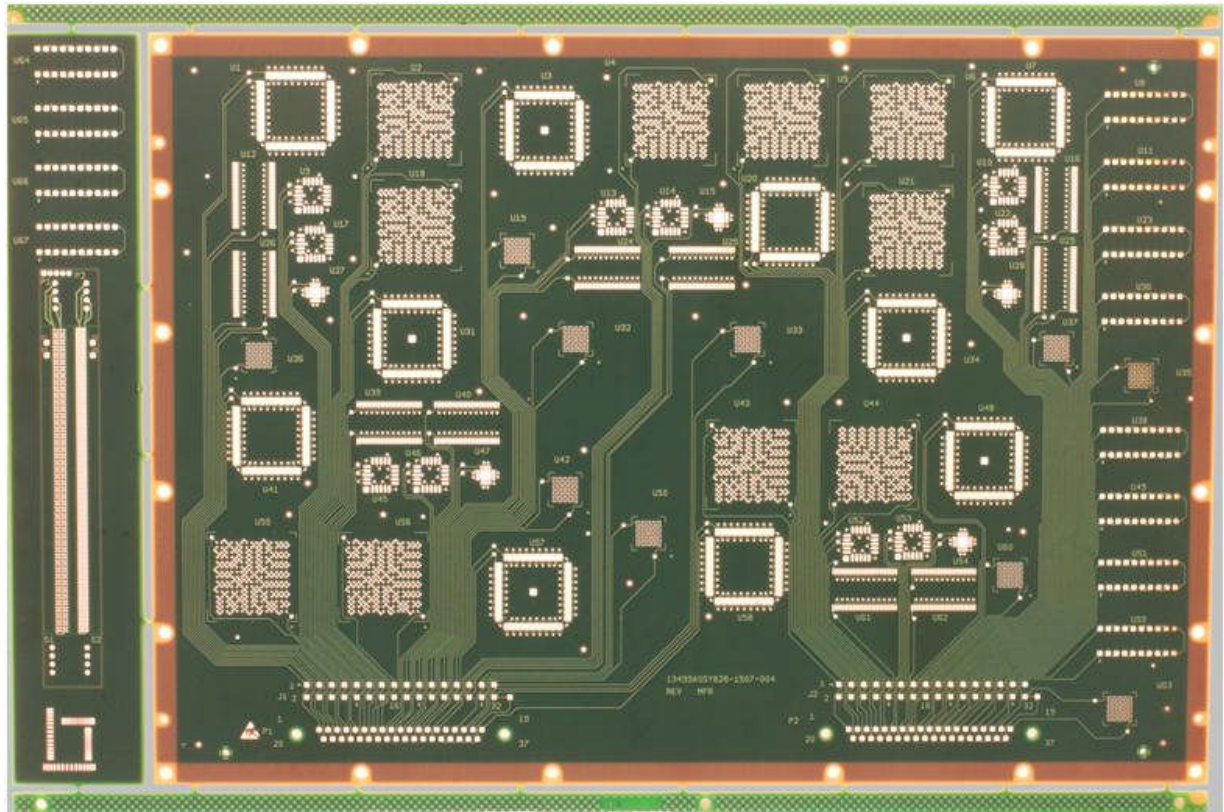


Figure 2 – NASA-DoD Lead-Free Electronics Project Test Vehicle Pre-Assembly

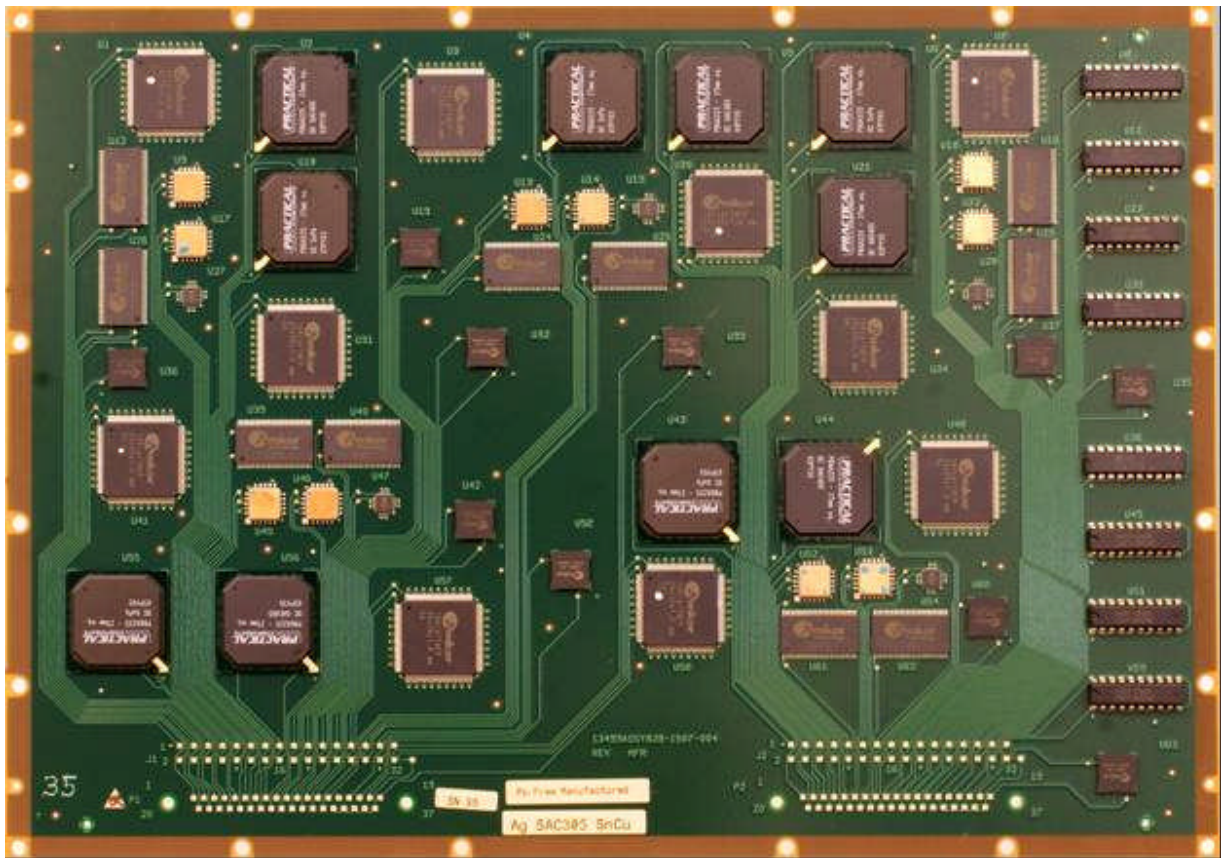


Figure 3 - NASA-DoD Lead-Free Electronics Project Test Vehicle Post-Assembly

3 Assembly

One hundred and ninety three (193) test vehicles were assembled by BAE Systems in Irving, Texas. One hundred and twenty (120) of these test vehicles were “Manufactured” PWA’s and seventy three (73) were “Rework” PWA’s (see Table 4).

Test vehicles were initially assembled per IPC J-STD-001D “Requirements for Soldered Electrical and Electronic Assemblies”, end-product Class 3 “High Performance Electronics Products”. Class 3 is defined in IPC J-STD-001D as “Includes products where continued high performance or performance-on-demand is critical, equipment downtime cannot be tolerated, end-use environment may be uncommonly harsh, and the equipment must function when required, such as life support or other critical systems.”

Please note that IPC J-STD-001DS “Space Applications Electronic Hardware Addendum to IPC J-STD-001D” and NASA-STD-8739.2 “Workmanship Standard for Surface Mount Technology” were not referenced during the assembly of the test vehicles.

“Manufactured” (Mfg.) test vehicles represent printed wiring assemblies newly manufactured for use in new product. Test vehicles being subjected to thermal cycle and combined environments

testing included forward and backward compatibility. Test vehicles assembled for vibration, mechanical shock and drop testing did not include forward and backward compatibility. The “Manufactured” test vehicles were assembled using immersion silver (Ag) and a limited number of electroless nickel / immersion gold (ENIG) finished glass fiber (GF) laminate (IPC-4101/26) printed circuit boards with a glass transition temperature, T_g , of 170°C minimum.

The “Rework” (Rwk.) test vehicles represent printed wiring assemblies manufactured and reworked prior to being tested. Solder mixing (SnPb/Pb-free & Pb-free/SnPb) was evaluated on all “Rework” test vehicles. The “Rework” test vehicles were assembled using immersion silver (Ag) and a limited number of electroless nickel / immersion gold (ENIG) finished glass fiber (GF) laminate (IPC-4101/26) printed circuit boards with a glass transition temperature, T_g , of 170°C minimum.

For this project, forward and backward compatibility have been defined as:

- Forward Compatibility is a SnPb component attached to a printed wiring assembly using Pb-free solder with a Pb-free profile.
- Backward compatibility is a Pb-free component attached to a printed wiring assembly using SnPb solder with a SnPb solder profile.

For all details relating to the assembly of the test vehicles, please see “NASA-DoD Pb-free Electronics Project; Project Plan – December 2009” (<http://teerm.nasa.gov>).

Table 4 – Test Vehicle Assembly Details

Test Vehicle Type	Reflow Solder	Wave Solder	Serial Numbers	Number of Boards
Lead-Free Rework All Test Vehicles	SAC305	SN100C	161-193	33
SnPb Rework All Test Vehicles	SnPb	SnPb	121-160	40
SnPb Manufactured Test Vehicles Thermal Cycle and Combined Environments Tests	SnPb	SnPb	1, 3, 5–14, 20 - 24	17
SnPb Manufactured Test Vehicles Vibration, Mechanical Shock and Drop Tests	SnPb	SnPb	2, 4, 15–19, 25-34	17
Lead-Free Manufactured Test Vehicles Thermal Cycle and Combined Environments Tests	SAC305	SN100C	35, 39, 41-45, 50-54, 69-73, 93, 95, 97	20
Lead-Free Manufactured Test Vehicles Vibration, Mechanical Shock and Drop Tests	SAC305	SN100C	36-38, 40, 46- 49, 55-68, 74- 92, 94, 96	43
Lead-Free Manufactured Test Vehicles Thermal Cycle and Combined Environments Tests	SN100C	SN100C	100, 102-106, 116-120	11
Lead-Free Manufactured Test Vehicles Vibration, Mechanical Shock and Drop Tests	SN100C	SN100C	101, 111-115	6
Lead-Free Manufactured Test Vehicles Crane Rework Effort	SN100C	SN100C	98-99, 107-110	6

Note - Lead-Free profiles were used for reflow and wave soldering of the “SnPb Rework All Test Vehicles”

3.1 NSWC Crane Assembly and Rework Effort

Thirty (30) of the one hundred and ninety three (193) test vehicles assembled by BAE Systems in Irving, Texas were built for Naval Surface Warfare Center (NSWC), Crane Division, a NASA-DoD Consortium member, in support of their Naval Supply Command (NAVSUP) sponsored “Logistics Impact of Pb-free Circuits/Components” project.

The 30 test vehicles were built as “Manufactured” (Mfg.) test vehicles using Pb-free solder alloys and Pb-free component finishes. Following assembly, NSWC Crane performed SnPb rework on random Pb-free DIP, TQFP-144, TSOP-50, and LCC components. BEST Inc. performed the QFN rework for NSWC Crane. Some of the components were reworked 2 times.

The goal of the NSWC Crane effort is to generate data supporting the qualification of existing SnPb rework procedures for military hardware built with Pb-free processes through analysis of thermal cycling, vibration, and drop test data including microsection analysis.

The test vehicles for the NSWC Crane Rework effort contained an assembly error in which PDIP components with two lead finishes (Sn and NiPdAu) were randomly inserted during assembly. This resulted in test vehicles with PDIP components that had incorrect component finishes in many component reference designator locations. With the assembly error identified, the actual PDIP component finishes were validated on each test vehicle and the rework matrix reconfigured to compensate for the assembly error. Table 5, Table 6, and Table 7 reflect PDIP locations having two possible component finish types; NiPdAu and Sn. Cells filled in gray indicate a component finish NOT placed onto the test vehicles.

The Quad Flatpack No-lead (QFN) was an active rework part for the NSWC Crane Rework Effort. Because of a fabrication error, U15 was missing a copper trace (see 3.2.2). For the Crane test vehicles, jumper wires were added to each thermal cycle, vibration and drop test board in order to capture test data for that location.

Table 5 – NSWC Crane Rework Effort; Vibration Test Boards

RefDes	Part/Finish	Vibration Test Board (Lead-Free Manufactured Batch F)								
		Number of Reworks								
		SN79	SN61	SN62	SN63	SN64	SN65	SN66	SN67	SN68
U16	TSOP-50/SnBi	1	2	1	2	1	2	1	2	1
U24	TSOP-50/SnBi	0	0	0	0	0	0	0	0	0
U26	TSOP-50/SnBi	1	0	1	0	1	0	1	0	1
U40	TSOP-50/SnBi	2	1	2	1	2	1	2	1	2
U62	TSOP-50/SnBi	0	1	0	1	0	1	0	1	0
U12	TSOP-50/Sn	0	0	0	0	0	0	0	0	0
U25	TSOP-50/Sn	1	2	1	2	1	2	1	2	1
U29	TSOP-50/Sn	2	1	2	1	2	1	2	1	2
U39	TSOP-50/Sn	1	0	1	0	1	0	1	0	1
U61	TSOP-50/Sn	0	1	0	1	0	1	0	1	0
U9	CLCC-20/SAC305	1	2	1	2	1	2	1	2	1
U10	CLCC-20/SAC305	2	1	2	1	2	1	2	1	2
U13	CLCC-20/SAC305	0	0	0	0	0	0	0	0	0
U14	CLCC-20/SAC305	0	0	0	0	0	0	0	0	0
U17	CLCC-20/SAC305	1	2	1	2	1	2	1	2	1
U22	CLCC-20/SAC305	2	1	2	1	2	1	2	1	2
U45	CLCC-20/SAC305	1	0	1	0	1	0	1	0	1
U46	CLCC-20/SAC305	0	1	0	1	0	1	0	1	0
U52	CLCC-20/SAC305	1	0	1	0	1	0	1	0	1
U53	CLCC-20/SAC305	0	1	0	1	0	1	0	1	0
U1	TQFP-144/Sn	1	2	1	2	1	2	1	2	1
U3	TQFP-144/Sn	0	0	0	0	0	0	0	0	0
U7	TQFP-144/Sn	2	1	2	1	2	1	2	1	2
U20	TQFP-144/Sn	0	0	0	0	0	0	0	0	0
U31	TQFP-144/Sn	1	2	1	2	1	2	1	2	1
U34	TQFP-144/Sn	2	1	2	1	2	1	2	1	2
U41	TQFP-144/Sn	1	0	1	0	1	0	1	0	1
U48	TQFP-144/Sn	0	1	0	1	0	1	0	1	0
U57	TQFP-144/Sn	1	0	1	0	1	0	1	0	1
U58	TQFP-144/Sn	0	1	0	1	0	1	0	1	0
U08	PDIP-20/NiPdAu			1						
U11	PDIP-20/NiPdAu			1						
U49	PDIP-20/NiPdAu			1					1	
U51	PDIP-20/NiPdAu		2	1	2	1	2	1	1	1
U59	PDIP-20/NiPdAu		1		1		1		1	
U08	PDIP-20/Sn	2	1		1	2	1	2	1	2
U11	PDIP-20/Sn	1	2		2	1	2	1	2	1
U23	PDIP-20/Sn		1		1		1		1	
U30	PDIP-20/Sn	1				1		1		1
U38	PDIP-20/Sn		1		1		1		1	
U49	PDIP-20/Sn	2	1		1	2	1	2		2
U51	PDIP-20/Sn	1								
U15	QFN/Sn	1	2	1	2	1	2	1	2	1
U27	QFN/Sn	2	1	2	1	2	1	2	1	2
U28	QFN/Sn	1	2	1	2	1	2	1	2	1
U47	QFN/Sn	1	1S*	1	1S*	1	1S*	1	1S*	1
U54	QFN/Sn	1S*	1	1S*	1	1S*	1	1S*	1	1S*

1S* = 1 rework with StencilMate®

Table 6 - NSWC Crane Rework Effort; Drop Test Boards

RefDes	Part/Finish	Drop Test Board (Lead-Free Manufactured Batch F)								
		Number of Reworks								
		SN60	SN80	SN81	SN82	SN83	SN84	SN85	SN86	SN87
U16	TSOP-50/SnBi	1	2	1	2	1	2	1	2	1
U24	TSOP-50/SnBi	0	0	0	0	0	0	0	0	0
U26	TSOP-50/SnBi	1	0	1	0	1	0	1	0	1
U40	TSOP-50/SnBi	2	1	2	1	2	1	2	1	2
U62	TSOP-50/SnBi	0	1	0	1	0	1	0	1	0
U12	TSOP-50/Sn	0	0	0	0	0	0	0	0	0
U25	TSOP-50/Sn	1	2	1	2	1	2	1	2	1
U29	TSOP-50/Sn	2	1	2	1	2	1	2	1	2
U39	TSOP-50/Sn	1	0	1	0	1	0	1	0	1
U61	TSOP-50/Sn	0	1	0	1	0	1	0	1	0
U9	CLCC-20/SAC305	1	2	1	2	1	2	1	2	1
U10	CLCC-20/SAC305	2	1	2	1	2	1	2	1	2
U13	CLCC-20/SAC305	0	0	0	0	0	0	0	0	0
U14	CLCC-20/SAC305	0	0	0	0	0	0	0	0	0
U17	CLCC-20/SAC305	1	2	1	2	1	2	1	2	1
U22	CLCC-20/SAC305	2	1	2	1	2	1	2	1	2
U45	CLCC-20/SAC305	1	0	1	0	1	0	1	0	1
U46	CLCC-20/SAC305	0	1	0	1	0	1	0	1	0
U52	CLCC-20/SAC305	1	0	1	0	1	0	1	0	1
U53	CLCC-20/SAC305	0	1	0	1	0	1	0	1	0
U1	TQFP-144/Sn	1	2	1	2	1	2	1	2	1
U3	TQFP-144/Sn	0	0	0	0	0	0	0	0	0
U7	TQFP-144/Sn	2	1	2	1	2	1	2	1	2
U20	TQFP-144/Sn	0	0	0	0	0	0	0	0	0
U31	TQFP-144/Sn	1	2	1	2	1	2	1	2	1
U34	TQFP-144/Sn	2	1	2	1	2	1	2	1	2
U41	TQFP-144/Sn	1	0	1	0	1	0	1	0	1
U48	TQFP-144/Sn	0	1	0	1	0	1	0	1	0
U57	TQFP-144/Sn	1	0	1	0	1	0	1	0	1
U58	TQFP-144/Sn	0	1	0	1	0	1	0	1	0
U08	PDIP-20/NiPdAu	1								
U11	PDIP-20/NiPdAu	1								
U49	PDIP-20/NiPdAu	1								
U51	PDIP-20/NiPdAu	1		1	2		2	1	2	1
U59	PDIP-20/NiPdAu				1	1	1		1	
U08	PDIP-20/Sn		1	2	1	2	1	2	1	2
U11	PDIP-20/Sn		1	1	2	1	2	1	2	1
U23	PDIP-20/Sn		1		1		1		1	
U30	PDIP-20/Sn			1		1		1		1
U38	PDIP-20/Sn		1		1		1		1	
U49	PDIP-20/Sn		1	2	1	2	1	2	1	2
U51	PDIP-20/Sn		1			1				
U15	QFN/Sn	2	2	1	2	1	2	1	2	1
U27	QFN/Sn	1	1	2	1	2	1	2	1	2
U28	QFN/Sn	1S*	2	1	2	1	2	1	2	1
U47	QFN/Sn	1	1S*	1	1S*	1	1S*	1	1S*	1
U54	QFN/Sn	1S*	1	1S*	1	1S*	1	1S*	1	1S*

1S* = 1 rework with StencilMate®

Table 7 - NSWC Crane Rework Effort; Thermal Cycle Test Boards

		Thermal Cycle -55°C to +125°C							
RefDes	Part/Finish	SAC Test Board (LF Mfg Batch F)				SN100C Test Board (LF Mfg Batch I)			
		Number of Reworks							
		SN46	SN47	SN48	SN49	SN107	SN108	SN109	SN110
U12	TSOP-50/Sn	1	0	2	0	1	0	2	0
U25	TSOP-50/Sn	2	0	1	2	2	0	1	2
U29	TSOP-50/Sn	0	1	2	0	0	1	2	0
U39	TSOP-50/Sn	1	2	0	1	1	2	0	1
U61	TSOP-50/Sn	0	1	2	0	0	1	2	0
U16	TSOP-50/SnBi	0	2	0	1	0	2	0	1
U24	TSOP-50/SnBi	1	2	0	1	1	2	0	1
U26	TSOP-50/SnBi	2	0	1	2	2	0	1	2
U40	TSOP-50/SnBi	2	0	1	2	2	0	1	2
U62	TSOP-50/SnBi	0	1	2	0	0	1	2	0
U9	CLCC-20/SAC305	0	1	2	0	0	1	2	0
U17	CLCC-20/SAC305	1	2	0	1	1	2	0	1
U13	CLCC-20/SAC305	2	0	1	2	2	0	1	2
U14	CLCC-20/SAC305	0	1	2	0	0	1	2	0
U52	CLCC-20/SAC305	1	2	0	1	1	2	0	1
U10	CLCC-20/SAC305	2	0	1	2	2	0	1	2
U22	CLCC-20/SAC305	0	1	2	0	0	1	2	0
U45	CLCC-20/SAC305	0	0	0	0	0	0	0	0
U46	CLCC-20/SAC305	0	0	0	0	0	0	0	0
U53	CLCC-20/SAC305	0	0	0	0	0	0	0	0
U1	TQFP-144/Sn	0	1	2	0	0	1	2	0
U3	TQFP-144/Sn	1	2	0	1	1	2	0	1
U7	TQFP-144/Sn	2	0	1	2	2	0	1	2
U20	TQFP-144/Sn	0	1	2	0	0	1	2	0
U31	TQFP-144/Sn	1	2	0	1	1	2	0	1
U34	TQFP-144/Sn	2	0	1	2	2	0	1	2
U41	TQFP-144/Sn	0	1	2	0	0	1	2	0
U48	TQFP-144/Sn	0	0	0	0	0	0	0	0
U57	TQFP-144/Sn	0	0	0	0	0	0	0	0
U58	TQFP-144/Sn	0	0	0	0	0	0	0	0
U08	PDIP-20/NiPdAu						1		
U11	PDIP-20/NiPdAu						1		
U23	PDIP-20/NiPdAu						1	1	
U38	PDIP-20/NiPdAu								1
U49	PDIP-20/NiPdAu								1
U51	PDIP-20/NiPdAu		1		1				
U59	PDIP-20/NiPdAu	1		1					1
U08	PDIP-20/Sn		1	2		1			1
U11	PDIP-20/Sn		1						
U23	PDIP-20/Sn	1	2		1	2			2
U30	PDIP-20/Sn	1	2		1				
U38	PDIP-20/Sn	2		1	2	2		1	
U49	PDIP-20/Sn	2		1	2		1	2	
U51	PDIP-20/Sn						1	2	
U59	PDIP-20/Sn					1	2		
U15	QFN/Sn	2	1S*	1	2	2	1S*	1	2
U47	QFN/Sn	1S*	1	2	1S*	1S*	1	2	1S*
U27	QFN/Sn	1S*	1	2	1S*	1S*	1	2	1S*
U28	QFN/Sn	1	2	1S*	1	1	2	1S*	1
U54	QFN/Sn	2	1S*	1	2	2	1S*	1	2

1S* = 1 rework with StencilMate*

Testing of the NSWC Crane test vehicles included -55°C to +125°C thermal cycling testing conducted by Rockwell Collins, Cedar Rapids, Iowa. The NSWC Crane test vehicles were tested with the NASA-DoD Lead-free Electronics test vehicles during -55°C to +125°C thermal cycle testing. Eight assemblies in all were tested. Each board was monitored for net resistance for all 63 components.

Drop testing, performed by Celestica, Toronto, Ontario, was conducted on the NSWC Crane test vehicles prior to testing the NASA-DoD Lead-free Electronics test vehicles. Initially, the testing procedures for both the NSWC Crane and NASA-DoD Lead-free Electronics test vehicles were to be identical. However, lessons learned during the testing of the NSWC Crane test vehicles lead the consortium to change the testing procedure for the NASA-DoD Lead-free Electronics test vehicles. Nine assemblies in all were tested. Each board was monitored for net resistance for all 63 components.

Vibration testing, performed by Celestica, Toronto, Ontario, was conducted on the NSWC Crane test vehicles since the facility that tested the NASA-DoD test vehicles could not accommodate the Crane vibration test vehicles. The testing followed the document specifications contained in the NASA-DoD Lead-Free Electronics Project Joint Test Protocol. Nine assemblies in all were tested. Each board was monitored for vibration response and net resistance for all 63 components. The assemblies were attached to the table with the supplied test fixture.

For all details relating to the assembly of the test vehicles, please see “NASA-DoD Lead-Free Electronics Project; Project Plan – March 2010” (<http://teerm.nasa.gov>).

3.2 Test Vehicle Assembly Irregularities

With all of the complexities built into the NASA-DoD Lead-Free Electronics Project design of experiment, test vehicle irregularities are bound to occur. Following are test vehicle irregularities that affect the collection of data from the test vehicles.

3.2.1 Chip Scale Package (CSP)

When reviewing the CSP data, please note that the CSP components on all test vehicles only have continuity in the outside solder balls. The wrong component configuration was used during test vehicle drafting. Traces interconnecting internal rows of balls to the outside row of balls do not exist on the test vehicles, Figure 4. In order for a CSP component failure to be recorded, breaks in both sides of the continuity box must occur, Figure 5.

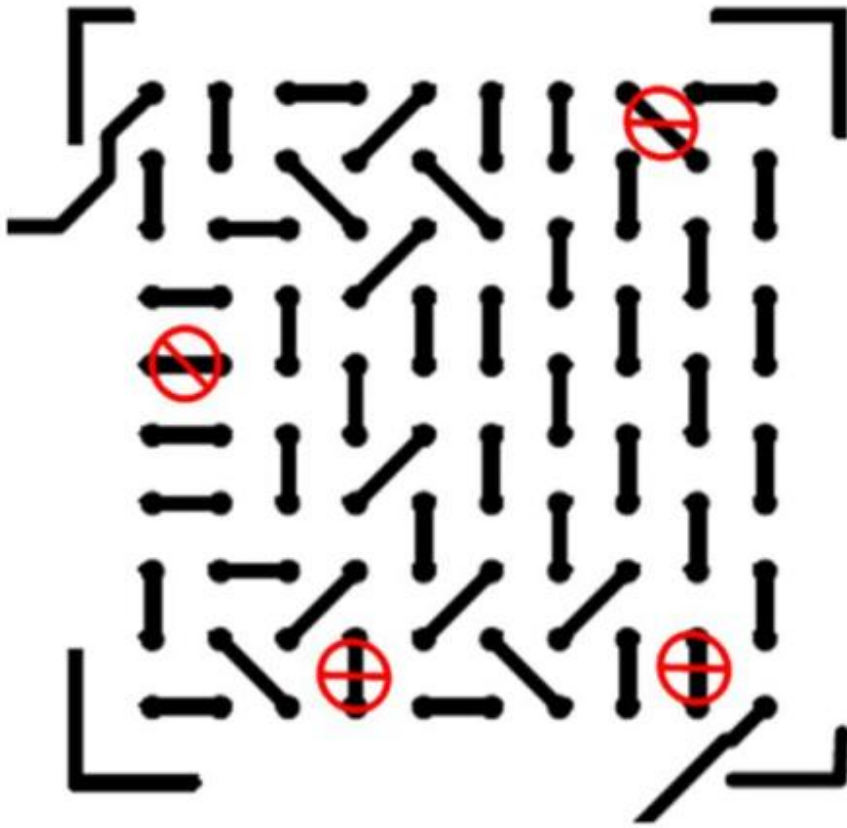


Figure 4 - Test Vehicle Drawing, Chip Scale Package (CSP)

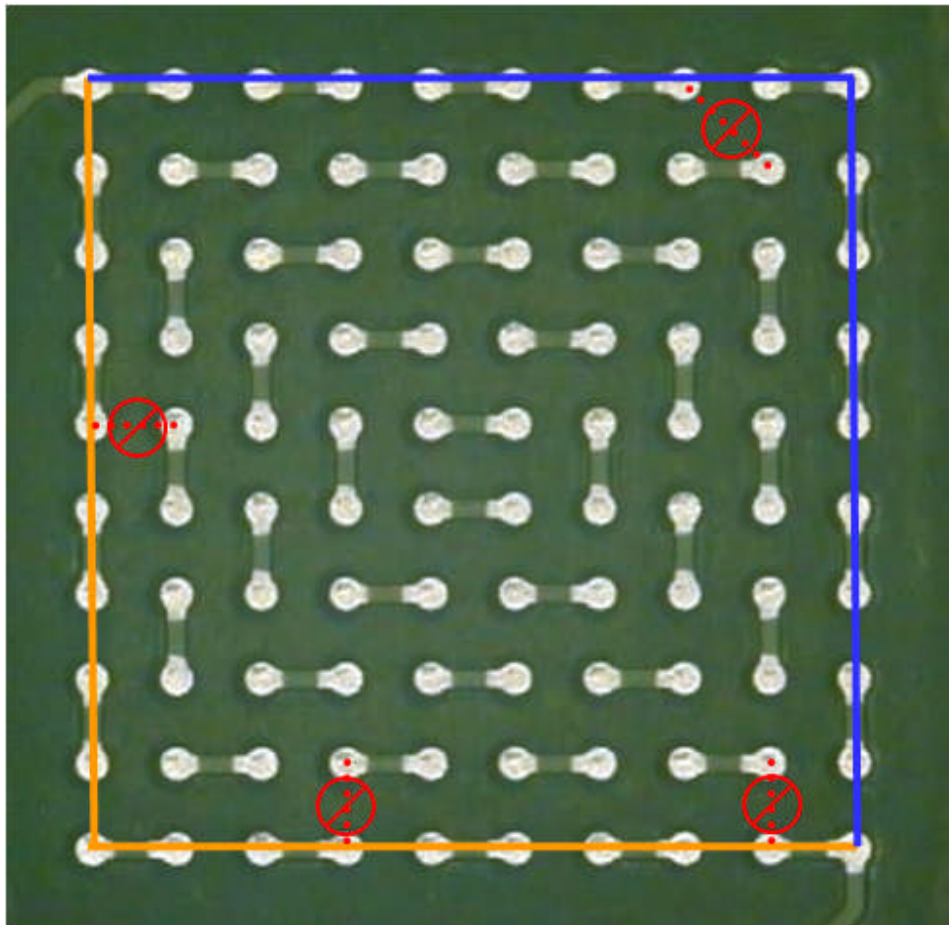


Figure 5 - Chip Scale Package (CSP) Continuity Loop

3.2.2 Quad Flat No leads (QFN), Location U15

Component location U15, a QFN, is missing a wire trace, Figure 6. During drafting, the trace was not included in the test vehicles drawing, Figure 7. Test data cannot be collected for this component unless a jumper wire is used in-place of the missing trace. Jumper wires were used for the thermal cycle test vehicles. For vibration, drop, mechanical shock and combined environments testing, it was determined that a jumper wire is not feasible. For the NSWCR Crane rework test vehicles, QFN U15 is an active rework component. For drop and vibration testing, a jumper wire was attached to each U15 location to permit collection of test data (see Figure 8).

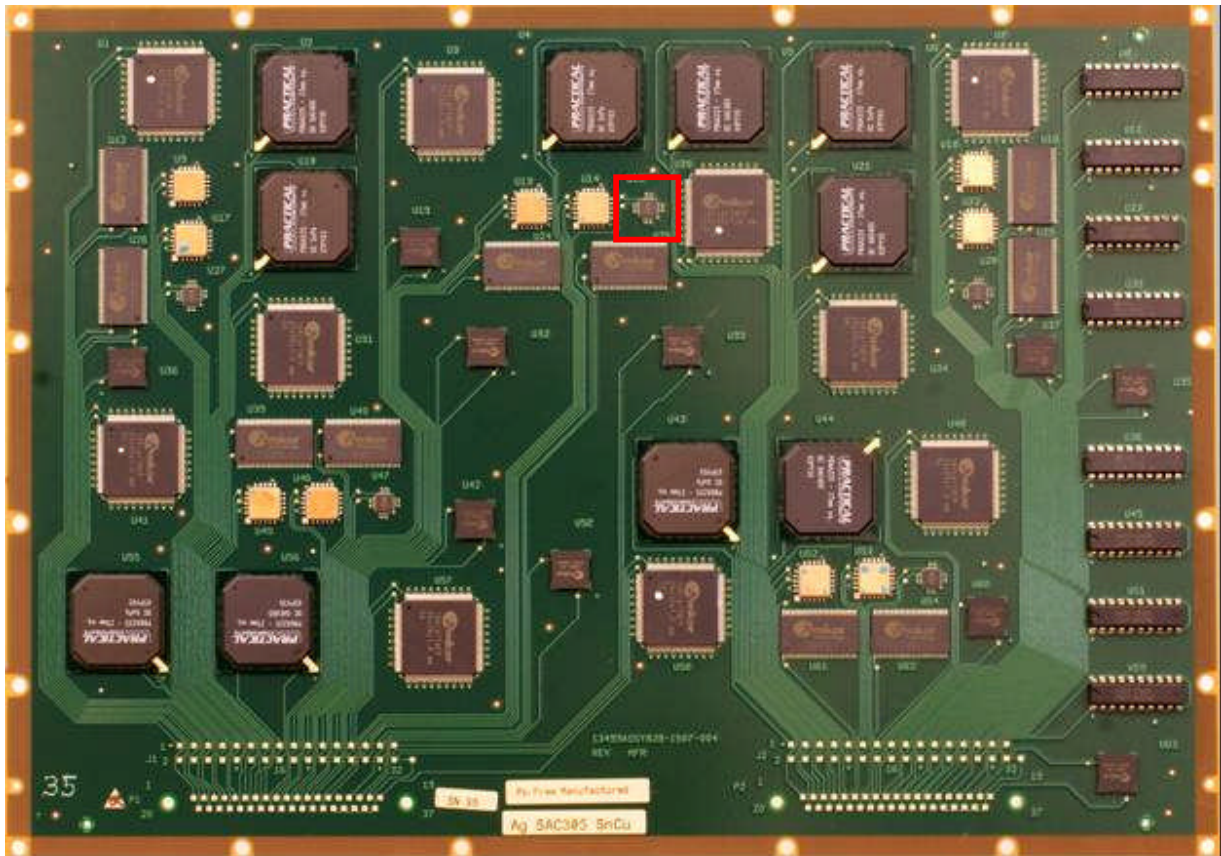


Figure 6 - Quad Flat No leads (QFN), Component Location U15

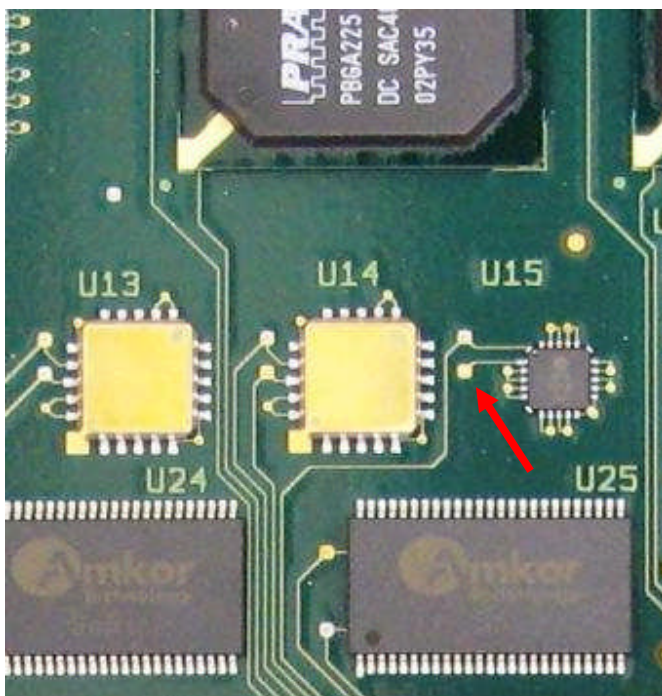


Figure 7 - Missing Trace, QFN – U15

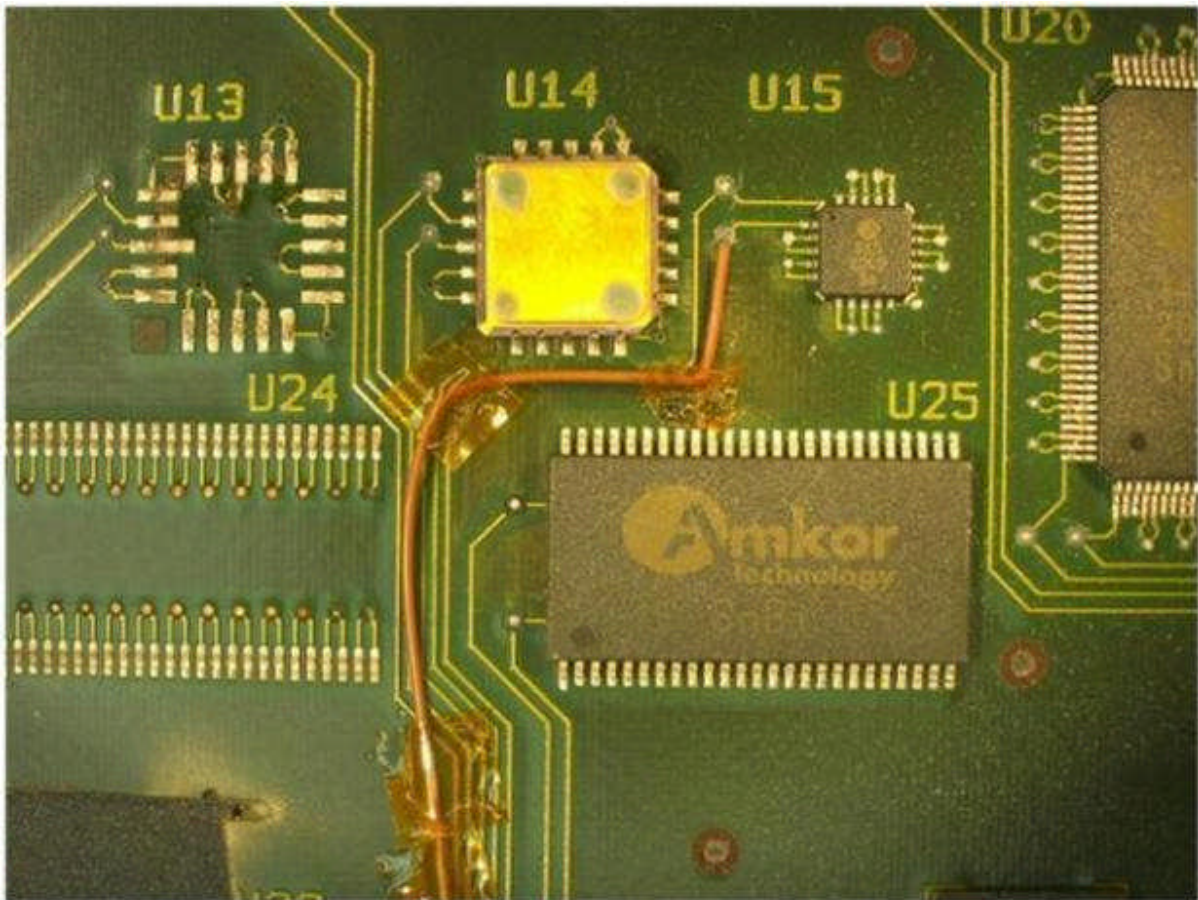


Figure 8 - Jumper Wire Attached to U15 Location to Permit Collection of Test Data

3.2.3 TSOP-50 Components Missing Internal Wire Bonds

The TSOP-50 components were found to be missing internal wire bonds during incoming component inspection. Numerous solutions were discussed by the stakeholders of the NASA-DoD Lead-Free Electronic Project. One solution agreed to by the group, was to add a jumper to the components for a few of the test vehicles (Figure 9). This option would have had to be worked following assembly, requiring 2000 jumpers, and dealt with during rework operations. With the jumper, only half of the component would be working. Instead of using jumpers to solve the TSOP component issue, Lockheed Martin provided the funding required to purchase new TSOP components from Amkor through Practical Components. The jumper option was used on a very limited basis; thermal cycle test vehicle (SN110), vibration test vehicle (SN61), and drop test vehicles (SN80 and SN86).

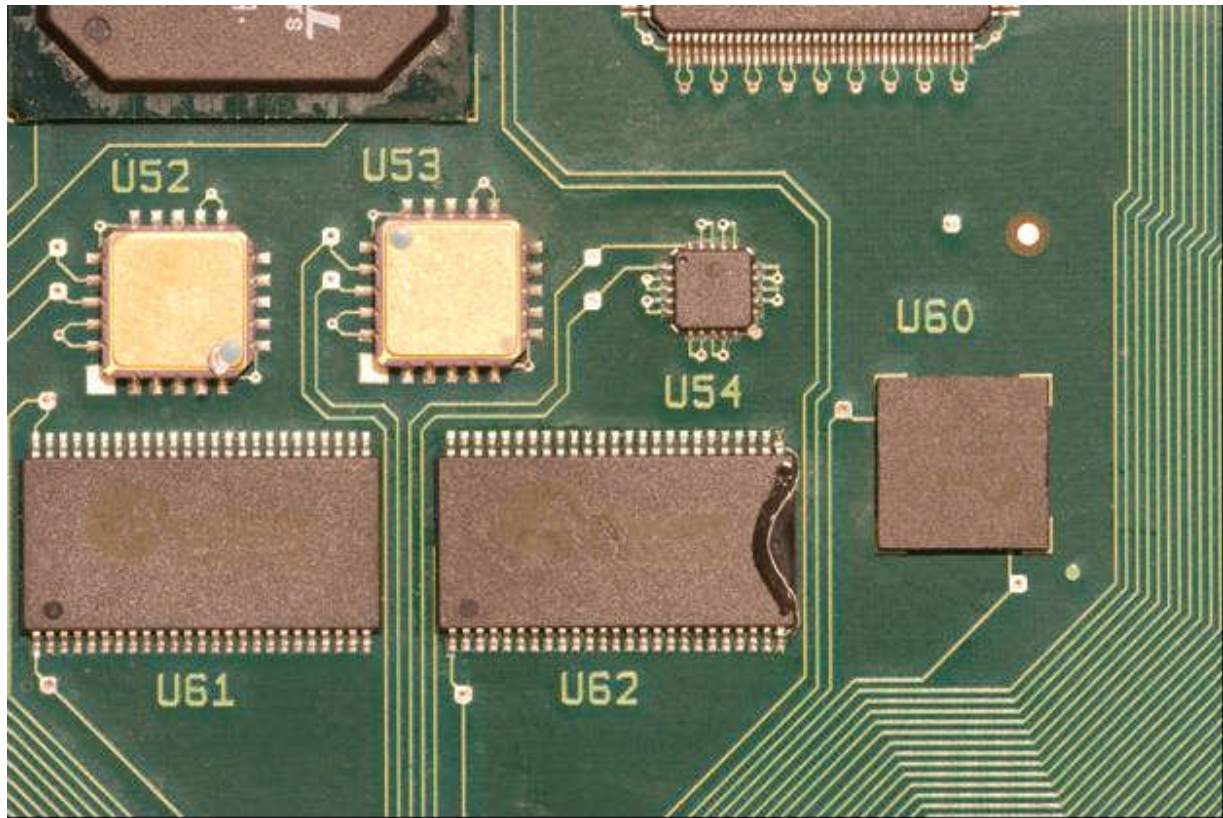


Figure 9 – TSOP Component Jumper

4 Test Methods

Project technical representatives identified the engineering, performance, and operational impact (supportability) requirements for printed wiring assemblies, reaching consensus on the tests, procedures and acceptance criteria to be applied. This information was documented in “NASA-DoD Lead-Free Electronics Project, Joint Test Protocol (JTP); September 2009” (<http://teerm.nasa.gov>).

The performance requirements and related tests for the NASA-DoD Lead-Free Electronics test vehicles are listed in Table 8. These tests were required by all military and aerospace systems that participated in the development of the NASA-DoD Lead-Free Electronics Project. Both “Manufactured” and “Rework” test vehicles were tested.

Table 8 - Test Vehicle Performance Requirements

Test	Location	Reference	Electrical Test	Acceptance Criteria ^(a)
Vibration	Boeing Seattle, WA	MIL-STD-810F Method 514.5 Procedure I	Electrical continuity failure	Better than or equal to SnPb controls
	Celestica Toronto, Ontario			
Mechanical Shock	Boeing Seattle, WA	MIL-STD-810F Method 516.5	Electrical continuity failure	Better than or equal to SnPb controls
	Boeing Seattle, WA			
Thermal Cycling	Boeing Seattle, WA	IPC-SM-785	Electrical continuity failure	Better than or equal to SnPb controls at 10% ^b Weibull cumulative failures
	Rockwell Collins Cedar Rapids, IA			
Combined Environments	Raytheon McKinney, TX	MIL-STD-810F Method 520.2	Electrical continuity failure	Better than or equal to SnPb controls at
	Raytheon McKinney, TX			
Drop Testing	Celestica Toronto, Ontario	JEDEC Standard JESD22-B110A	Electrical continuity failure	Better than or equal to SnPb controls
	Celestica Toronto, Ontario			
Interconnect Stress Test (IST)	PWB Interconnect Solutions Inc. Toronto, Ontario	IPC-TM-650-2.6.26	Electrical continuity testing	3 thermal cycles simulate assembly and 6 thermal cycles simulate assembly and rework
Copper Dissolution	Celestica Toronto, Ontario	IPC-TM-650-2.1.1 ASTM-E-3	Cross section/ metallographic analysis	N/A
	Rockwell Collins Cedar Rapids, IA			

^a Failure of a test board in a specific test does not necessarily disqualify a Pb-free solder alloy for use in an application for which that test does not apply. Electrical performance requirements for a particular circuit apply only to parts containing that circuit.

^b 10% noncompliance of minimal Weibull distribution data for Thermal Cycling and Combined Environments Testing was selected because it was a compromise between the 63.2% failures which is taken as normal life, and 1% failures (or first failure) which is most important in high reliability systems.

5 Test Results

5.1 Vibration Test

5.1.1 Vibration Test Method

This test quantifies solder joint failures on the test vehicles during exposure to vibration. The limits identified in the vibration testing were used to compare performance differences in the Pb-free test alloys and mixed solder joints vs. the baseline standard SnPb (63/37) alloy.

The testing satisfies the general requirements of MIL-STD-810F (Test Method Standard for Environmental Engineering Considerations and Laboratory Tests) Method 514.5 (Vibration) and was performed using the following procedure:

- Confirm the electrical continuity of each test channel prior to testing. One channel was used per component.
- Place the PWAs into a test fixture in random order and mount the test fixture onto an electrodynamic shaker.

- Conduct a step stress test in the Z-axis only (i.e., perpendicular to the plane of the circuit board). Most failures occur with displacements applied in the Z-axis as those results in maximum board bending for each of the major modes.
- Run the test using the stress steps shown in Figure 10 and Table 9. Subject the test vehicles to 8.0 g_{rms} for one hour. Then increase the Z-axis vibration level in 2.0 g_{rms} increments, shaking for one hour per step until the 20.0 g_{rms} level is completed. Then subject the test vehicles to a final one hour of vibration at 28.0 g_{rms}.
- Continuously monitor the electrical continuity of the solder joints during the test using event detectors with shielded cables. All wires used for monitoring were soldered directly to the test vehicles and then glued to the test vehicles (with stress relief) to minimize wire fatigue during the test.
- A complete modal analysis was conducted on one test vehicle using a laser vibrometer system in order to determine the resonant frequencies and the actual deflection shapes for each mode

The stakeholders agreed that a stress step test representing increasingly severe vibration environments was appropriate for this test. A step stress test is required since a test conducted at a constant 8.0 g_{rms} level (Step 1) would take thousands of hours to fail the same number of components as a step stress test. This is because some locations on a circuit assembly experience very low stresses and severe vibration is required in order to fail components at these locations. The shape of the PSD (Power Spectral Density) curve for each step stress level was designed so that all of the major resonances of the test vehicles would be excited by the random vibration input. The PSD curves presented in MIL-STD-810F were used as guides for the creation of this step stress test but were not directly duplicated.

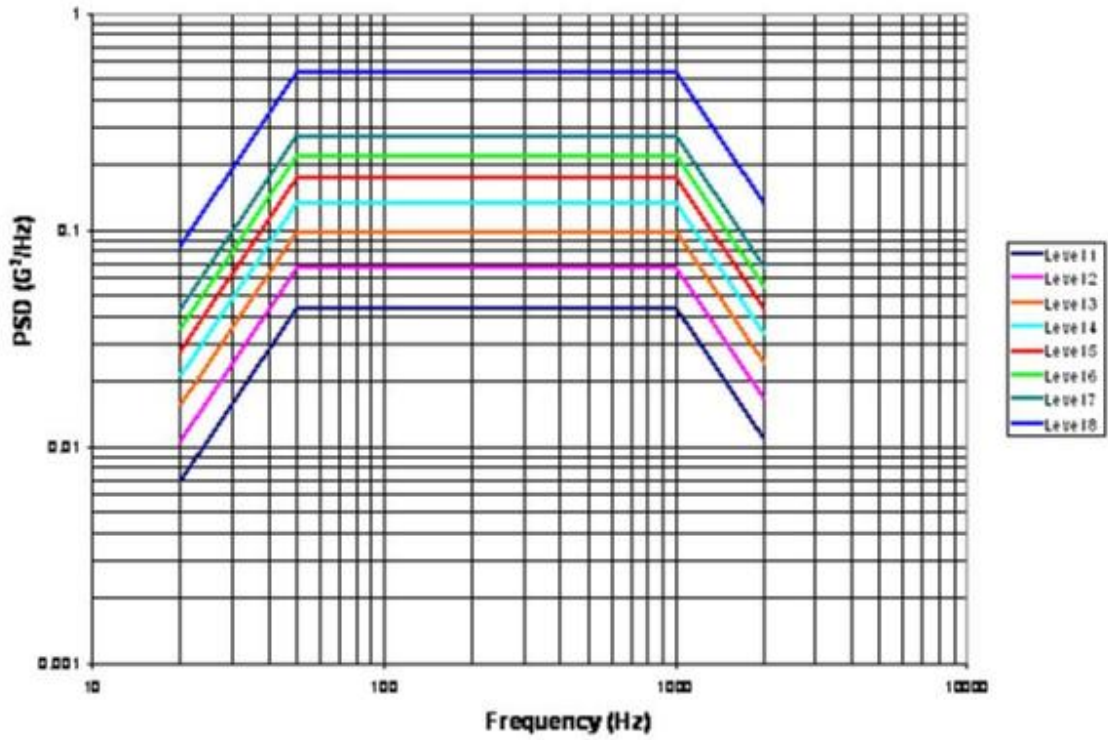


Figure 10 - Vibration Spectrum

Table 9 - Vibration Profile

Level 1	Level 2	Level 3
20 Hz @0.00698 G ² /Hz	20 Hz @0.0107 G ² /Hz	20 Hz @0.0157 G ² /Hz
20 - 50 Hz @ +6.0 dB/octave	20 - 50 Hz @ +6.0 dB/octave	20 - 50 Hz @ +6.0 dB/octave
50 - 1000 Hz @0.0438 G ² /Hz	50 - 1000 Hz @0.067 G ² /Hz	50 - 1000 Hz @0.0984 G ² /Hz
1000 -2000 Hz @ -6.0 dB/octave	1000 - 2000 Hz @ -6.0 dB/octave	1000 - 2000 Hz @ -6.0 dB/octave
2000 Hz @ 0.0 109 G ² /Hz	2000 Hz @ 0.0 167 G ² /Hz	2000 Hz @ 0.0245 G ² /Hz
Composite = 8.0 g_{rms}	Composite = 9.9 g_{rms}	Composite = 12.0 g_{rms}
Level 4	Level 5	Level 6
20 Hz @ 0.02 14 G ² /Hz	20 Hz @ 0.0279 G ² /Hz	20 Hz @ 0.0354 G ² /Hz
20 - 50 Hz @ +6.0 dB/octave	20 - 50 Hz @ +6.0 dB/octave	20 - 50 Hz @ +6.0 dB/octave
50 - 1000 Hz @ 0.134 G ² /Hz	50 - 1000 Hz @ 0.175 G ² /Hz	50 - 1000 Hz @ 0.22 15 G ² /Hz
1000 -2000 Hz @ -6.0 dB/octave	1000 - 2000 Hz @ -6.0 dB/octave	1000 - 2000 Hz @ -6.0 dB/octave
2000 Hz @ 0.0334 G ² /Hz	2000 Hz @ 0.0436 G ² /Hz	2000 Hz @ 0.0552 G ² /Hz
Composite = 14.0 g_{rms}	Composite = 16.0 g_{rms}	Composite = 18.0 g_{rms}
Level 7	Level 8	
20 Hz @ 0.0437 G ² /Hz	20 Hz @ 0.0855 G ² /Hz	
20 - 50 Hz @ +6.0 dB/octave	20 - 50 Hz @ +6.0 dB/octave	
50 - 1000 Hz @ 0.2734 G ² /Hz	50 - 1000 Hz @ 0.5360 G ² /Hz	
1000 -2000 Hz @ -6.0 dB/octave	1000 - 2000 Hz @ -6.0 dB/octave	
2000 Hz @0.0682 G ² /Hz	2000 Hz @0.1330 G ² /Hz	
Composite = 20.0 g_{rms}	Composite = 28.0 g_{rms}	

5.1.2 NASA-DoD Test Vehicle Vibration Testing Results Summary

The complete test report, “NASA-DoD Lead-Free Electronics Project: Vibration Test”, can be found on the NASA TEERM website (<http://teerm.nasa.gov>).

The objective of this study was to determine the effects of random vibration on the relative reliability of Pb-free and tin/lead solder joints (i.e., which solder survived the longest). Modal data and strain data were also collected during this study in an effort to provide data that would be useful to those that may want to try to model the behavior of the NASA-DoD test vehicle.

Twenty seven test vehicles were delivered to Boeing for vibration testing. These consisted of 5 SnPb “Manufactured” test vehicles; 6 Pb-free “Manufactured” test vehicles assembled with SAC305 paste; 5 Pb-free “Manufactured” test vehicles assembled with SN100C paste; 6 SnPb “Rework” test vehicles; and 5 Pb-free “Rework” test vehicles. Most of the test vehicles had an immersion silver PWB finish except for one SAC305 “Manufactured” test vehicle (Test Vehicle 96) with ENIG PWB finish and one SnPb “Rework” test vehicle (Test Vehicle 157) with ENIG PWB finish.

Table 10 shows the percent of each component type that failed on both the “Manufactured” and the “Rework” test vehicles at the end of the test. Notice that the QFN-20’s were resistant to failure due to vibration.

Table 10 - Percentage of Components Failed (Includes Mixed Solders)

Component	% of Components Failed During Vibration Testing				
	"Manufactured" Test Vehicles			"Rework" Test Vehicles	
	SnPb Paste	SAC305 Paste	SN100C Paste	SnPb Paste	Pb-Free Paste
BGA-225	84	98	100	100	100
CLCC-20	32	43	90	35	68
CSP-100	62	73	70	62	80
PDIP-20	98	92	100	88	96
QFN-20	0	21	20	8	10
TQFP-144	60	63	64	70	70
TSOP-50	62	73	86	77	80

Figure 11 shows when the components failed on Test Vehicle 74. The failures are color coded according to how many test minutes were required to cause the failure (red = 1 to 60 test minutes; orange = 61 to 120 minutes; yellow = 121 to 180 minutes; green = 181 to 240 minutes; blue = 241 to 300 minutes; purple = 301 to 360 minutes; pink = 361-420 minutes; and white =

421 to 480+ minutes). In general, the components tended to fail first down the centerline and along the edges of the test vehicle (near the wedgelocks). Therefore, the first component failures coincide with the regions of highest strain as shown in Figure 12.

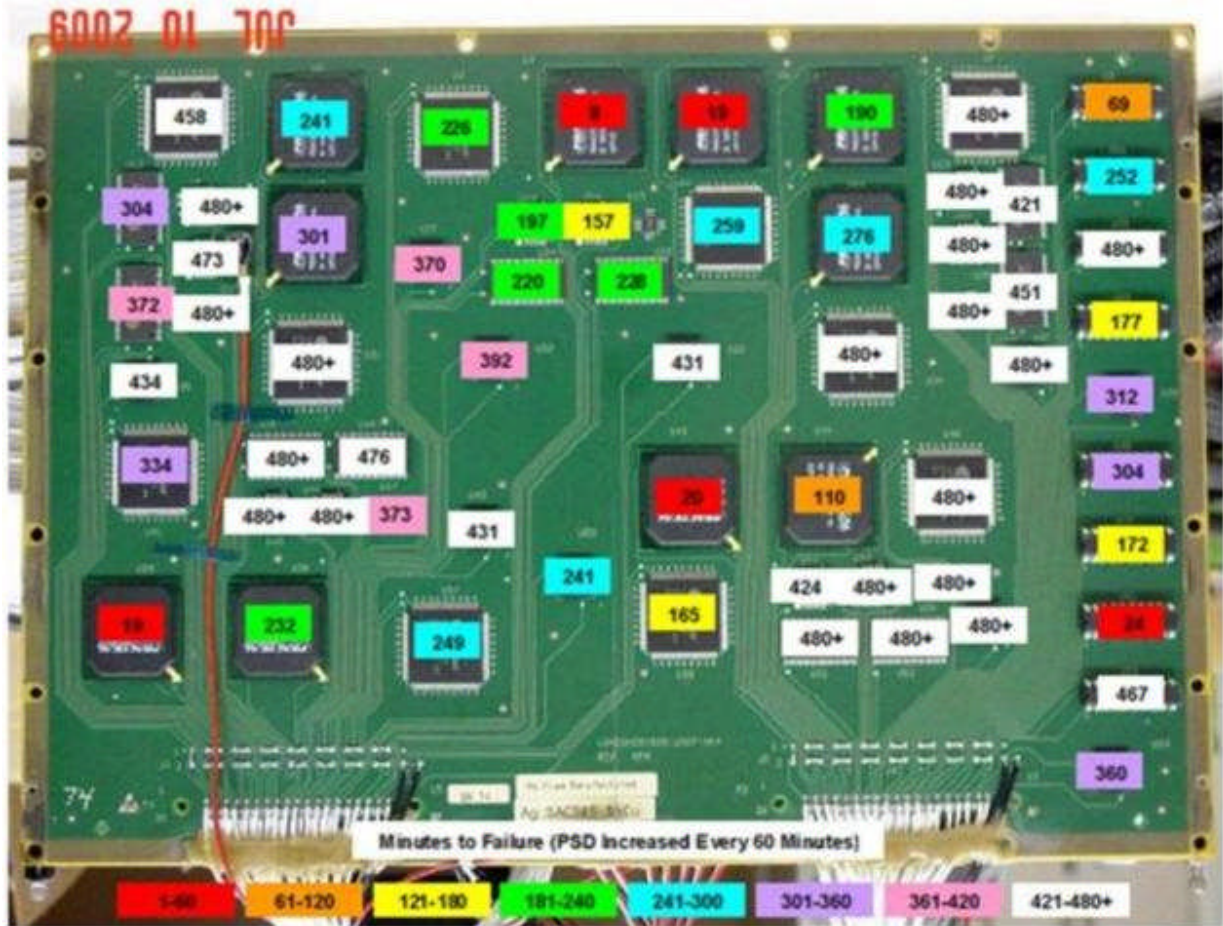


Figure 11 - Test Minutes Required for Components to Fail (Test Vehicle 74 Data)

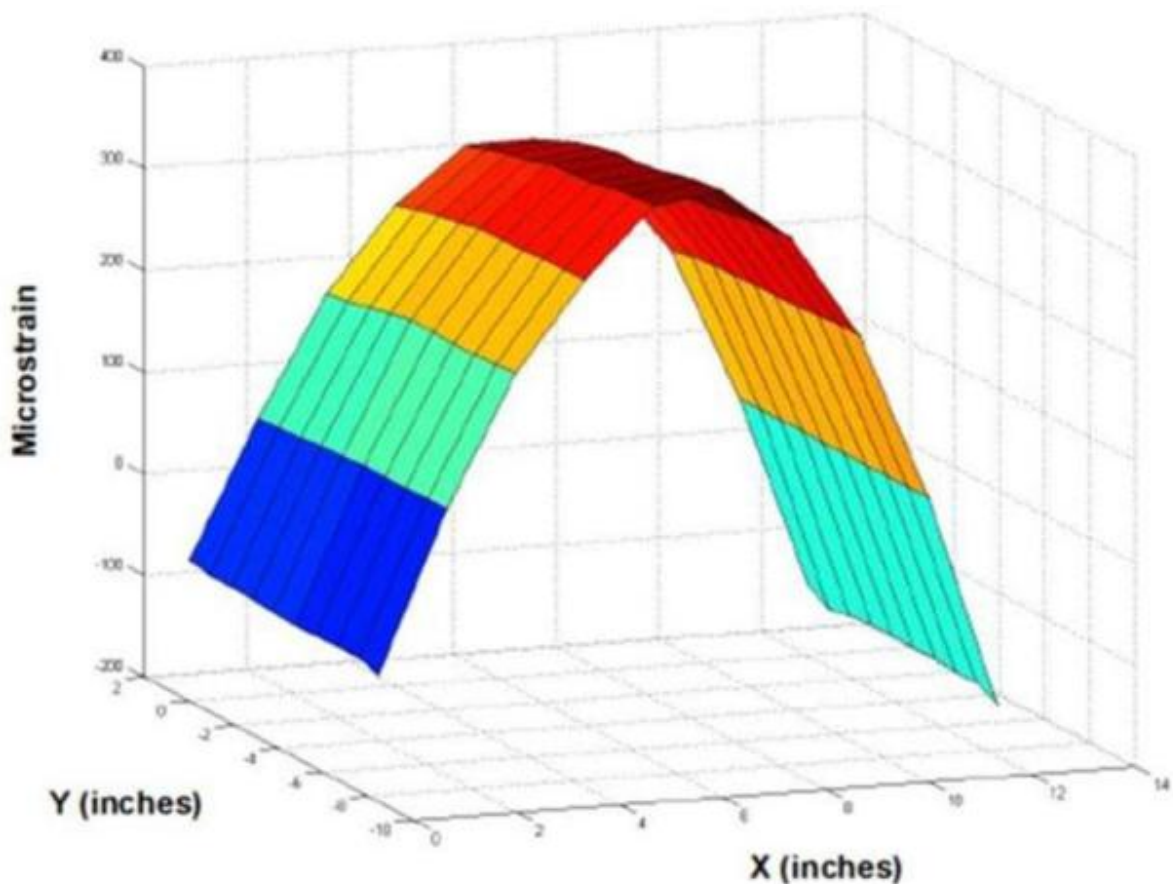


Figure 12 - Full Field Peak Strains at 65 Hz (1G Sine Dwell, Test Vehicle 74)

The overall results of the vibration testing are summarized in Table 11. If a solder alloy/component finish combination performed as well or better than the SnPb control, it was assigned the number “1” and the color “green”. Solders that performed worse than the SnPb control were assigned a “2” and the color “yellow”. Solders that performed much worse than the SnPb control were assigned a “3” and the color “red”.

The rankings in Table 11 are somewhat subjective due to the scatter in the data for some component types. The TSOP data was difficult to interpret since the orientation of the TSOP on the test vehicle appeared to influence how the solder/component finish combinations performed relative to the Sn37Pb/SnPb controls. Weibull plots were not used since the test conditions were changed during the test (i.e., the PSD was increased every 60 minutes) which renders the Weibull parameters meaningless.

Table 11 - Ranking of Solder Alloy/Component Finish Combinations

Relative Ranking (Solder Alloy / Component Finish)												
BGA-225	Sn37Pb/ Sn37Pb	SAC305/ SAC405	Sn37Pb/ SAC405	SAC305/ Sn37Pb	Rwk Flux Only/ Sn37Pb	Rwk Flux Only/ SAC405	Rwk Sn37Pb/SAC405 (SnPb Profile)	Rwk Sn37Pb/SAC405 (Pb-Free Profile)	SN100C/ SAC405			
	1	3	3	1	3	3	3	3	3			
CLCC-20	Sn37Pb/ Sn37Pb	SAC305/ SAC305	Sn37Pb/ SAC305	SAC305/ Sn37Pb	SN100C/ SAC305							
	1	3	2	3	3							
CSP-100	Sn37Pb/ Sn37Pb	SAC305/ SAC105	Sn37Pb/ SAC105	SAC305/ Sn37Pb	Rwk Flux Only/ Sn37Pb	Rwk Flux Only/ SAC105	Rwk Sn37Pb/SAC105 (SnPb Profile)	Rwk Sn37Pb/SAC105 (Pb-Free Profile)	SN100C/ SAC105			
	1	1	1	2	1	2	1	3	1			
PDIP-20	Sn37Pb/ SnPb	SN100C/ Sn	Sn37Pb/ NiPdAu	Rwk Sn37Pb/ Sn	Rwk Sn100C/ Sn	SN100C/ NiPdAu						
	1	3	2	3	3	3						
QFN-20	Sn37Pb/ Sn37Pb	SAC305/ Sn	Sn37Pb/ Sn	SAC305/ Sn37Pb	SN100C/ Sn							
	1	2	1	1	2							
TQFP-144	Sn37Pb/ Sn	SAC305/ Sn	Sn37Pb/ NiPdAu	SAC305/ NiPdAu	Sn37Pb/ Sn37Pb Dip	SAC305/ SAC305 Dip	SN100C/ Sn					
	1	1	1	2	1	2	1					
TSOP-50	Sn37Pb/ SnPb	Sn37Pb/ Sn	Sn37Pb/ SnBi	SAC305/ Sn	SAC305/ SnBi	SAC305/ SnPb	Rwk Sn37Pb/ SnPb	Rwk Sn37Pb/Sn (SnPb Profile)	Rwk Sn37Pb/Sn (Pb-free Profile)	Rwk SAC305/ SnBi	SN100C/ Sn	SN100C/ SnBi
	1	2*	2*	2*	2*	2	2	2*	2*	2	2	2
*Performance relative to Sn37Pb control may depend on orientation of the TSOP												
1 = as good as or better than Sn37Pb control				2 = worse than Sn37Pb control				3 = much worse than Sn37Pb control				

5.1.3 NSWC Crane Test Vehicle Vibration Testing Results Summary

The complete test report, “Vibration Testing Report for Crane; TOL0901051”, can be found on the NASA TEERM website (<http://teerm.nasa.gov>).

For this effort, 9 NSWC Crane test vehicles were subjected to vibration testing per the test method outlined in section 5.1. The vibration testing resulted in electrical failures in over 80% of all components; see Table 12 and Table 13 for details. In total, 63 components on each board were in-situ resistance monitored during the vibration testing. An average of 51 components failed electrically on each board.

Table 12 - Component Percentage Failure by Force Level

Vibration	Components Failed	%	Total %
8	51	9.0	9
10	45	7.9	16.9
12	43	7.6	24.5
14	39	6.9	31.4
16	39	6.9	38.3
18	59	10.4	48.7
20	73	12.9	61.6
28	111	19.6	81.1

Table 13 - Component Detachments

Vibration Level	Card	Components
20	79	U16
28	61	U16, U29
	62	U12, U16
	64	U16
	65	U7, U12, U16, U29
	66	U12, U16, U29
	67	U7, U12, U16, U29, U34
	79	U29

A comparison of the results of the testing on the as-manufactured components vs. the reworked components is shown in Table 14. This table shows the package style of the component and identifies each by its approximate location on the board, as well as the assigned reference designator. A summary of the manufacturing conditions is included for convenience.

For each test group, two statistics are included. These are the average time to failure in minutes, T_f , and the standard deviation of the time to failure, also in minutes. These statistics are shown for both the as-manufactured and the reworked conditions. In Table 14, any samples which did not fail have been assigned a T_f of 480 minutes, the time at which the test was suspended. This decision was made to prevent skewing the data toward earlier failure times.

Table 14 - Results of Testing on As-Manufactured and Reworked Components

	Zone Site		Manufactured Conditions			As-Manufactured		1 st SnPb Rework		Statistics		
			Solder	Lead	Board	Average Tf	Standard Deviation	Average Tf	Standard Deviation	F-Test	P-Value	Variance Check
CLCC-20	1	U52	SAC305	SAC305	ImAg	360	162	446	19	1.39	0.2763	0.001
	2	U45	SAC305	SAC305	ImAg	465	25	457	27	0.2	0.6654	0.9
	2	U46	SAC305	SAC305	ImAg	451	26	431	54	0.56	0.4793	0.215
	2	U53	SAC305	SAC305	ImAg	465	12	456	29	0.39	0.5533	
PDIP-20	3	U59	SN100C	NiPdAu	ImAg	480	0	480	0	NA	NA	NA
	3	U23	SN100C	Sn	ImAg	480	0	480	0	NA	NA	NA
	3	U30	SN100C	Sn	ImAg	150	197	158	91	0.01	0.9378	0.237
	3	U38	SN100C	Sn	ImAg	162	213	462	25	7.78	0.0316	0.005
QFN-20	1	U47	SAC305	Sn	ImAg	347	48	401	39	1.3	0.2762	0.632
	2	U27	SAC305	Sn	ImAg	480	0	477	4.5	1.3	0.2924	NA
	2	U28	SAC305	Sn	ImAg	480	0	445	32	5.47	0.047	NA
	2	U54	SAC305	Sn	ImAg	480	0	480	0	NA	NA	NA
TQFP-144	1	U57	SAC305	Sn	ImAg	271	101	310	21	0.74	0.4172	0.012
	1	U58	SAC305	Sn	ImAg	220	54	251	35	0.96	0.359	0.462
	2	U48	SAC305	Sn	ImAg	439	5	344	111	3.83	0.0914	0.00005
	3	U41	SAC305	Sn	ImAg	392	56	440	32	2.54	0.1553	0.352
TSOP-50	1	U61	SAC305	Sn	ImAg	439	5	344	111	3.87	0.0899	0.002
	2	U39	SAC305	Sn	ImAg	457	20	439	29	1.18	0.313	0.566
	2	U62	SAC305	SnBi	ImAg	472	11	351	158	0.1284	2.97	0.0002
	3	U26	SAC305	SnBi	ImAg	362	55	360	53	0	0.9571	0.709

In order to determine whether a significant change occurred between the two conditions, an F-test was performed on the data. The results are shown, along with the associated p-value. Any case where the p-value is less than 0.05 (5%), can be considered significant at the 95% level. For significant results we can conclude that the shift in the means between the two conditions is distinguishable from one another. In the other cases, we do not have enough evidence to reject the hypothesis that the means are the same. Figure 13 shows a graph of the actual differences between the test groups. In this graph, the vertical axis shows the delta Tf, or the Tf of the reworked samples minus the Tf for the as-manufactured samples. If the delta Tf is positive, the average Tf for the reworked samples was higher than the average Tf for the as-manufactured parts. If the delta Tf is negative, the average Tf for the reworked samples was lower than the average Tf for the as-manufactured parts.

Looking at Figure 13, overall, it appears that rework had minimal effect in most cases. There are only five sets of tests where the absolute value of the delta Tf was 75 or larger. In two cases, the CLCC-20 and PDIP-20, the delta Tf was positive, and for three others, aTQFP-144 and two TSOP-50s, it was negative.

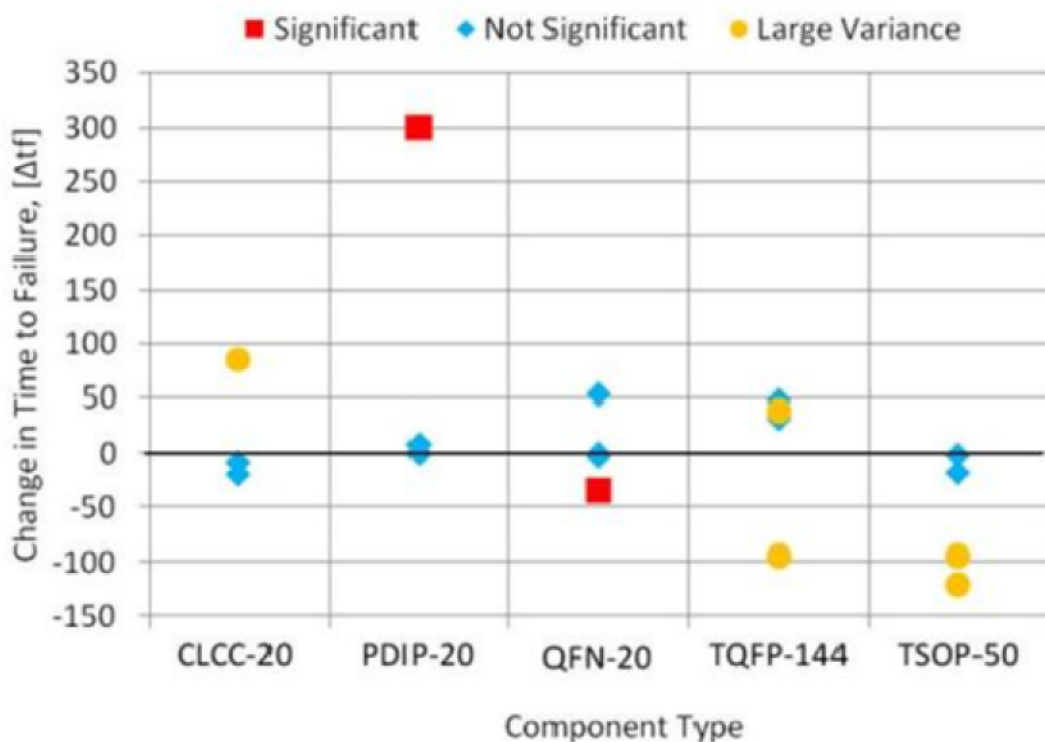


Figure 13 - The difference in average time to failure for each component type when comparing as-manufactured parts to reworked parts. A positive change indicates an increased time to failure after rework.

Starting with the cases where the reworked samples failed more quickly, there were two test runs where the reworked TSOP-50s did not perform as well as samples in the as-manufactured condition. In one run, the reworked parts failed 121 minutes earlier. This was U62, and the difference can be attributed to one outlier; an early life failure on just one reworked sample. Another TSOP, U61 failed an average of 95 minutes earlier after rework. The test results are shown in Figure 14.

Figure 14 is shown as a box and whisker plot. The box is an icon which covers the middle half of the data. The whiskers extend out the minimum and maximum data points. The middle blue line is the median or middle data point.

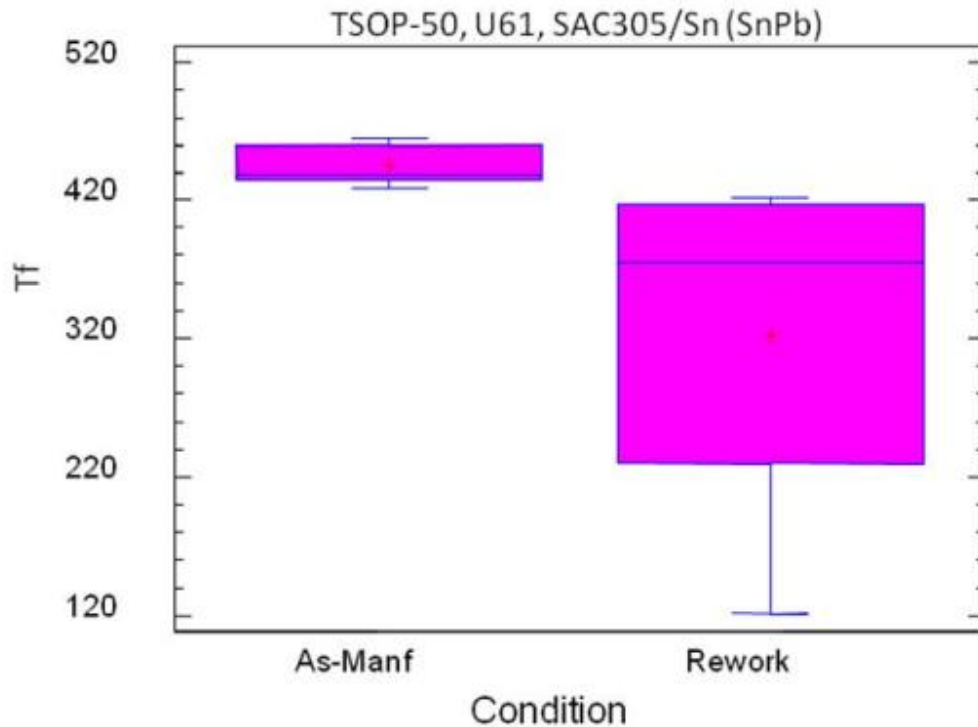


Figure 14 - Test results for U61, in the As-Manufactured Condition and after Rework

The final case is a TQFP-144, U48, which failed 95 minutes quicker after rework than before. In this test run, the as-manufactured components had an average Tf of 439 minutes, while the reworked components had a Tf of 344 minutes.

In two cases, the reworked samples lasted much longer than as-manufactured samples. The most extreme example was a test run where PDIP-20, U38, lasted 300 minutes longer after rework. A graph of the results is shown in Figure 15.

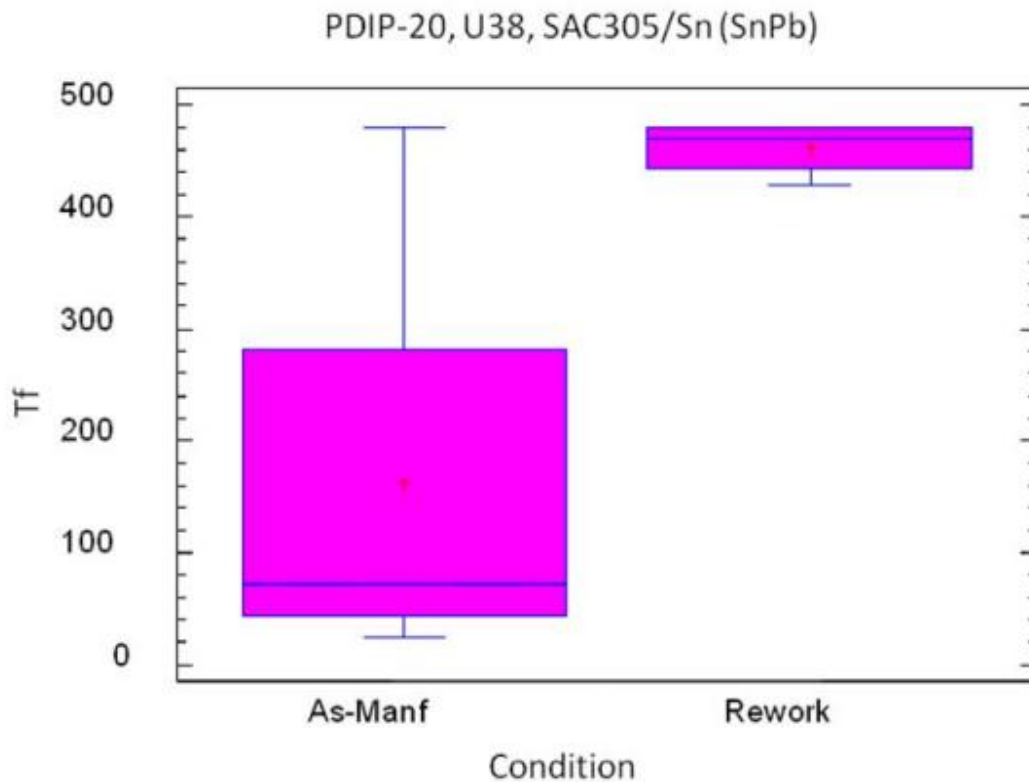


Figure 15 - Results of PDIP-20, U38 in As-Manufactured Condition and after Rework

These extreme results are due to three early life failures of the as-manufactured components, all failing in the first 80 minutes. The final as-manufactured sample survived the test, operating successfully after 480 minutes.

Finally, a CLCC-20, U52, lasted 82 minutes longer after rework than the as-manufactured samples. Reviewing the data, this is due to one early life failure in the as-manufactured samples. Reviewing the F-test results, there were only two cases where the differences between the “as-manufactured” and “reworked” test conditions were large enough to be statistically significant. These are denoted with red boxes on Figure 16. In all other cases, the results were not significant. Since statistical significance is a relative benchmark, this may be due to one of several factors. One factor is the difference in response between the test conditions, or the time to failure, in our case. If the difference is not large enough, the results will not be significant. Another factor is sample size. With more samples, the test will be more sensitive to smaller differences in the response. In our case, we had relatively few samples, four per test group in some cases. In order to maintain the significance level of 95%, fewer samples meant that the power of the test would be decreased. The final factor is unexplained variation in the data. It is harder to detect a “signal” in the data if there are high levels of “noise.” We have mentioned several outliers, unusual results, and dispersion of the results.

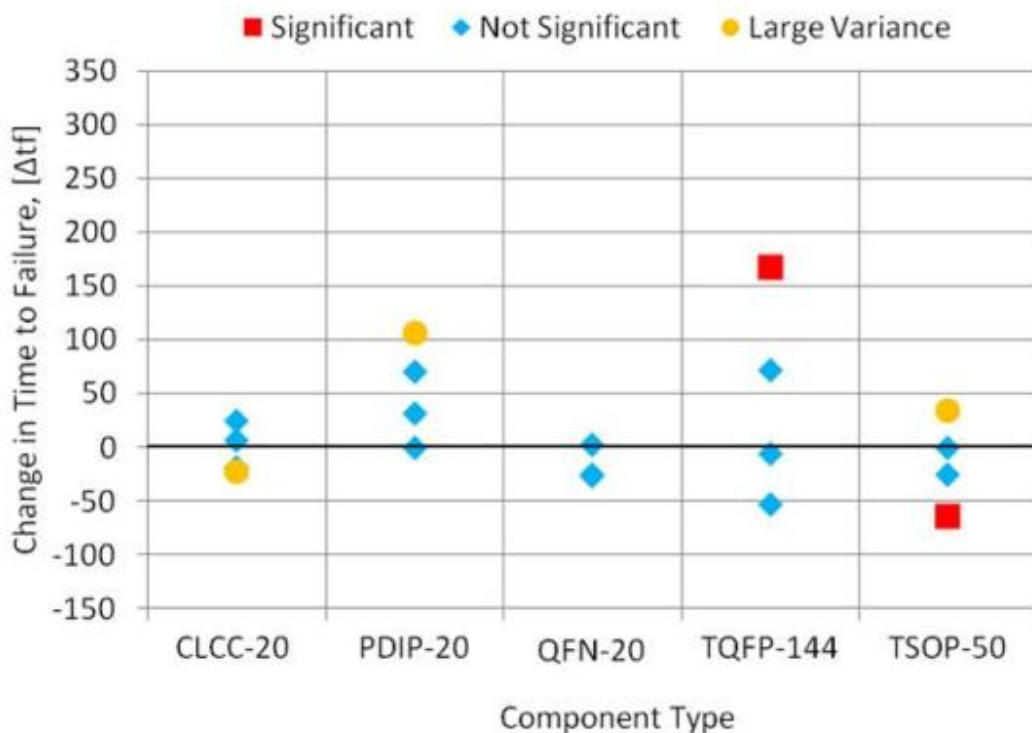


Figure 16 - The difference in average time to failure for each component type when comparing the 1st SnPb rework to the 2nd SnPb rework. A positive change indicates an increased time to failure after the 2nd rework.

Another potential “noise” problem is large differences in variation between sample test groups. When we performed the F-tests, we tested for differences in the variation between the groups using Bartlett’s Test. The p-values for the variance check are shown in Table 15. Cases where the p-value is less than 0.05 (5%) show that there is a significant difference in the variation between the sample test groups. The significant results are shown as circles on Figure 16. Difference in variation between the test groups can distort the F-test results.

Table 15 - Results of Tests on Components Reworked Once vs. Twice

	Zone Site		Manufactured Conditions			1st Rework		2nd Rework		Statistics		
			Solder	Component	Board	Average Tf	Standard Deviation	Average Tf	Standard Deviation	F-Test	P-Values	Variance Check
CLCC-20	2	U10	SAC305	SAC305	ImAg	407	44	413	72	0.02	0.8849	0.404
	2	U22	SAC305	SAC305	ImAg	421	45	446	37	0.86	0.3821	0.75
	3	U09	SAC305	SAC305	ImAg	417	10	394	69	0.44	0.532	0.011
	3	U17	SAC305	SAC305	ImAg	480	0	461	38	1.3	0.294	NA
PDIP-20	3	U51	SN100C	NiPdAu	ImAg	323	190	393	128	0.31	0.5989	0.57
	3	U08	SN100C	Sn	ImAg	368	223	475	9	0.92	0.3746	0.0003
	3	U11	SN100C	Sn	ImAg	480	0	480	0	NA	NA	NA
	3	U49	SN100C	Sn	ImAg	75	87	106	124	0.13	0.7303	0.63
QFN-20	1	U15	SAC305	Sn	ImAg	117	48	90	49	0.67	0.4386	0.979
	2	U27	SAC305	Sn	ImAg	478	5	480	0	1.3	0.2924	NA
	2	U28	SAC305	Sn	ImAg	446	33	421	36	1.19	0.3116	0.867
TOFP-144	2	U07	SAC305	Sn	ImAg	258	95	330	44	2.36	0.1681	0.185
	2	U31	SAC305	Sn	ImAg	422	42	416	27	0.07	0.8049	0.472
	2	U34	SAC305	Sn	ImAg	213	145	380	11	6.78	0.0375	0.0002
	3	U01	SAC305	Sn	ImAg	377	33	324	73	2.13	0.1877	0.174
TSOP-50	1	U25	SAC305	Sn	ImAg	170	14	145	43	1.56	0.2517	0.07
	3	U29	SAC305	Sn	ImAg	394	71	428	17	1.07	0.3344	0.023
	2	U40	SAC305	SnBi	ImAg	381	12	317	46	7.15	0.0318	0.048
	3	U16	SAC305	SnBi	ImAg	386	28	385	34	0	0.9681	0.755

Out of the 9 test vehicles tested, 33 parts representing electrical failures were selected for cross-section analysis. Test vehicles were submitted to Celestica's Performance Innovation Laboratories for physical failure analysis. The cross-sections revealed a high degree of damage throughout the solder joints. This damage occurred across all cross-sectioned parts and did not seem to correlate to the part type, location on the board or type of solder, i.e. no significant difference between the Pb-free (non-reworked) parts and the reworked SnPb parts.

5.1.3.1 CLCC Components

All of the tested CLCC-20s had SAC305 component finish. None of these solder joints were reworked. Solder cracks we observed around every solder joint. The cross sections of all CCLC-20 packages were performed on corner pads. Each cross section revealed cracking across the length of the solder, see Figure 17. SN67 also showed voiding, in this case the crack traveled along the void, see Figure 18.

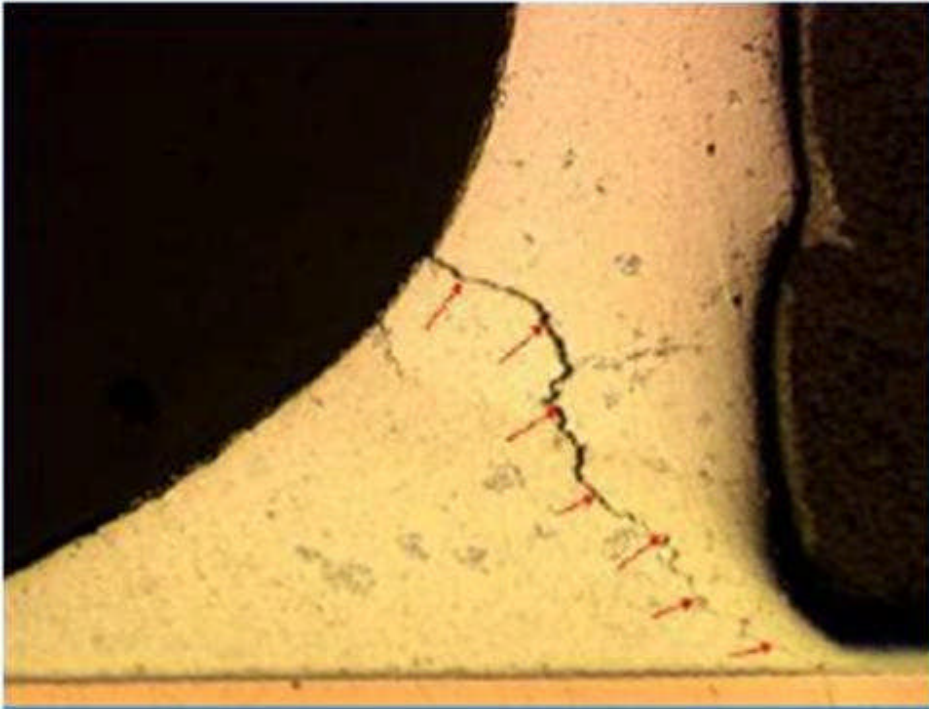


Figure 17 - SN63 U52, Left Side Pad

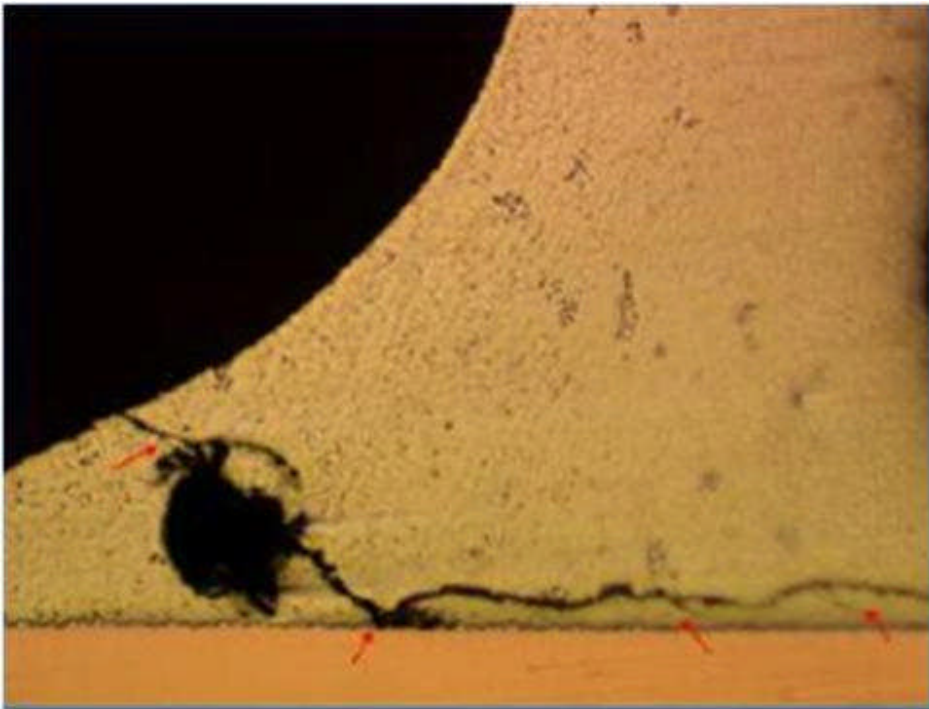


Figure 18 - SN67 U52, Left Side Pad

5.1.3.2 QFN Components

All of the QFN-20 packages were fabricated using Sn finish and were exposed to one or two reworks with SnPb solder. Approximately half of the solder joints exhibited cracks which ran along the component pad. There does not appear to be a correlation between the cracked solder and the number of re-work cycles to which the part was exposed. Cross sections of the QFN-20 packages reveal that the cracks propagated along the component pad, see Figure 19 and Figure 20.

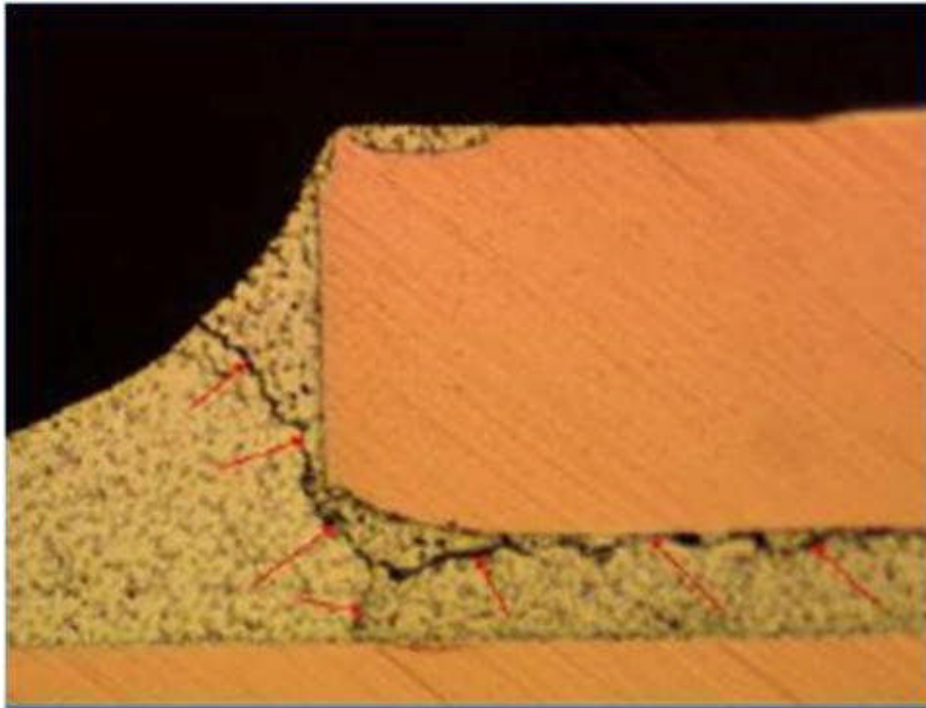


Figure 19 - SN63 U54, Left Side Pad

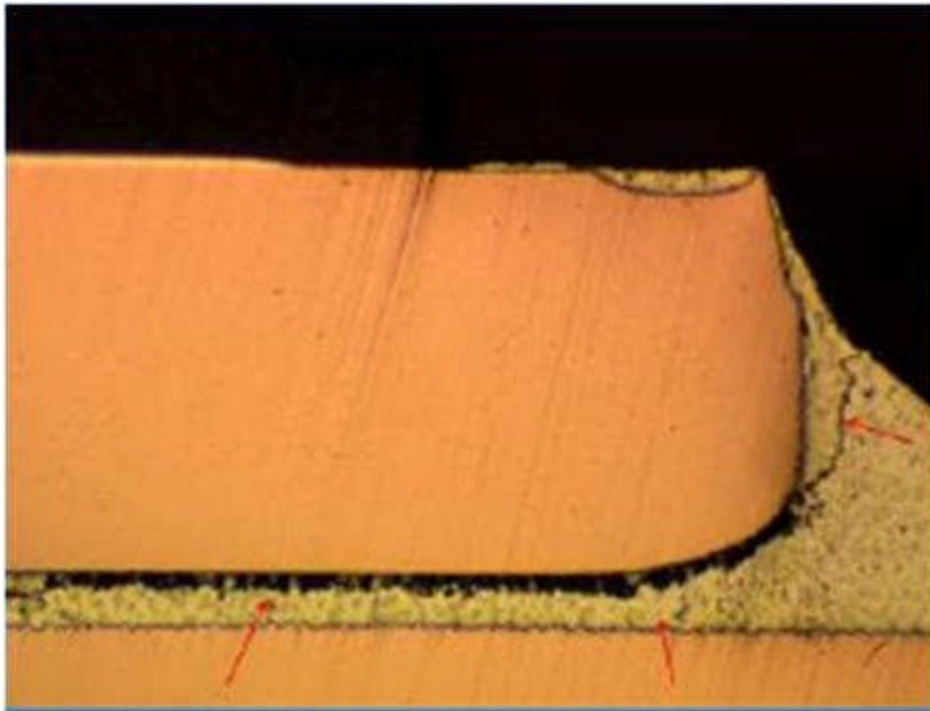


Figure 20 - SN68 U28, Right Side Pad

5.1.3.3 TQFP Components

All of the TQFP-144 packages were fabricated using Sn finish on the leads, and four of the nine were exposed to one or two re-work cycles with SnPb solder. All of the solder joints experienced significant cracking. Additionally, eight leads broke, all corresponding to components that did not undergo any re-work and therefore contained only Pb-free solder.

Cross-sectioning revealed cracks in the actual copper leads of the TQFP-144 packages. This damage was observed only on parts which were not reworked and therefore the solder joint was Pb-free. This is to be expected as the Pb-free solder is stiffer than the SnPb solder and transfers the stress to the weaker copper leads. Figure 21 and Figure 22 illustrate TQFP-144 packages which were not reworked and therefore contain only Pb-free solders.

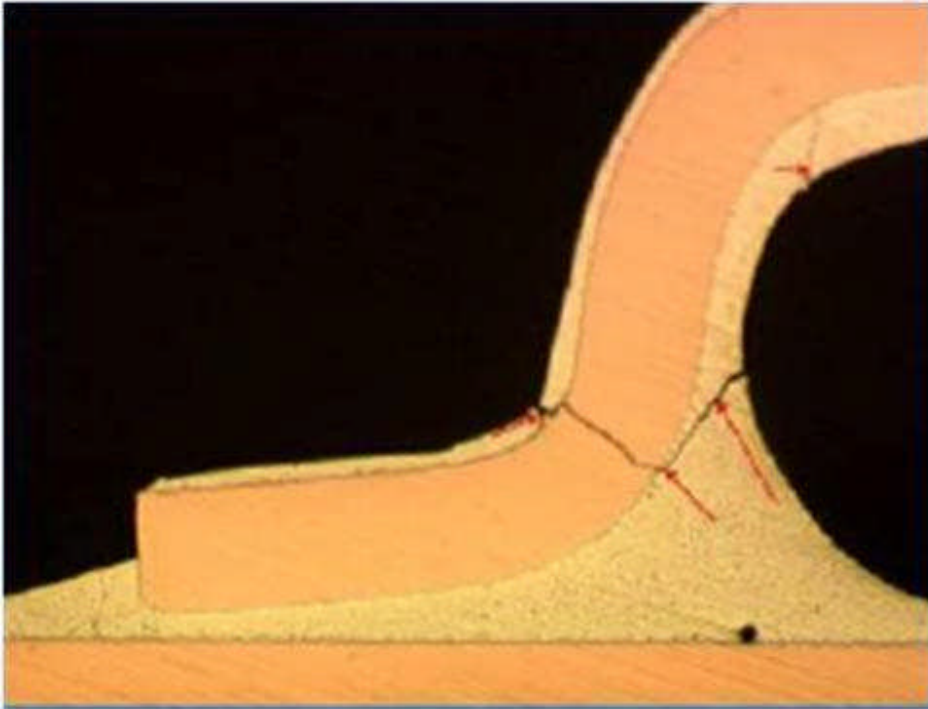


Figure 21 - SN63 U41. Left Lead

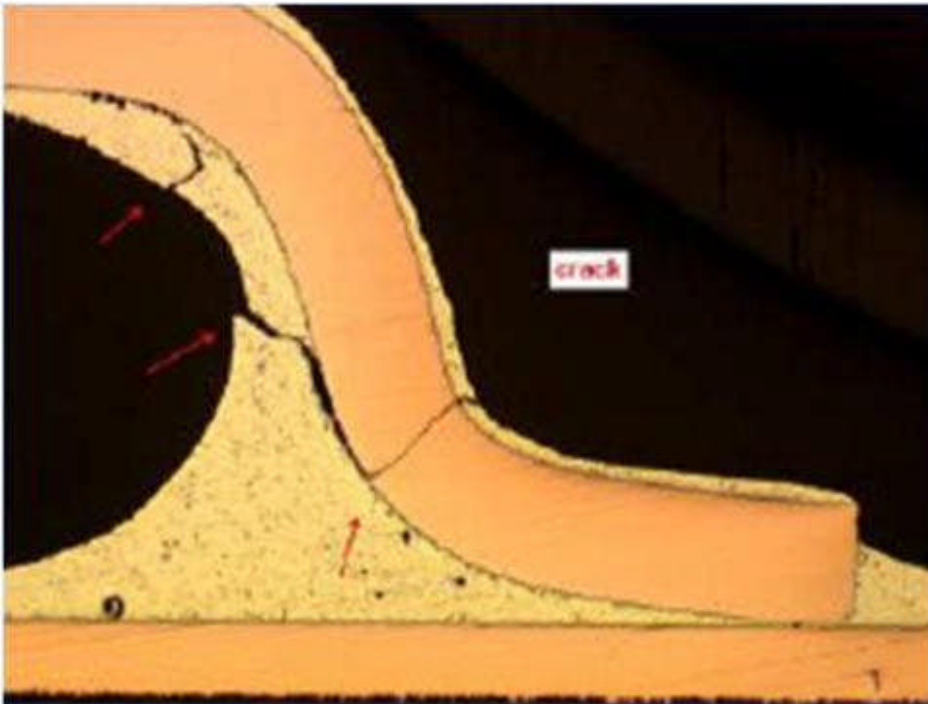


Figure 22 - SN61 U20 Right Lead

Cross-sections of TQFP-144 packages which were re-worked, either once or twice, revealed cracked solder joints in all cases. However, all of the leads on these samples survived see Figure 23 and Figure 24.

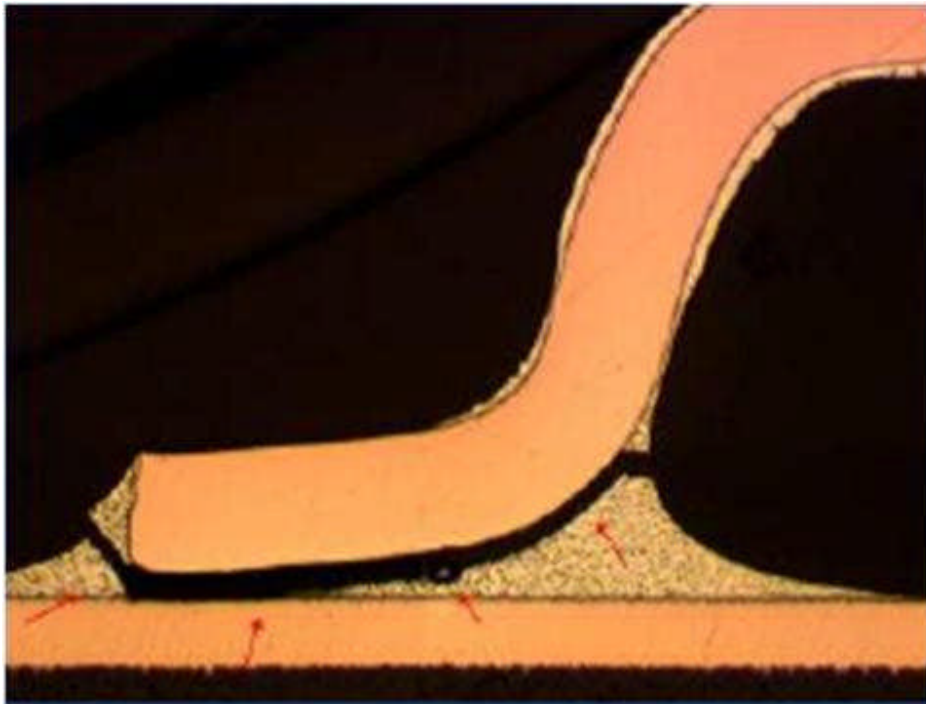


Figure 23 - SN67 U31 Left Lead

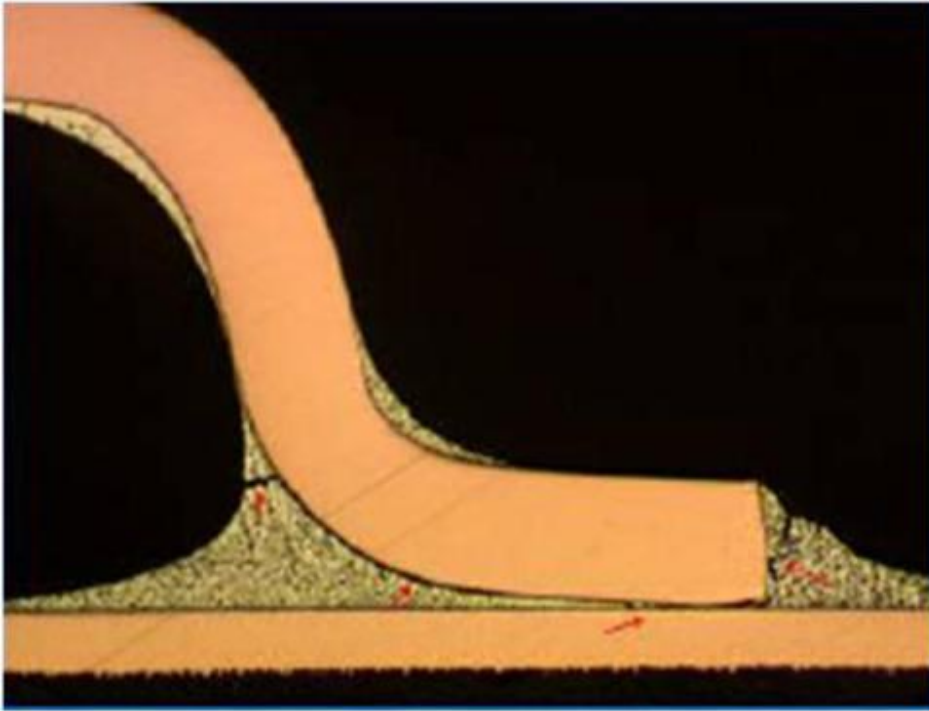


Figure 24 - SN68 U31, Right Lead

5.1.3.4 TSOP Components

Of the twenty one TSOPs tested, seven fell off of the board during the vibration test and were therefore not cross sectioned. All of these parts were in an area closest to the edge of the board. Among the cross sectioned parts, all of the leads remained intact however almost all of the solder joints experienced significant cracking. The TSOPs had finishes of either Sn or SnBi, and two thirds were re-worked either one or two times using SnPb solder. There does not appear to be any correlation between the lead finish or the number of re-works with the incident of cracking in the solder joint.

SN79 U12 (Figure 25) and SN66 U62 (Figure 26) are examples of TSOPs which did not undergo any re-work. They have Sn and SnBi finishes respectively. Both experienced severe solder joint cracking on both sides of the component.

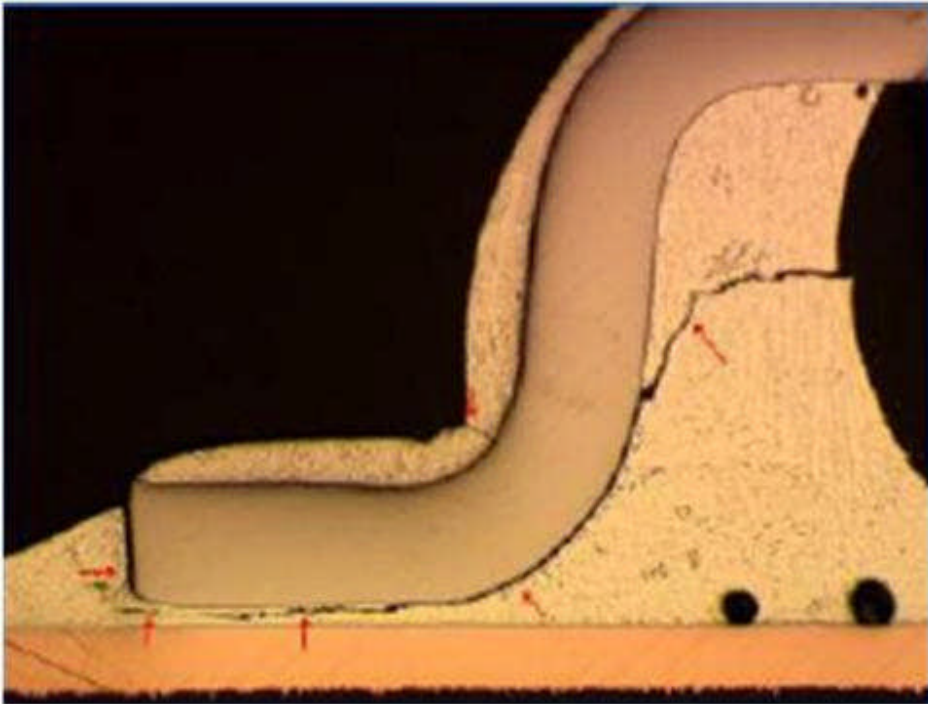


Figure 25 - SN79 U12, Left Lead

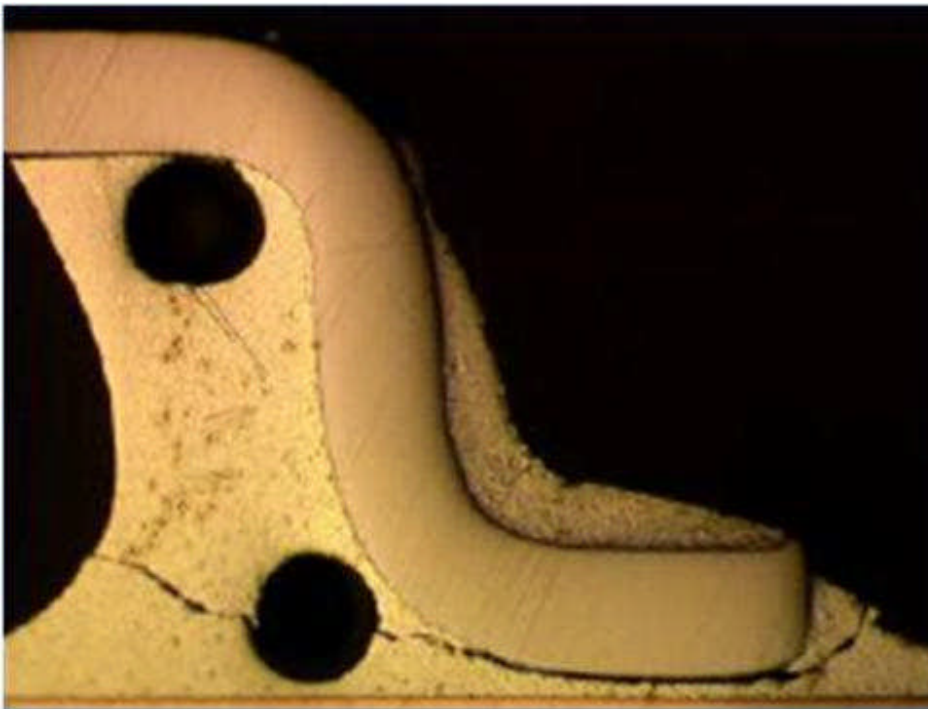


Figure 26 - SN66 U62, Right Lead

SN65 U62 (Figure 27) and SN63 U61 (Figure 28) are examples of parts which underwent one rework cycle with SnPb solder. They have Sn and SnBi finishes respectively and both components

showed significant cracking within the solder at both sides of the component. This is consistent with all parts which have undergone one re-work cycle.

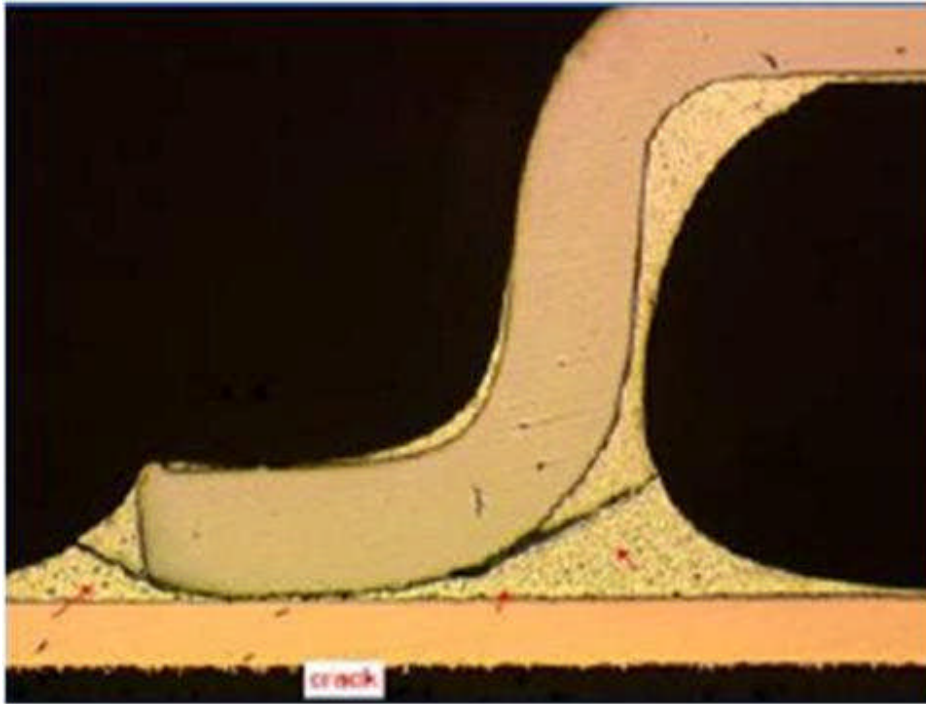


Figure 27 - SN65 U62, Left Lead

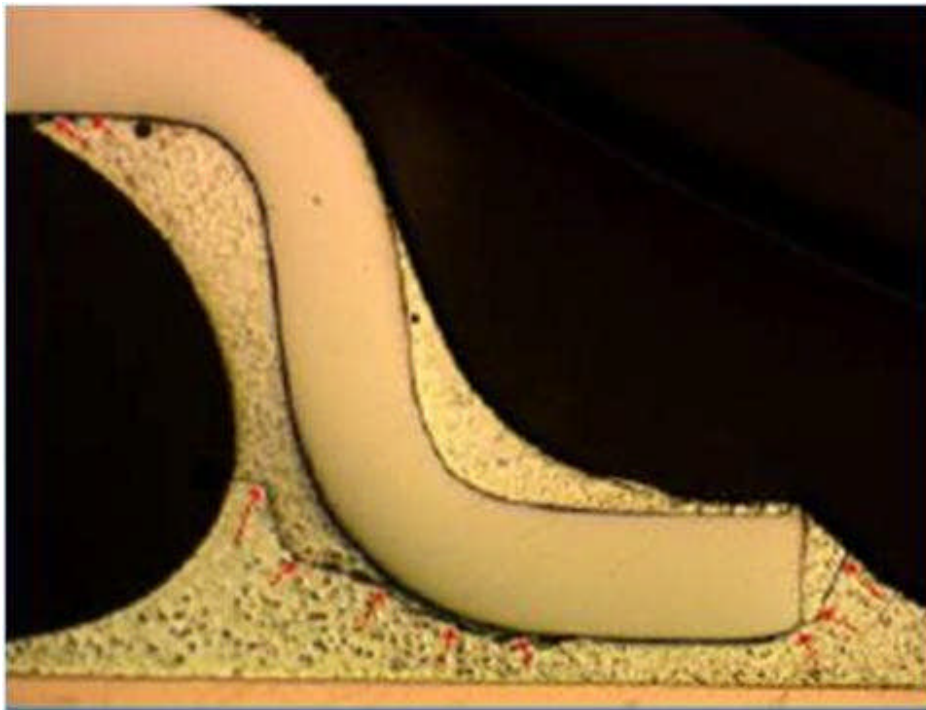


Figure 28 - SN63 U61, Right Lead

SN63 U16 (Figure 29) and SN68 U29 (Figure 30) were both re-worked twice with SnPb solder. SN63 U16 is finished with SnBi and SN68 U29 is finished with Sn. The SnBi part experienced extensive solder cracking through-out. The Sn finished part experienced solder cracking at one side of the component.

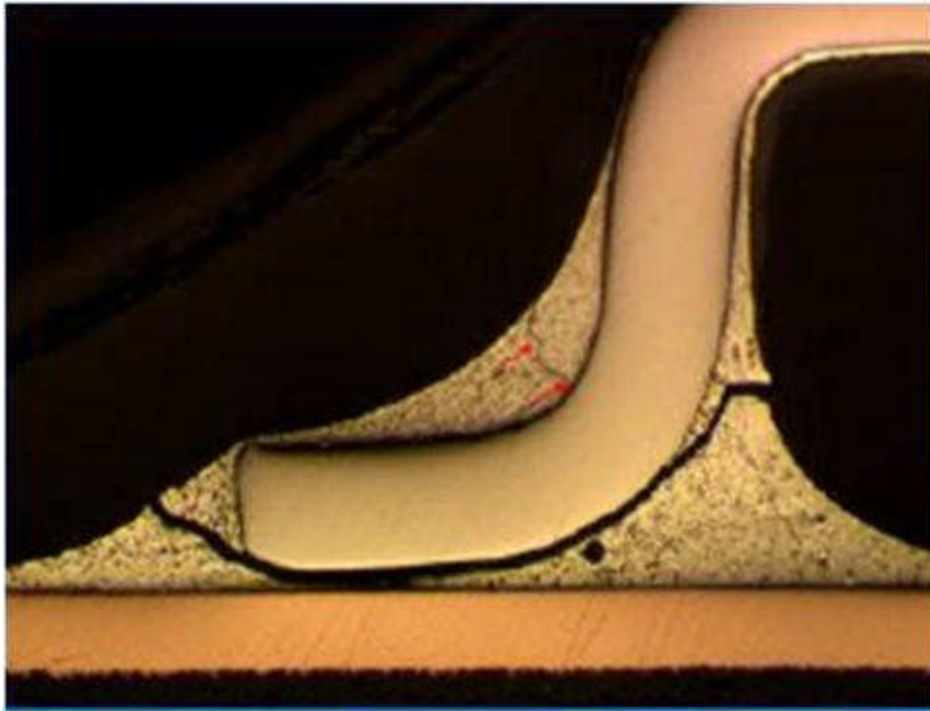


Figure 29 - SN63 U16, Left Lead

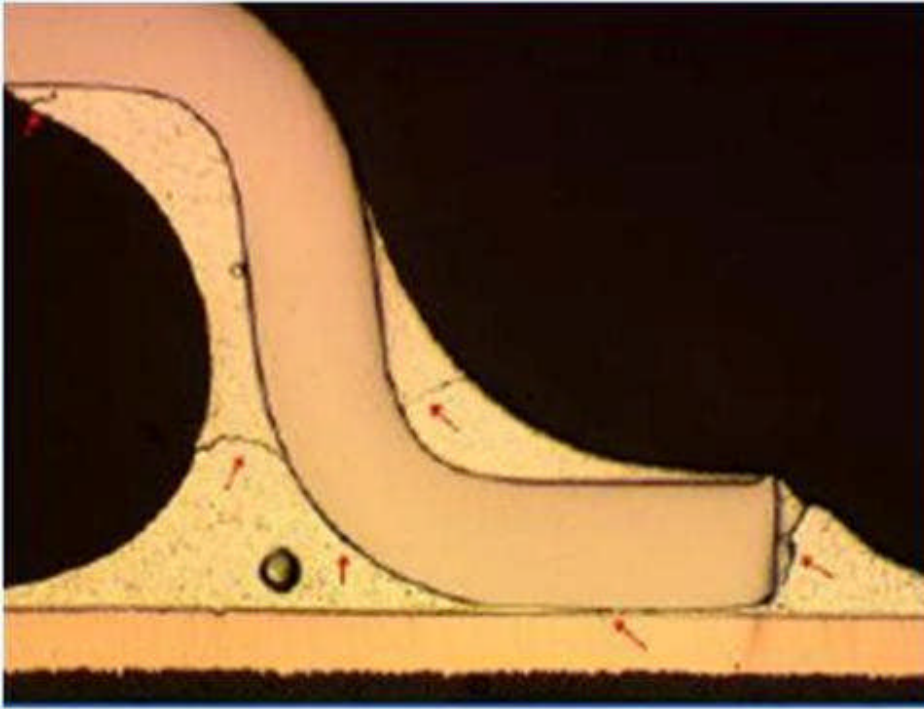


Figure 30 - SN68 U29, Right Lead

Based on the limited number of cross-section completed, there does not appear to be a correlation between component lead finish and the damage to the leads or bulk solder. The TQFPs show some correlation to number of re-work cycles and damaged leads, as only those leads which did not undergo any re-work broke. As the re-work solder was SnPb, this would indicate that the leads with Pb-free solder joints broke, while those with some Pb in the solder survived.

5.2 Mechanical Shock Test

5.2.1 Mechanical Shock Test Method

The purpose of this test was to determine the resistance of solders to the stresses associated with high-intensity shocks. Testing was performed in accordance with the requirements specified in MIL-STD-810F (with modifications). A step stress shock test was performed to maximize the number of failures generated which allowed comparisons of solder reliability.

The test vehicles were mounted in a fixture on an electro-dynamic shaker. The required shock response spectrum (SRS) was programmed into the digital shock controller which in turn generated the required transient shock time history.

Testing followed MIL-STD-810F, Method 516.5 with the following modifications: (1)100 shocks applied per test level (rather than 3) and all of the shocks applied in the Z-axis, and (2) the shock transients applied at the levels specified in MIL-STD-810F, Method 516.5 for the Functional Test for Flight Equipment, the Functional Test for Ground Equipment, and the Crash Hazard Test for Ground Equipment followed the modified parameters given in Table 16. Additional step stress test was then conducted (per Table 16 and Figure 31) with the shocks being applied in the Z-axis only. For Level 6 (300 G's), 400 shocks were applied instead of 100. Testing continued until a majority (approximately 63 percent) of components failed. Shock levels, pulse durations and/or frequencies may be modified during testing based on the actual capabilities of the electrodynamic shaker used.

The test SRS shall be within +3dB and -1.5dB of the nominal requirement over a minimum of 90% of the frequency band when using a 1/12-octave analysis bandwidth. The remaining 10% of the frequency band shall be within +6dB and -3dB of the nominal requirement.

The electrical continuity of the solder joints was continuously monitored during the test. All test results were recorded.

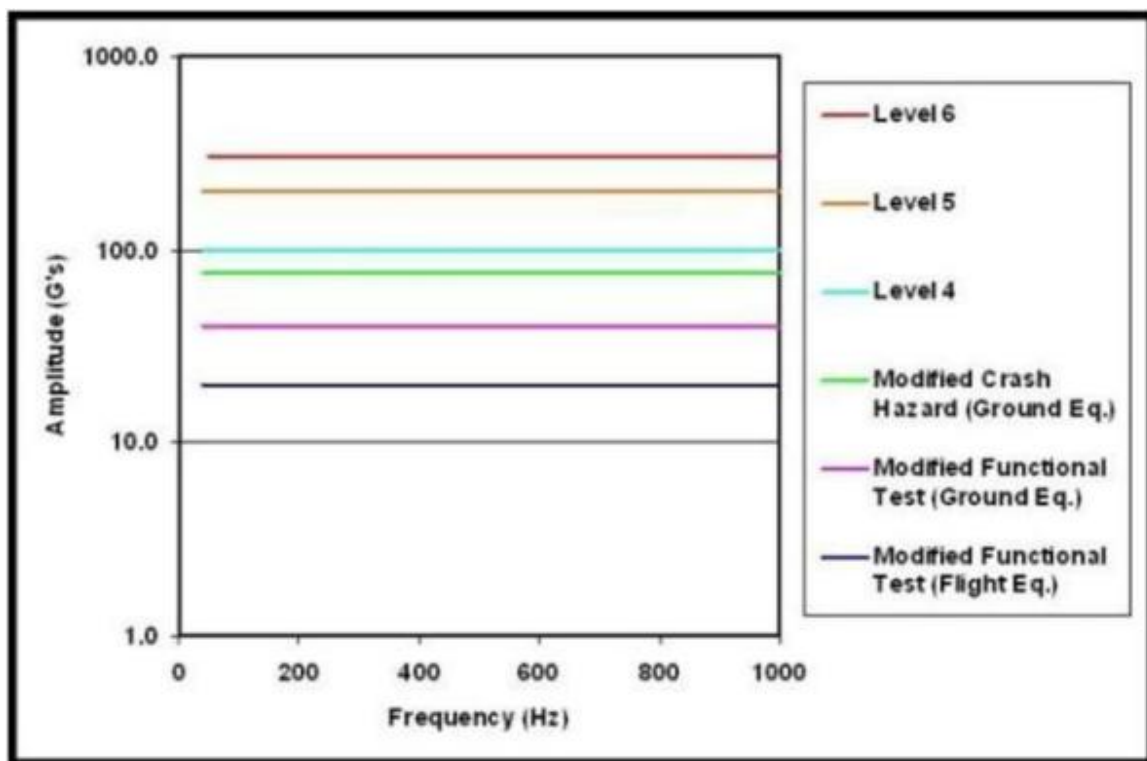


Figure 31 - Mechanical Shock SRS Test Levels

Table 16 - Mechanical Shock Test Methodology – Test Procedure

Parameters	The shock transients were applied perpendicular to the plane of the board and were increased after every 100 shocks (i.e., a step stress test). For Level 6 (300 G's), 400 shocks were applied. Frequency range is 40 to 1000 Hz. SRS damping: 5%			
	Test Shock Response Spectra	Amplitude (G's)	Te (msec)	Shocks per Level
	Modified Functional Test for Flight Equipment (Level 1)	20	<30	100
	Modified Functional Test for Ground Equipment (Level 2)	40	<30	100
	Modified Crash Hazard Test for Ground Equipment (Level 3)	75	<30	100
	Level 4	100	<30	100
	Level 5	200	<30	100
	Level 6	300	<30	400
Number of Test Vehicles Required				
Mfg. SnPb = 5		Mfg. LF = 5		
Rwk. SnPb = 5	Rwk. SnPb {ENIG} = 1		Rwk. LF = 5	
Trials per Specimen		1		

5.2.2 Mechanical Shock Testing Results Summary

The complete test report, “NASA-DoD Lead-Free Electronics Project: Mechanical Shock Test”, can be found on the NASA TEERM website (<http://teerm.nasa.gov>).

The overall results of the mechanical shock testing are summarized in Table 17. If a solder alloy/component finish combination performed as well or better than the SnPb control, it was assigned the number “1” and the color “green”. Solders that performed worse than the SnPb control were assigned a “2” and the color “yellow”. For those cases where both the SnPb controls and a Pb-free solder had few or no failures after 900 shock pulses, they were not ranked.

The rankings in Table 17 are somewhat subjective since the data for some component types contained a lot of scatter and other component types had few failures which complicated the ranking process. In addition, if some of the component/solder combinations had only a few early failures, these failures did not count in the ranking process.

In general, the pure Pb-free systems (SAC305/SAC405 balls, SAC305/SAC105 balls, SAC305/Sn, and SN100C/Sn) performed as well or better than the SnPb controls (SnPb/SnPb or SnPb/Sn).

For mixed technologies, SnPb solder balls combined with SAC305 paste (and reflowed with a Pb-free profile) performed as well as the SnPb controls on both the BGA's and the CSP's. In

contrast, SnPb solder paste combined with either SAC405 or SAC105 balls (and reflowed with a SnPb thermal profile) underperformed the SnPb/SnPb controls.

Rework operations on the PDIP's and TSOP's reduced the reliability of both the SnPb and the Pb-free solders when compared to the unreworked SnPb/SnPb controls. In contrast, rework of SnPb and SAC405 BGA's and SAC105 CSP's using flux only gave equivalent performance to the unreworked SnPb/SnPb controls. Pb-free BGA's reworked with SnPb paste and SAC405 balls (and a Pb-free thermal profile) were also equivalent to the SnPb controls.

Table 17 - Shock Testing; Relative Ranking (Solder/Component Finish)

Relative Ranking (Solder Alloy / Component Finish)										
	Sn37Pb/ Sn37Pb	SAC305/ SAC405	Sn37Pb/ SAC405	SAC305/ Sn37Pb	Rwk Flux Only/ Sn37Pb	Rwk Flux Only/ SAC405	Rwk Sn37Pb/SAC405 (SnPb Profile)	Rwk Sn37Pb/SAC405 (Pb-Free Profile)		
BGA-225	1	1	2	1	1	1	2	1		
CLCC-20	1	2	2	2						
CSP-100	1	1	2	1	2	1	2	2		
PDIP-20	1	1	1	2	2					
QFN-20	X	X	X	X						
TQFP-144	1	1	1	1	1	2				
TSOP-50	X	X	X	X	X	X	2	2	2	2
X = Not enough failures to rank										
1 = as good as or better than Sn37Pb control					2 = worse than Sn37Pb control			3 = much worse than Sn37Pb control		

5.2.2.1 BGA Components

Many of the BGA failures (SnPb/SnPb balls, SAC305/SAC405 balls, and mixed technologies) were due to pad cratering. This suggests that Pb-free laminates may be the weakest link for large area array components.

Microsections made at the end of Mechanical Shock Testing showed that the corner solder joints failed first. The SnPb/SnPb sections showed pad cratering, PWB trace cracking, and solder joint cracking on the component side (Figure 32).

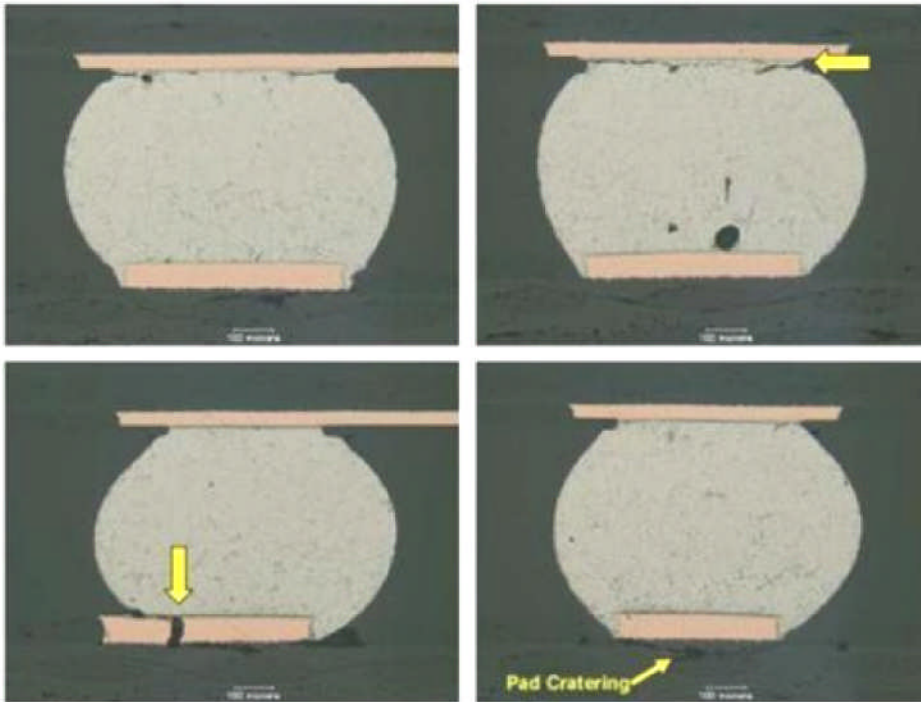


Figure 32 - Test Vehicle 34 - Four Corner Balls of BGA U6 (SnPb Solder/SnPb Balls)

The SAC305/SAC405 sections showed PWB trace cracking and solder joint cracking at the component side intermetallic layer (Figure 33). Which failure mechanism occurred first could not be determined from the microsections.

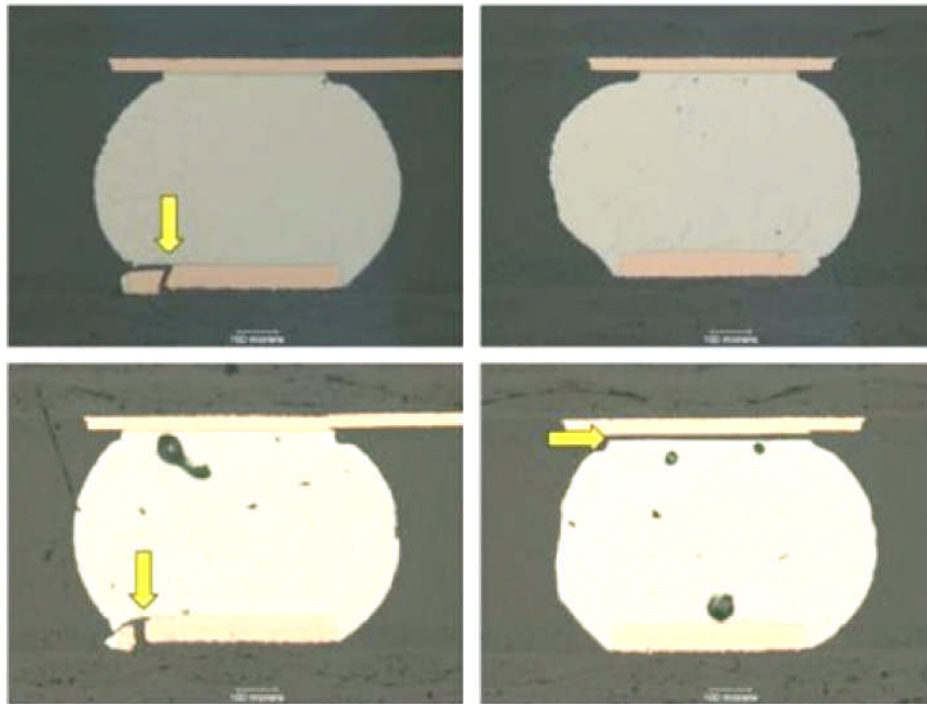


Figure 33 - Test Vehicle 89 - Four Corner Balls of BGA U2 (SAC305 Solder/SAC405 Balls)

A number of BGA's fell off of the test vehicles during the shock test which allowed the failure mechanisms to be examined more closely.

Surprisingly, on the SnPb/SnPb BGA's that fell off, almost 100% of the solder joints failed by pad cratering. The BGA balls and associated PWB copper pads were missing from the test vehicles (Figure 34 and Figure 35).



Figure 34 - Test Vehicle 30 BGA U2 with Missing Pads (SnPb Solder/SnPb Balls)

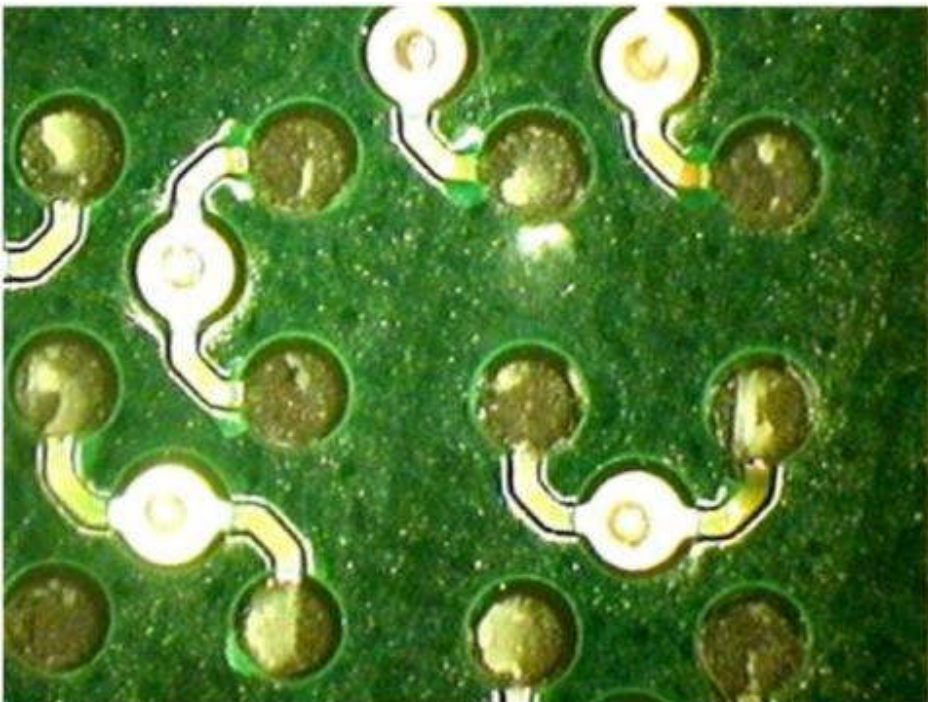


Figure 35 - Test Vehicle 30 BGA U4 with Missing Pads (SnPb Solder/SnPb Balls)

No SAC305/SAC405 BGA's fell off during the test. The only purely Pb-free BGA that fell off was one reworked using flux only and a BGA with SAC405 balls. For this BGA, 16% of the

balls remained with the PWB with the solder joints failing on the component side (although most of the remaining balls also showed signs of PWB pad cratering). The balance of the BGA balls and associated PWB copper pads were missing from the test vehicle (Figure 36 and Figure 37).



Figure 36 - Test Vehicle 193 BGA U21 with Missing Pads (Flux Only/SAC405 Balls)

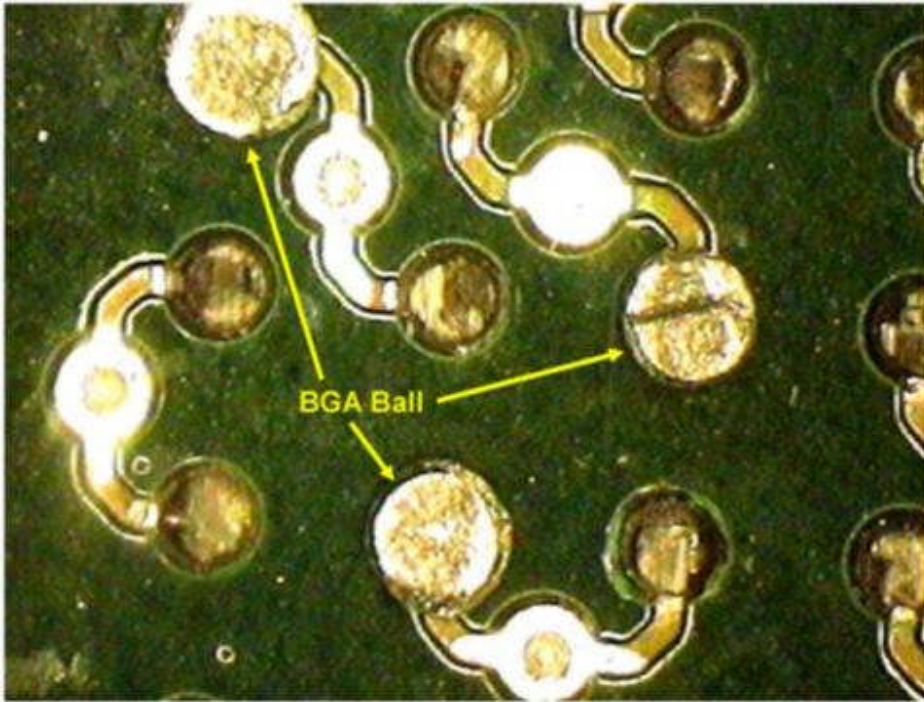


Figure 37 - Test Vehicle 193 BGA U21 with Missing Pads (Flux Only/SAC405 Balls)

5.2.2.2 CLCC Components

For the CLCC-20 components, the SnPb/SnPb controls outperformed the combinations of SAC305/SAC305, SnPb/SAC305, and SAC305/SnPb (Figure 38).

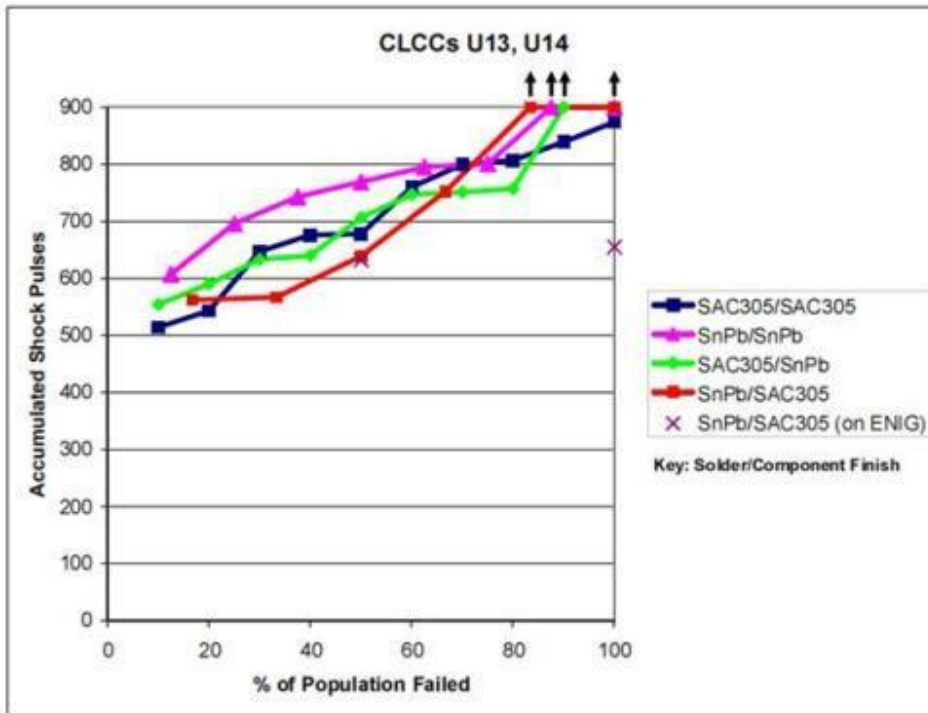


Figure 38 - Combined Data from CLCC's U13 and U14

Test vehicle inspections made at the end of Mechanical Shock Testing showed cracks in a CLCC solder joint (Figure 39).

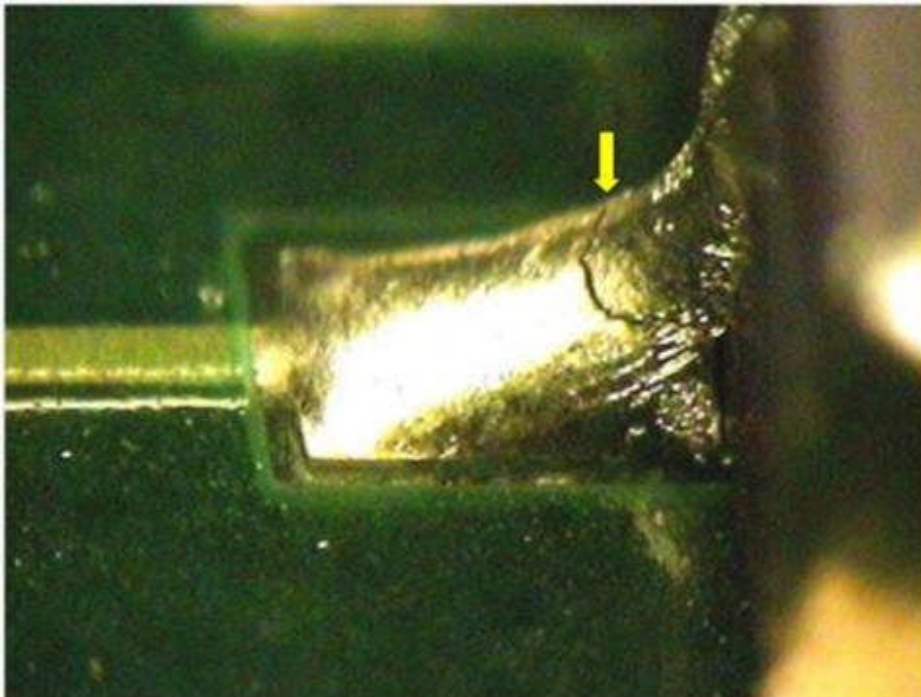


Figure 39 - Test Vehicle 191 CLCC U10 (Cracked SAC305/SnPb Solder Joint)

5.2.2.3 CSP Components

The CSP daisy chain pattern on the test vehicles was incorrect with the result that only the outer perimeter balls of each CSP formed an electrically continuous path (Figure 40). In order for a CSP to be detected as failed, both legs of the outer perimeter needed to fail.

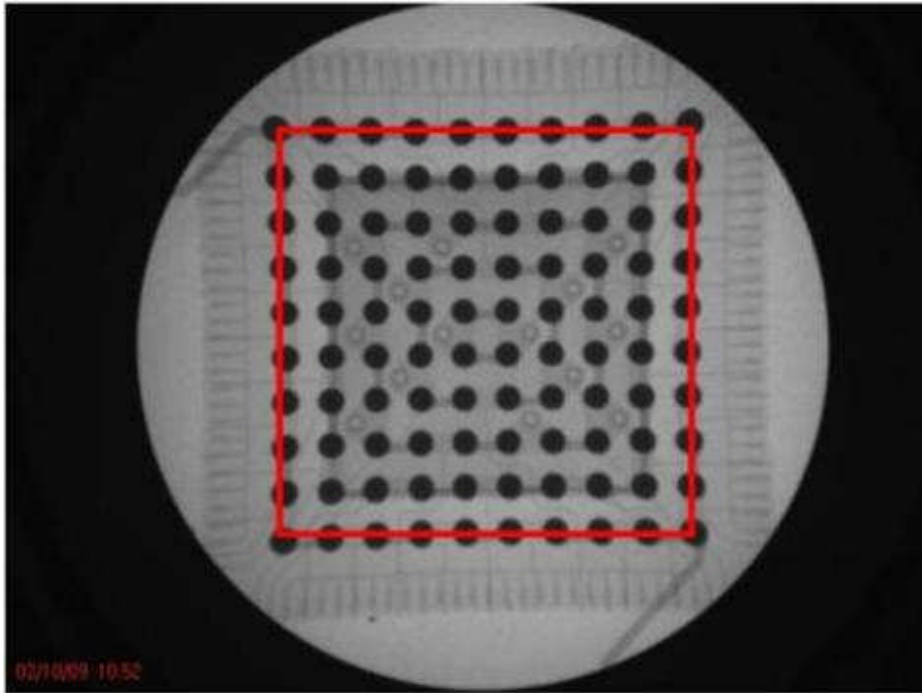


Figure 40 - X-Ray of a CSP-100 (Showing that only the outer balls form a daisy-chain (Red Lines).)

The combination of SAC305 solder/SAC105 balls generally performed as well as the SnPb/SnPb controls in mechanical shock. Microsections made at the end of the test showed that the corner solder joints failed first. The SnPb/SnPb solder joints formed cracks primarily on the component side (Figure 41). The SAC305/SAC105 solder joints formed cracks primarily on the component side and also showed evidence of pad cratering (Figure 42).

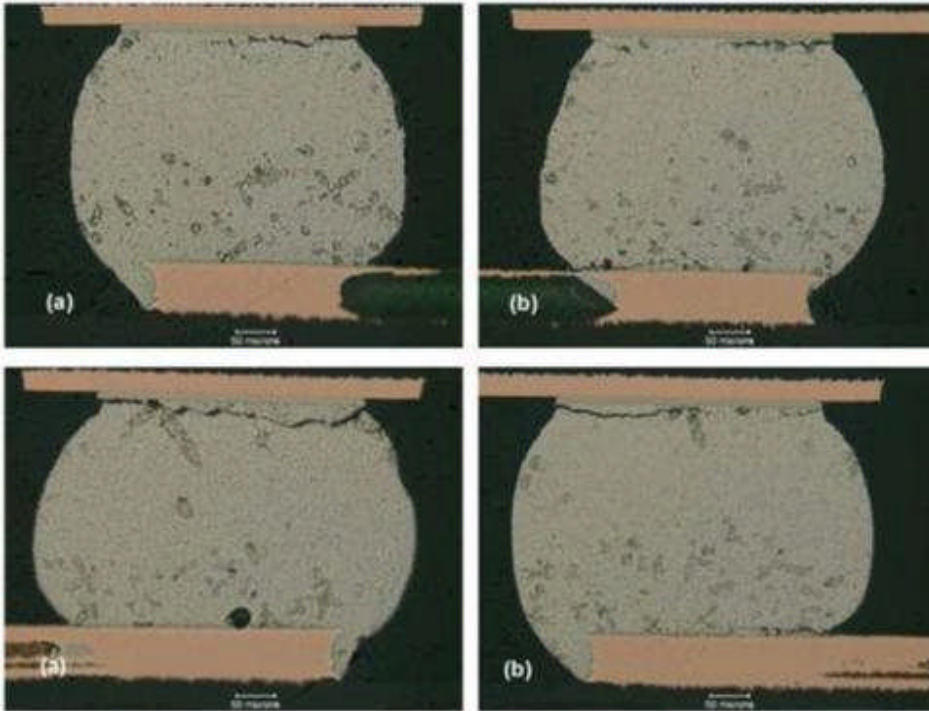


Figure 41 - Test Vehicle 34 – CSP U33
 (a) Corner Ball, (b) Ball Adjacent to Corner Ball (SnPb Solder/SnPb Balls)

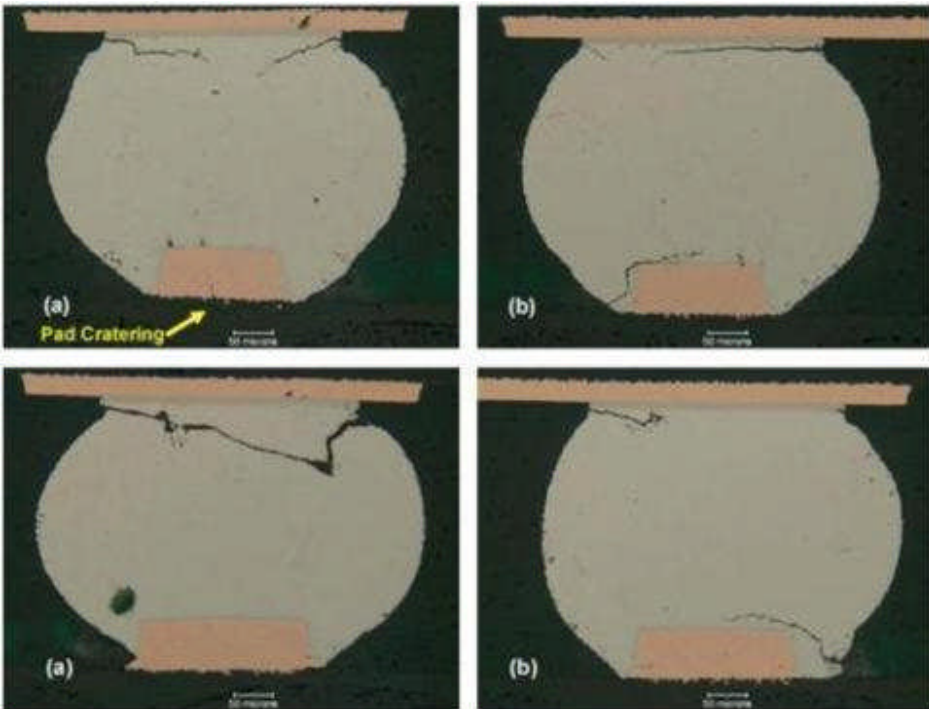


Figure 42 - Test Vehicle 89 – CSP U33
 (a) Corner Ball, (b) Ball Adjacent to Corner Ball (SAC305 Solder/SAC105 Balls)

5.2.2.4 PDIP Components

The combination of SN100C solder/Sn component finish generally performed as well as the SnPb/SnPb controls in mechanical shock although some of the SN100C/Sn solder joints failed early. Microsections made at the end of the test showed that the corner solder joints failed before the other solder joints. The topside solder fillet would crack first followed by cracking of the lead where it necks down at the top of the PTH (Figure 43 and Figure 44).

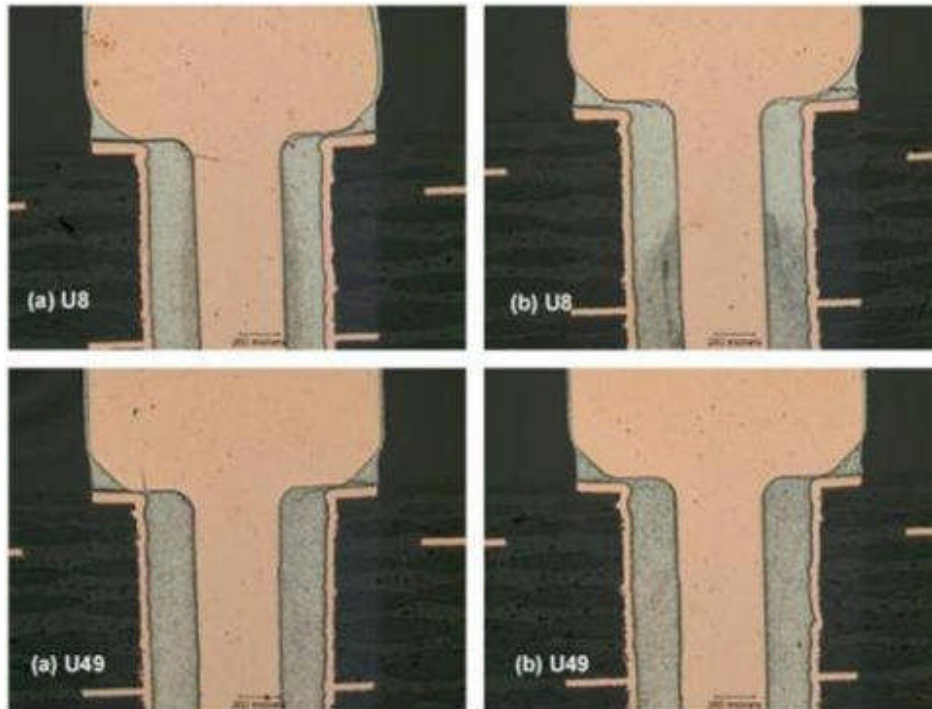


Figure 43 - Test Vehicle 34 – PDIPs U8 and U49 (a) Corner Lead, (b) Lead Adjacent to Corner Lead (SnPb Solder/SnPb Finish)

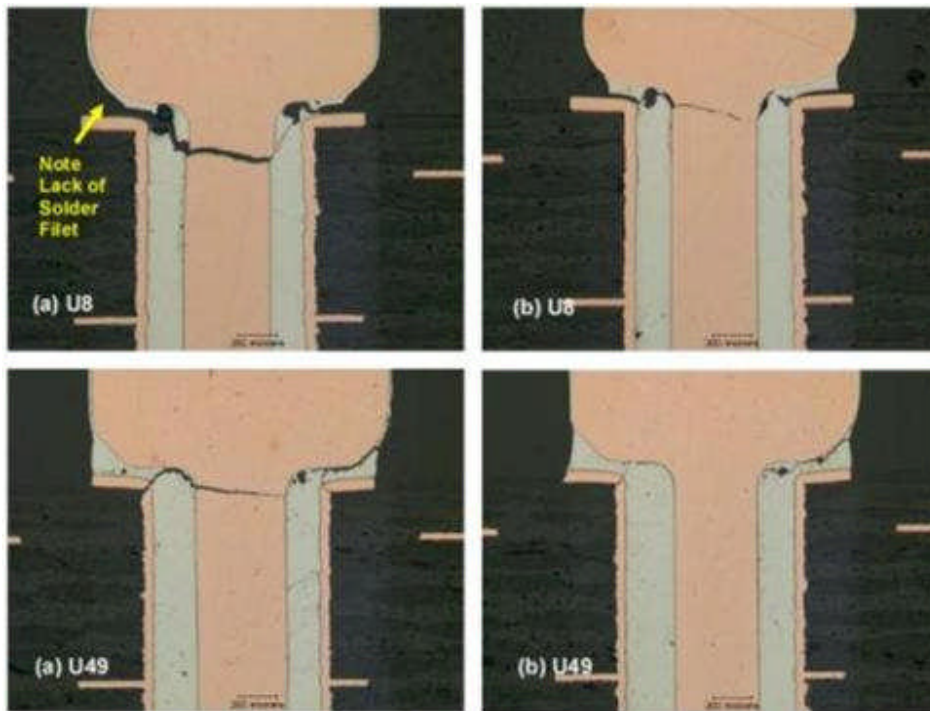


Figure 44 - Test Vehicle 89 – PDIPs U8 and U49 (a) Corner Lead, (b) Lead Adjacent to Corner Lead (SN100C Solder/Sn Finish)

Another observation is that many of the PDIP's soldered with SN100C exhibited trace cracking at the corner solder joints (Figure 45 and Figure 46). This failure mode was not observed as often with the PDIP's assembled with SnPb solder.

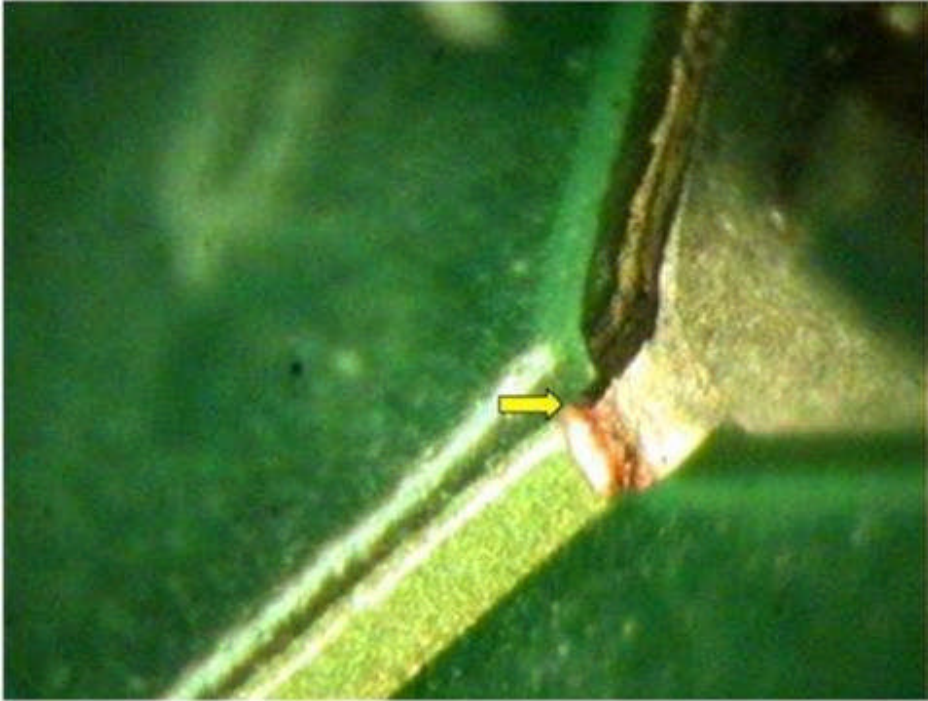


Figure 45 - Test Vehicle 89 PDIP U30 (Cracked Trace, SN100C)

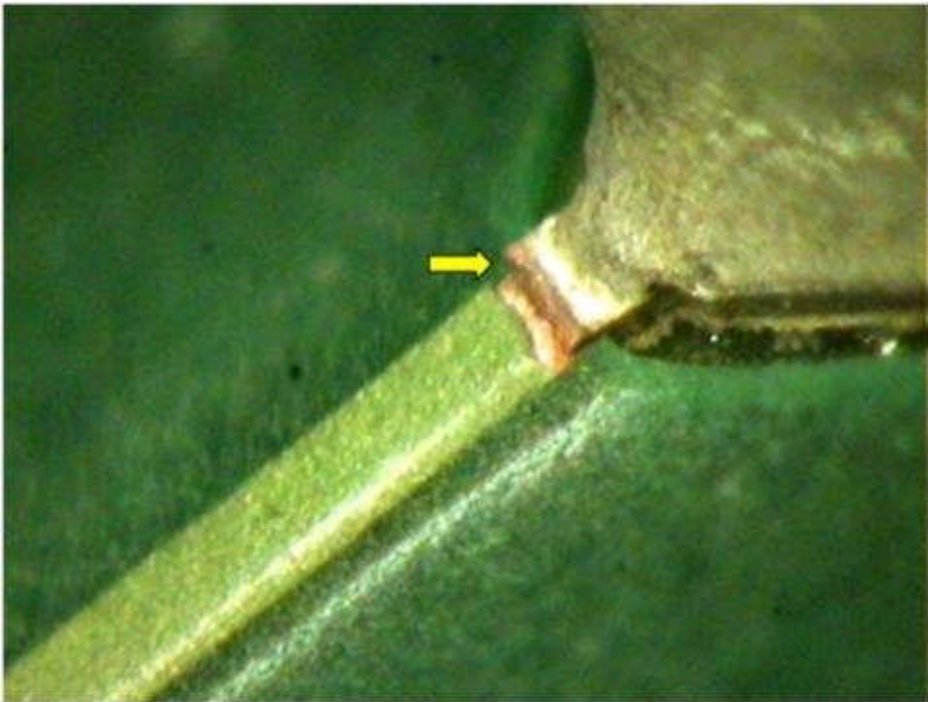


Figure 46 - Test Vehicle 89 PDIP U38 (Cracked Trace, SN100C)

Several of the earliest failures on the “Manufactured” test vehicles were SN100C/Sn solder joints. One possible cause is that some of the SN100C joints did not have a substantial topside solder filet (Figure 47). This could have resulted in a point of high stress concentration where the PDIP lead necked down resulting in premature failure of the lead. The trace cracking mentioned above is another possible cause for the early failures. Many of the PDIP’s that failed early exhibited both failure modes so it could not be definitely determined which occurred first.

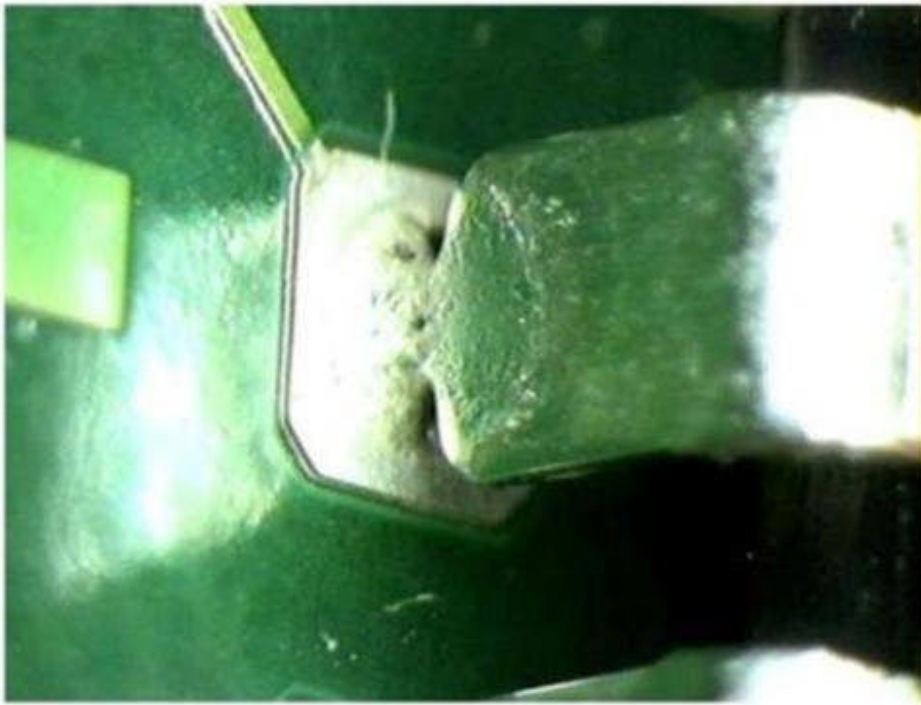


Figure 47 - Test Vehicle 89 PDIP U51 (SN100C)

5.2.2.5 QFN Components

The QFN components were resistant to failure under the conditions of this test. Only two QFN’s failed (on Shocks 827 and 873) and they were both SAC305/Sn. Not enough failures occurred to rank the solders. A PWB trace required for electrically monitoring QFN U15 was missing on every test vehicle due to a design error. Therefore, no data was generated for this component.

5.2.2.6 TQFP Components

Most of the TQFP-144’s had broken and/or missing leads at the end of the test (Figure 48). Since most of the failures appeared to be due to broken leads, the scatter in the test data for all of the TQFP solder/finish combinations was small. SAC305/Sn was equivalent in performance to SnPb/Sn, SnPb/NiPdAu (on immersion Ag), and SnPb/NiPdAu (on ENIG). SAC305/NiPdAu was superior to the SnPb/Sn controls in performance.

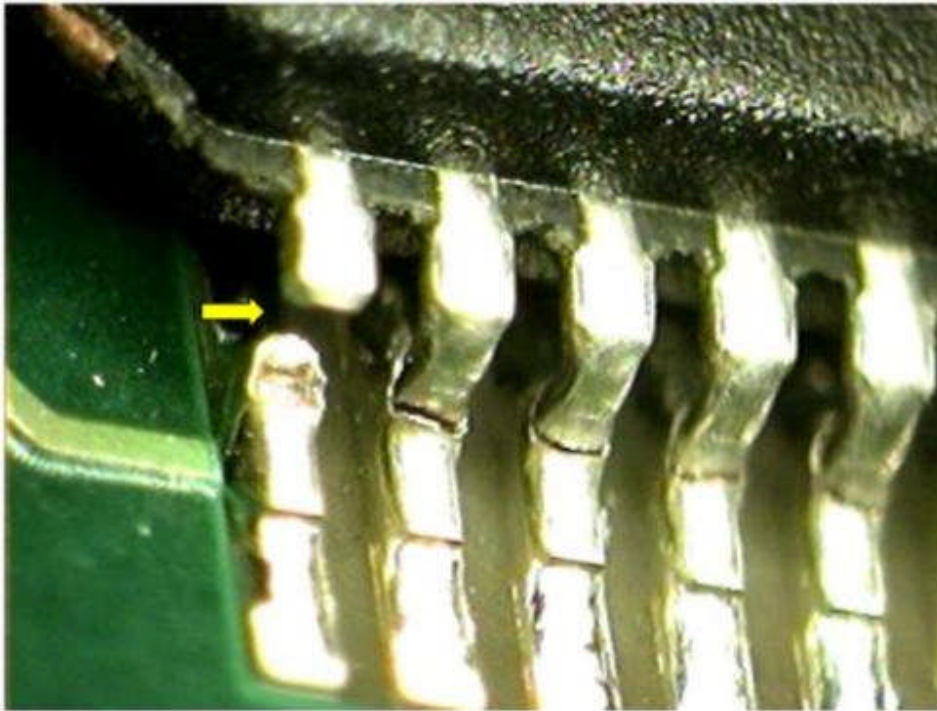


Figure 48 - Test Vehicle 89 TQFP U3 (Cracked Leads, Missing Lead)

For this test, some Sn-plated TQFP-144 leads were dipped into either molten SnPb or SAC305 to evaluate the effectiveness of the hot solder dipping on tin whisker formation. The combination of SnPb/SnPb Dip was equivalent to the SnPb/Sn control in performance but the SAC305/SAC305 Dip performance was inferior to that of the SnPb/Sn control due to some early failures (Figure 49).

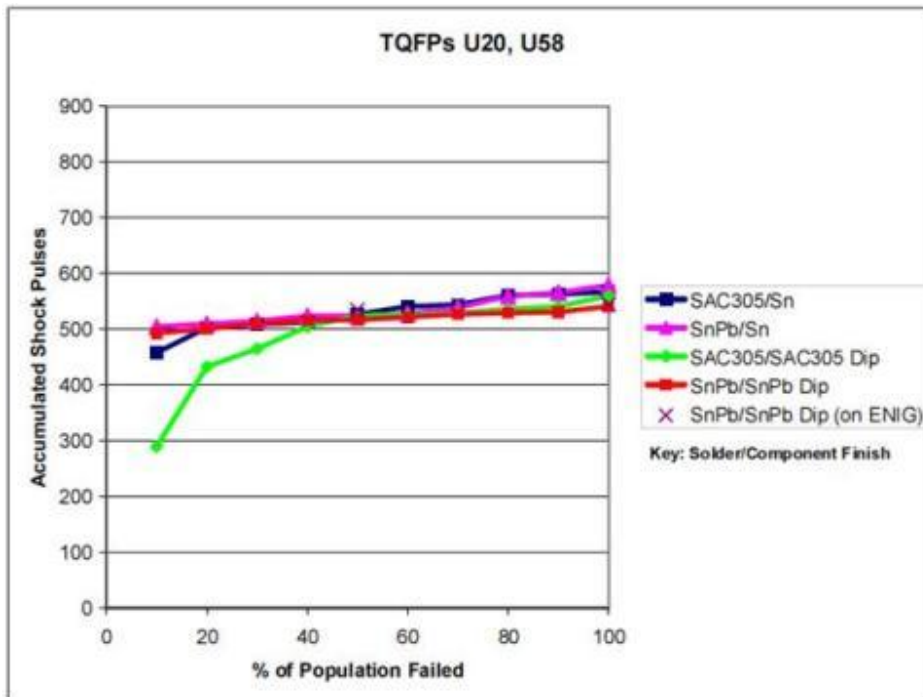


Figure 49 - Combined Data from TQFP's U20 and U58

5.2.2.7 TSOP Components

TSOP components that were not reworked were resistant to failure under the mechanical shock conditions of this test and the lack of failures made it impossible to rank the solder/finish combinations. Un-reworked SnPb/Sn on ENIG did have a few failures but they occurred late in the test. Mixed solder/finish combinations also had few failures.

Rework had a definite negative effect on performance. SnPb/SnPb reworked with SnPb/SnPb and SAC305/Sn reworked with SnPb/Sn underperformed the un-reworked SnPb/SnPb controls which had no failures (Figure 50).

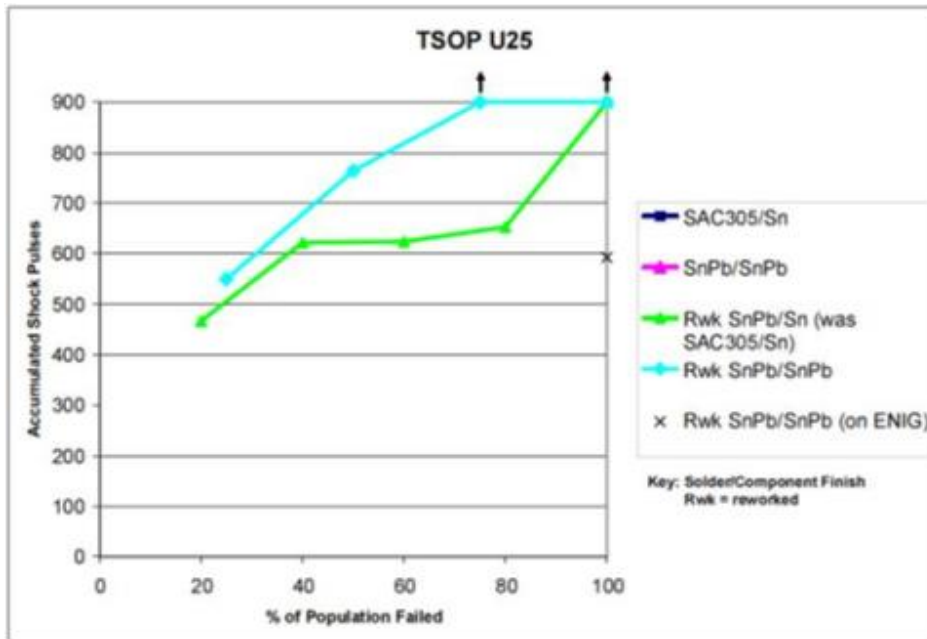


Figure 50 - TSOP U25 Data

SnPb/SnPb reworked with SnPb/Sn and SAC305/SnBi reworked with SAC305/SnBi underperformed the un-reworked SnPb/SnPb and SAC305/SnBi controls which had no failures (Figure 51).

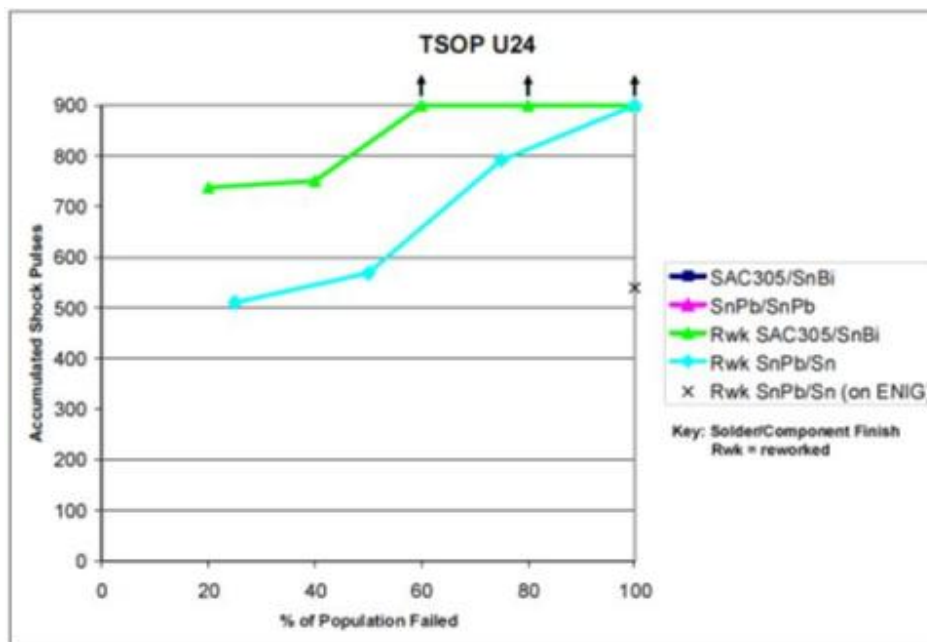


Figure 51 - TSOP U24 Data

Test vehicle inspection made at the end of Mechanical Shock Testing showed cracks in a TSOP solder joint (Figure 52).

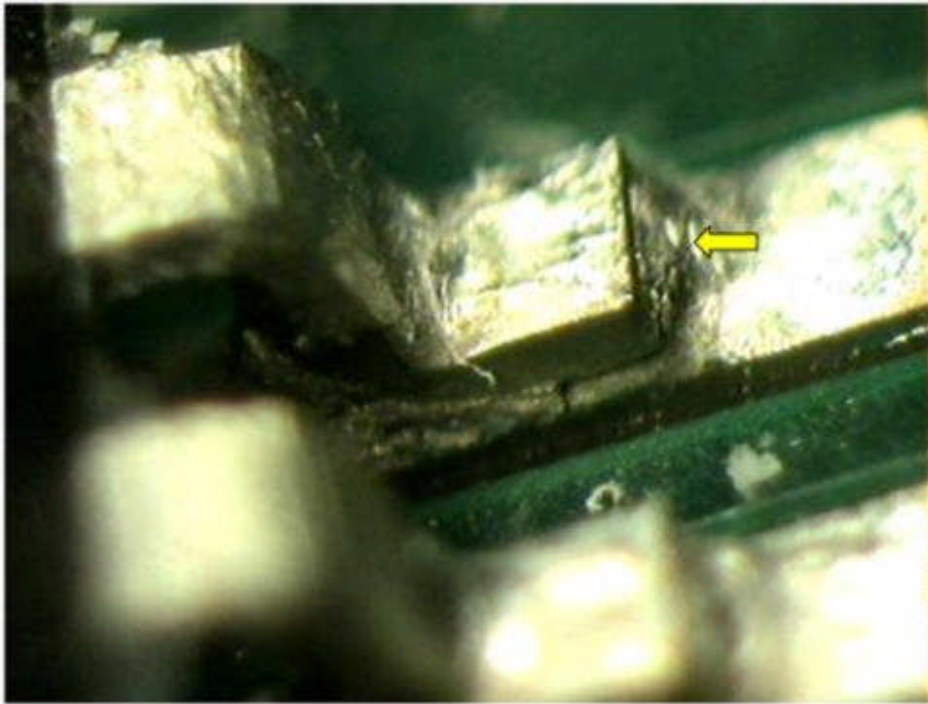


Figure 52 - Test Vehicle 34 TSOP U61 (Cracked SnPb/SnPb Solder Joint)

5.3 Combined Environments Test

5.3.1 Combined Environments Test Method

The Combined Environments Test (CET) for the NASA-DoD Lead-Free Electronics Project was based on a modified Highly Accelerated Life Test (HALT), a process in which products are subjected to accelerated environments to find weak links in the design and/or manufacturing process.

The CET process can identify design and process related problems in a much shorter time frame than other development tests. In this project, CET was used determine the operation and endurance limits of the solder alloys by subjecting the test vehicles to accelerated environments. The limits identified in CET were used to compare performance differences in the Pb-free test alloys and mixed solder joints vs. the baseline standard SnPb (63/37) alloy. The primary accelerated environments are temperature extremes (both limits and rate of change) and vibration (pseudo-random six degrees of freedom [DOF]) used in combination.

This test was performed utilizing a temperature range of -55 to 125°C with $20^{\circ}\text{C}/\text{minute}$ ramps. The dwell times at each temperature extreme are the times required to stabilize the test sample plus a 15-minute soak. 10 g_{rms} pseudo-random vibration was applied for the duration of the thermal cycle. Testing was continued until sufficient data was generated to obtain statistically significant Weibull plots indicating relative solder joint endurance (cycles to failure) rates. If significant failure rates were not evidenced after 50 cycles, the vibration levels were increased in increments of 5 g_{rms} and continued cycling for an additional 50 cycles. The process was repeated until all parts failed or 55 g_{rms} was reached.

Table 18 - Combined Environments Test Methodology

Parameters	<ul style="list-style-type: none"> ▪ -55°C to $+125^{\circ}\text{C}$ ▪ Number of cycles ≥ 500 ▪ $20^{\circ}\text{C}/\text{minute}$ ramp ▪ 15 minute soak ▪ Vibration for duration of thermal cycle ▪ 10 g_{rms}, initial ▪ Increase 5 g_{rms} after every 50 cycles ▪ 55 g_{rms}, maximum 		
Number of Test Vehicles Required			
Mfg. SnPb = 5	Mfg. LF = 5	Mfg. LF {SN100C} = 5	Mfg. LF {ENIG} = 1
Rwk. SnPb = 5	Rwk. SnPb {ENIG} = 1	Rwk. LF = 5	
Trials per Specimens		1	

Table 19 - Combined Environments Testing Vibration Level and Cycle Correlation

Cycle(s)	Vibration Level (g _{rms})
0 to 50	10
51 to 100	15
101 to 150	20
151 to 200	25
201 to 250	30
251 to 300	35
301 to 350	40
351 to 400	45
401 to 450	50
451 to 500+	55

5.3.2 Combined Environments Test Results Summary

The complete test report, “NASA/DOD Lead-Free Electronics Project: Combined Environments Test”, can be found on the NASA TEERM website (<http://teerm.nasa.gov>).

Overall, the component type had the greatest effect on solder joint reliability performance. The plated-through-hole components {PDIP-20} proved to be more reliable than the surface mount technology components. Of the surface mount technology, the TQFP-144 and QFN-20 components performed the best while the BGA-225 components performed the worst.

The solder alloy had a secondary effect on solder joint reliability. In general, tin-lead finished components soldered with tin-lead solder paste were the most reliable. In general, tin-silver copper soldered components were less reliable than the tin-lead soldered controls. The lower reliability of the tin-silver-copper 305 solder joints does not necessarily rule out the use of tin silver copper solder alloy on military electronics. In several cases, tin-silver-copper 305 solder performed statistically as good as or equal to the baseline, tin-lead solder.

The effect of tin-lead contamination on BGA-225 components degrades early life performance of tin-copper solder paste. It can also degrade early life performance of tin-silver-copper 305 solder paste. The effect of tin-lead contamination on BGA-225 components soldered with tin-silver-copper 305 solder paste was less than the effect on tin-lead contamination on tin-copper solder.

CSP-100 components are the exception, where tin-lead CSP-100 components soldered with tin-silver-copper 305 solder paste performed better than or equal to tin-lead CSP-100 components soldered with tin-lead solder paste. The chip scale package components were not drafted correctly during the design stage, therefore CSP-100 components results can only be used to compare within chip scale packages.

The probability plots of soldering tin-lead and tin-silver-copper 305 solder components onto electroless nickel immersion gold (ENIG) finished test vehicles were compared using BGA-225 and CLCC-20 components. In general, tin-lead components soldered with tin-silver-copper 305 solder paste onto immersion gold performed better than tin-silver-copper 305 components

soldered onto ENIG finished test vehicles. One exception is the performance of tin-lead CLCC-20 components soldered with tin-silver-copper 305 solder paste onto ENIG test vehicle performing better than the immersion gold test vehicle. Keep in mind, the ENIG sample size consisted of only two test vehicles.

In general, reworked components were less reliable than the unreworked components. This is especially true with reworked Pb-free CSP-100, reworked Pb-free BGA-225 and unreworked Pb-free TQFP-144 components; these components did not survive beyond 200 cycles. The exceptions were the immersion gold plated-through-hole components, nickel-palladium-gold TQFP-144, matte tin and tin-lead QFN-20, and tin PDIP-20 components where a majority of these components were soldered with tin-lead solder and did not fail. Approximately, 37% of rework test vehicle components soldered with tin-lead solder paste failed, whereas, 53% of rework test vehicle components soldered with tin-silver-copper 305 solder paste failed. This suggests that reworking surface mount technology components with Pb-free solder continues to pose processing challenges.

When comparing the performance of components soldered onto the two different test vehicle board finishes of immersion silver and electroless nickel immersion gold (ENIG), the immersion silver finish of the manufactured test vehicles had better reliability of solder joints than components soldered onto and ENIG surface finish. This is supported in several of the 2-parameter Weibull plots generated with the data.

Data from the Combined Environments Test was segregated by component type, component finish and solder alloy, see Table 20 and Table 21. Test vehicles soldered with tin-lead solder had the fewest solder joint failures overall. Test vehicles soldered with tin-silver-copper solder were second best. Lastly, the test vehicles soldered with tin-copper solder paste had the worst performance.

Table 20 - Number of Failed Components by Board Finish, Component, Component Finish and Solder Alloy on Manufactured Test Vehicles

Board Finish	Component	Finish	Solder	Number of Failed Components
Im. Ag	BGA-225	SAC405	SAC305	76% (19 of 25)
			SN100C	76% (19 of 25)
			SnPb	92% (23 of 25)
		SnPb	SAC305	84% (21 of 25)
			SN100C	88% (22 of 25)
			SnPb	60% (15 of 25)
Im. Ag	CLCC-20	SAC305	SAC305	96% (24 of 25)
			SN100C	96% (24 of 25)
			SnPb	92% (23 of 25)
		SnPb	SAC305	100% (25 of 25)
			SN100C	88% (22 of 25)
			SnPb	84% (21 of 25)
Im. Ag	CSP-100	SAC105	SAC305	32% (8 of 25)
			SN100C	44% (11 of 25)
			SnPb	68% (17 of 25)
		SnPb	SAC305	20% (5 of 25)
			SN100C	48% (12 of 25)
			SnPb	16% (4 of 25)
Im. Ag	PDIP-20	NiPdAu	SN100C	0% (0 of 28)
			SnPb	0% (0 of 20)
		Sn	SN100C	10% (5 of 52)
			SnPb	0% (0 of 20)
Im. Ag	PTH	Im. Ag	SN100C	0% (0 of 10)
			SnPb	0% (0 of 5)
Im. Ag	QFN-20	Matte Sn	SAC305	20% (5 of 25)
			SN100C	40% (10 of 25)
			SnPb	20% (5 of 25)
Im. Ag	TQFP-144	Matte Sn	SAC305	24% (6 of 25)
			SN100C	52% (13 of 25)
			SnPb	32% (8 of 25)
		SnPb Dip	SAC305	0% (0 of 25)
			SN100C	60% (15 of 25)
			SnPb	8% (2 of 25)
Im. Ag	TSOP-50	SnBi	SAC305	92% (23 of 25)
			SN100C	92% (23 of 25)
			SnPb	64% (16 of 25)
		SnPb	SAC305	60% (15 of 25)
			SN100C	84% (21 of 25)
			SnPb	64% (16 of 25)

Table 21 - Number of Failed Components by Board Finish, Component, Component Finish and Solder Alloy on Manufactured Test Vehicles

Board Finish	Component	Finish	Solder	Number of Failed Components
ENIG	BGA-225	SAC405	SAC305	0% (0 of 5)
		SnPb	SAC305	100% (5 of 5)
ENIG	CLCC-20	SAC305	SAC305	60% (3 of 5)
		SnPb	SAC305	60% (3 of 5)
ENIG	CSP-100	SAC105	SAC305	0% (0 of 5)
		SnPb	SAC305	0% (0 of 5)
ENIG	PDIP-20	Sn	SN100C	0% (0 of 8)
ENIG	PTH	ENIG	SN100C	0% (0 of 1)
ENIG	QFN-20	Matte Sn	SAC305	20% (1 of 5)
ENIG	TQFP-144	Matte Sn	SAC305	0% (0 of 5)
		SnPb Dip	SAC305	0% (0 of 5)
ENIG	TSOP-50	SnBi	SAC305	20% (1 of 5)
		SnPb	SAC305	20% (1 of 5)

Data from the Combined Environments Test, rework test vehicles, was segregated by component type, component finish and solder alloy, see Table 22 and Table 23. Test vehicles soldered with or reworked with tin-lead solder had the fewest solder joint failures. Test vehicles soldered with tin-silver-copper solder were second best. Lastly, the test vehicles soldered with tin-copper solder had the worst performance.

Table 22 - Number of Failed Components by Board Finish, Component, Component Finish, Solder Alloy, New Component Finish and Rework Solder on Rework Test Vehicles

Board Finish	Component	Finish	Solder	New Component Finish	Rework Solder	Number of Failed Components	
Im. Ag	BGA-225	SAC405	SAC305	SAC405	Flux Only	60% (9 of 15)	
					SnPb	33% (5 of 15)	
			SnPb			50% (10 of 20)	
		SnPb	SAC305				65% (13 of 20)
			SnPb	SAC405	SnPb		80% (12 of 15)
				SnPb	Flux Only		20% (3 of 15)
Im. Ag	CLCC-20	SAC305	SnPb			98% (49 of 50)	
		SnPb	SAC305			100% (50 of 50)	
Im. Ag	CSP-100	SAC105	SAC305	SAC105	Flux Only	20% (3 of 15)	
					SnPb	93% (14 of 15)	
			SnPb			60% (3 of 5)	
		SnPb	SAC305				55% (11 of 20)
			SnPb	SAC105	SnPb		0% (0 of 15)
				SnPb	Flux Only		7% (1 of 15)
Im. Ag	PDIP-20	NiPdAu	SnPb			0% (0 of 15)	
		Sn	SN100C	Sn	SN100C	7% (1 of 15)	
			SnPb			20% (2 of 10)	
		SnPb	SnPb	Sn	SnPb	7% (2 of 30)	
Im. Ag	PTH	ImAg	SN100C			13% (2 of 15)	
			SnPb			40% (4 of 10)	
Im. Ag	QFN-20	Matte Sn	SnPb			0% (0 of 5)	
		SnPb	SAC305			0% (0 of 5)	
Im. Ag	TQFP-144	NiPdAu	SAC305			20% (5 of 25)	
			SnPb			24% (6 of 25)	
		SAC305	SAC305			0% (0 of 25)	
		SnPb Dip	SnPb			0% (0 of 25)	
Im. Ag	TSOP-50	Sn	SAC305	Sn	SnPb	44% (11 of 25)	
			SnPb			12% (3 of 25)	
		SnBi	SAC305	SnBi	SAC305		60% (6 of 10)
			SnPb			20% (3 of 15)	
		SnPb	SAC305				90% (9 of 10)
			SnPb	Sn	SnPb		67% (10 of 15)
				SnPb	SnPb		33% (5 of 15)
			SnPb	SnPb	Sn	SnPb	
		SnPb	SnPb		50% (5 of 10)		
		SnPb	SnPb		60% (6 of 10)		

Table 23 - Number of Failed Components by Board Finish, Component, Component Finish, Solder Alloy, New Component Finish and Rework Solder on Rework Test Vehicles

Board Finish	Component	Finish	Solder	New Component Finish	Rework Solder	Number of Failed Components
ENIG	BGA-225	SAC405	SnPb			75% (3 of 4)
		SnPb	SnPb	SAC405	SnPb	100% (3 of 3)
		SnPb	SnPb	SnPb	Flux Only	33% (1 of 3)
ENIG	CLCC-20	SAC305	SnPb			100% (10 of 10)
ENIG	CSP-100	SAC105	SnPb			25% (1 of 4)
		SnPb	SnPb	SAC105	SnPb	33% (1 of 3)
		SnPb	SnPb	SnPb	Flux Only	0% (0 of 3)
ENIG	PDIP-20	NiPdAu	SnPb			0% (0 of 3)
		Sn	SnPb			33% (1 of 3)
		SnPb	SnPb	Sn	SnPb	0% (0 of 2)
ENIG	PTH	ENIG	SnPb			0% (0 of 1)
ENIG	QFN-20	Matte Sn	SnPb			20% (1 of 5)
ENIG	TQFP-144	NiPdAu	SnPb			20% (1 of 5)
		SnPb Dip	SnPb			60% (3 of 5)
ENIG	TSOP-50	Sn	SnPb			33% (1 of 3)
		SnBi	SnPb			33% (1 of 3)
		SnPb	SnPb	Sn	SnPb	100% (2 of 2)
		SnPb	SnPb	SnPb	SnPb	100% (2 of 2)

5.3.3 Combined Environments Failure Analysis

After completing Combined Environments Testing, the test vehicles were removed from the test chamber and inspected per J-STD-001, Class 3 requirements. The components selected for failure analysis are listed in Table 24.

Table 24 - Components selected for failure analysis based on when a failure was recorded during Combined Environments Testing

Test Vehicle	Component Location	Reason for Failure Analysis	FA Performed by
21	U34	Mfg group - No signal, failed at 0 cycles	COM DEV
21	U57	Mfg group - Failed at cycle 1	COM DEV
23	U30	Mfg group - Survived 650 cycles, surrounded by components that fell off	Nihon Superior
23	U43	Mfg group - Failed at 120 cycles, located near center of TV	Nihon Superior
72	U29	Mfg group - Location in chamber (low fails); failed at 161 cycles	Nihon Superior
117	U4	Mfg group - Failed at 20 cycles; SN100C solder paste used	Lockheed Martin
119	U36	Mfg group - Surrounded by components that fell off; failed at 233 cycles	COM DEV
119	U39	Mfg group - Surrounded by components that fell off; failed at 318 cycles	COM DEV
140	U11	Rwk group - Damaged pad from rework - Failed at 398 cycles	Lockheed Martin
142	U13	Rwk group - Adjacent to Reworked components, survived all 650 cycles	COM DEV
158	U6	Rwk group - Reworked component failed at cycle 1	Nihon Superior
180	U21	Rwk group - Reworked component failed at cycle 1	Nihon Superior
181	U56	Rwk group - Reworked component failed at cycle 1	COM DEV
181	U25	Rwk group - Reworked component failed at cycle 1	COM DEV
183	U41	Rwk group - Failed at cycle 1, was not reworked	Lockheed Martin

5.3.3.1 Test Vehicle 21

Component location U34 is a TQFP-144 component from SnPb manufactured (Batch C), soldered with SnPb on SnPb dip component finish. This component did not have a signal and failed before one complete cycle.

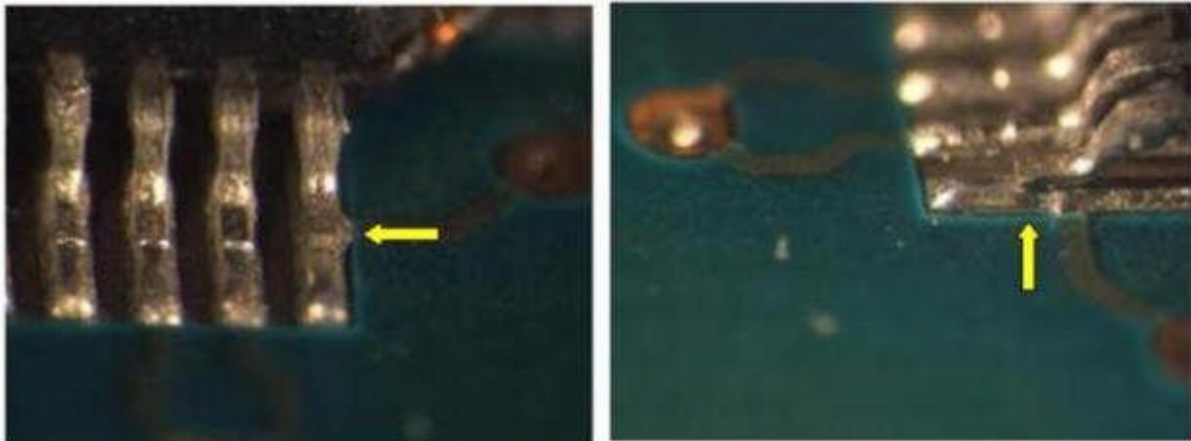


Figure 53 - TV21 U34; Optical Micrograph of Insufficient Solder Observed on Lead 72 at 49X Magnification

Component location U57 is a TQFP-144 component from SnPb manufactured (Batch C), soldered with SnPb on SnPb dip component finish. This component failed at cycle one.

Figure 54 is the optical micrograph of residue that was found between leads in two locations. The image on the left shows residue between leads 35 and 36, magnified at 38X. The image on the right shows residue between leads 38 and 39, magnified at 38X.



Figure 54 - TV21 U57; Optical Micrograph, Residue between Leads

Figure 55 shows Scanning Electron Microscope (SEM) images taken of the residue found from the images in Figure 54. The image on the left shows the residue that was found between leads 35 and 36, magnified at 90X. The image on the right shows the residue found between leads 38 and 39, magnified at 55X.

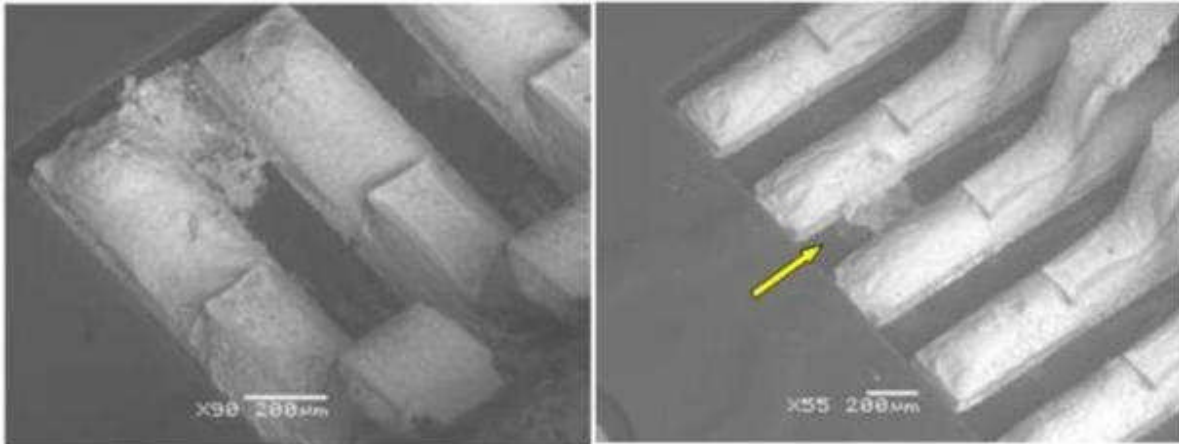


Figure 55 - TV21 U57; Optical Micrograph, Residue between Leads

The possible cause for the immediate failure at cycle one can be found in the Figure 56. The Optical micrograph shows component lead 1 does not contact solder on PWB pad at 49X magnification.

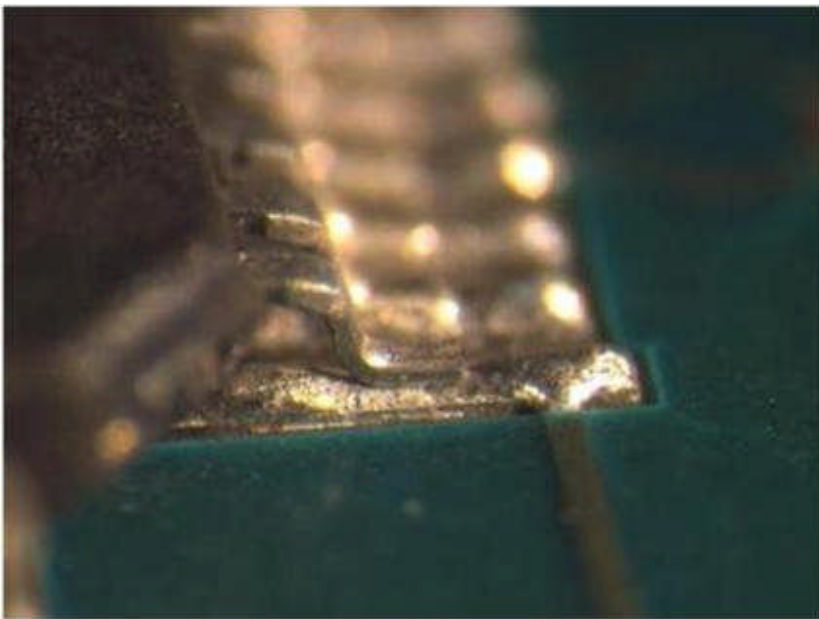


Figure 56 - TV21 U57; Optical Micrograph, Component Lead 1

5.3.3.2 Test Vehicle 23

Component location U30 is a PDIP-20 from the SnPb manufactured (Batch C), soldered with SnPb on tin plated component finish. This component survived all 650 cycles of combined environments testing and it was surrounded by components that fell off during testing. Figure 57, the red boxes highlight the two leads that were magnified to indicate observed cracking in the solder joints. The image in the upper right is of lead 11, which indicates two areas with cracking. The image in the bottom left is the top portion of lead 11 and the bottom right image is of lead 10 showing a small crack near the pad. Crack has not caused an electrical failure, yet.

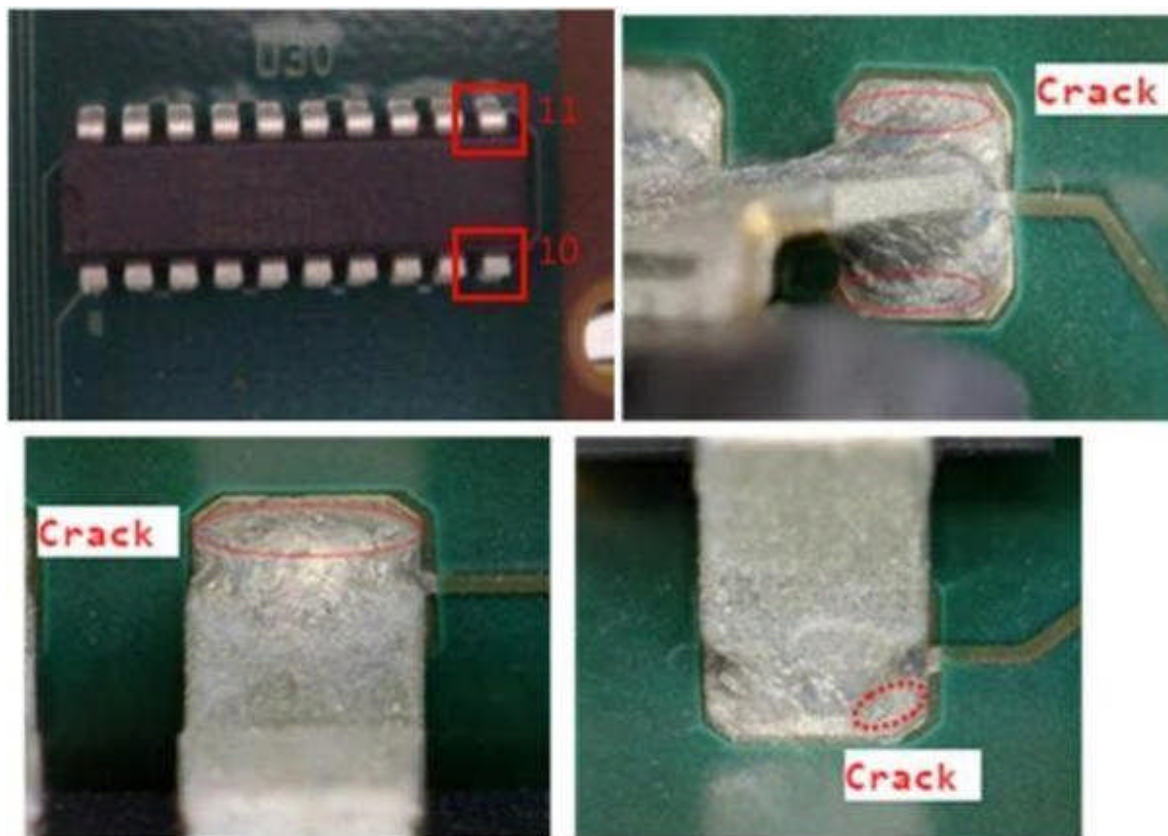


Figure 57 - TV23 U30; Optical Micrograph, PDIP-20

Figure 58 shows cross-sectional micrographs of PDIP-20 leads where the two images on the top are indicating the lead numbering. The cross-sections of leads 1, 5, 19 and 20 were selected as an example of the leads that had large quantities of voids, relative to the other component leads. The dotted lines indicate solder cracks that were found; no break off solder was found during failure analysis.

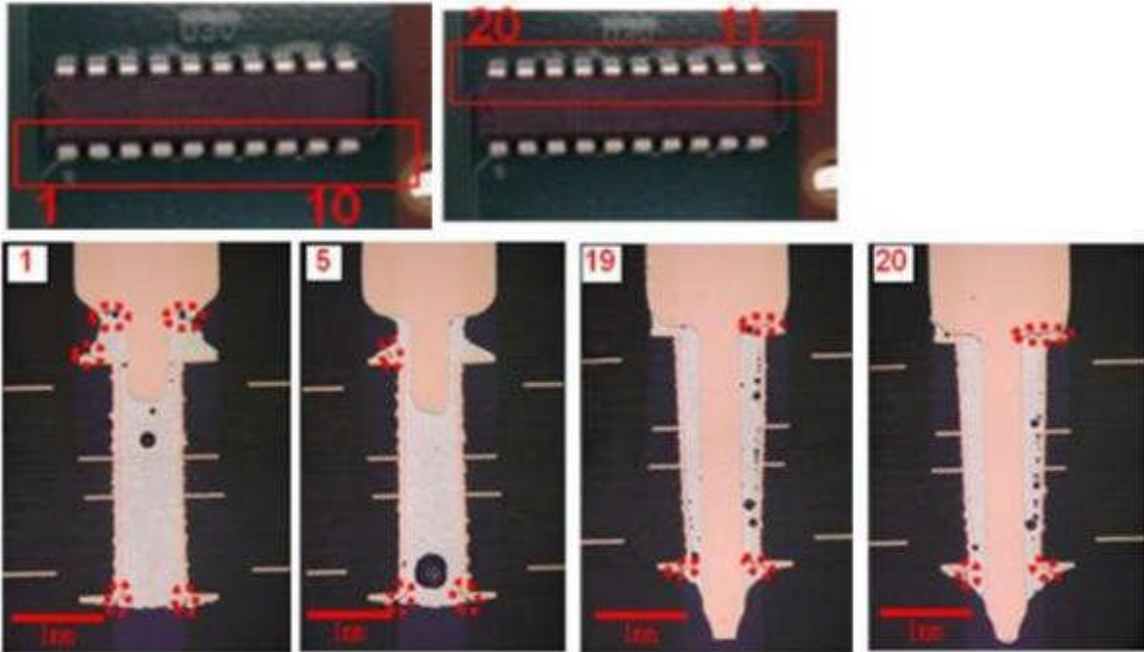


Figure 58 - TV23 U30; Cross-Sectional Micrographs of PDIP-20 Leads

The micrographs in Figure 59 show progression of analysis for lead 9 of PDIP-20 component beginning with upper left and following the arrows to the image on the bottom right. This analysis found silver (bottom right) within the solder joint. The source of the silver may have been the immersion silver board finish.

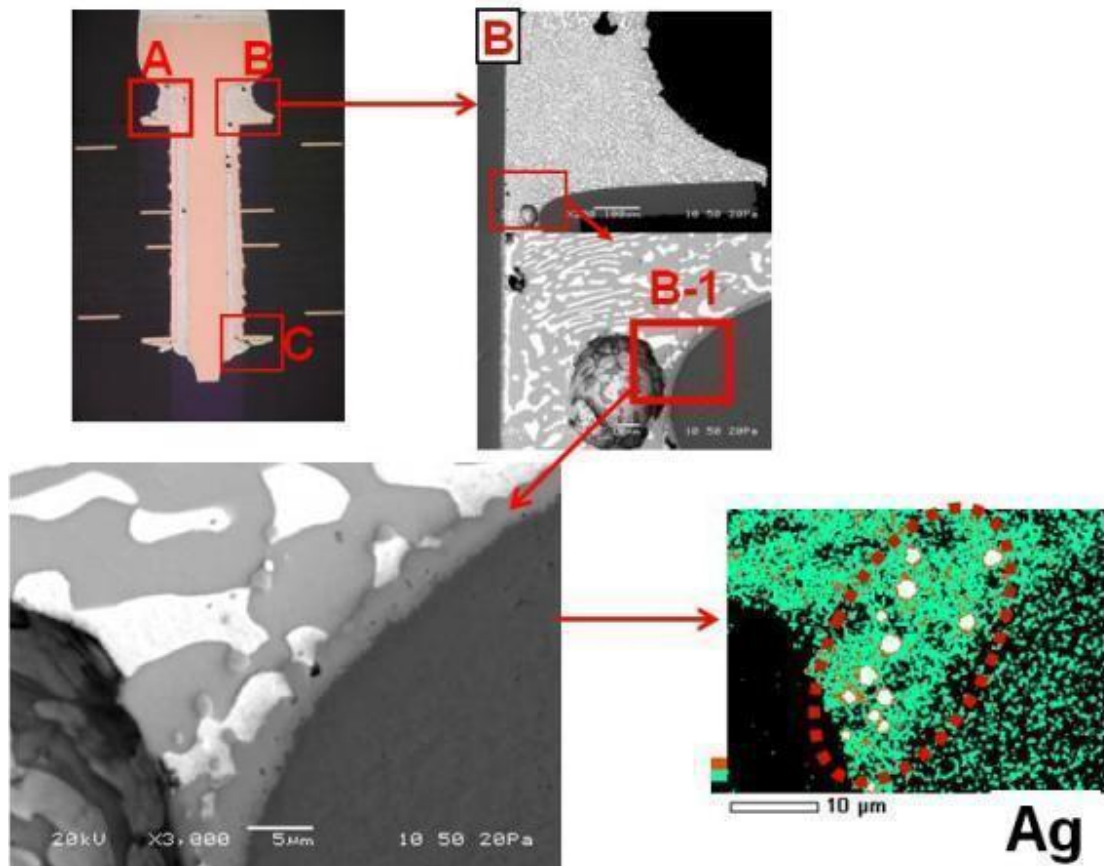


Figure 59 - TV23 U30; Micrographs, Lead 9 of PDIP-20

5.3.3.2.1 Component location U43

Component location U43 is a BGA-225 from the SnPb manufactured (Batch C), soldered with SnPb with SAC405 component finish located near the center of the test vehicle. This component failed at 120 cycles of combined environments. In Figure 60, yellow circles indicate solder joints with high resistance and red circles indicating failed solder joints that are open.

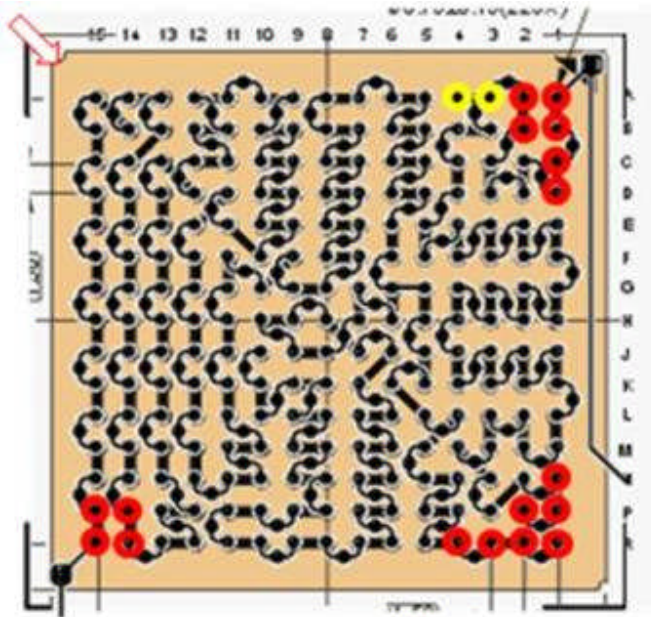


Figure 60 - TV23 U43; FA Results, BGA-225, Location U43

Cross-sectional micrographs in Figure 61 show different solder structure in lands on board (3, 4, 7, 8) and lands on component (1, 2, 5, 6). Cracking to open along land on board observed at 3-A.

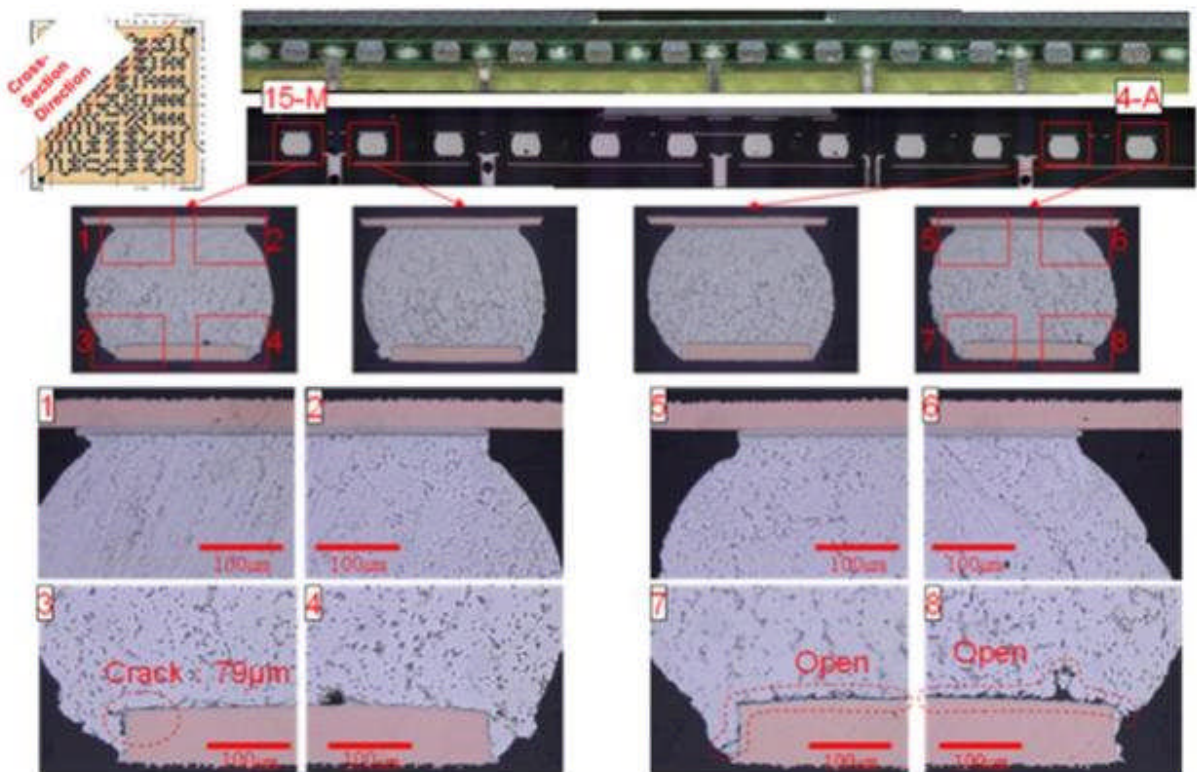


Figure 61 - TV23 U43; Cross-Sectional Micrographs

Cross-sectional micrographs in Figure 62 show different solder structure in lands on board (3, 4) and lands on component (1, 2). Cracking to open along land on board observed at 1-A and 15-Q.

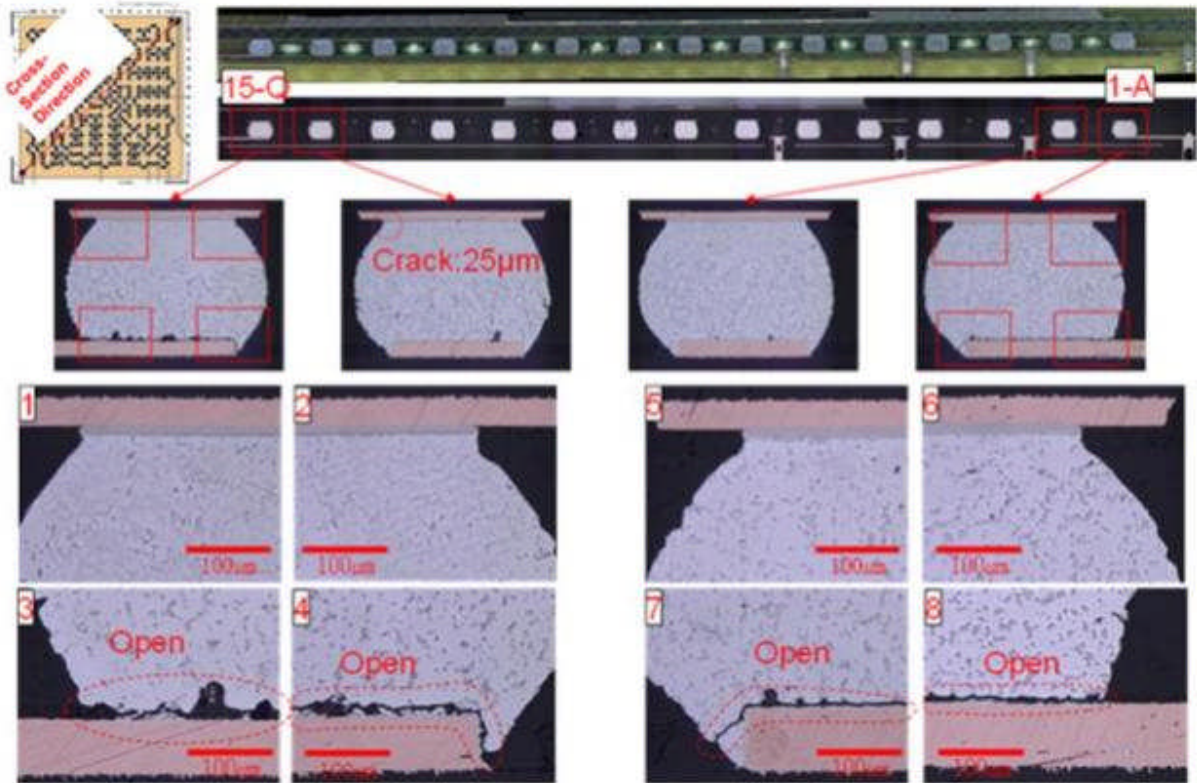


Figure 62 - TV23 U43; Cross-Sectional Micrographs

In Figure 63 SEM mapping shows segregation of Pb around land on board. Cracking found in the part Pb segregated.

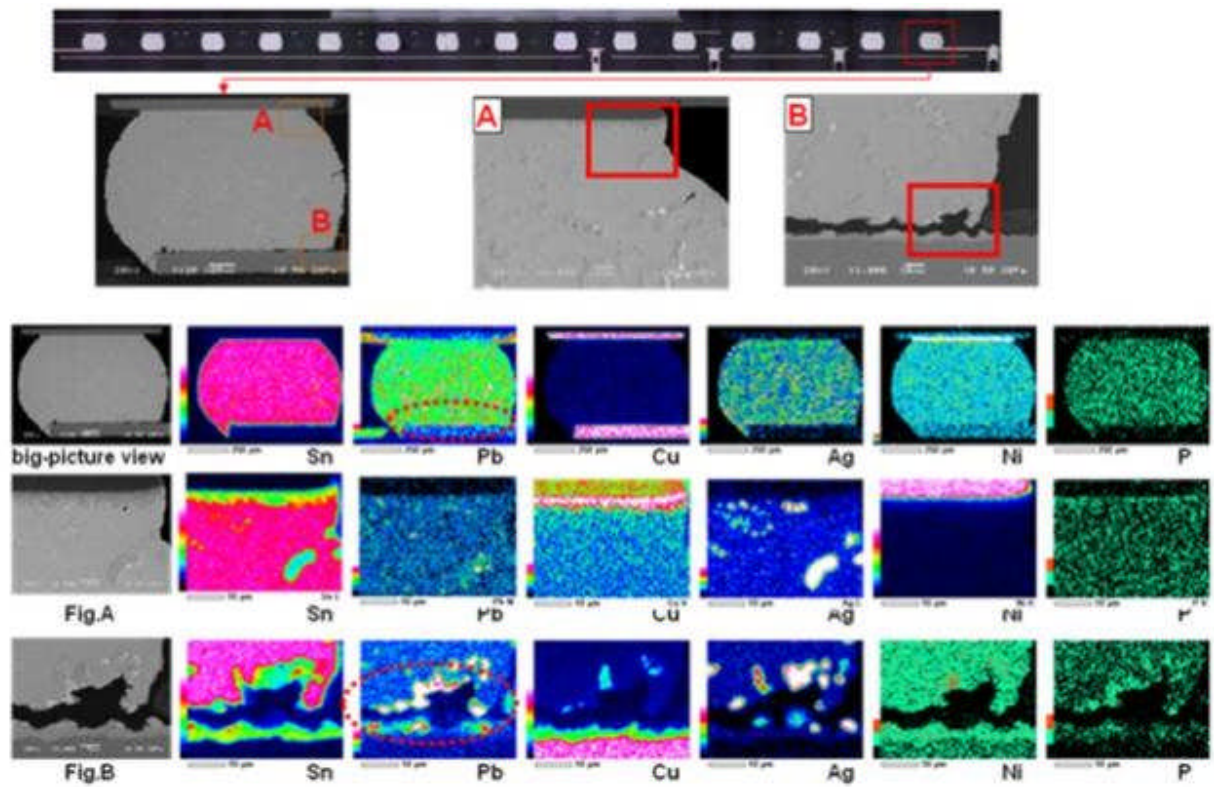


Figure 63 - TV23 U43; SEM Mapping

In Figure 64 the distance between component and board at each sphere is almost the same under the chip in the center. The distance becomes smaller further to the end. Comparing the distance at [1-A] and [15-Q], [1-A] has smaller distance.

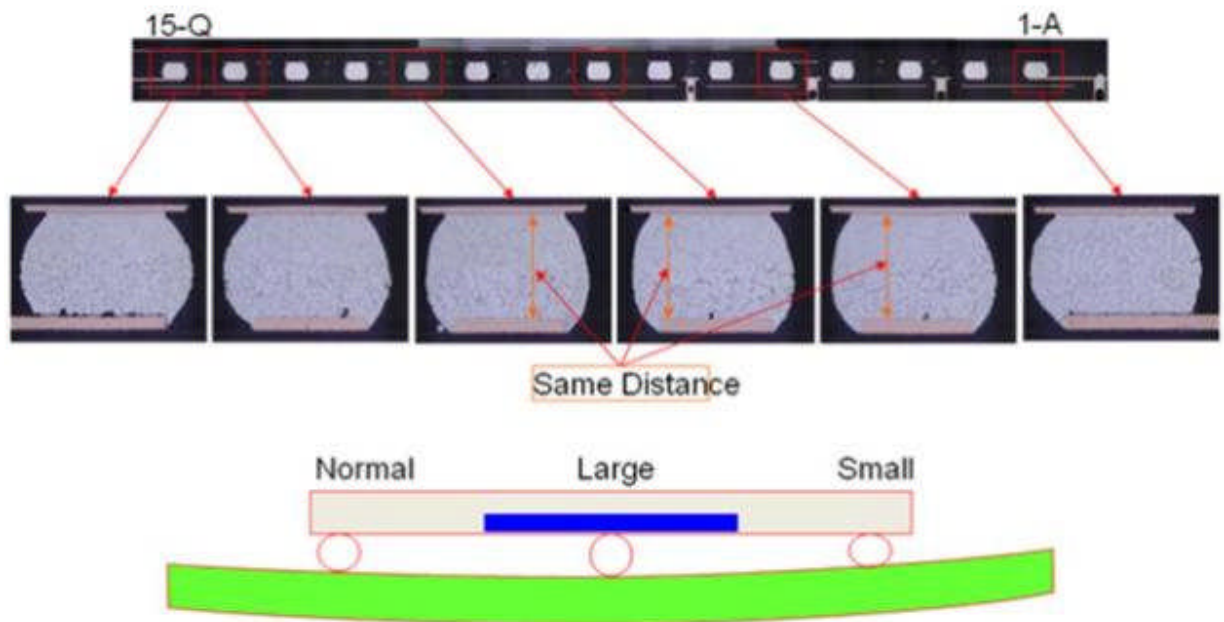


Figure 64 - TV23 U43; Cross-Sectional Micrographs Show Warping

5.3.3.3 Test Vehicle 72, component U29

Component location U29 is a TSOP-50 soldered with SAC305 on SnPb component finish. This component failed at 161 cycles of combined environments testing.

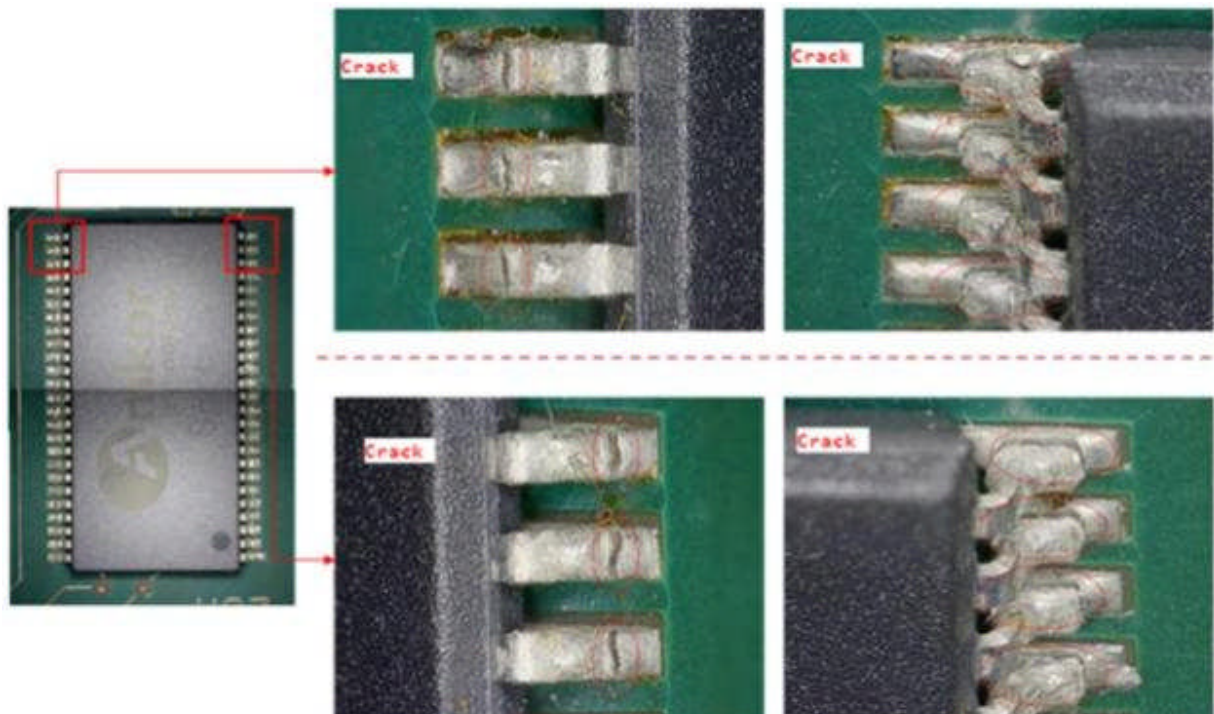


Figure 65 - TV72 U29; Visual Inspection Showing Cracked Solder Joints

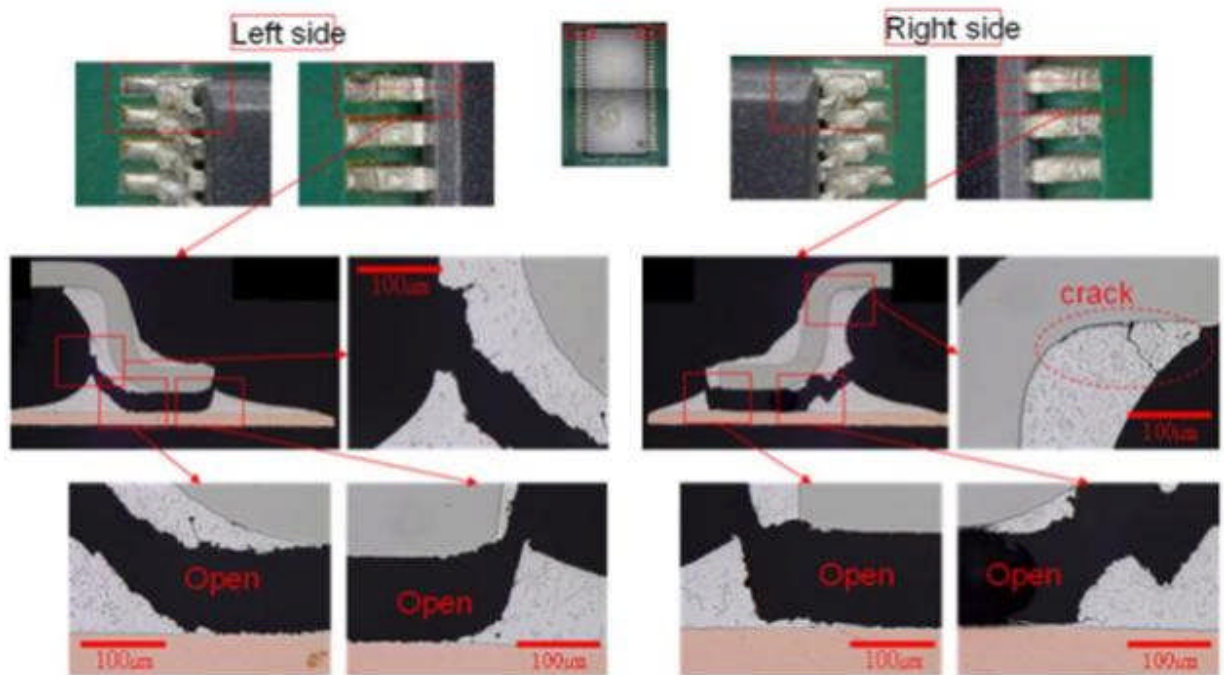


Figure 66 - TV72 U29; Cross-Section Micrographs Showing Open Solder Joints

As observed in Figure 67, more Pb was found from the right lead. Source of Pb is from the lead plating.

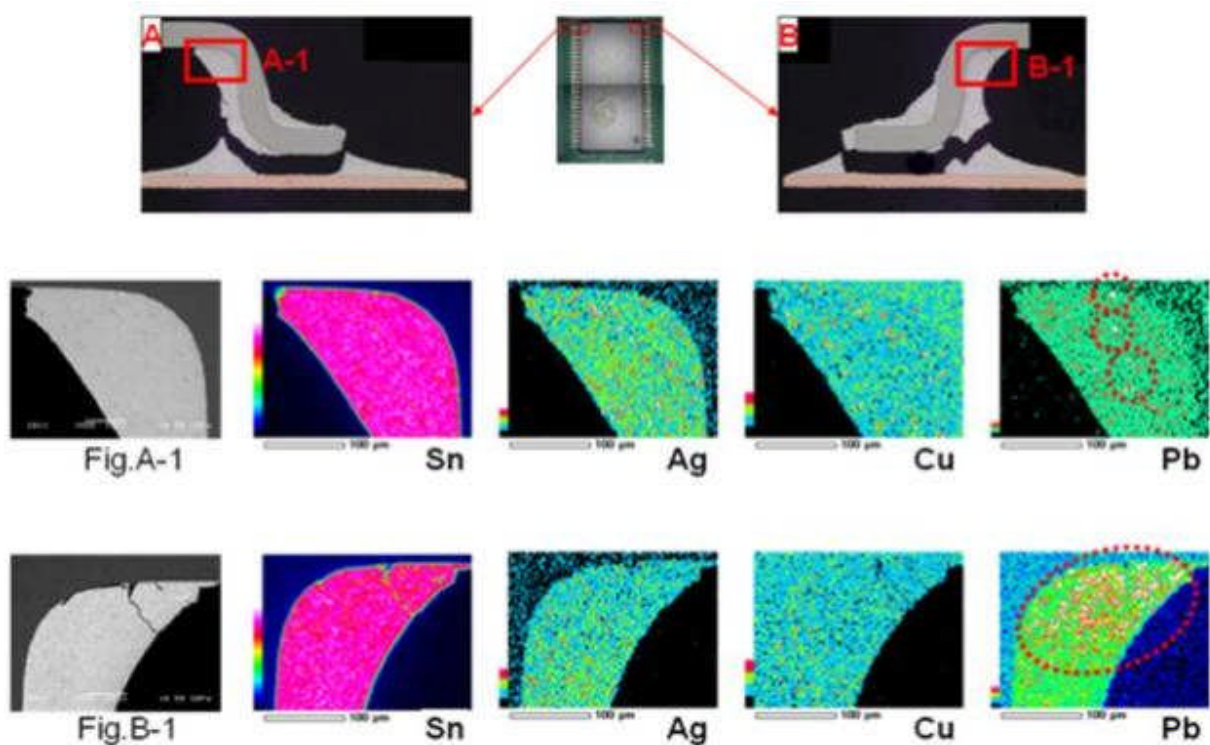


Figure 67 - TV72 U29; SEM Mapping, Pb was Found Around Upper Part of the Both Leads

5.3.3.4 Test Vehicle 117

Component location U4 is a BGA-225 component from Pb-free manufactured (Batch G), soldered with SN100C solder paste on SnPb component finish. This component failed after twenty cycles. Figure 68 shows the orientation of the corner solder balls for the cross-sections in Figure 69.



Figure 68 - TV117 U4; Orientation of the Corner Solder Balls

Figure 69 shows cross-sectional micrographs of corner solder balls depicting cracks at component pads on views A, B and C. Crack at the PWB pad detected on view D.

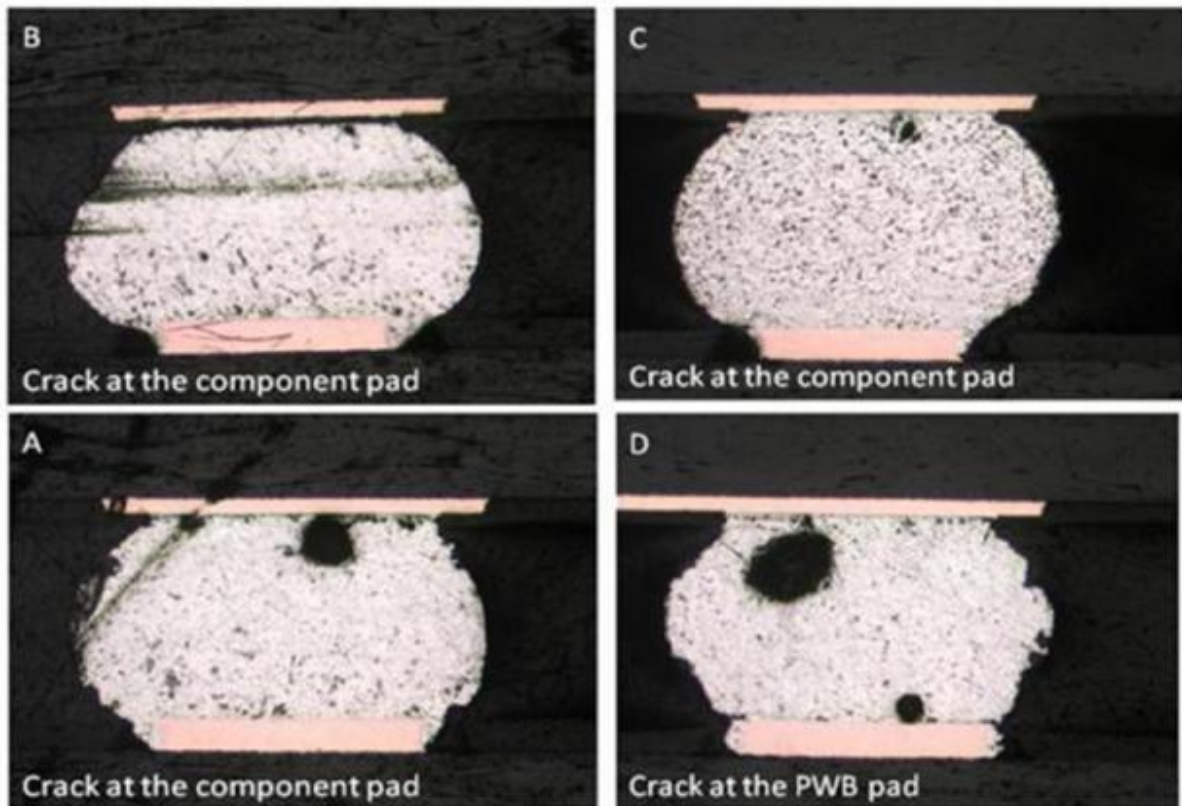


Figure 69 - TV117 U4; Cross-Sectional Micrographs of Corner Solder Balls

There was a progression of cracking between sides A/D and B/C, which can be visually represented in Figure 70. Red on top of the solder ball is cracking observed at the component interface. Red on the bottom of the solder ball is cracking observed at the PWB pad interface. Red on both the top and bottom of the solder ball is cracking observed at both the component and PWB pad interface. No red indicates an intact solder joint.

For this BGA-225 component, cracking was observed on both the second and third rows in from the perimeter row. No cracking was observed on solder balls beneath the component die.

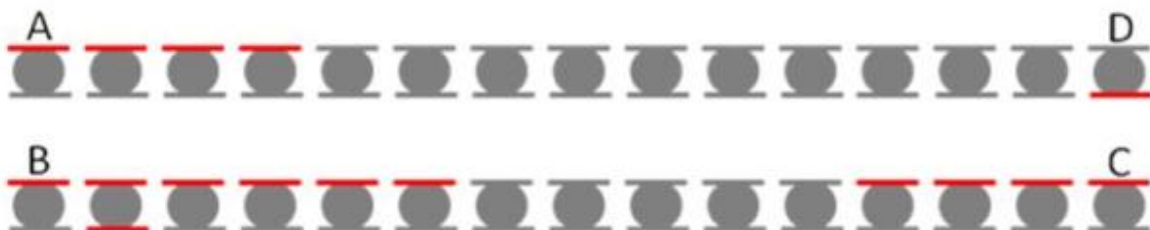


Figure 70 - TV117 U4; Diagram Showing Progression of Cracking in Component

5.3.3.5 Test Vehicle 119

Component location U36 is a CSP-100 component from lead-free manufactured (Batch G), soldered with SN100C solder paste on SAC105 component finish. This component was surrounded by components that fell off during testing and failed after 233 cycles.

Figure 71 is an x-ray image of the center region of the CSP-100 component in location U36. The PCB solder mask has a crack and is not homogeneous.

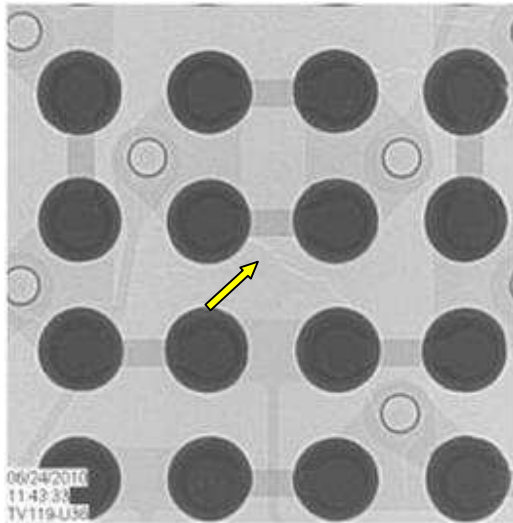


Figure 71 - TV119 U36; X-Ray Image, CSP-100

Figure 72 is an x-ray image for reference of the cross-section analysis in Figure 73. The number '1' and yellow circle indicate the location of pin 1 and the letter 'A' and dotted line indicate the row and level chosen for grinding.

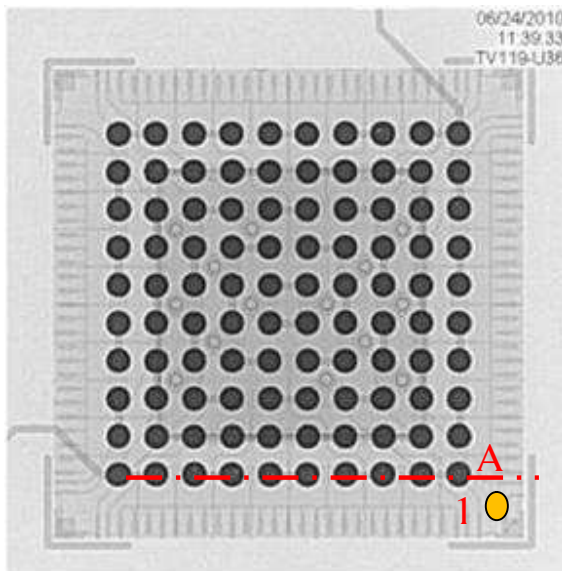


Figure 72 - TV119 U36; X-Ray Image for Reference of the Cross-Section Analysis

In Figure 73 on the left, cross-sectional micrographs of solder ball A1, A2, A9 and A10, at 274X magnification. On the right, the corresponding SEM images for solder ball A1 (300X), A2 (250X), A9 (220X) and A10 (220X).

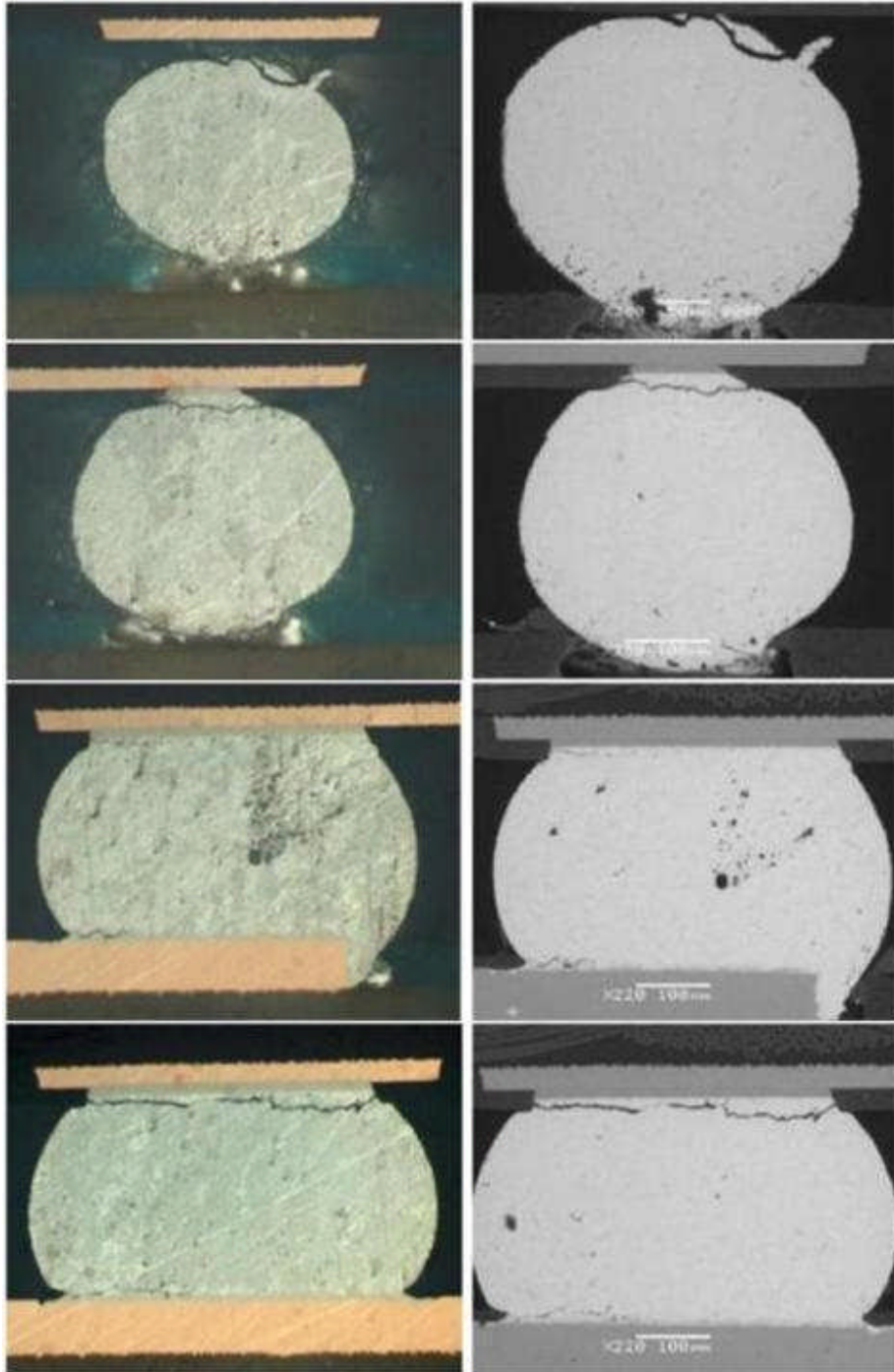


Figure 73 - TV119 U36; Cross-Sectional Micrographs of Solder Balls A1, A2, A9 and A10

Component location U39 is a TSOP-50 component from lead-free manufactured (Batch G), soldered with SN100C solder paste on SnPb component finish. This component was surrounded by components that fell off during testing and failed after 318 cycles. In Figure 74, an optical micrograph at 49X magnification showing cracked solder joints and cracks in the solder mask between leads 47 and 50.

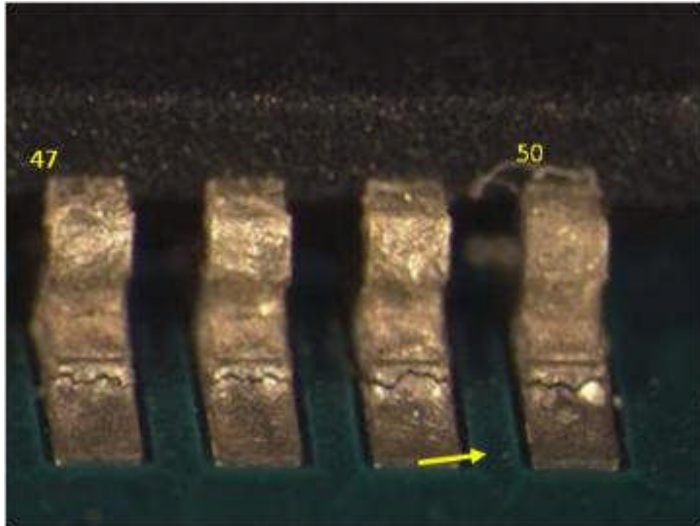


Figure 74 - TV119 U39; Optical Micrograph at 49X Magnification

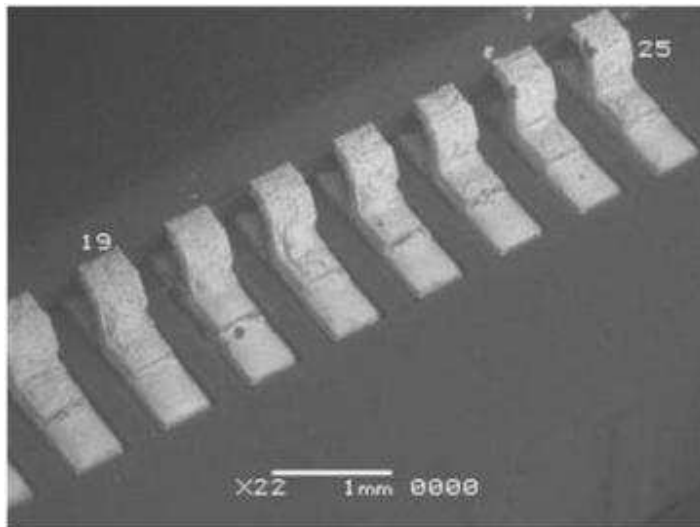


Figure 75 - TV119 U39; SEM Image of Leads 19-25 at 22X Magnification

Figure 76, SEM image, on the left is lead 25 at 70X magnification. SEM image on the right is lead 48-50 at 50X magnification.

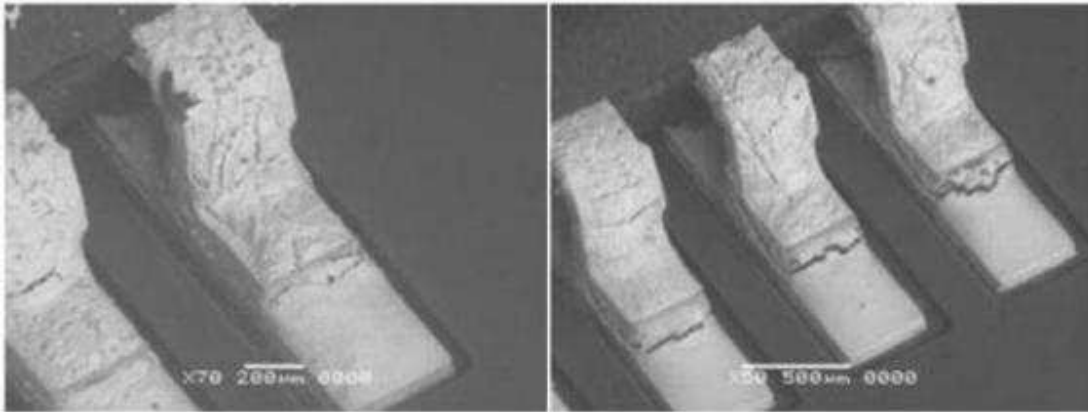


Figure 76 - TV119 U39; SEM Image, Lead 25

Figure 77, cross-sectional micrograph, on the left is lead 1 at 49X magnification. Micrograph on the right is lead 1 at 136X magnification.

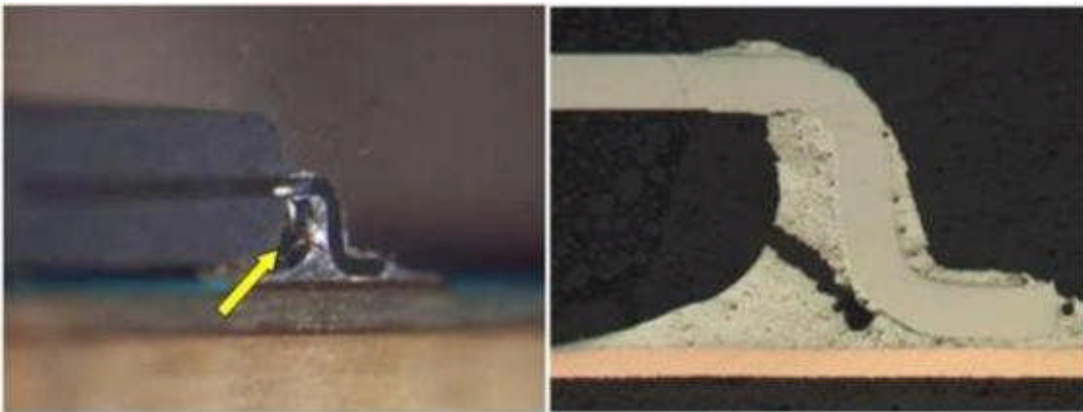


Figure 77 - TV119 U39; Cross-Sectional Micrograph, Lead 1

Figure 78, cross-sectional micrograph, on the left is lead 50 at 49X magnification. Micrograph on the right is lead 50 at 136X magnification.

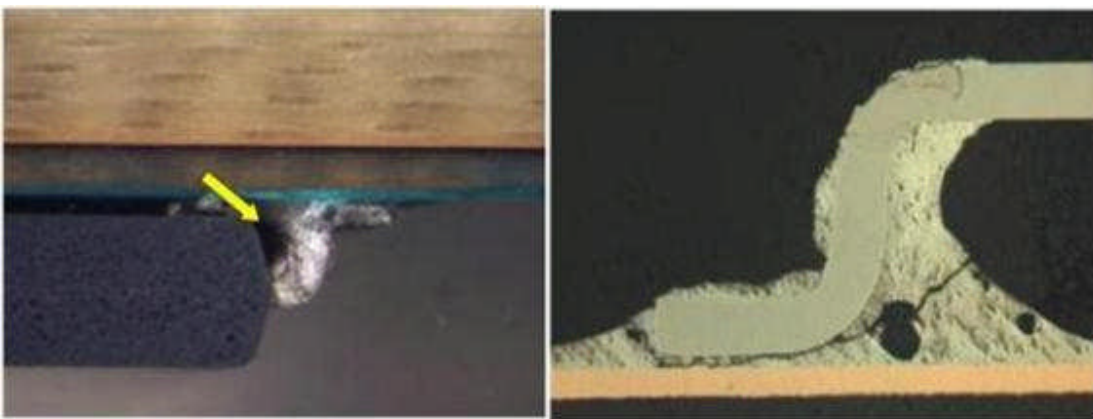


Figure 78 - TV119 U39; Cross-Sectional Micrograph, Lead 50

5.3.3.6 Test Vehicle 140

Component location U11 is a PDIP-20 from SnPb rework (Batch B), soldered with SnPb on SnPb component finish. This component had a damaged pad from the rework process and failed after 398 cycles. For the optical micrograph in Figure 79, on the left shows the suspect lead. Cross-sectional micrograph on the right is the suspect lead.

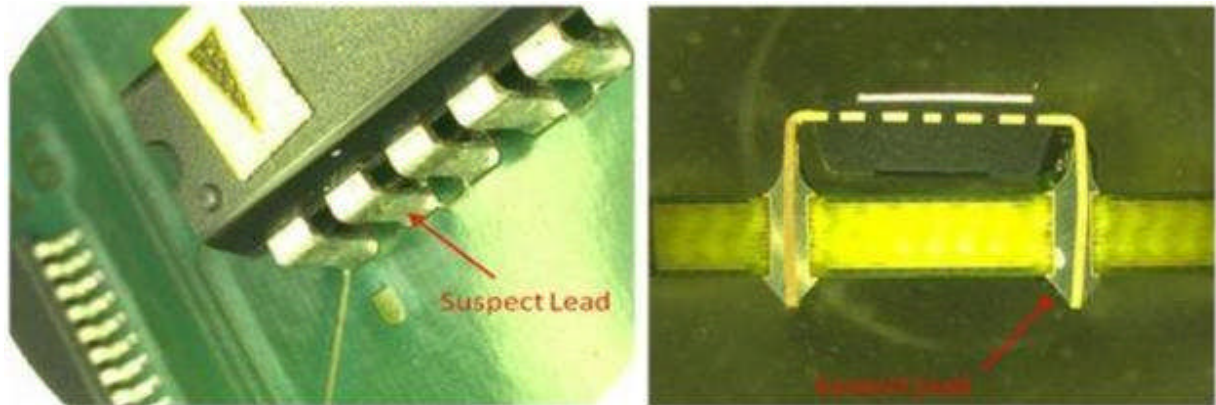


Figure 79 - TV140 U11; Optical Micrograph

Figure 80 shows the cross-sectional micrographs of the suspect lead in the PDIP-20 component showing solder joint crack initiation and lifted land.

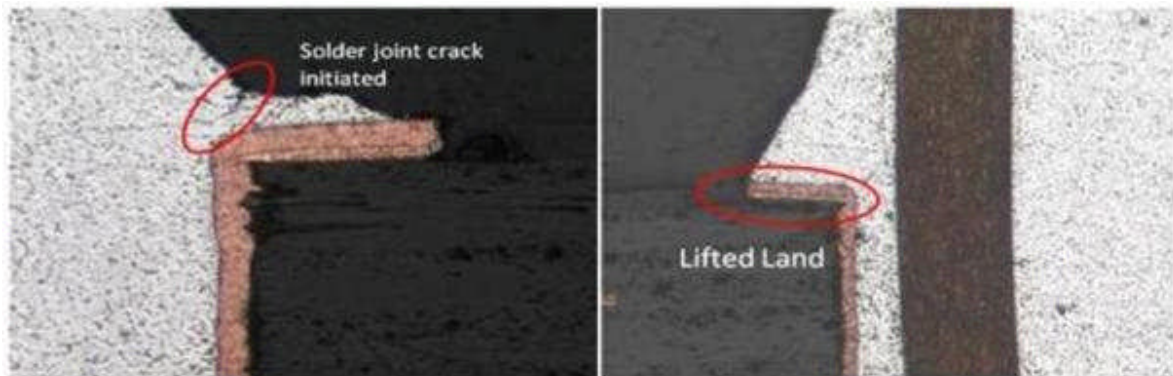


Figure 80 - TV140 U11; Cross-Sectional Micrographs, Suspect PDIP-20 Lead

5.3.3.7 Test Vehicle 142

Component location U13 is a CLCC-20 component from SnPb rework (Batch B), soldered with SnPb on SAC305 component finish. This component was adjacent to reworked components and survived all 650 cycles of testing.

Figure 81, optical micrograph, on the left shows the CLCC package lead numbering. Micrograph on the right shows an improperly sealed lid on the side for leads 1 – 5 where lead 1 is on the left at 19X magnification.

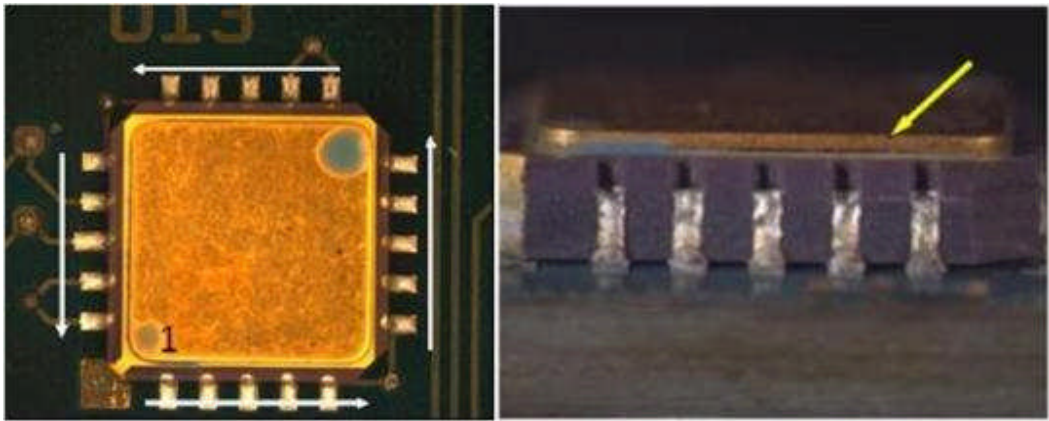


Figure 81 - TV142 U13; Optical Micrograph, CLCC Package Lead

For Figure 82, on the left are leads 6 – 10 starting with lead 6 on the left and on the right are leads 11 – 15 starting with lead 11 on the left. Minor solder cracking is visible.

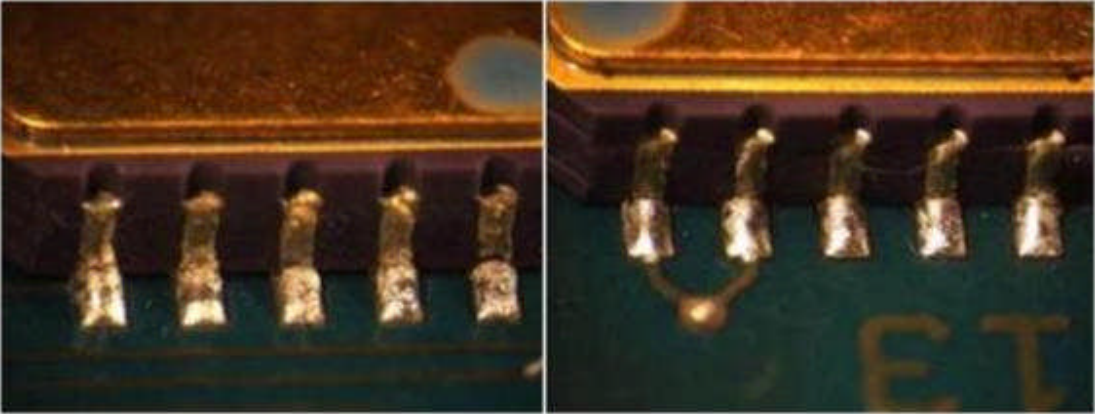


Figure 82 - TV142 U13 Optical Micrographs of CLCC-20 Leads at 24X Magnification

In Figure 83, on the left is the overall x-ray image and on the right is an x-ray of leads 6 – 10 with lead 6 being on the bottom.

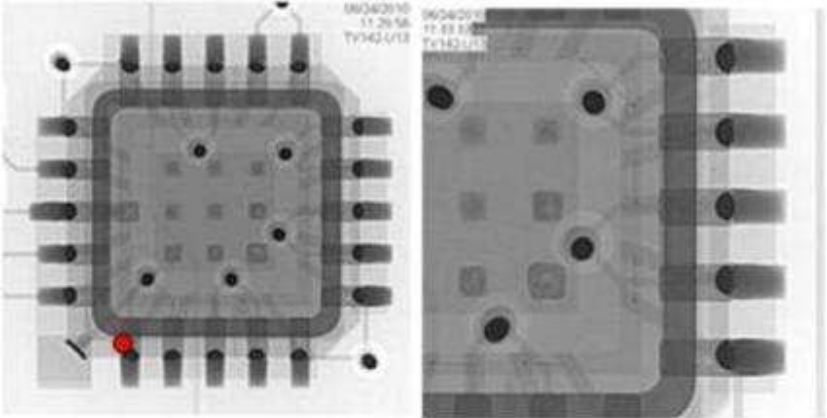


Figure 83 - TV142 U13 X-Ray Inspection of CLCC-20 Component.

In Figure 84 on the left are leads 6 – 10 which have some visible solder cracks and on the right are leads 16 – 20 and do not have solder cracks.

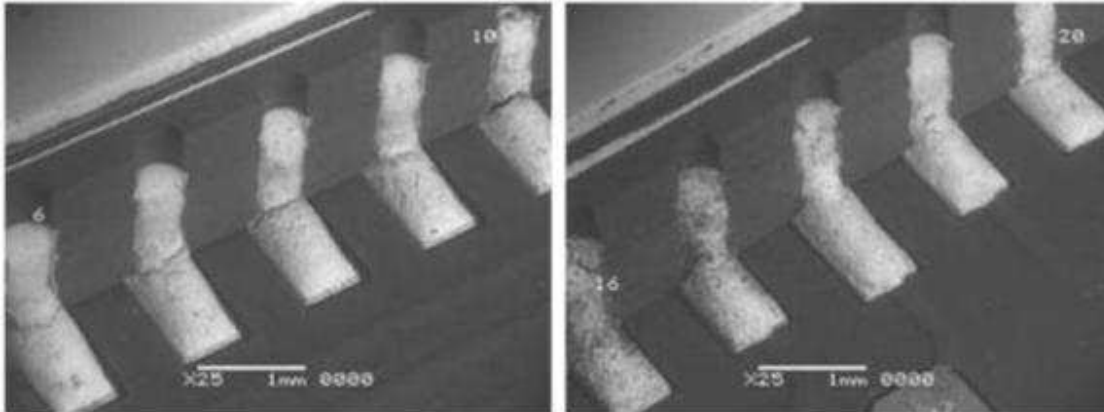


Figure 84 - TV142 U13 SEM Images of Component at 25X Magnification

In Figure 85, the upper left image is lead 8 where the arrow indicates a solder crack. The upper right image is lead 10 where a solder crack is also visible. The lower left image is lead 11 and the lower right image is lead 20.

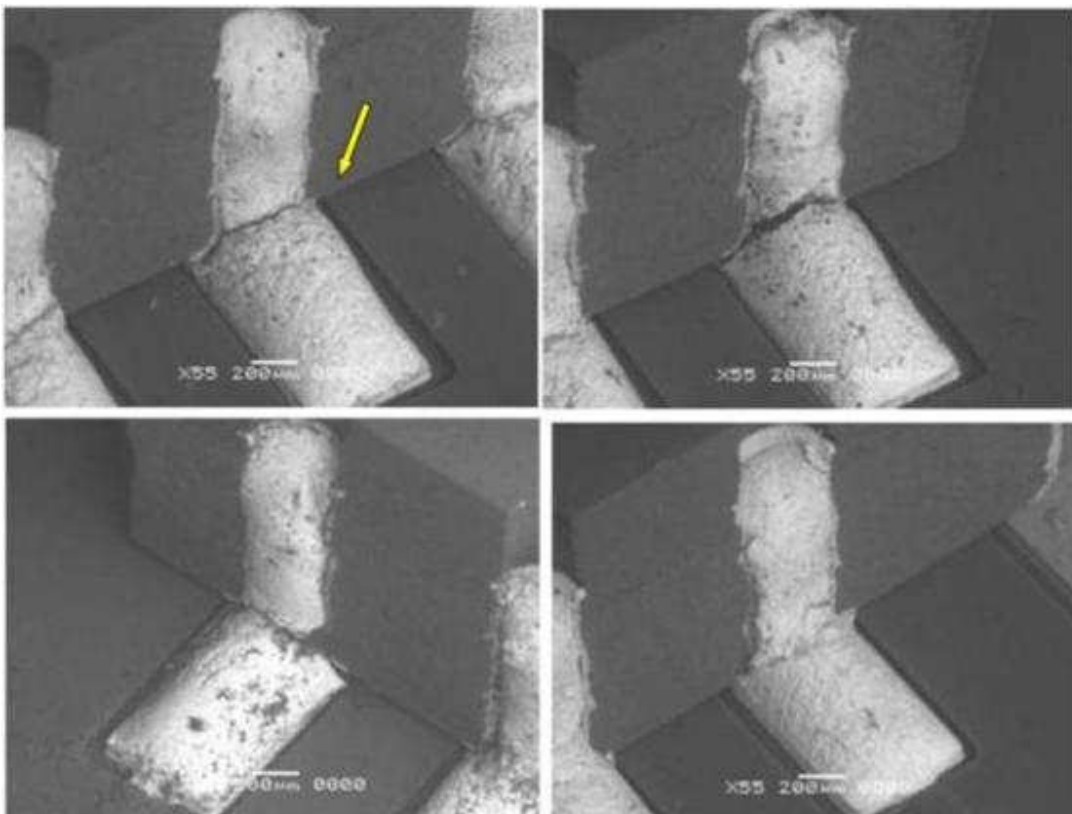


Figure 85 - TV142 U13 SEM Images of Selected Leads at 55X Magnification.

Figure 86 is an optical micrograph indicating the grinding levels of U13 CLCC-20 component.

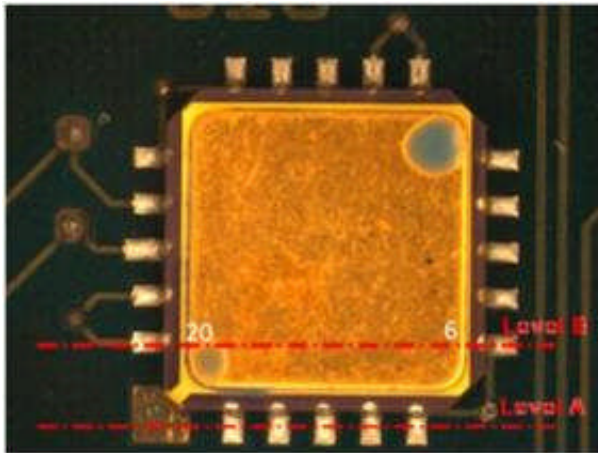


Figure 86 - TV142 U13; CLCC-20 Component

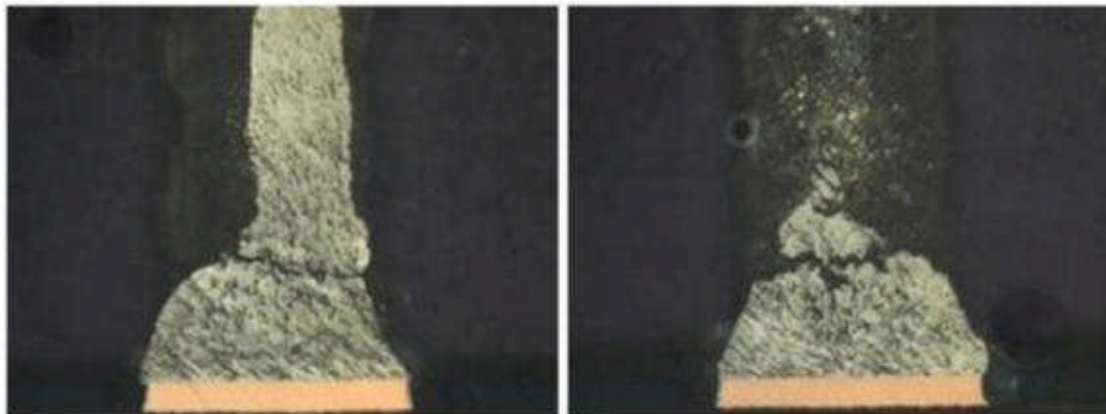


Figure 87, cross-sectional micrographs of lead 1 (left) and lead 5 (right) solder joints, grinding level A, at 136X magnification.

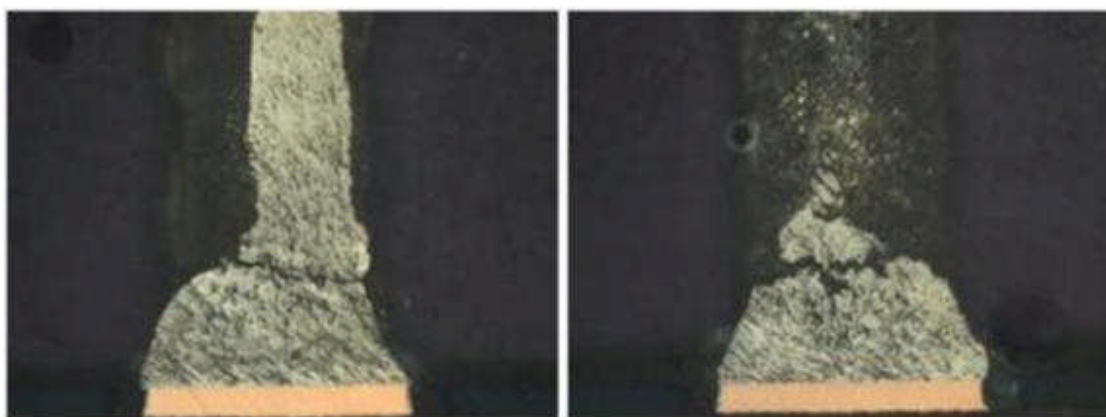


Figure 87 - TV142 U13; Cross-Sectional Micrographs of Lead 1 and Lead 5

Figure 88, cross-sectional micrograph, on the left shows grinding level A of leads 1 – 5 where the arrows indicate separation of the solder joints from the copper pads at 24X magnification. Micrograph on the right is lead 6 at 38X magnification just prior to grinding to level B.

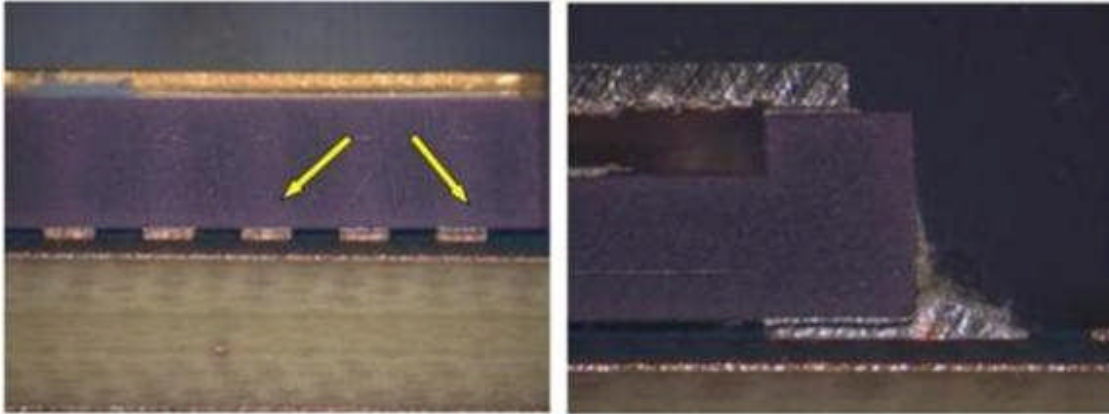


Figure 88 - TV142 U13; Cross-Sectional Micrograph

Figure 89, SEM image, on the left is the cross-section of lead 6 after grinding to level B at a 150X magnification. SEM image on the right is the cross-section of lead 20 after grinding to level B at 55X magnification.

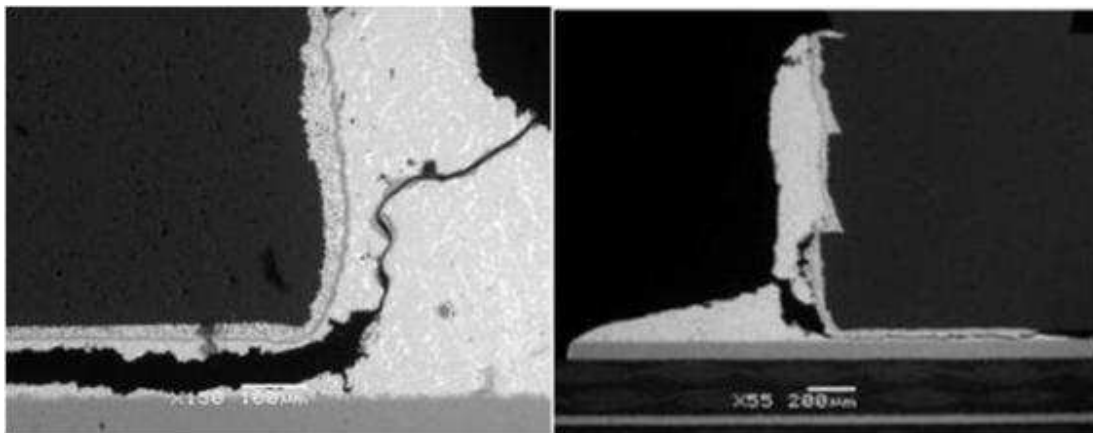


Figure 89 - TV142 U13; SEM Image

5.3.3.8 Test Vehicle 158, U6

Component location U6 is a reworked SnPb BGA-225 component soldered with SnPb solder paste, removed and replaced with a SAC405 BGA-225 component soldered with SnPb solder paste on an ENIG PWB. This component failed during the first cycle.

In Figure 90, the red circles indicate failed solder joints that are open.

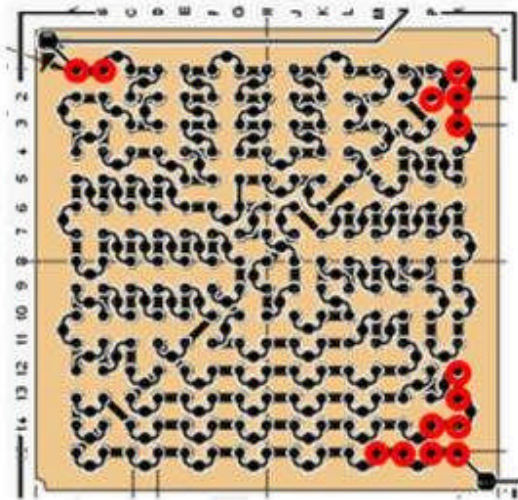


Figure 90 - TV158 U6; FA Results

The cross-sectional micrographs in Figure 91 show different solder structure in lands on board (7, 8) and lands on component (5, 6). Cracking to open along component land observed at 15-N.

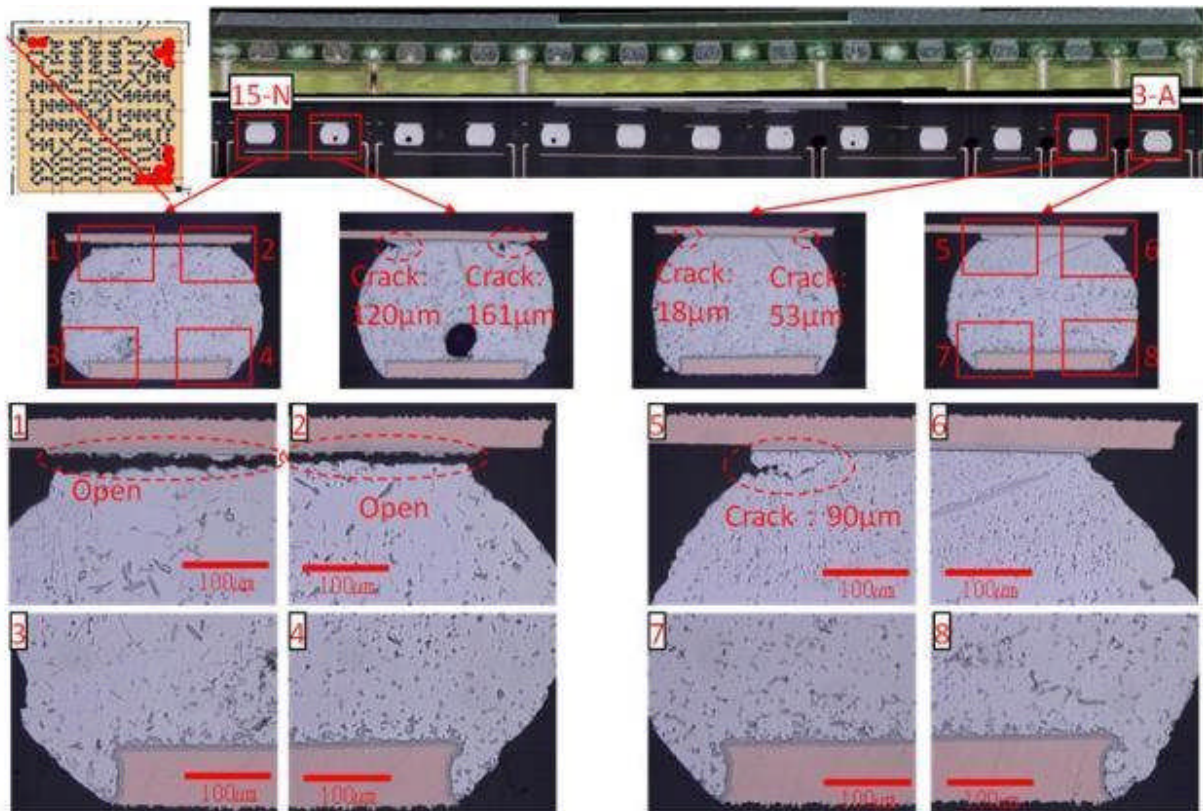


Figure 91 - TV158 U6; Cross-Sectional Micrographs

Figure 92 cross-sectional micrographs show different solder structure in lands on board (1, 2, 7, 8) and lands on component (3, 4, 5, 6). Cracking to open along PWB land found at 15-P.

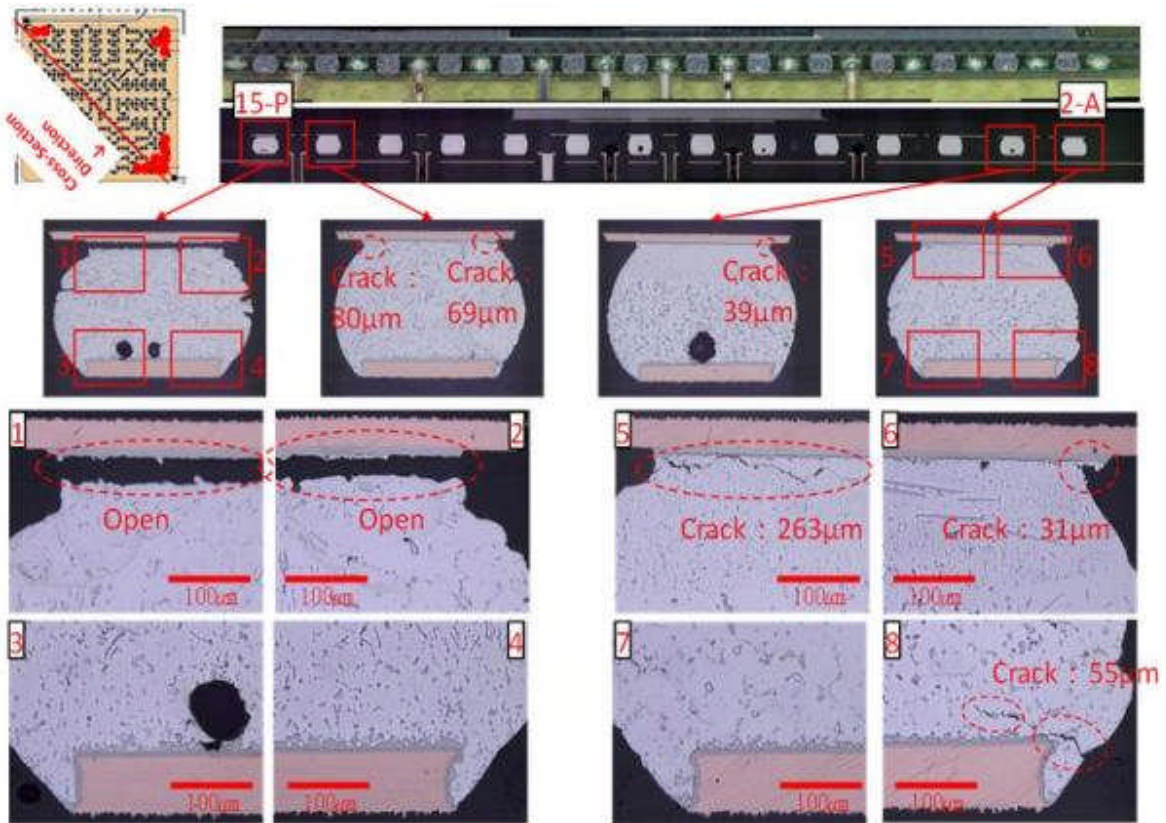


Figure 92 - TV158 U6; Cross-Sectional Micrographs

Cross-sectional micrographs in Figure 93 show different solder structure in lands on board (7, 8) and lands on component (5, 6). Cracking to open inside solder found at 1-A. Open joint along land on component found at 15-N.

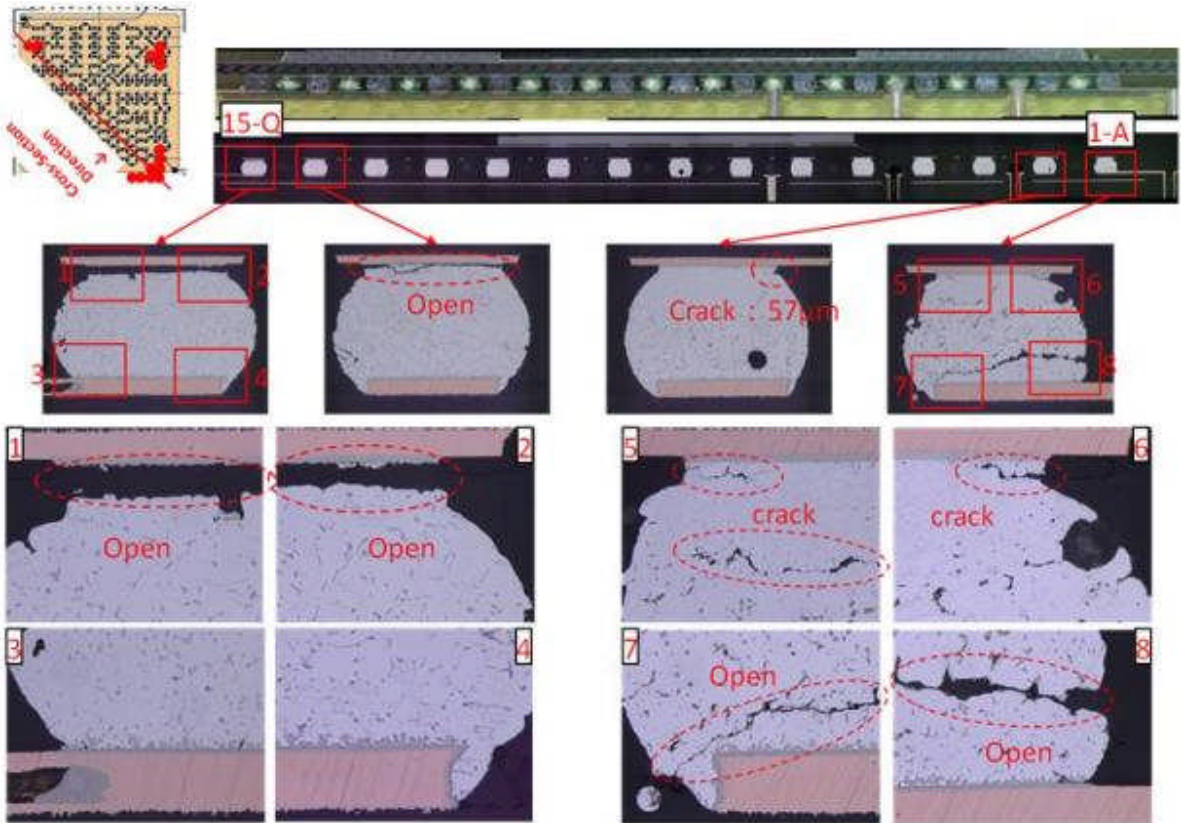


Figure 93 - TV158 U6; Cross-Sectional Micrographs

SEM mapping in Figure 94 shows segregation of Ag around land on component and segregation of Pb around PWB land. Higher concentrations of Pb detected in the cracking / breaking area.

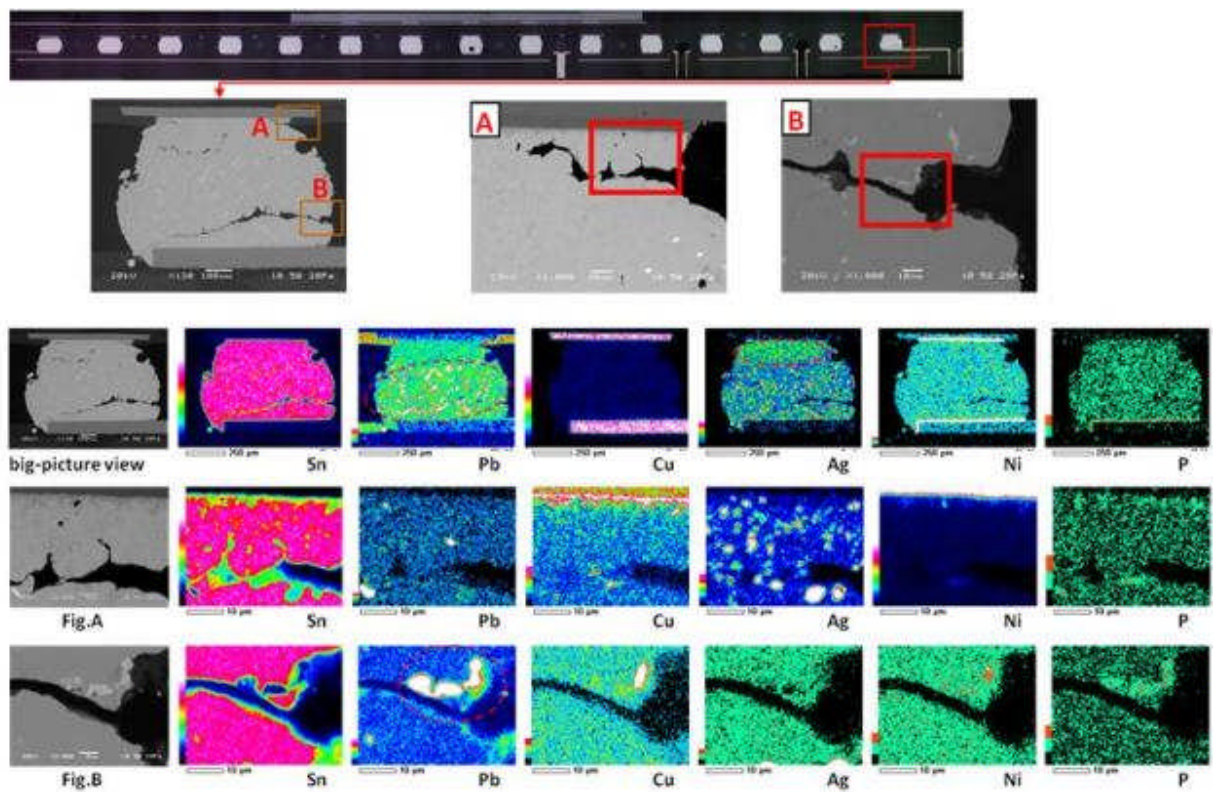


Figure 94 - TV158 U6; SEM Mapping

SEM mapping in Figure 95 shows solder is well blended over all except around component land where higher levels of Pb and cracking were found. Segregation of P from the ENIG board finish, however, no cracking detected.

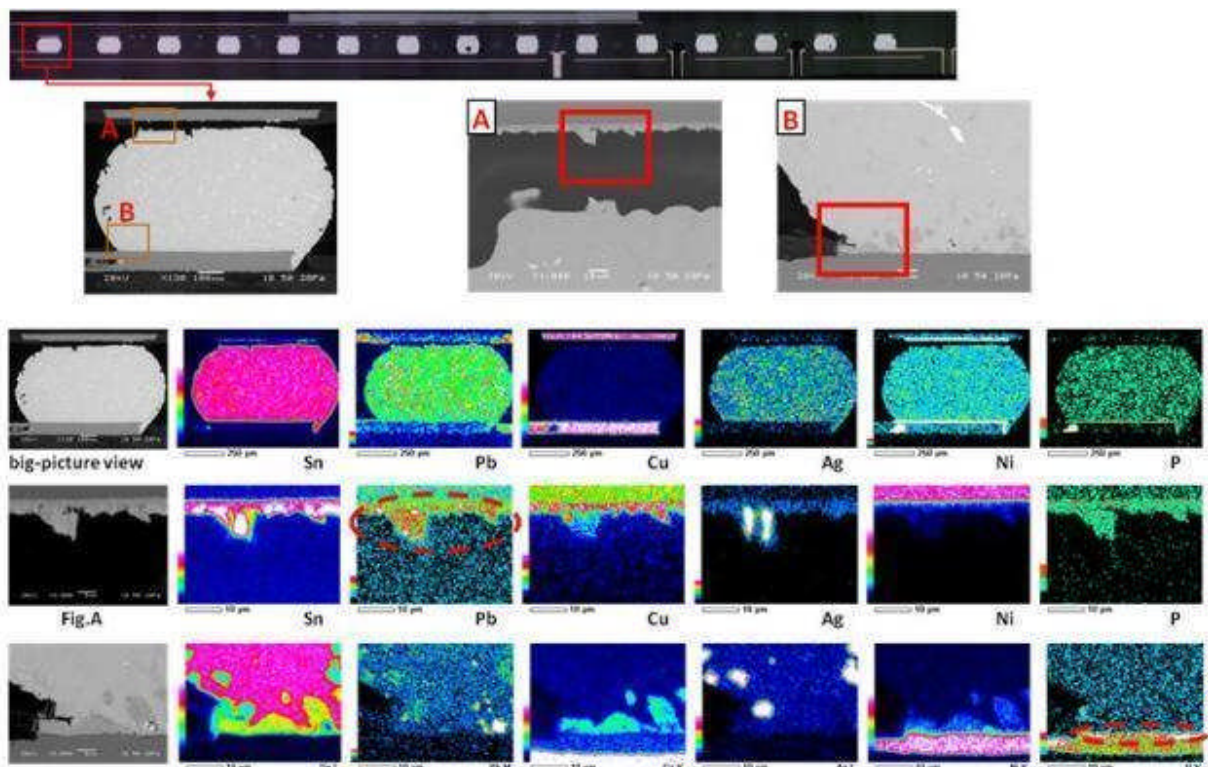


Figure 95 - TV158 U6; SEM Mapping

In Figure 96 the distance between component and board at each sphere is almost the same under the chip in the center. The distance becomes smaller further to the end. Comparing the distance at [1-A] and [15-Q], [1-A] has smaller distance.

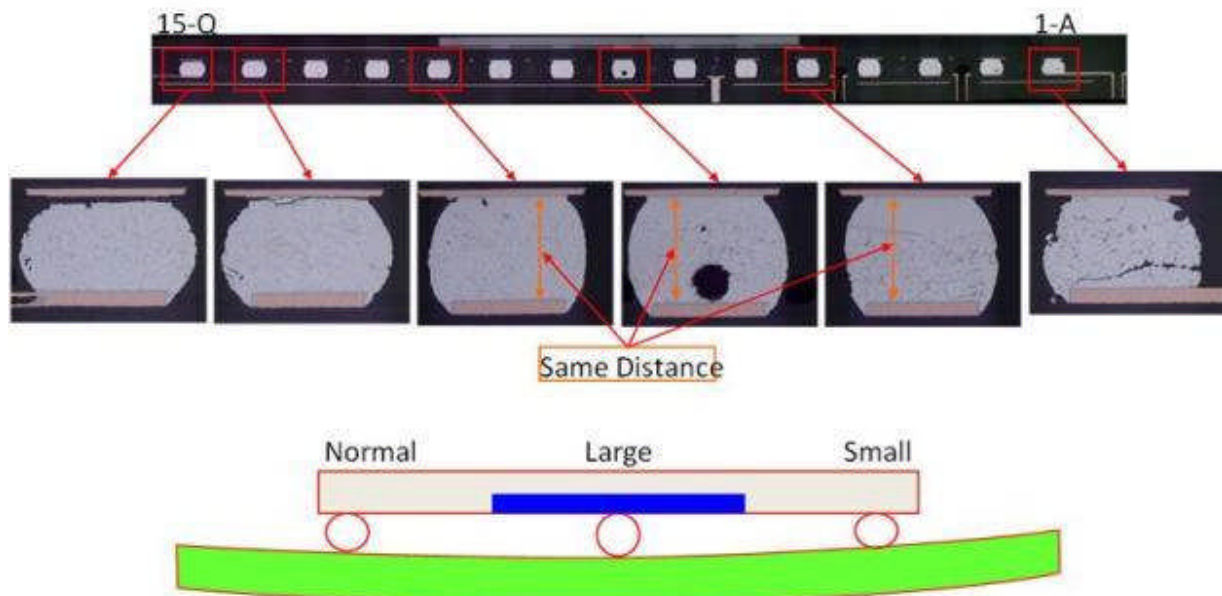


Figure 96 - TV158 U6; Cross-Sectional Micrographs Show Warping on BGA-225

5.3.3.9 Test Vehicle 180

Component location U21 is a reworked BGA-225 soldered with SAC305 on SAC405 component finish and replaced with SAC405 BGA-225 soldered with flux only. This component failed on cycle one and was reworked prior to combine environments testing.

In Figure 97 the yellow circles are solder joints with high resistance and red circles are failed solder joints that are open.

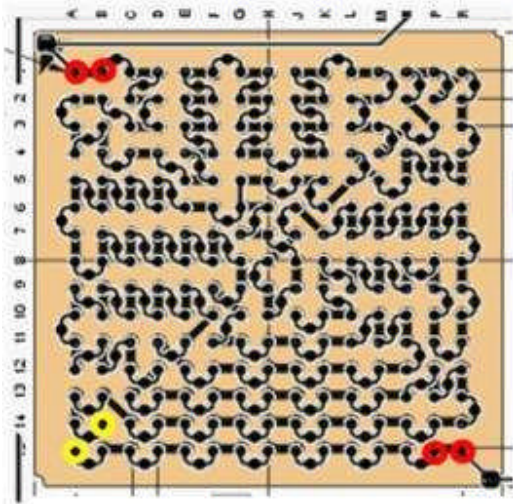


Figure 97 - TV180 U21; FA Results

In Figure 98 the cross-sectional micrographs show cracking to opens on board side (1, 2, 5, 6).

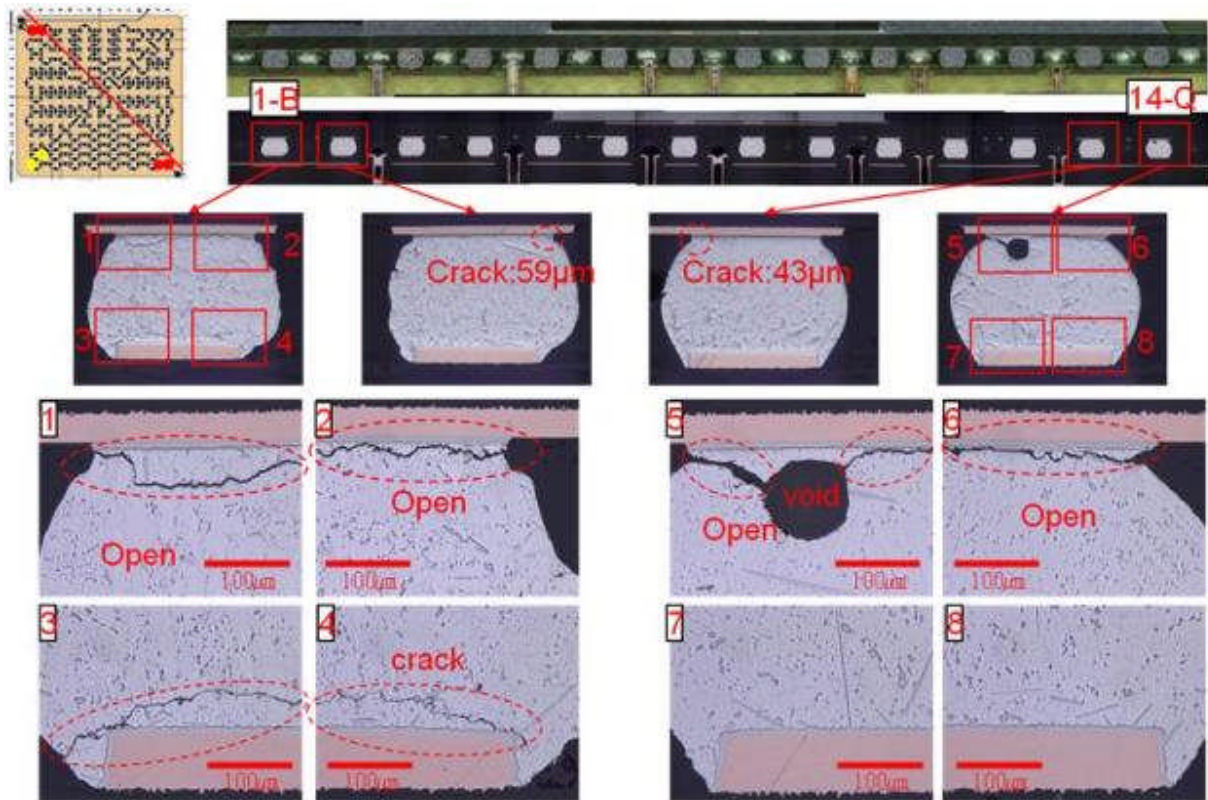


Figure 98 - TV180 U21; Cross-Sectional Micrographs

In Figure 99 the cross-sectional micrographs show cracking to open solder joints around both land on board and component (3, 4, 5, 6). Large intermetallic compounds observed around land on board (3, 4, 7, 8).

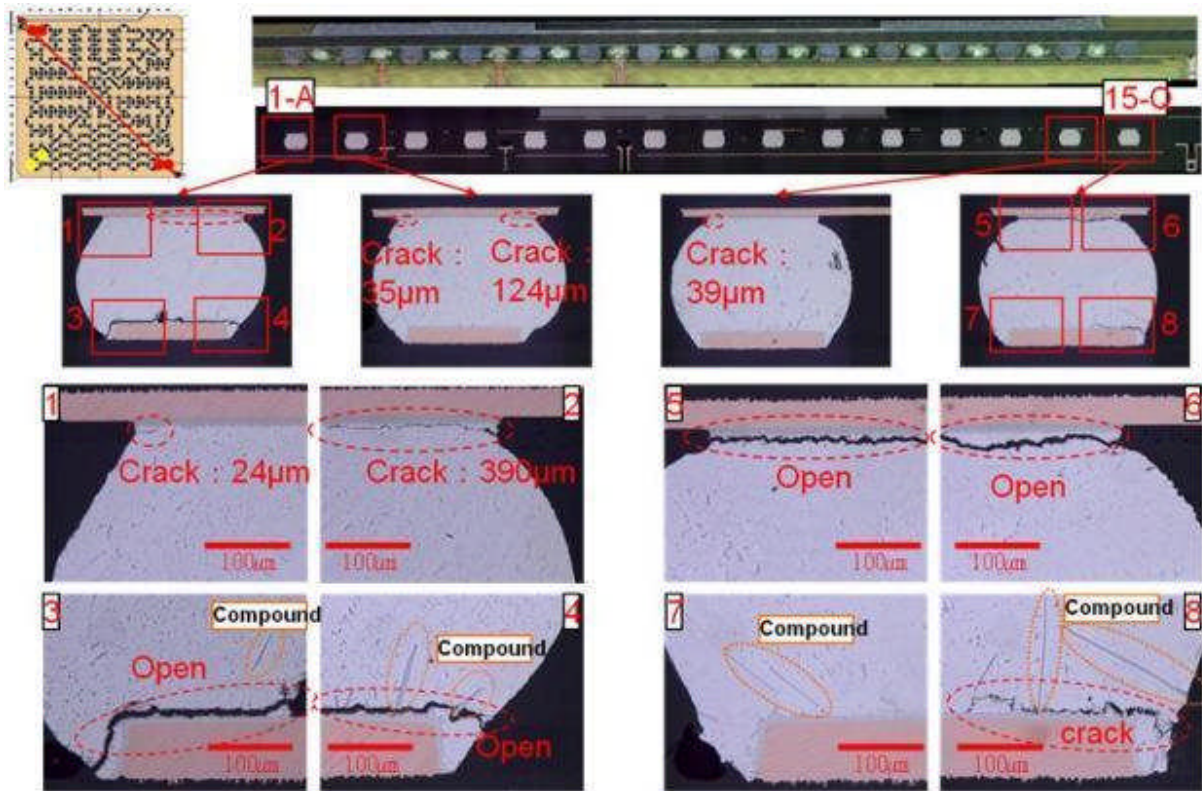


Figure 99 - TV180 U21; Cross-Sectional Micrographs

SEM mapping in Figure 100 shows cracks inside solder as well as cracking to open between IMC and solder, or inside solder.

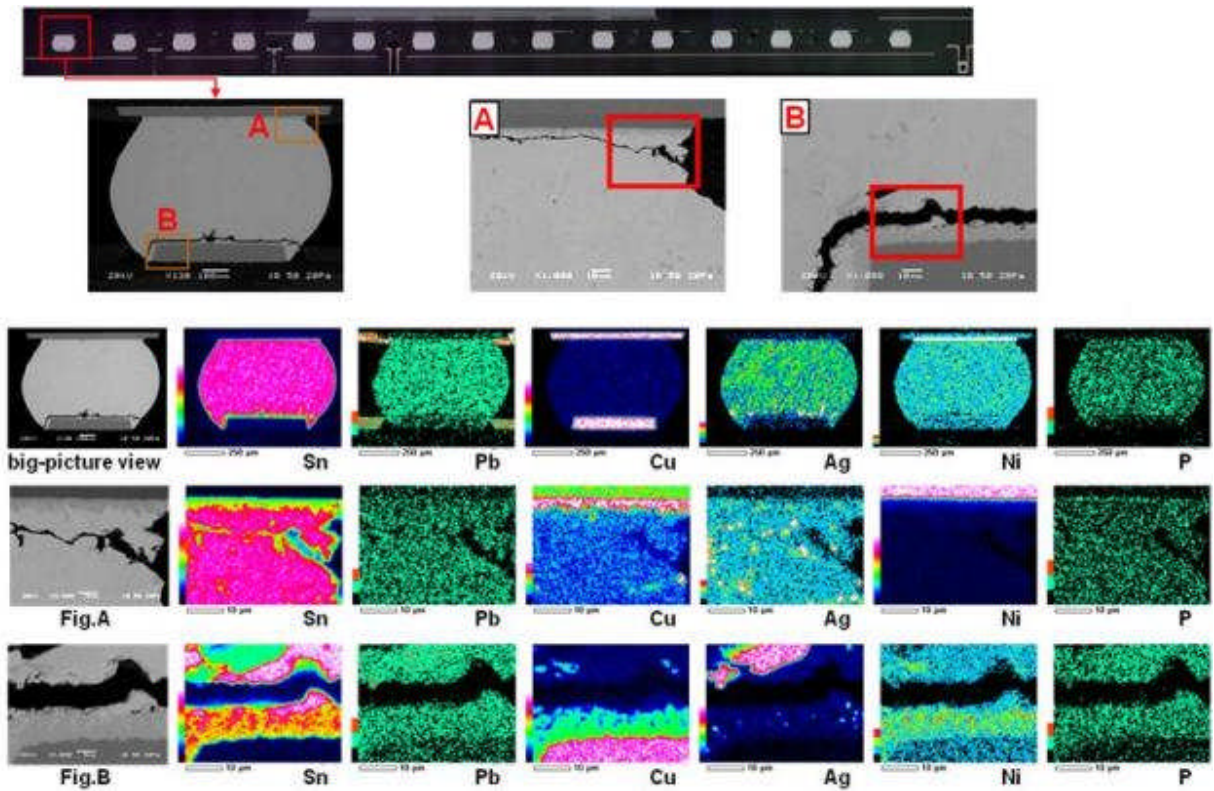


Figure 100 - TV180 U21; SEM Mapping

5.3.3.10 Test Vehicle 181

Component location U56 is a BGA-225 from the Pb-free rework (Batch A), soldered with SAC305 on SAC405 component finish. This component failed on cycle one and was reworked prior to combine environments testing.

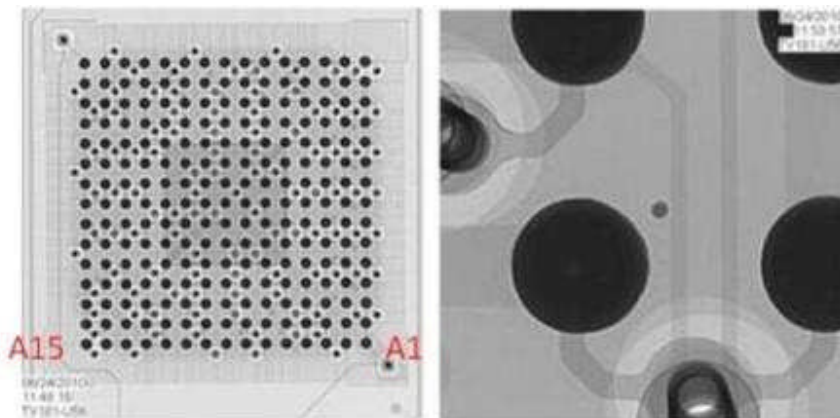


Figure 101 - X-Ray Inspection of TV181 U56 BGA-225

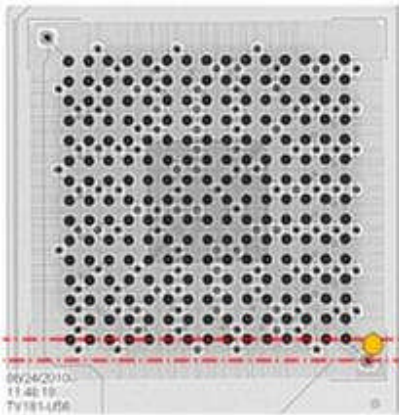


Figure 102 - TV181 U56; X-Ray Image Showing the Grinding Levels

In Figure 103 the image on the left is at 24X magnification and the image on the right is at 136X magnification.

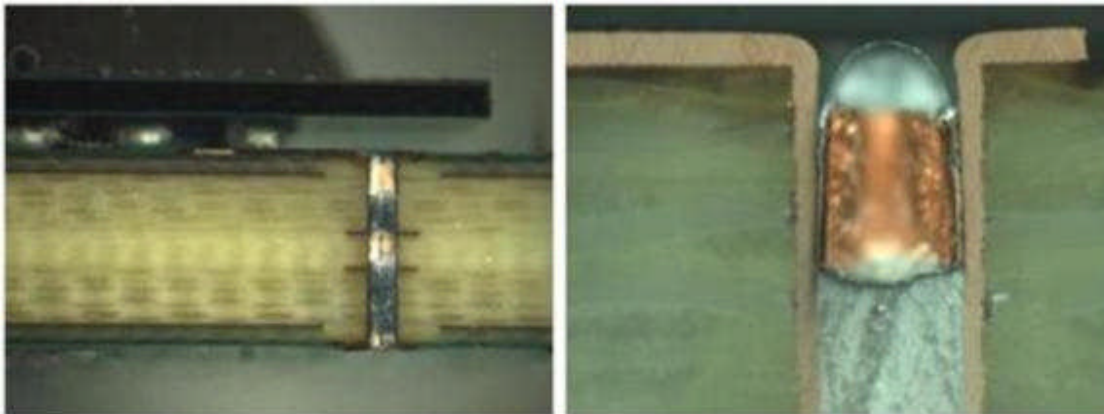


Figure 103 - TV181 U56; Cross-Sectional Micrographs of Via Hole Connected to Ball A1

In Figure 104 the image on the top left is solder ball A1 at 136X magnification. The image on the top right is solder ball A7 at 274X magnification. On the bottom left, is solder ball A9 and on the bottom right is solder ball A11, both at 136X magnification.

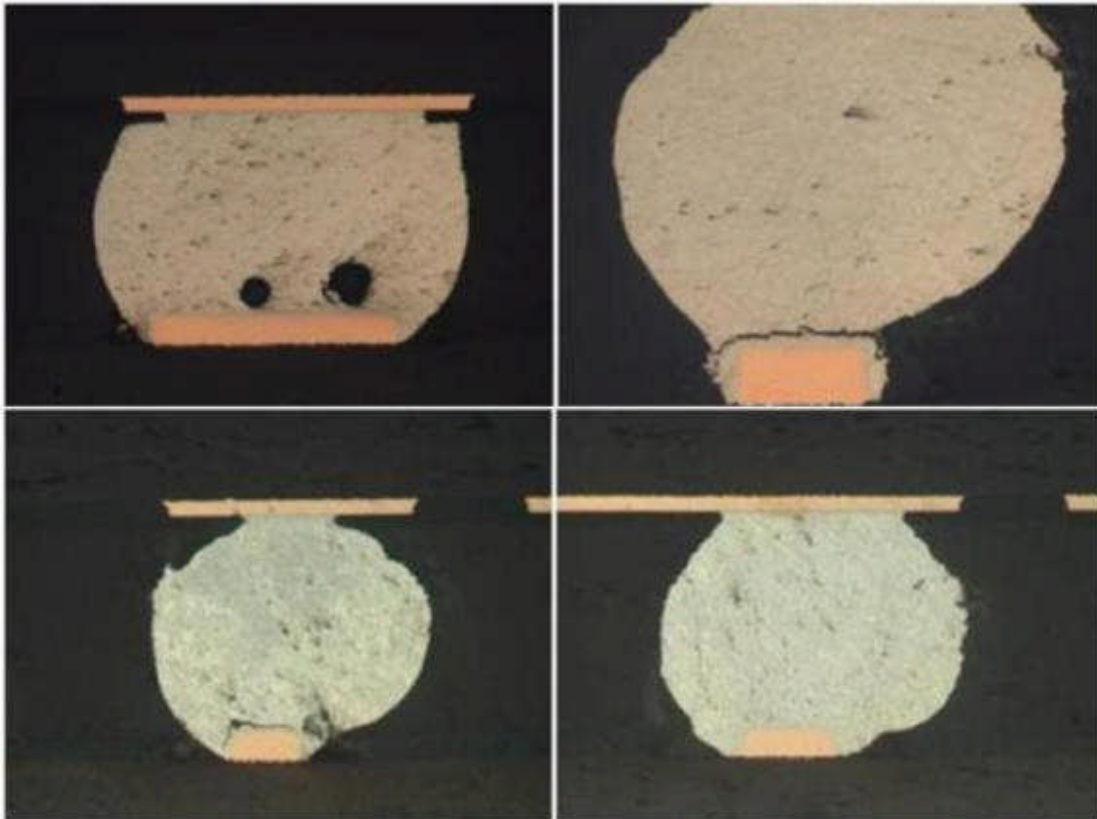


Figure 104 - TV181 U56; Cross-Sectional Micrographs of Solder Balls

In Figure 105 the image on the left is at 140X magnification and the image on the right is at 370X magnification.

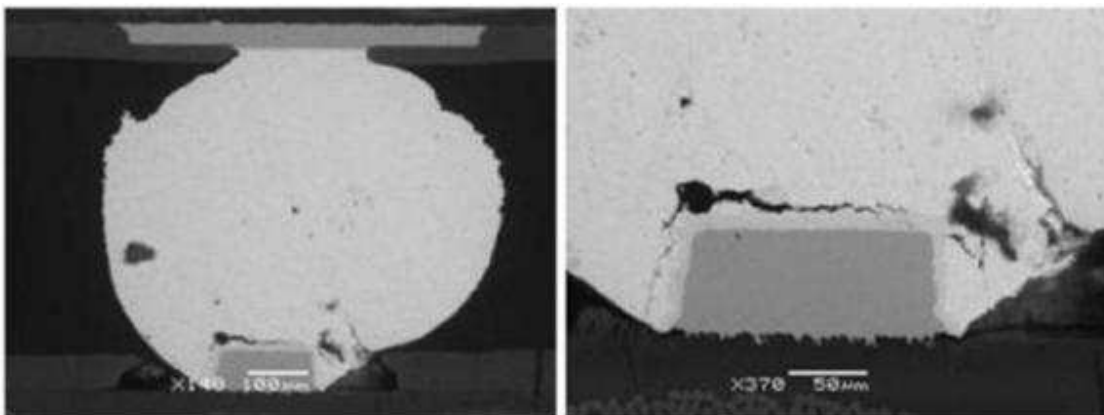


Figure 105 - TV181 U56; SEM Image of Solder Ball A9 Cross-Section

Component location U25 is a TSOP-50 from the Pb-free rework (Batch A), soldered with SAC305 on tin component finish. This component failed on cycle one and was reworked prior to combine environments testing.

In Figure 106 the optical micrograph on the left is the lead numbering and the image on the right is of leads 21-25. The arrows indicate cracked solder mask and the arrow on lead 22 indicates a solder disturbance at 49X magnification.

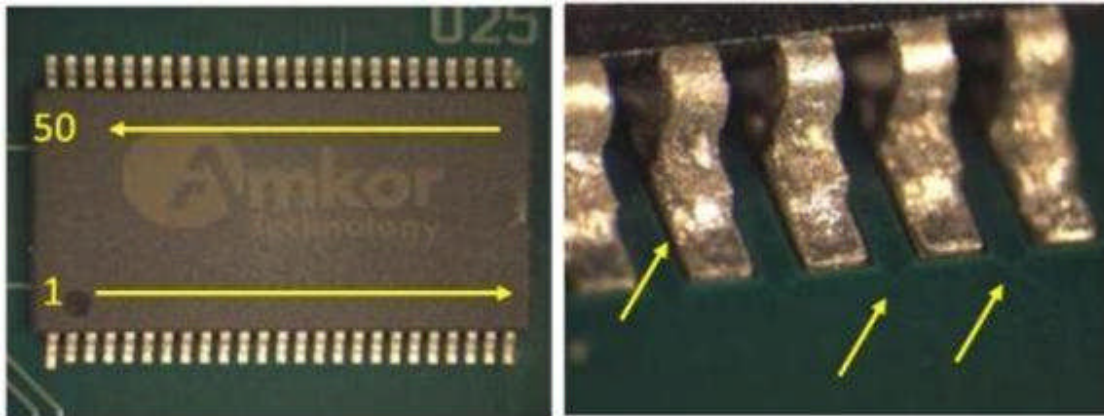


Figure 106 - TV181 U25; Optical Micrographs

In Figure 107 x-ray images of leads 22 -25 on the left and lead 22 on the right.

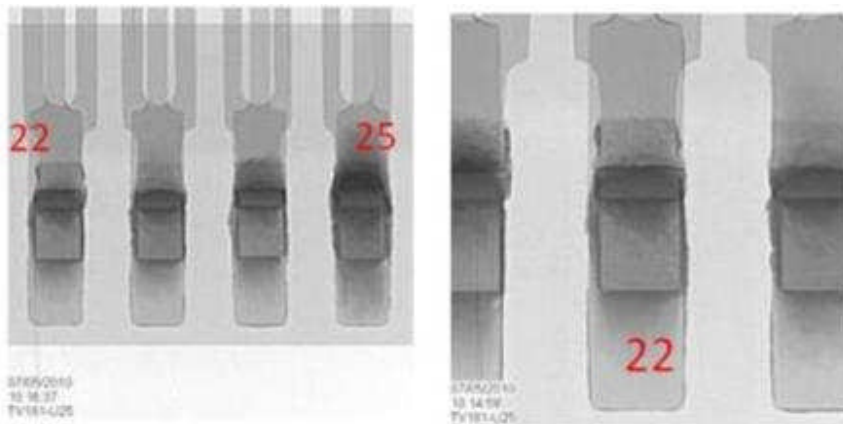


Figure 107 - TV181 U25; X-Ray Images of Component Leads

Figure 108 shows SEM images of leads 19-25 on the left and leads 44-50 on the right at a magnification of 22X.

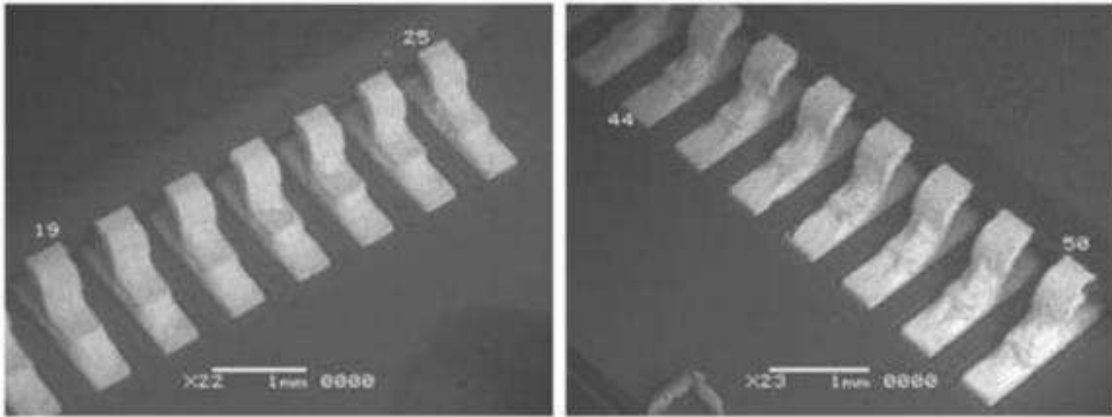


Figure 108 - TV181 U25; SEM Images

Optical micrographs in Figure 109 show grinding levels in the image on the left and a cross-sectional view of lead 1, level 1, at 30X magnification on the right.

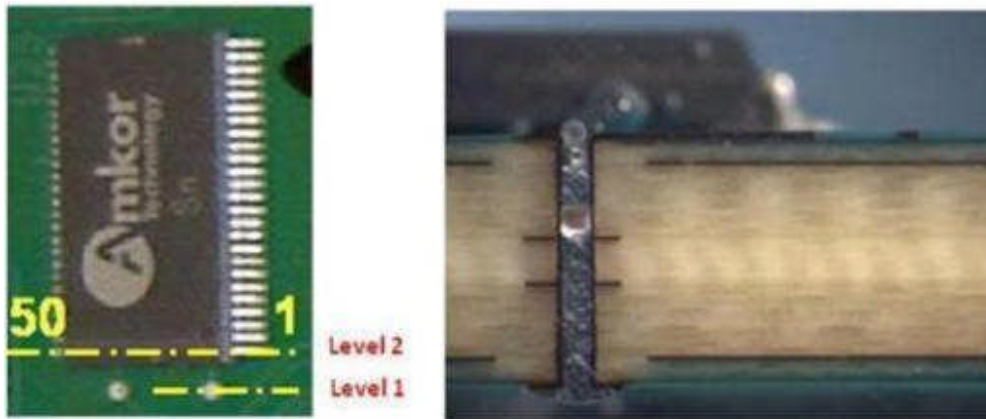


Figure 109 - TV181 U25; Optical Micrographs

Figure 110 shows cross-sectional micrographs of lead 2 (left) and lead 50 (right), level 2 grinding, at 136X magnification.

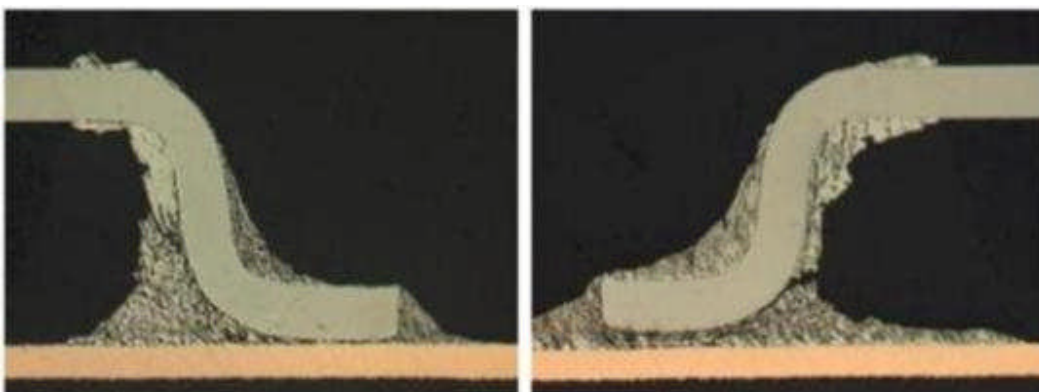


Figure 110 - TV181 U25; Cross-Sectional Micrographs

Figure 111 shows a SEM image of cross-section lead 2, level 2 grinding at 150X magnification.

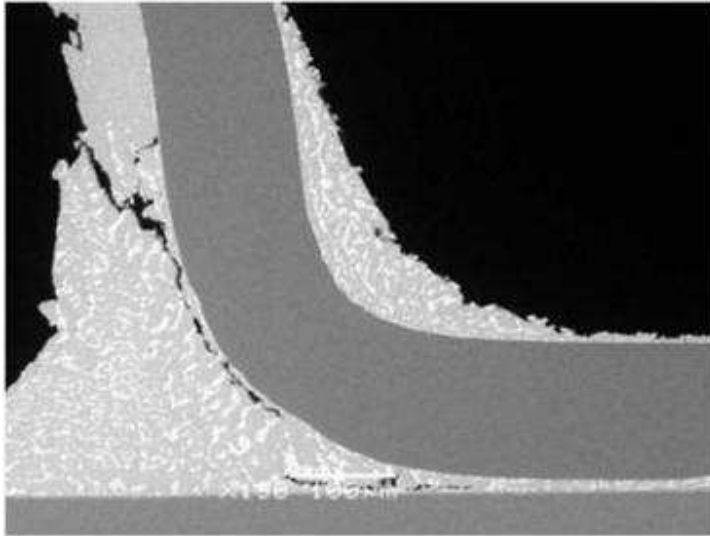


Figure 111 - TV181 U25; SEM Image

5.3.3.11 Test Vehicle 183

Component location U41 is a TQFP-144 from Pb-free rework (Batch A), soldered with SAC 305 on SAC305 dip component finish. This component failed on cycle one and was not reworked.

Figure 112 shows inadequate solder joint resulting in no connection between the lead and the pad.

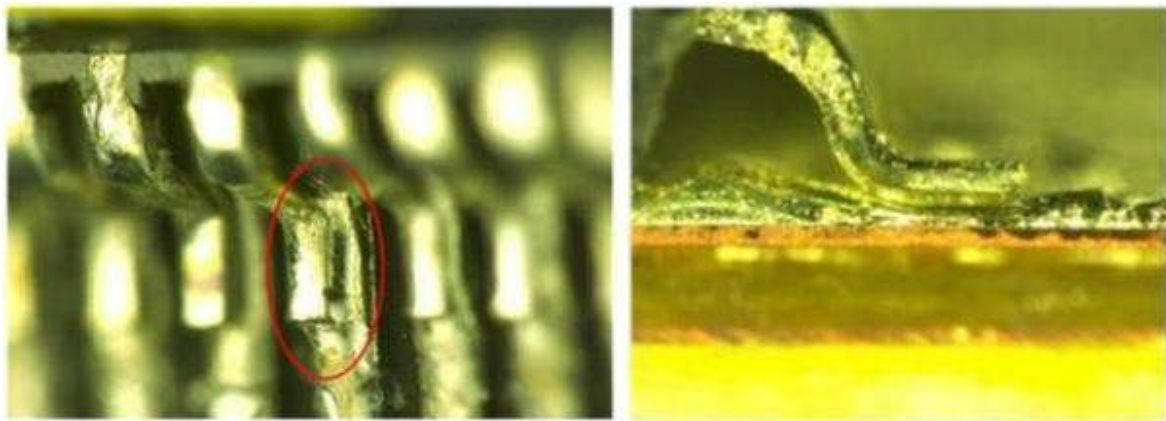
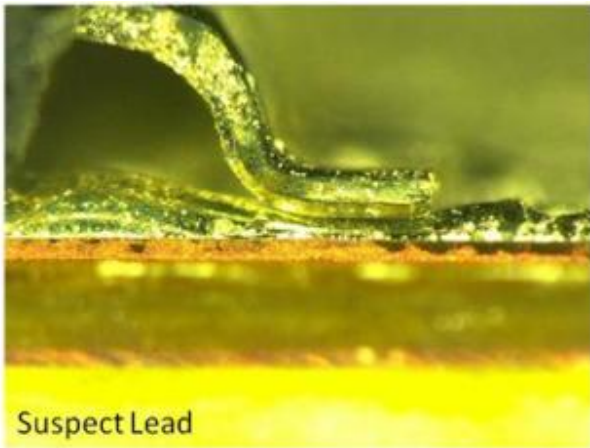
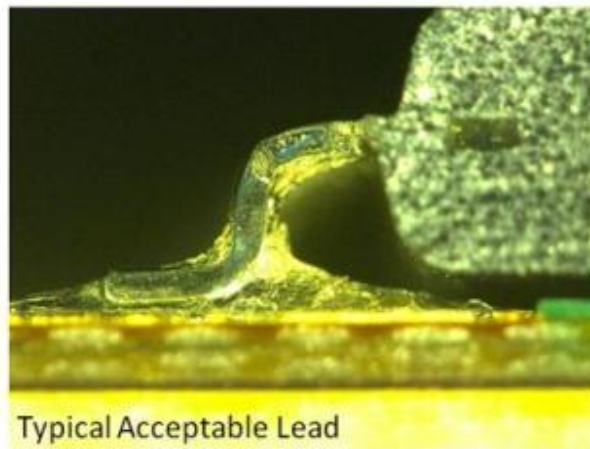


Figure 112 - TV183 U 41; Optical Micrographs of Suspect Lead

Figure 113 shows cross-sectional micrographs of component leads comparing suspect lead to a typical acceptable lead.



Suspect Lead



Typical Acceptable Lead

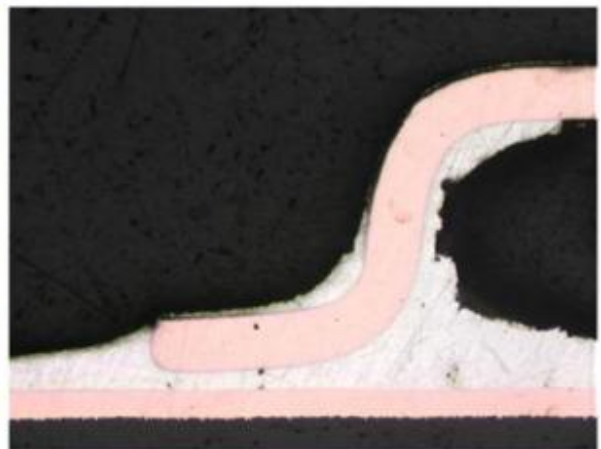


Figure 113 - TV183 U 41; Cross-Sectional Micrographs

5.3.4 Combined Environments Test Summary Tables

Table 26 and Table 28 provide a qualitative comparative summary of the relative performance of the Pb-free solder alloys based on N1, N10 and N63. Table 26 is for “Manufactured” test vehicles and Table 28 is for “Rework” test vehicles. Please note, for Table 28, the data for SnPb/SnPb Manufactured test vehicles was used as the baseline for the relative solder performance, rework test vehicles. All comparisons are based on a two-parameter Weibull analysis of the data.

Baseline SnPb data and other solder alloy/component finish data which is within 5% of the baseline is denoted with a 0. Single symbols, – or +, denote data that is 5% to 20% above (+) or below (-) the baseline. Double symbols, -- or ++, denote data that is more than 20% above (++) or below (--) the baseline. Green cells denote performance better than the SnPb baseline. Yellow cells denote performance worse than the SnPb baseline. Red cells denote data that is grossly worse than the SnPb baseline. Numerical values can be found in the “Weibull Numbers” Tables.

Table 25 - Combined Environments Test; Summary of Manufactured Test Vehicle Test Results

Board Finish	Component	Alloy	Finish	Nf (1%)	Nf (10%)	Nf (63.2%)
ENIG	BGA-225	SAC305	SAC405			
ENIG	BGA-225	SAC305	SnPb	17	76	323
ENIG	CLCC-20	SAC305	SAC305	156	299	560
ENIG	CLCC-20	SAC305	SnPb	214	333	508
ENIG	CSP-100	SAC305	SAC105			
ENIG	CSP-100	SAC305	SnPb			
ENIG	PDIP-20	SN100C	Sn			
ENIG	PTH	SN100C	ENIG			
ENIG	QFN-20	SAC305	Matte Sn			
ENIG	TQFP-144	SAC305	Matte Sn			
ENIG	TQFP-144	SAC305	SnPb Dip			
ENIG	TSOP-50	SAC305	SnBi			
ENIG	TSOP-50	SAC305	SnPb			
ImAg	BGA-225	SAC305	SAC405	70	224	683
ImAg	BGA-225	SN100C	SAC405	54	182	586
ImAg	BGA-225	SnPb	SAC405	22	58	146
ImAg	BGA-225	SAC305	SnPb	35	142	539
ImAg	BGA-225	SN100C	SnPb	10	68	428
ImAg	BGA-225	SnPb	SnPb	64	226	757
ImAg	CLCC-20	SAC305	SAC305	153	267	456
ImAg	CLCC-20	SN100C	SAC305	85	204	470
ImAg	CLCC-20	SnPb	SAC305	158	278	475
ImAg	CLCC-20	SAC305	SnPb	141	237	390
ImAg	CLCC-20	SN100C	SnPb	121	239	461
ImAg	CLCC-20	SnPb	SnPb	258	373	530
ImAg	CSP-100	SAC305	SAC105	409	536	694
ImAg	CSP-100	SN100C	SAC105	229	422	757
ImAg	CSP-100	SnPb	SAC105	186	338	600
ImAg	CSP-100	SAC305	SnPb	453	553	669
ImAg	CSP-100	SN100C	SnPb	331	480	684
ImAg	CSP-100	SnPb	SnPb	458	539	629
ImAg	PDIP-20	SN100C	NiPdAu			
ImAg	PDIP-20	SnPb	NiPdAu			
ImAg	PDIP-20	SN100C	Sn	327	638	1209
ImAg	PDIP-20	SnPb	Sn			
ImAg	PTH	SN100C	ImAg			
ImAg	PTH	SnPb	ImAg			
ImAg	QFN-20	SAC305	Matte Sn			
ImAg	QFN-20	SN100C	Matte Sn	478	520	564
ImAg	QFN-20	SnPb	Matte Sn			

Board Finish	Component	Alloy	Finish	Nf (1%)	Nf (10%)	Nf (63.2%)
ImAg	TQFP-144	SAC305	Matte Sn	452	535	629
ImAg	TQFP-144	SN100C	Matte Sn	235	417	720
ImAg	TQFP-144	SnPb	Matte Sn	308	488	757
ImAg	TQFP-144	SAC305	SnPb Dip			
ImAg	TQFP-144	SN100C	SnPb Dip	265	432	691
ImAg	TQFP-144	SnPb	SnPb Dip			
ImAg	TSOP-50	SAC305	SnBi	169	313	562
ImAg	TSOP-50	SN100C	SnBi	82	181	389
ImAg	TSOP-50	SnPb	SnBi	268	413	625
ImAg	TSOP-50	SAC305	SnPb	132	312	713
ImAg	TSOP-50	SN100C	SnPb	88	226	560
ImAg	TSOP-50	SnPb	SnPb	136	318	718

Table 26 - Combined Environments Test; Relative Solder Performance, Manufactured Test Vehicles

Board Finish	Component	Alloy	Finish	Nf (1%)	Nf (10%)	Nf (63.2%)
ImAg	BGA-225	SAC305	SAC405	+	0	-
ImAg	BGA-225	SN100C	SAC405	-	-	--
ImAg	BGA-225	SnPb	SAC405	--	--	--
ImAg	BGA-225	SAC305	SnPb	--	--	--
ImAg	BGA-225	SN100C	SnPb	--	--	--
ImAg	BGA-225	SnPb	SnPb	0	0	0
ImAg	CLCC-20	SAC305	SAC305	--	--	-
ImAg	CLCC-20	SN100C	SAC305	--	--	-
ImAg	CLCC-20	SnPb	SAC305	--	--	-
ImAg	CLCC-20	SAC305	SnPb	--	--	--
ImAg	CLCC-20	SN100C	SnPb	--	--	-
ImAg	CLCC-20	SnPb	SnPb	0	0	0
ImAg	CSP-100	SAC305	SAC105	-	0	+
ImAg	CSP-100	SN100C	SAC105	--	--	--
ImAg	CSP-100	SnPb	SAC105	--	--	0
ImAg	CSP-100	SAC305	SnPb	0	0	0
ImAg	CSP-100	SN100C	SnPb	--	-	+
ImAg	CSP-100	SnPb	SnPb	0	0	0
ImAg	TSOP-50	SAC305	SnBi	++	0	--
ImAg	TSOP-50	SN100C	SnBi	--	--	--
ImAg	TSOP-50	SnPb	SnBi	++	+	-
ImAg	TSOP-50	SAC305	SnPb	0	0	0
ImAg	TSOP-50	SN100C	SnPb	--	--	--
ImAg	TSOP-50	SnPb	SnPb	0	0	0

Table 27 - Combined Environments Test; Summary of Rework Test Vehicle Test Results

Board Finish	Component	Alloy	Finish	New Finish	Rework Solder	Nf (1%)	Nf (10%)	Nf (63.2%)
ENIG	BGA-225	SnPb	SAC405			149	281	514
ENIG	BGA-225	SnPb	SnPb	SAC405	SnPb	234	326	447
ENIG	BGA-225	SnPb	SnPb	SnPb	Flux Only			
ENIG	CLCC-20	SnPb	SAC305			143	220	333
ENIG	CSP-100	SnPb	SAC105					
ENIG	CSP-100	SnPb	SnPb	SAC105	SnPb			
ENIG	CSP-100	SnPb	SnPb	SnPb	Flux Only			
ENIG	PDIP-20	SnPb	NiPdAu					
ENIG	PDIP-20	SnPb	Sn					
ENIG	PDIP-20	SnPb	SnPb	Sn	SnPb			
ENIG	PTH	SnPb	ENIG					
ENIG	QFN-20	SnPb	Matte Sn					
ENIG	TQFP-144	SnPb	NiPdAu					
ENIG	TQFP-144	SnPb	SnPb Dip			244	376	568
ENIG	TSOP-50	SnPb	Sn					
ENIG	TSOP-50	SnPb	SnBi					
ENIG	TSOP-50	SnPb	SnPb	Sn	SnPb	250	393	606
ENIG	TSOP-50	SnPb	SnPb	SnPb	SnPb	55	161	447
ImAg	BGA-225	SAC305	SAC405	SAC405	Flux Only	278	413	603
ImAg	BGA-225	SAC305	SAC405	SAC405	SnPb	239	411	690
ImAg	BGA-225	SnPb	SAC405			203	368	651
ImAg	BGA-225	SAC305	SnPb			86	226	570
ImAg	BGA-225	SnPb	SnPb	SAC405	SnPb	39	118	337
ImAg	BGA-225	SnPb	SnPb	SnPb	Flux Only	345	432	536
ImAg	CLCC-20	SnPb	SAC305			158	260	419
ImAg	CLCC-20	SAC305	SnPb			143	222	338
ImAg	CSP-100	SAC305	SAC105	SAC105	Flux Only	315	513	820
ImAg	CSP-100	SAC305	SAC105	SAC105	SnPb	9	56	331
ImAg	CSP-100	SAC305	SAC105			284	432	648
ImAg	CSP-100	SnPb	SAC105			200	337	554
ImAg	CSP-100	SAC305	SnPb					
ImAg	CSP-100	SnPb	SnPb	SAC105	SnPb			
ImAg	CSP-100	SnPb	SnPb	SnPb	Flux Only			
ImAg	PDIP-20	SnPb	NiPdAu					

Board Finish	Component	Alloy	Finish	New Finish	Rework Solder	Nf (1%)	Nf (10%)	Nf (63.2%)
ImAg	PDIP-20	SN100C	Sn	Sn	SN100C			
ImAg	PDIP-20	SN100C	Sn					
ImAg	PDIP-20	SnPb	Sn					
ImAg	PDIP-20	SnPb	SnPb	Sn	SnPb	233	412	711
ImAg	PTH	SN100C	ImAg					
ImAg	PTH	SnPb	ImAg					
ImAg	QFN-20	SnPb	Matte Sn					
ImAg	QFN-20	SAC305	SnPb					
ImAg	TQFP-144	SAC305	NiPdAu					
ImAg	TQFP-144	SnPb	NiPdAu					
ImAg	TQFP-144	SAC305	SAC305			8	143	2242
ImAg	TQFP-144	SnPb	SnPb Dip			343	612	1065
ImAg	TSOP-50	SAC305	Sn	Sn	SnPb	180	339	622
ImAg	TSOP-50	SnPb	Sn			437	544	670
ImAg	TSOP-50	SAC305	SnBi	SnBi	SAC305	237	344	490
ImAg	TSOP-50	SAC305	SnBi			288	427	623
ImAg	TSOP-50	SnPb	SnBi			262	438	716
ImAg	TSOP-50	SAC305	SnPb			164	426	1064
ImAg	TSOP-50	SnPb	SnPb	Sn	SnPb	305	445	640
ImAg	TSOP-50	SnPb	SnPb	SnPb	SnPb	163	310	574

Table 28 - Combined Environments Test; Relative Solder Performance, Rework Test Vehicles

TV	Board Finish	Component	Alloy	Finish	New Finish	Rework Solder	Nf (1%)	Nf (10%)	Nf (63.2%)
RWK	ImAg	BGA-225	SAC305	SAC405	SAC405	Flux Only	++	++	-
RWK	ImAg	BGA-225	SAC305	SAC405	SAC405	SnPb	++	++	-
RWK	ImAg	BGA-225	SAC305	SnPb			++	0	--
RWK	ImAg	BGA-225	SnPb	SAC405			++	++	-
RWK	ImAg	BGA-225	SnPb	SnPb	SAC405	SnPb	--	--	--
RWK	ImAg	BGA-225	SnPb	SnPb	SnPb	Flux Only	++	++	--
MFG	ImAg	BGA-225	SnPb	SnPb			0	0	0
RWK	ImAg	CLCC-20	SAC305	SnPb			--	--	--
RWK	ImAg	CLCC-20	SnPb	SAC305			--	--	--
MFG	ImAg	CLCC-20	SnPb	SnPb			0	0	0
RWK	ImAg	CSP-100	SAC305	SAC105	SAC105	Flux Only	--	-	++
RWK	ImAg	CSP-100	SAC305	SAC105	SAC105	SnPb	--	--	--
RWK	ImAg	CSP-100	SAC305	SAC105			--	-	0
RWK	ImAg	CSP-100	SAC305	SnPb					
RWK	ImAg	CSP-100	SnPb	SAC105			--	--	-
RWK	ImAg	CSP-100	SnPb	SnPb	SAC105	SnPb			
RWK	ImAg	CSP-100	SnPb	SnPb	SnPb	Flux Only			
MFG	ImAg	CSP-100	SnPb	SnPb			0	0	0
RWK	ImAg	TSOP-50	SAC305	Sn	Sn	SnPb	++	+	-
RWK	ImAg	TSOP-50	SAC305	SnBi	SnBi	SAC305	++	+	--
RWK	ImAg	TSOP-50	SAC305	SnBi			++	++	-
RWK	ImAg	TSOP-50	SAC305	SnPb			++	++	++
RWK	ImAg	TSOP-50	SnPb	Sn			++	++	-
RWK	ImAg	TSOP-50	SnPb	SnBi			++	++	0
RWK	ImAg	TSOP-50	SnPb	SnPb	Sn	SnPb	++	++	-
RWK	ImAg	TSOP-50	SnPb	SnPb	SnPb	SnPb	+	0	-
MFG	ImAg	TSOP-50	SnPb	SnPb			0	0	0

5.4 Thermal Cycle -55°C to +125°C Test

5.4.1 Thermal Cycle -55°C to +125°C Test Method

This test determines a test specimen's resistance to degradation from thermal cycling. The limits identified in thermal cycle testing were used to compare performance differences in the Pb-free test alloys and mixed solder joints vs. the baseline standard SnPb (63/37) alloy.

This test was performed in accordance with IPC-SM-785 (*Guidelines for Accelerated Reliability Testing of Surface Mount Solder Attachments*) and the following procedure:

- Continuously monitor the electrical continuity of the solder joints during the test. It is desirable to continue thermal cycling until 63% of each component type fails.

Table 29 - Thermal Cycling Test Methodology; -55°C to +125°C

Parameters	<ul style="list-style-type: none"> ▪ -55°C to +125°C ▪ 5 to 10°C/minute ramp ▪ 30 minute high temperature dwell ▪ 10 minute low temperature dwell 		
Number of Test Vehicles Required			
Mfg. SnPb = 5	Mfg. LF = 5	Mfg. LF {SN100C} = 5	Mfg. LF {ENIG} = 1
Rwk. SnPb = 5	Rwk. SnPb {ENIG} = 1	Rwk. LF = 5	
Trials per Specimen	1		

5.4.2 Thermal Cycle -55°C to +125°C Testing Results Summary

The -55°C to +125°C thermal cycle testing was terminated after 4068 total thermal cycles. At that point, all of the components had reached an N63 statistical value (except for the QFN-20 component style) thus allowing for a complete statistical analysis of the compiled failure data. The Manufactured test vehicle failure rates are shown in Table 30 and Reworked test vehicle failure rates are shown in Table 31.

Table 30 - Manufactured Test Vehicle Component Population Failure Rates after 4068 Thermal Cycles

Component Type	Total Failures	Population	Percent Failed
CLCC-20	280	305	92%
QFN-20	6	135	4%
QFP-144	274	287	95%
PBGA-225	236	283	83%
PDIP-20	82	218	38%
CSP-100	163	241	68%
TSOP-50	236	238	99%

Table 31 - Reworked Test Vehicle Component Population Failure Rates after 4068 Thermal Cycles

Component Type	Total Failures	Population	Percent Failed
PBGA-225	48	66	73%
PDIP-20	36	64	56%
CSP-100	25	64	37%
TSOP-50	99	99	100%

The physical failure and statistical analysis for each component type was completed with the following sections summarizing the results for each specific component style. It should be noted that the test vehicles remained in the thermal cycle chamber the entire 4068 cycles. Individual components remained in the test chamber after they had failed to avoid damaging the solder joints of other components on the test vehicles due to handling/movement. This resulted in some continuing solder joint microstructure evolution after the initial component failure, which is evident in some of the physical failure analysis pictures. The data in the following plots do not include thermal cycle results that showed a failure after 1 cycle.

5.4.2.1 Ceramic Leadless Chip Carriers (CLCC-20) Results

5.4.2.1.1 Statistical Analysis

The CLCC-20 components had accumulated 92% population failure after the completion of 4068 thermal cycles. The CLCC-20 components were included on the test vehicles because of their poor reliability track record on electronic assemblies used in harsh environments. Industry data (1) has demonstrated that the CLCC component style undergoes solder joint integrity degradation under IPC Class 3 use environments due to coefficient of thermal expansion (CTE) mismatch with the printed wiring assembly. CLCC-20 components had six different combinations (SAC/SAC, SAC/SnPb, SnPb/SAC, SnPb/SnPb, SN100C/SAC, SN100C/SnPb) tested and the Weibull characteristics show N63 values ranging from 952 cycles to 1954 cycles for the immersion silver test vehicles. The SnPb/SnPb combination had best thermal cycle performance with remaining solder alloy/component finish combinations having similar performance results. The solder alloy/component surface finish combination results for the ENIG test vehicles revealed no clear favored combination as the results populations were statistically indistinguishable from each other. The TQFP-144 components reworked as part of the NSWC Crane population had no preferred thermal cycle result solder alloy/component finish combination.

The Weibull plots in Figure 114, Figure 115, and Figure 116 summarize the CLCC-20 thermal cycle test results.

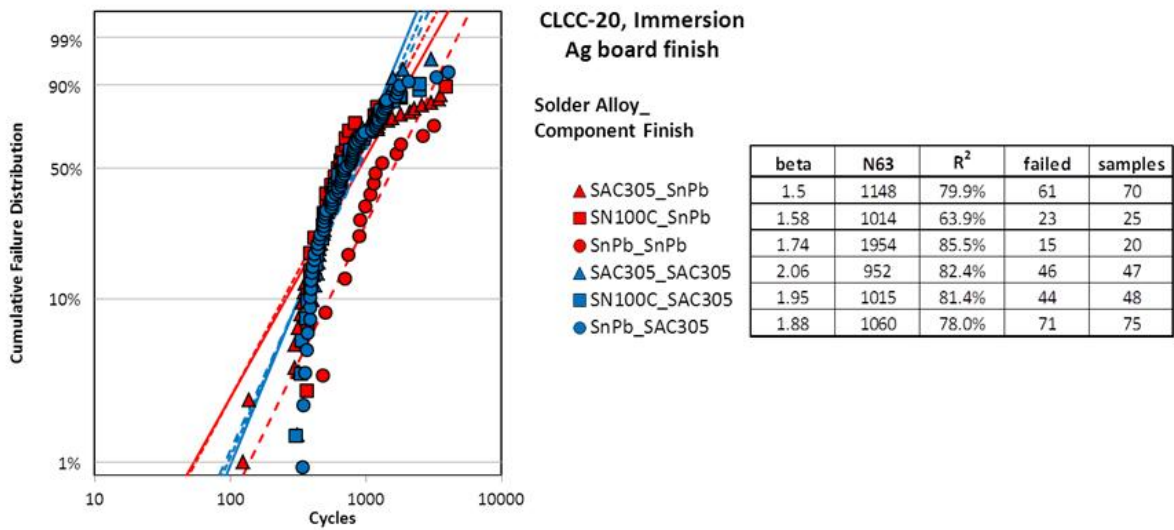


Figure 114 - CLCC-20 Weibull Plot for Immersion Silver Test Vehicle

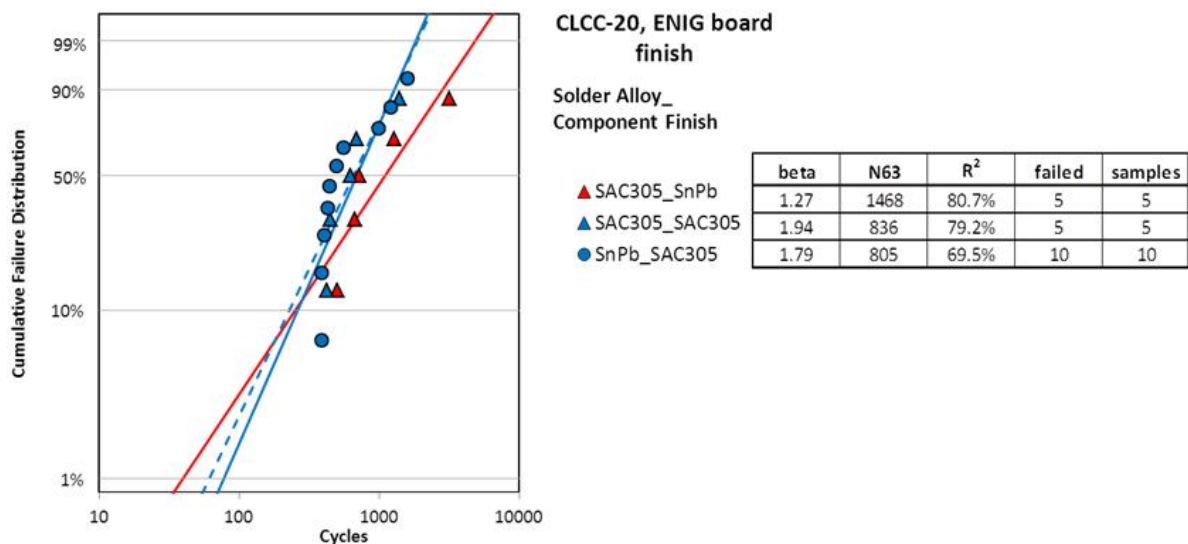


Figure 115 - CLCC-20 Weibull Plot for Immersion Silver Test Vehicle

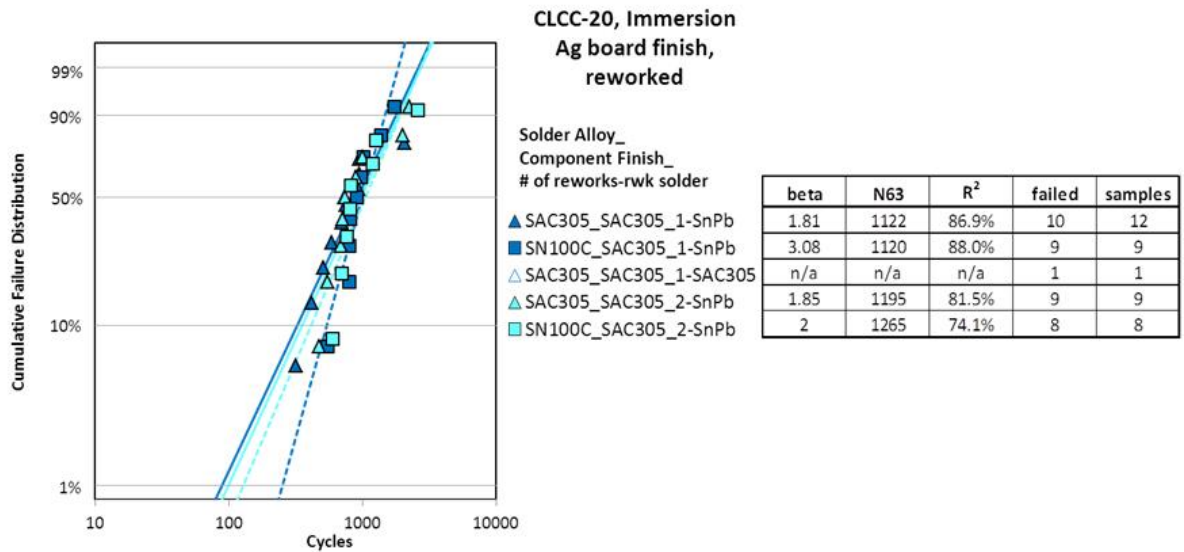


Figure 116 - NWSC Crane Reworked CLCC-20 Weibull Plot

5.4.2.1.2 Physical Failure Analysis

Metallographic cross-sectional analysis was conducted on the CLCC-20 components to document the solder joint failure location, crack morphology and solder joint microstructure. General physical failure observations of the failed CLCC-20 components were:

- The cracks in the solder joints initiated under the components and traversed at a 45° angle thru the solder fillets. The crack formation and location are in agreement with industry published data of CLCC failure modes (2), (3).
- The solder joint geometries and wetting angles were acceptable and met industry workmanship criteria
- The solder joint microstructures were reasonably homogenous with no segregation regions observed in the mixed metallurgy cases

Figure 117 through Figure 121 illustrate the typical CLCC-20 solder joint failures observed.



Figure 117 - CLCC-20 Component on Test Vehicle after 4068 Thermal Cycles

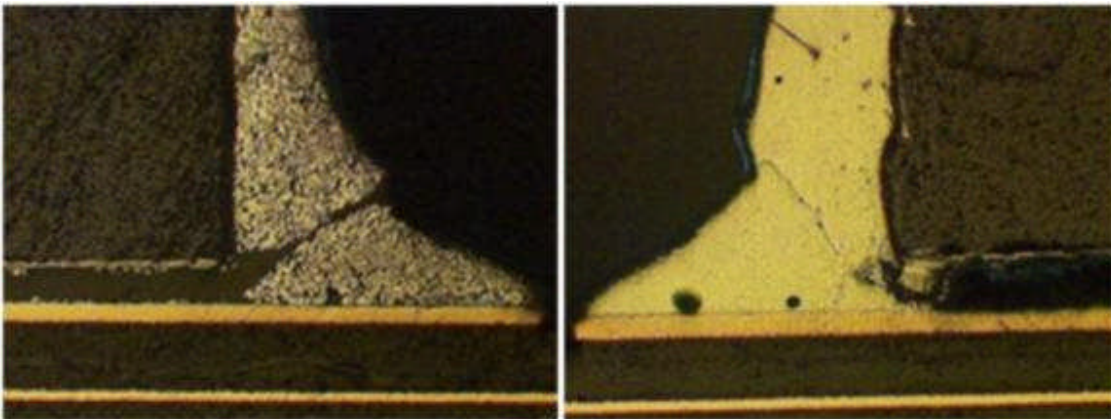


Figure 118 - CLCC-20 Solder Joints; Left - Board 5, Component U14, SnPb/SnPb, Failed @ 2625 Cycles; Right - Board 43, Component U14, SAC305/SAC305, Failed @ 513 Cycles

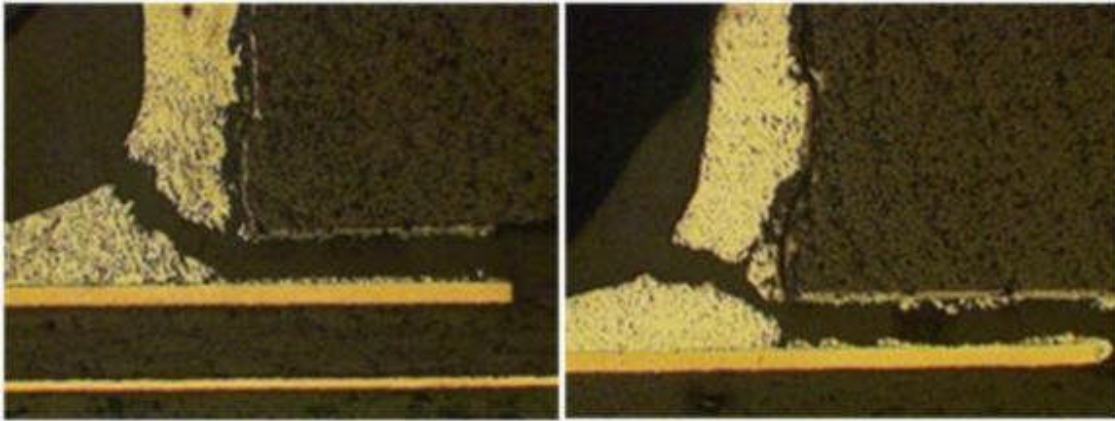


Figure 119 - CLCC-20 Solder Joints; Left - Board 164, Component U14, SAC305/SnPb, Failed @ 1248 Cycles; Right - Board 126, Component U14, SnPb/SAC305, Failed @ 2064 Cycles

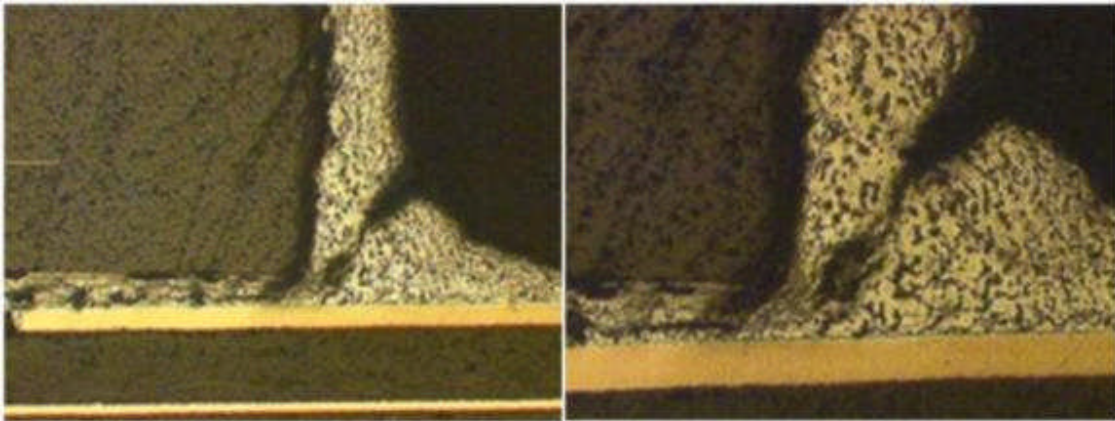


Figure 120 - CLCC-20 Solder Joints, Board 103, Component U22, SN100C/SnPb, Failed @ 828 Cycles

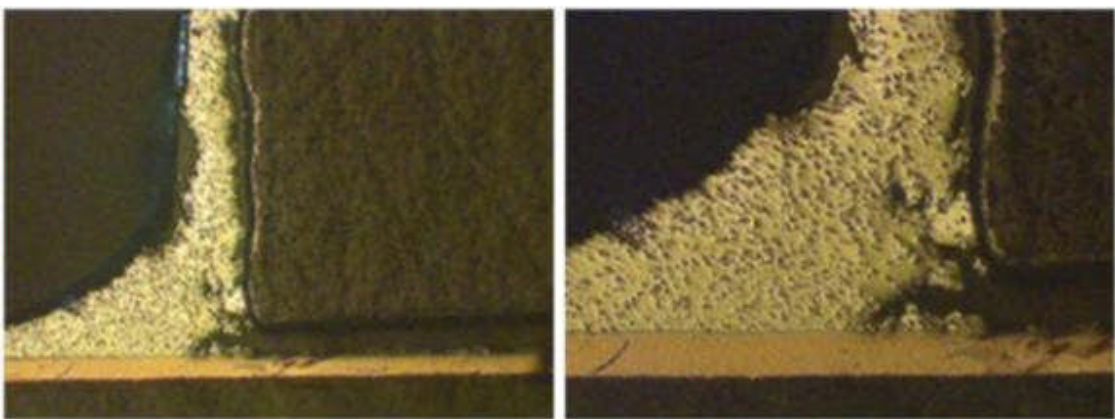


Figure 121 - CLCC-20 Solder Joints, Board 104, Component U14, SN100C/SAC305, Failed @ 304 Cycles

5.4.2.2 Quad Flatpack No-Lead (QFN-20) Results

5.4.2.2.1 Statistical Analysis

The QFN-20 components had accumulated 4% population failure after the completion of 4068 thermal cycles and were the most robust component type in the investigation. QFN-20 components had three different combinations (SAC/Sn, SN100C/Sn, SnPb/Sn) tested. Calculation of Weibull statistics was only possible for the SN100C/Sn alloy/component finish combination due to the low number of solder joint failures. The robustness of the QFN component style was demonstrated as none of the solder alloy/component finish combination accumulated any significant number of failures. R. Coyle et al published results showing for a QFN-48 package that SnPb solder alloy performed better than a SAC405 solder alloy in a 0C - 100C thermal cycle test conditions(4). The investigation QFN-20 data is not in agreement with that result, however, differences in the test components may be the reason for the different thermal cycle results. No alloy/component finish preferred combination conclusions could be made due to the lack of solder joint failures for the NWSA Crane reworked CLCC-20 components.

The Weibull plots in Figure 122 and Figure 123 summarize the QFN-20 thermal cycle test results.

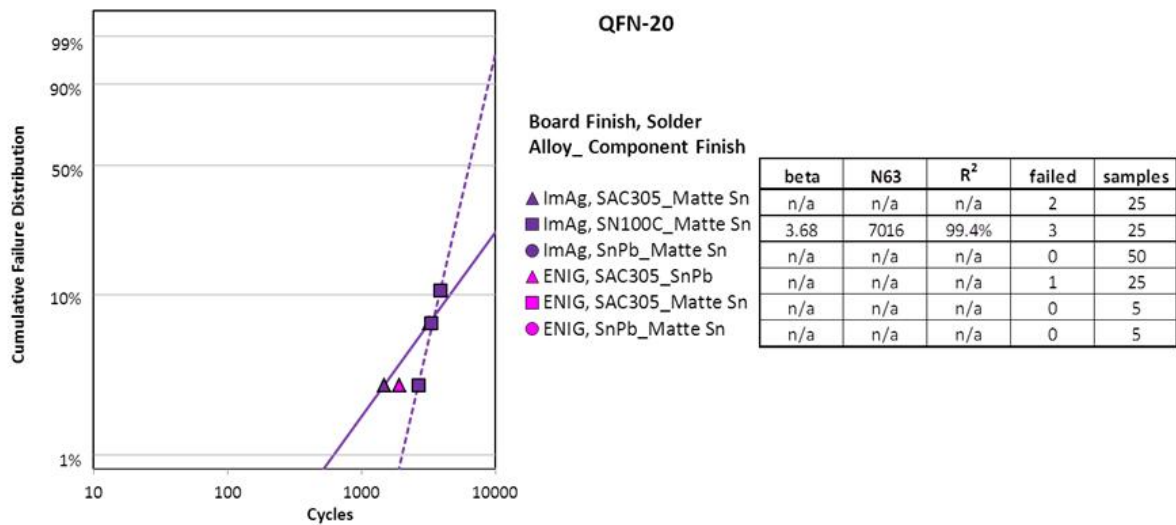


Figure 122 - QFN-20 Weibull Plot for Immersion Silver and ENIG PWB Finishes

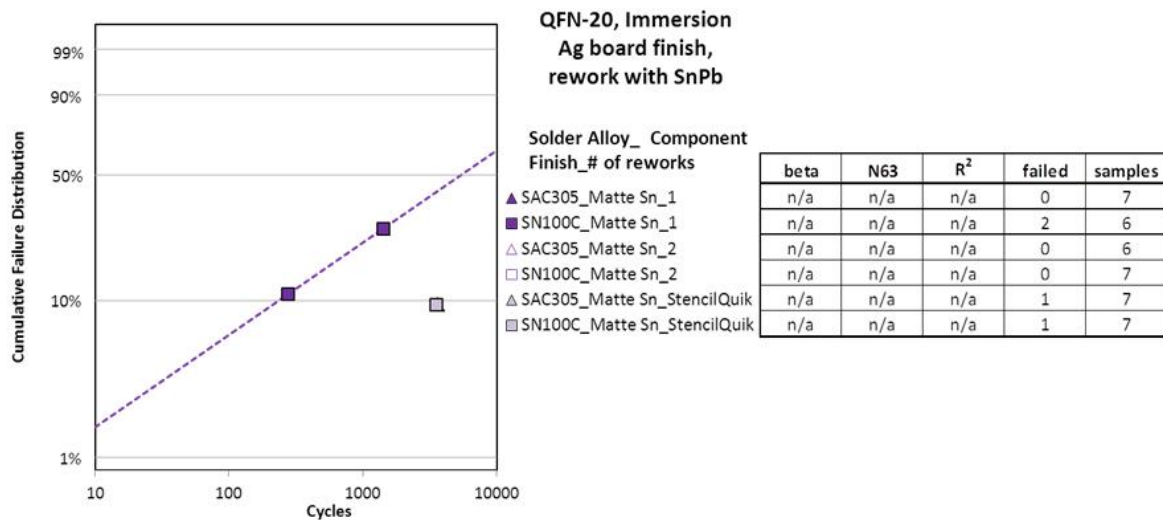


Figure 123 - NWSC Crane Reworked QFN-20 Weibull Plot

5.4.2.2.2 Physical Failure Analysis

Metallographic cross-sectional analysis was conducted on the QFN-20 components to document the solder joint failure location, crack morphology and solder joint microstructure. General physical failure observations of the failed QFN-20 components were:

- The cracks in the solder joints initiated in the bottom terminated pads and traversed towards the lead toe. The crack formation and location are in agreement with industry published data of QFN failure modes (4), (5).
- The solder joint geometries and wetting angles were acceptable and met industry workmanship criteria. The ground pad on the QFN-20 components achieved 50% minimum solder coverage and no cracking was observed in that solder joint.
- The solder joint microstructures were homogenous with no segregation regions observed. The solder paste alloy completely dominated the solder joint microstructure regardless of the component surface finish.
- The Stencil Quik reworked solder joints were significantly thicker than the traditionally reworked solder joints (Figure 130 and Figure 131).

Figure 124 through Figure 131 illustrate the typical QFN-20 solder joint failures observed.

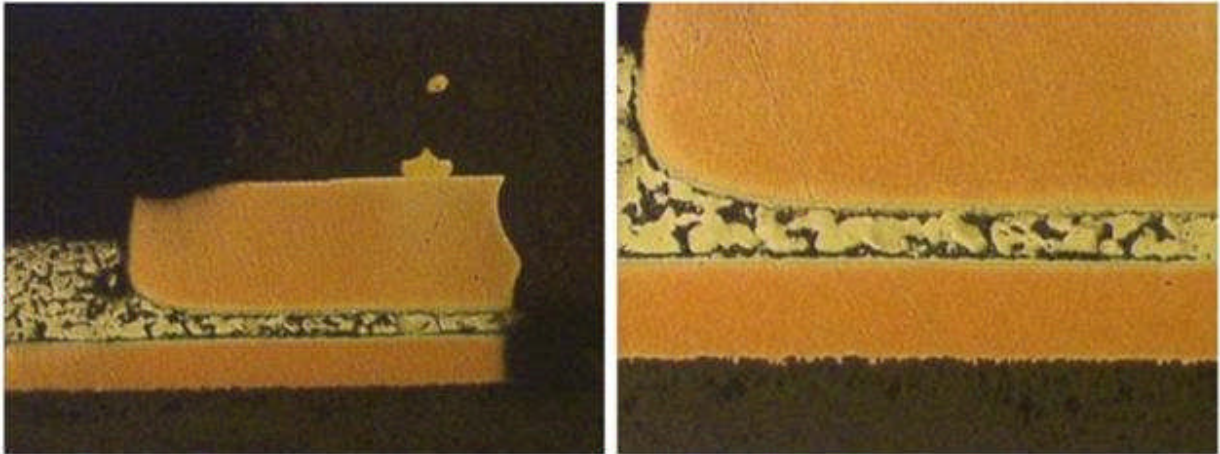


Figure 124 - QFN-20 Solder Joints, Board 6, Component U27, SnPb/Sn Dipped, Did Not Fail (DNF)

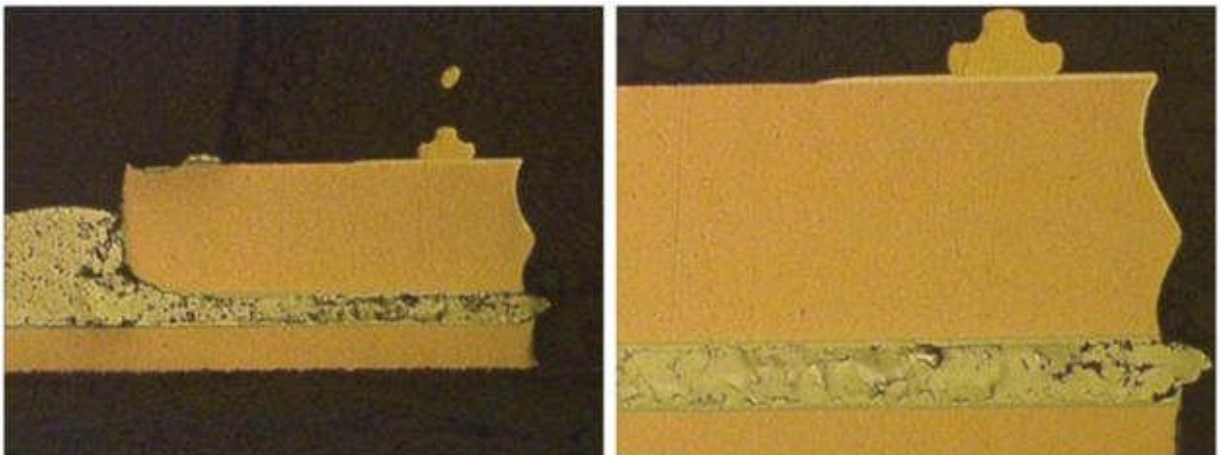


Figure 125 - QFN-20 Solder Joints, Board 42, Component U54, SAC305/Sn, DNF

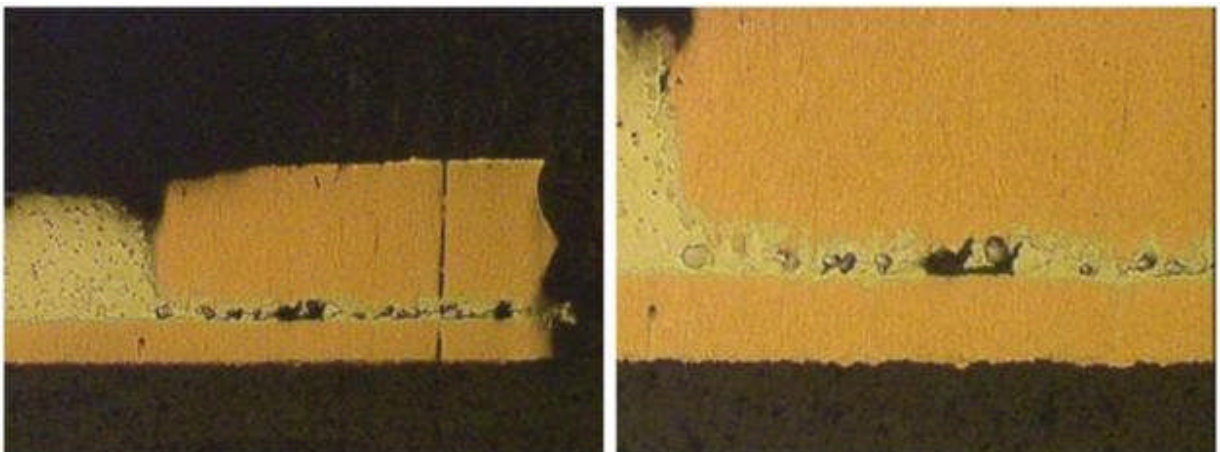


Figure 126 - QFN-20 Solder Joints, Board 104, Component U27, SN100C/Sn, DNF

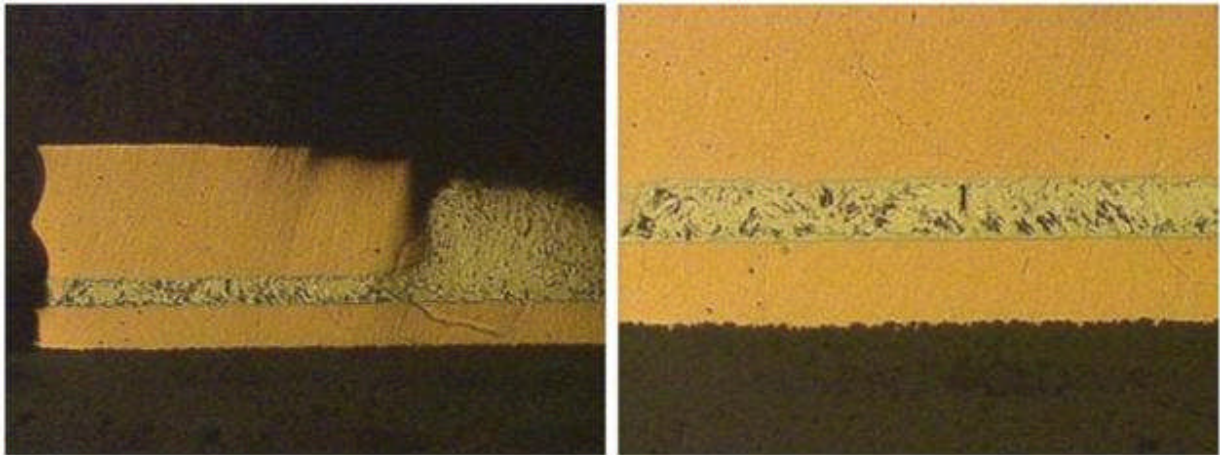


Figure 127 - QFN-20 Solder Joints, Board 167, Component U15, SAC305/SnPb, DNF

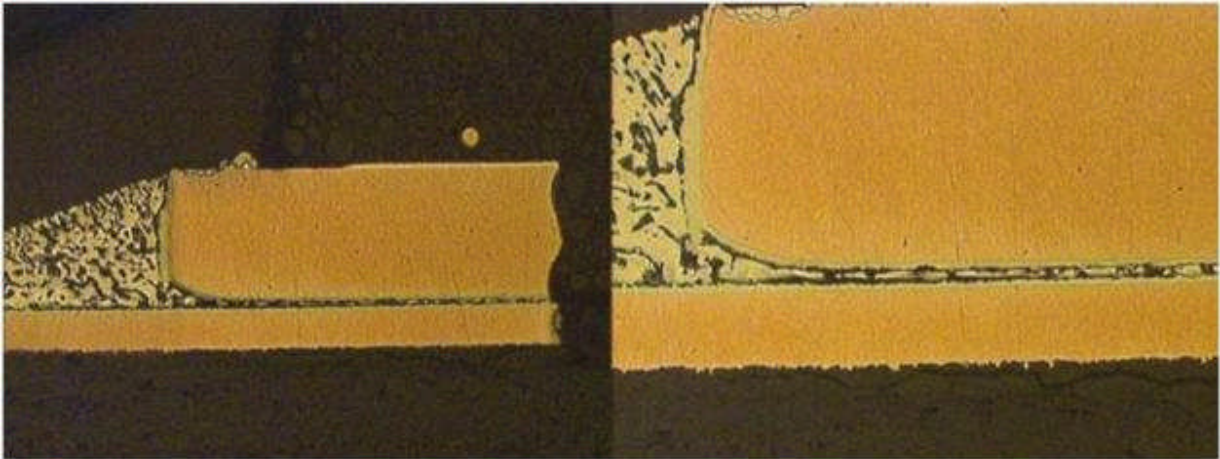


Figure 128 - QFN-20 Solder Joints, Board 107, Component U28, SN100C/Sn, Reworked with SnPb Paste, 1 Rework Failed @ 277 Cycles

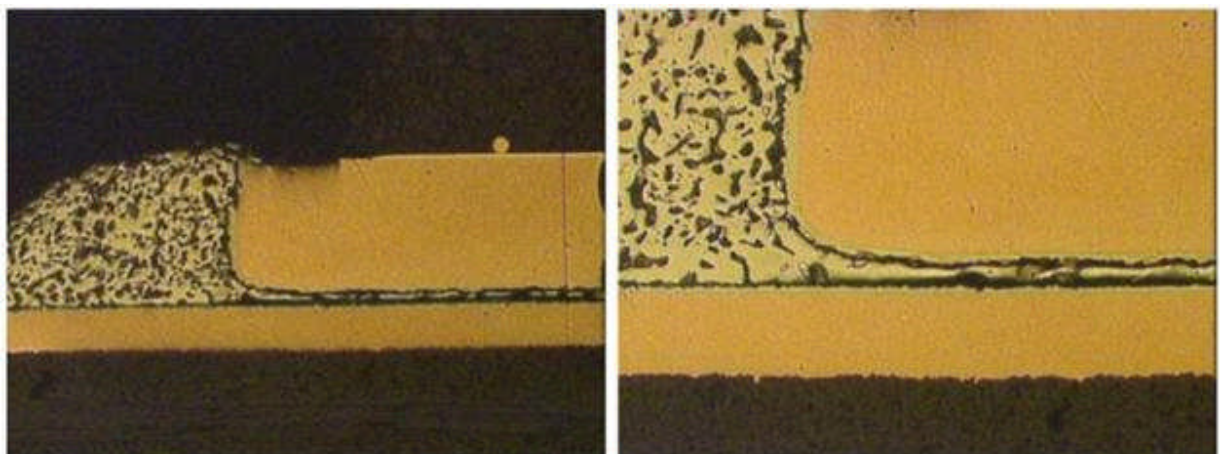


Figure 129 - QFN-20 Solder Joints, Board 108, Component U28, SN100C/Sn, Reworked with SnPb Paste, 2 Reworks, DNF

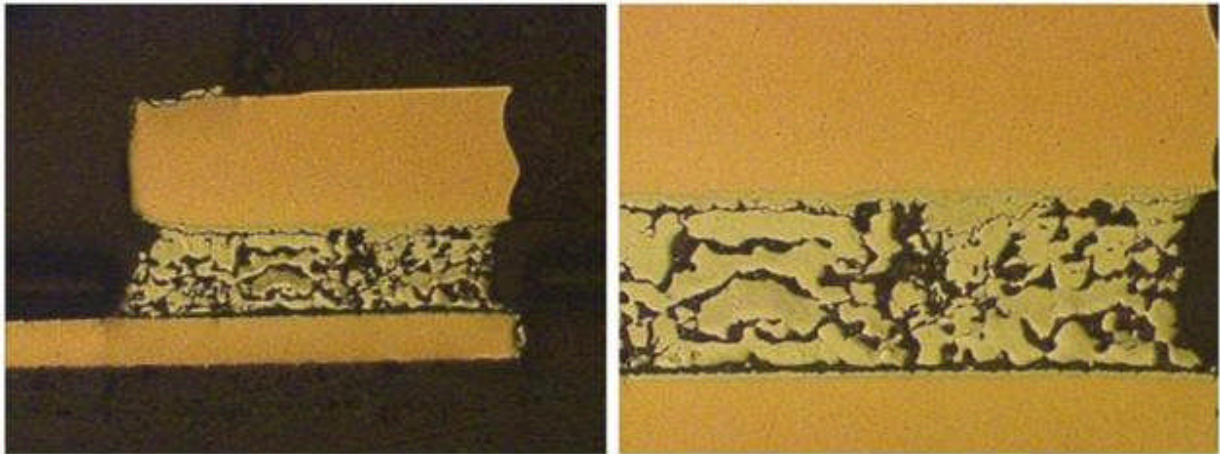


Figure 130 - QFN-20 Solder Joints, Board 109, Component U28, SN100C/Sn, Reworked with Stencil Quik, 1 Rework, DNF

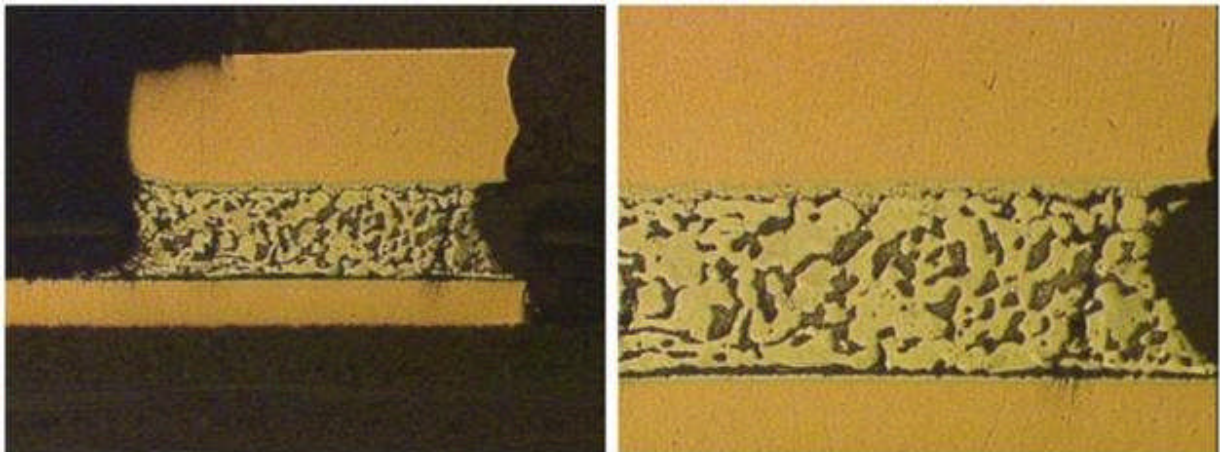


Figure 131 - QFN-20 Solder Joints, Board 47, Component U15, SAC305/Sn, Reworked with Stencil Quik, 1 Rework, Failed @ 3660 Cycles

5.4.2.3 Quad Flatpack Package (QFP-144) Results

5.4.2.3.1 Statistical Analysis

The TQFP-144 components had accumulated 95% population failure after the completion of 4068 thermal cycles. TQFP-144 components had eight different combinations (SAC/Sn, SAC/SnPb, SAC/SAC, SnPb/NiPdAu, SnPb/SnPb, SnPb/Sn, SN100C/Sn, SN100C/SnPb) and the Weibull characteristics show very similar N63 values for the immersion silver test vehicles. None of the solder alloy/component finish combinations performed significantly better than another. This is not a surprising result as QFP components have excellent industry solder joint integrity under a variety of conditions due to the package lead compliancy. The solder alloy/component surface finish combination results for the ENIG test vehicles revealed no clear favored combination as the results populations were statistically indistinguishable from each

other. The TQFP-144 components reworked as part of the NSWC Crane population had no preferred thermal cycle result solder alloy/component finish combination.

The Weibull plots in Figure 132 through Figure 134 summarize the TQFP-144 thermal cycle test results.

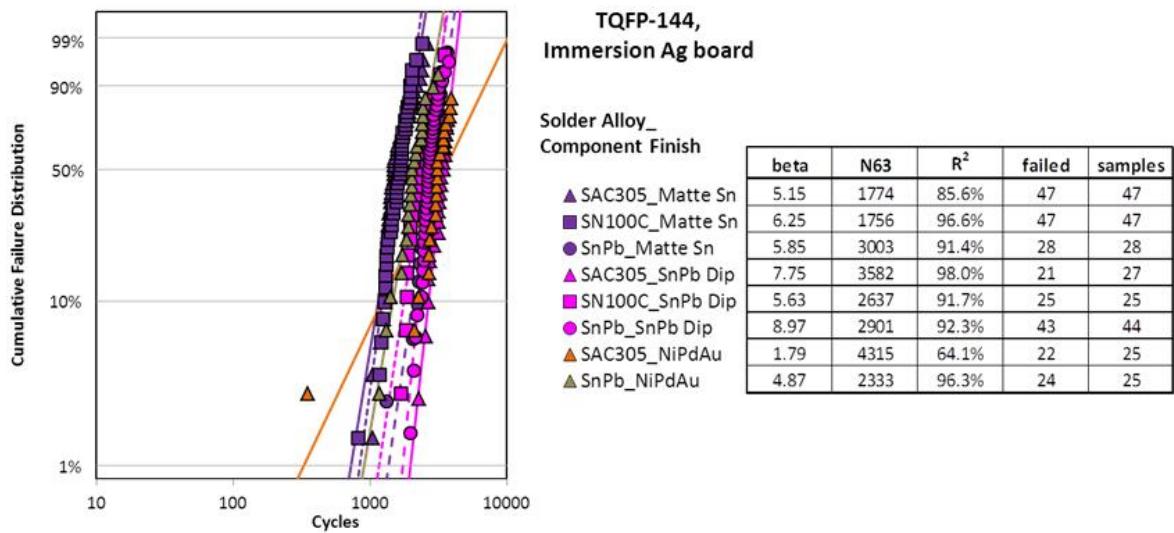


Figure 132 - TQFP-144 Weibull Plot for Immersion Silver PWB Finish

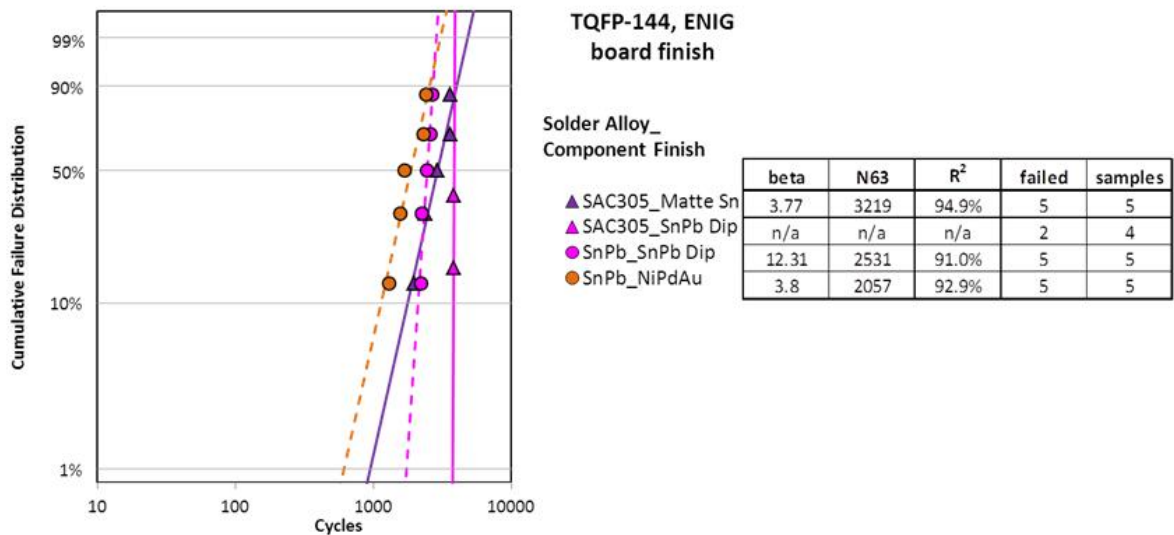


Figure 133 - TQFP-144 Weibull Plot for ENIG PWB Finish

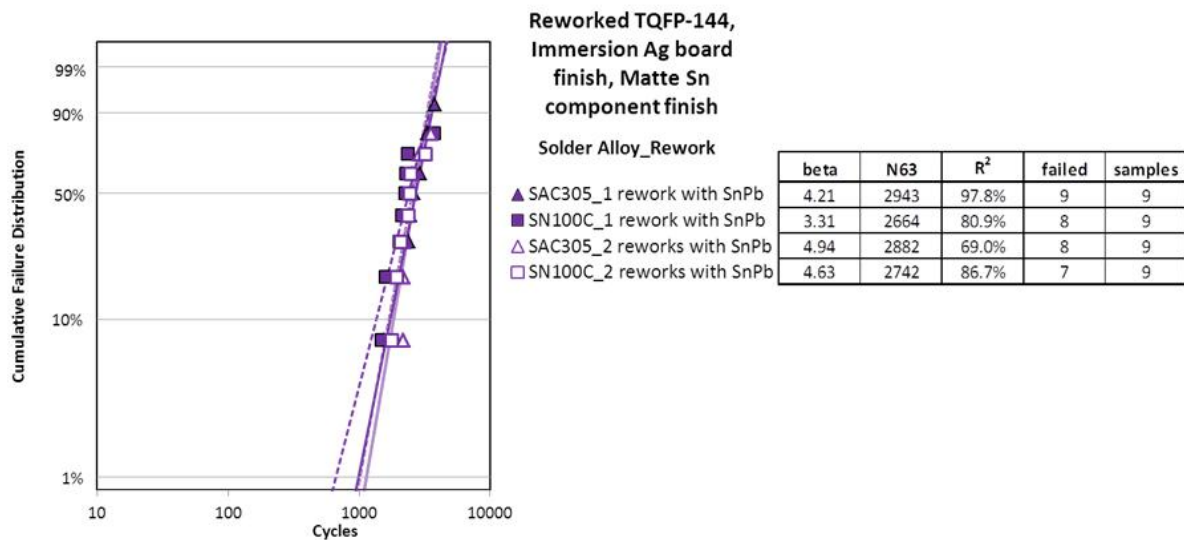


Figure 134 - NSWC Crane Reworked TQFP-144 Weibull Plot

5.4.2.3.2 Physical Failure Analysis

Metallographic cross-sectional analysis was conducted on the TQFP-144 components to document the solder joint failure location, crack morphology and solder joint microstructure. General physical failure observations of the failed TQFP-144 components were:

- The cracks in the solder joints initiated in the heel fillet region and traversed under the foot towards the lead toe. The crack formation and location are in agreement with industry knowledge of QFP failure modes (1).
- The solder joint geometries and wetting angles were acceptable and met industry workmanship criteria. There were a number of instances where the solder did flow into the upper lead bend region which is acceptable per industry standards.
- The solder joint microstructures were reasonably homogenous with no segregation regions observed in the mixed metallurgy cases.

Figure 135 through Figure 143 illustrate the typical TQFP-144 solder joint failures observed.

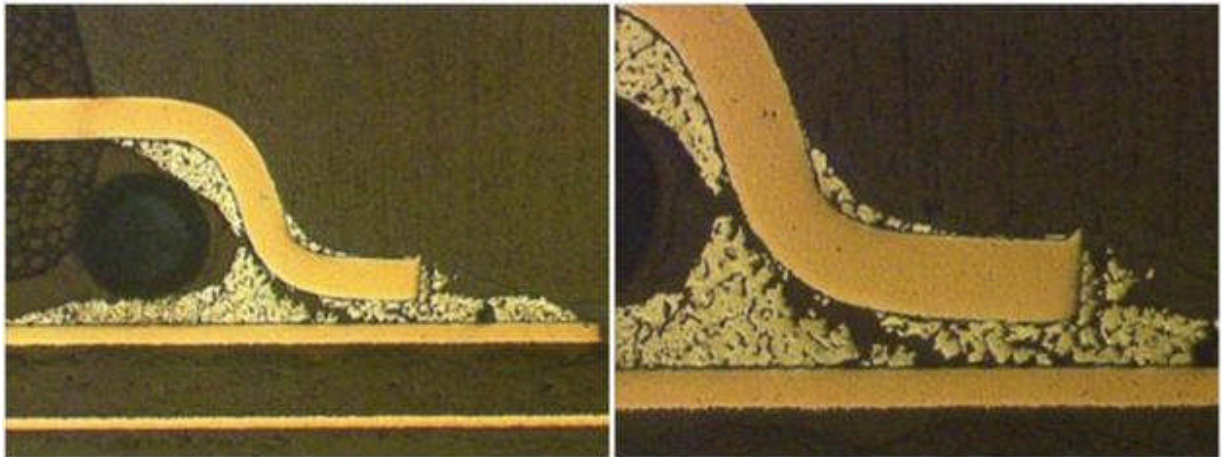


Figure 135 - TQFP-144 Solder Joints, Board 9, Component U48, SnPb/SnPb Dipped, Failed @ 2648 Cycles

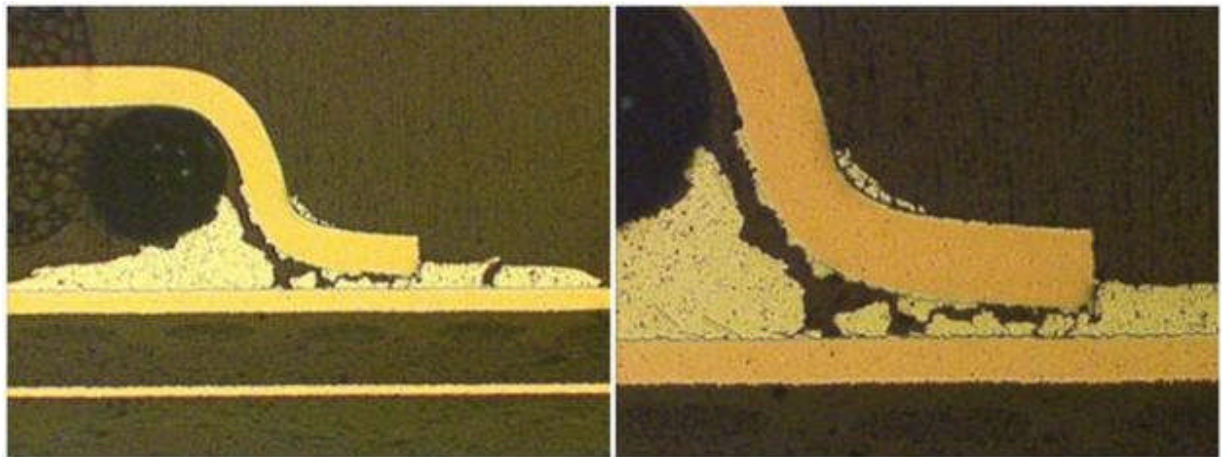


Figure 136 - TQFP-144 Solder Joints, Board 41, Component U20, SAC305/SnPb Dipped, Failed @ 3541 Cycles

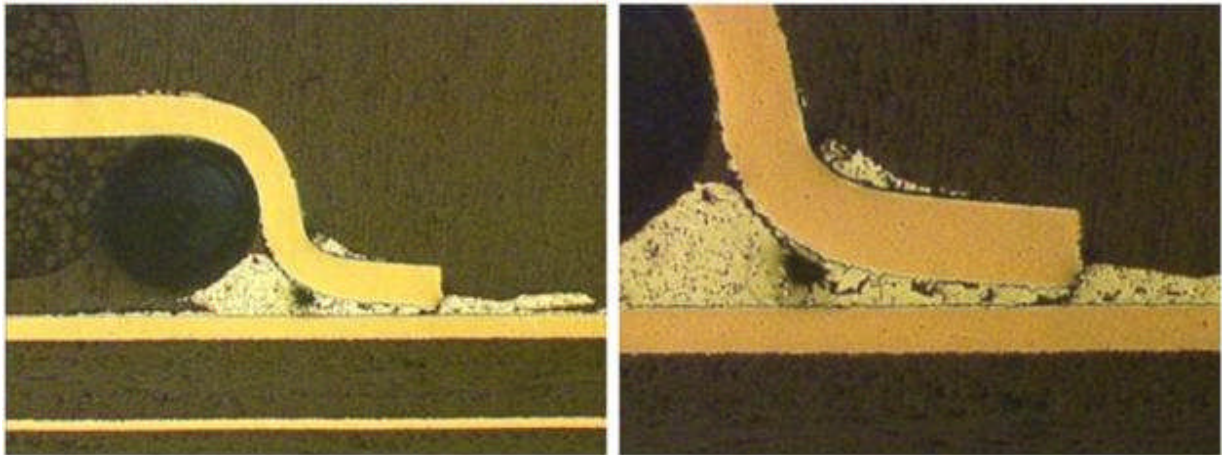


Figure 137 - TQFP-144 Solder Joints, Board 106, Component U20, SN100C/SnPb Dipped, Failed @ 3258 Cycles

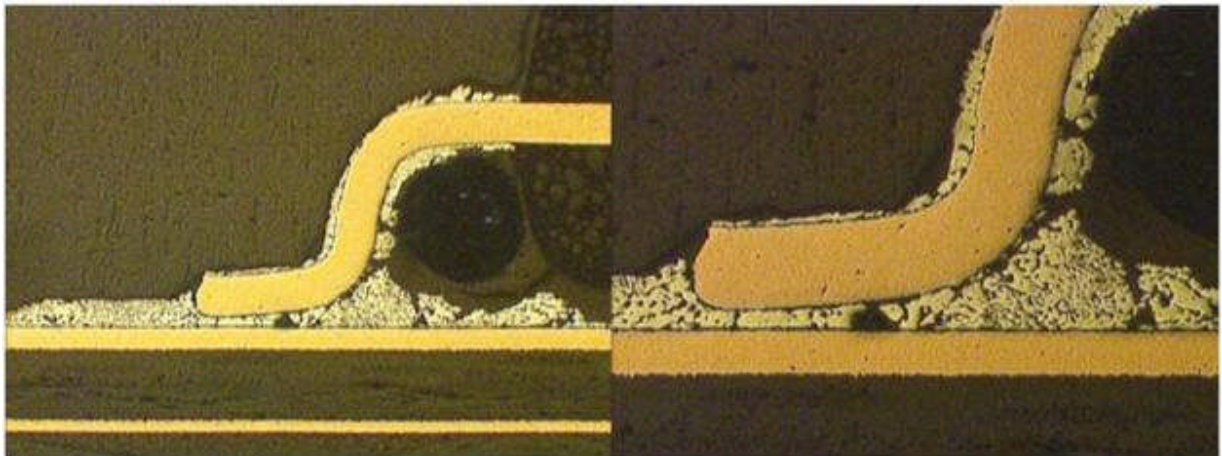


Figure 138 - TQFP-144 Solder Joints, Board 9, Component U1, SnPb/Sn, Failed @ 1 Cycle

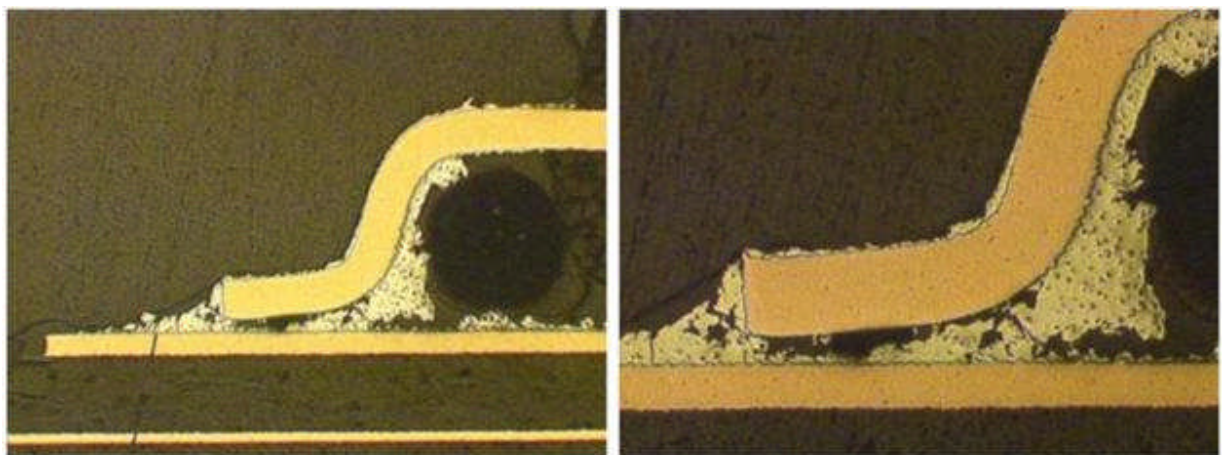


Figure 139 - TQFP-144 Solder Joints, Board 49, Component U57, SAC305/Sn, Failed @ 1430 Cycles

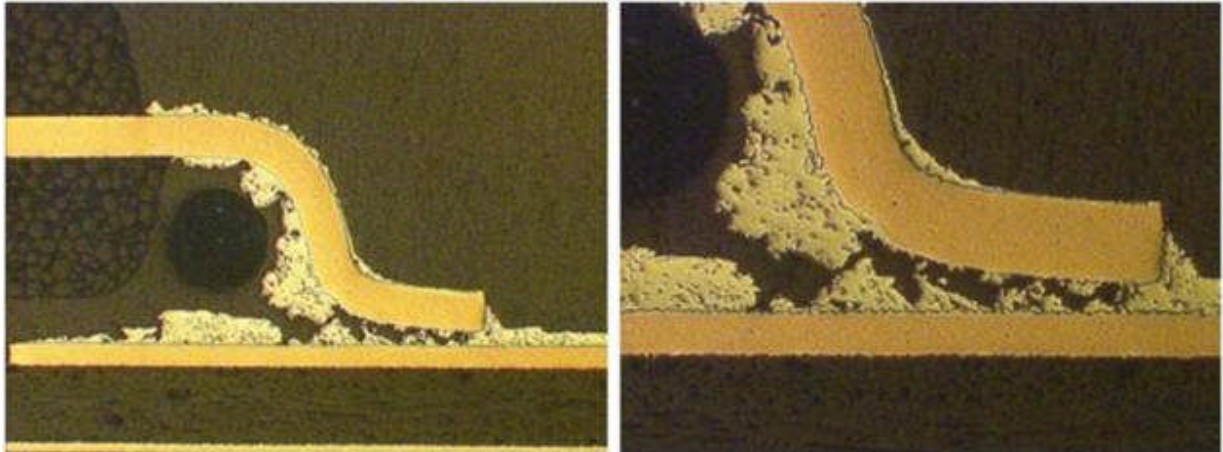


Figure 140 - TQFP-144 Solder Joints, Board 103, Component U48, SN100C/Sn, Failed @ 1712 Cycles

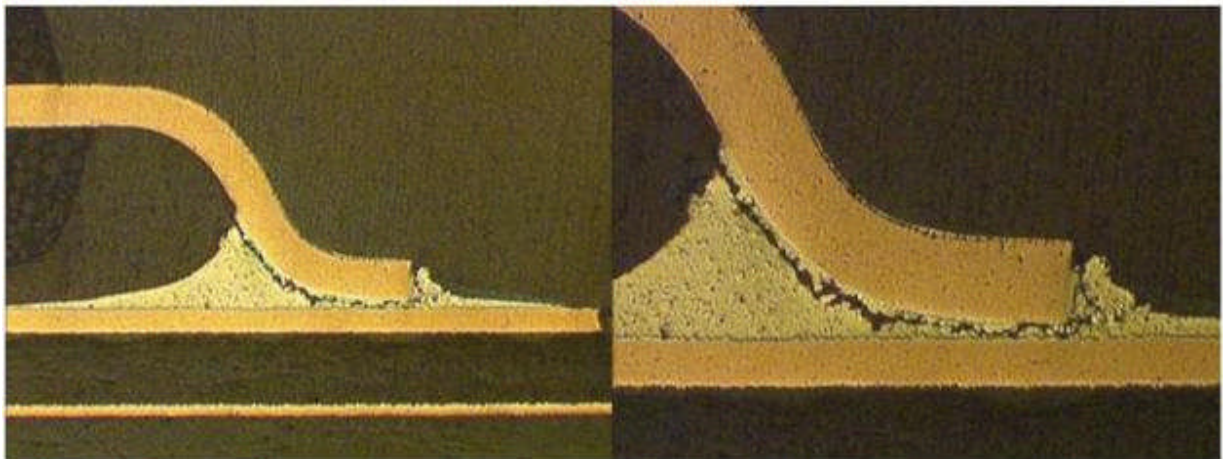


Figure 141 - TQFP-144 Solder Joints, Board 167, Component U57, SAC305/NiPdAu, Failed @ 3478 Cycles

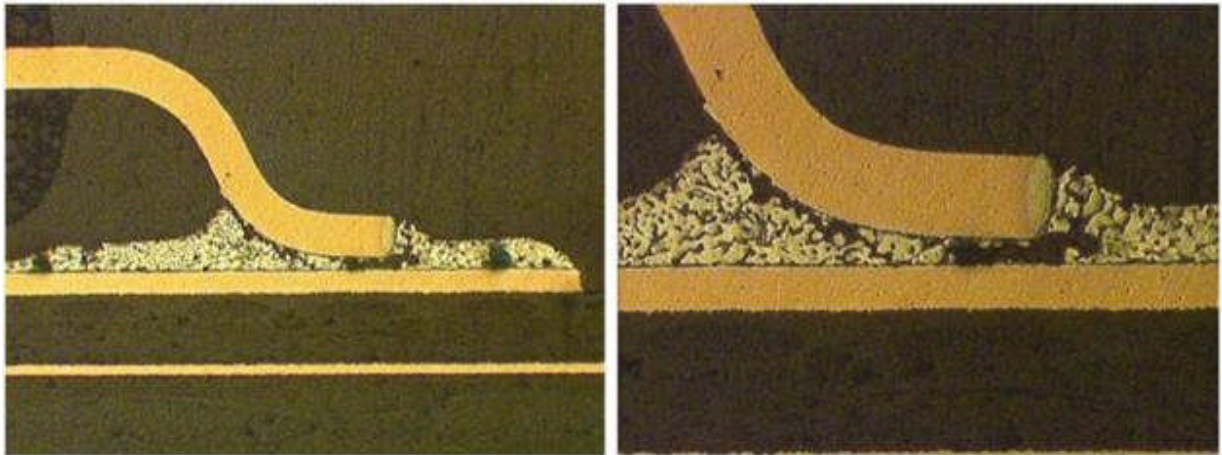


Figure 142 - TQFP-144 Solder Joints, Board 127, Component U3, SnPb/NiPdAu, Failed @ 1744 Cycles

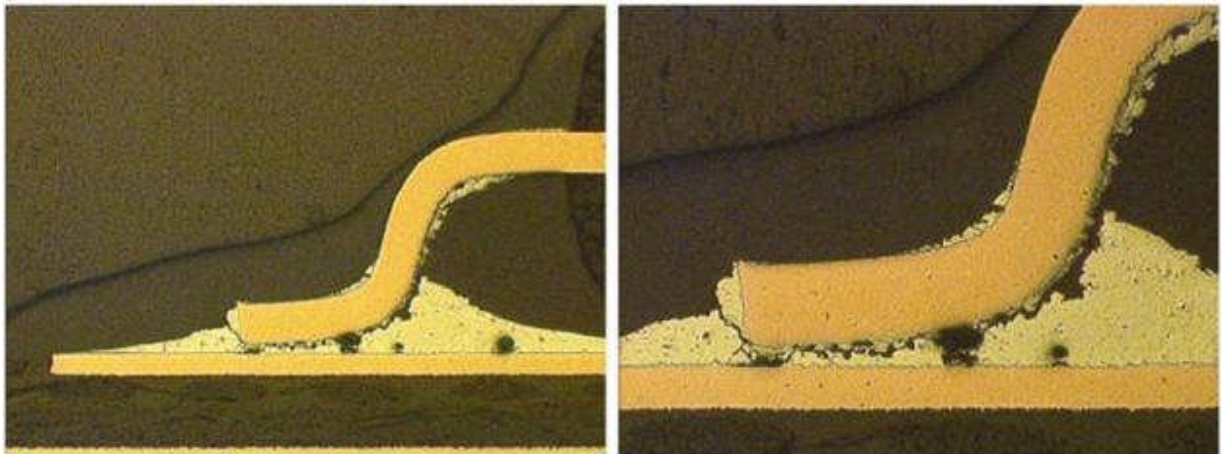


Figure 143 - TQFP-144 Solder Joints, Board 164, Component U7, SAC305/SAC305, Failed @ 2359 Cycles

5.4.2.4 Ball Grid Array (PBGA-225) Results

5.4.2.4.1 Statistical Analysis

The PBGA-225 components had accumulated 83% population failure after the completion of 4068 thermal cycles. PBGA-225 components had six different combinations (SAC/SAC, SAC/SnPb, SN100C/SAC, SN100C/SnPb, SnPb/SAC, SnPb/SnPb) tested. The non-mixed solder alloy/component finish combinations - SnPb/SnPb, SAC305/SAC405, SN100C/SAC405 - had better thermal cycle performance than the mixed metallurgy combinations. This result is in agreement with the JCAA/JGPP program PBGA thermal cycle results. The number of solder joint failures for the ENIG test vehicles was very small and therefore no conclusions were made.

The reworked PBGA-225 components had accumulated 73% population failure after the completion of 4068 thermal cycles. The same failure trend was observed for the reworked PBGA-225 as observed for the manufactured PBGA-225 components: non-mixed solder

alloy/component finish combinations had better thermal cycle performance than the mixed metallurgy combinations. The small number of solder joint failures for the ENIG test vehicles was very small and therefore no conclusions were made.

The Weibull plots in Figure 144 thru Figure 147 summarize the PBGA-225 thermal cycle test results.

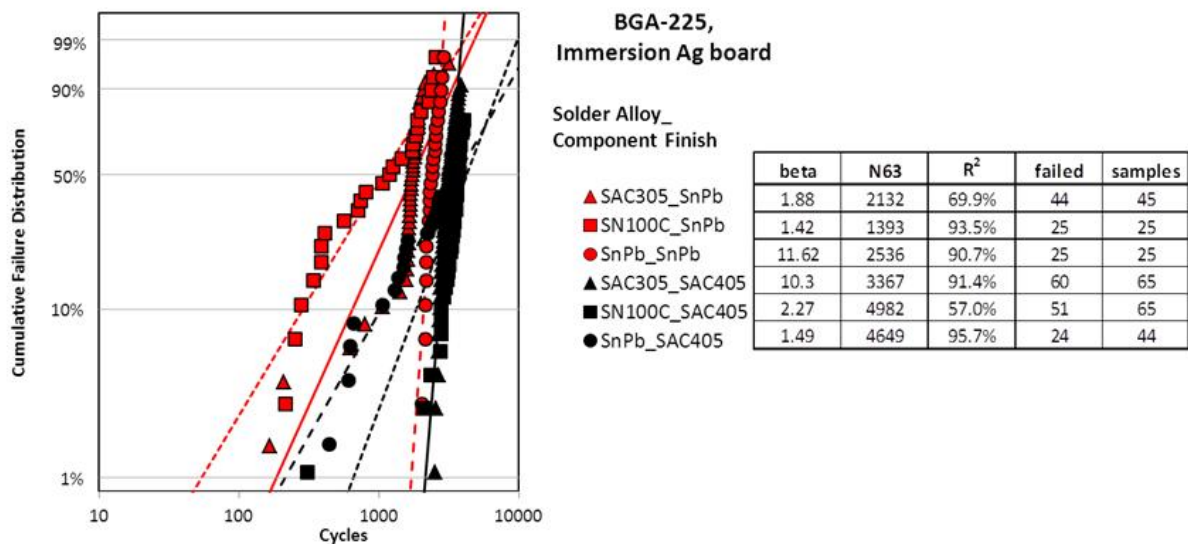


Figure 144 - PBGA-225 Weibull Plot for Immersion Silver PWB Finish

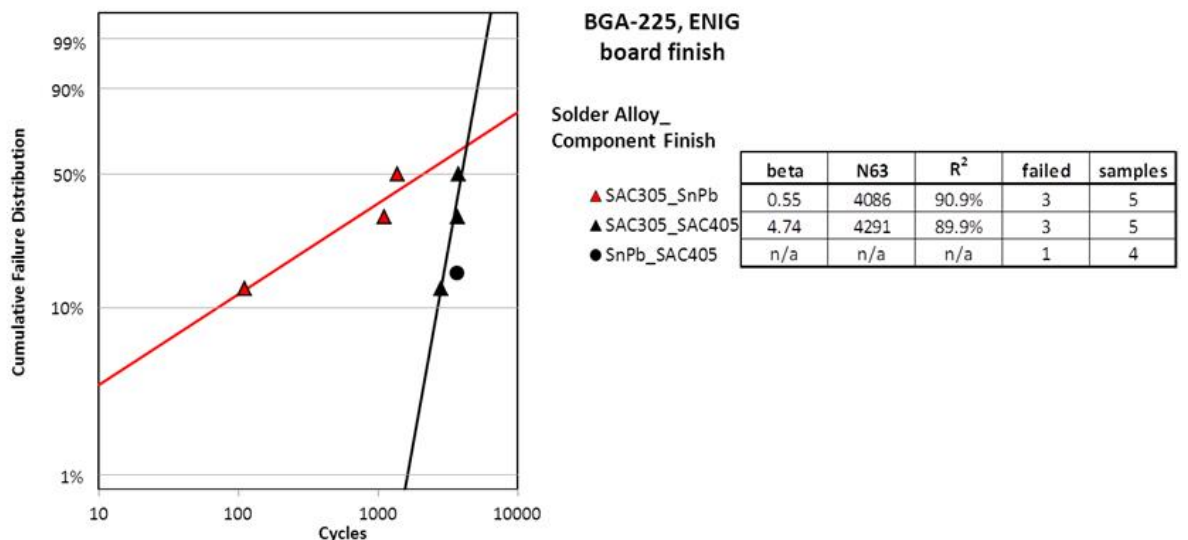


Figure 145 - PBGA-225 Weibull Plot for ENIG PWB Finish

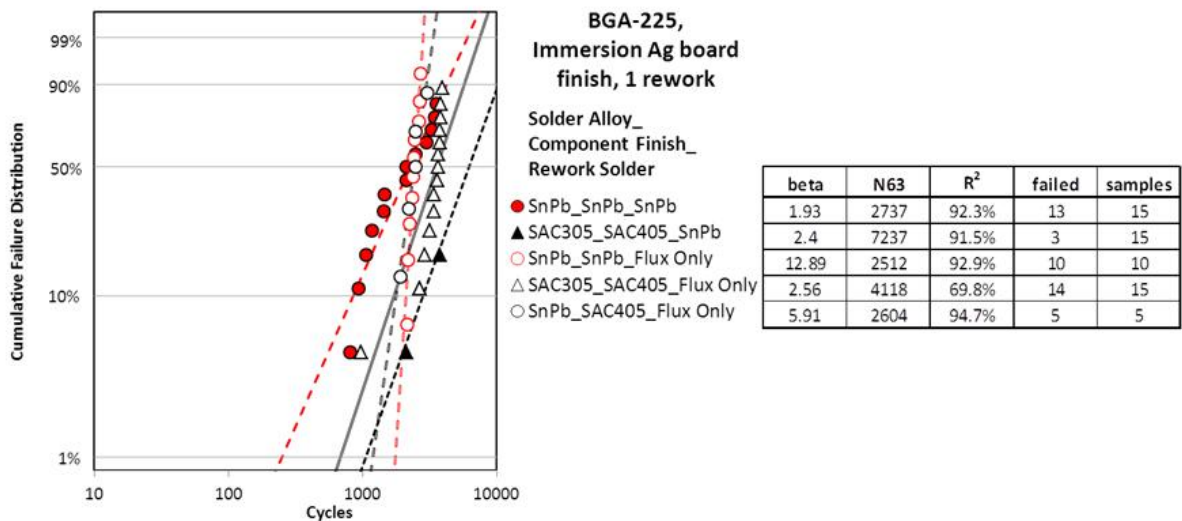


Figure 146 - Reworked PBGA-225 Weibull Plot for Immersion Silver Finish

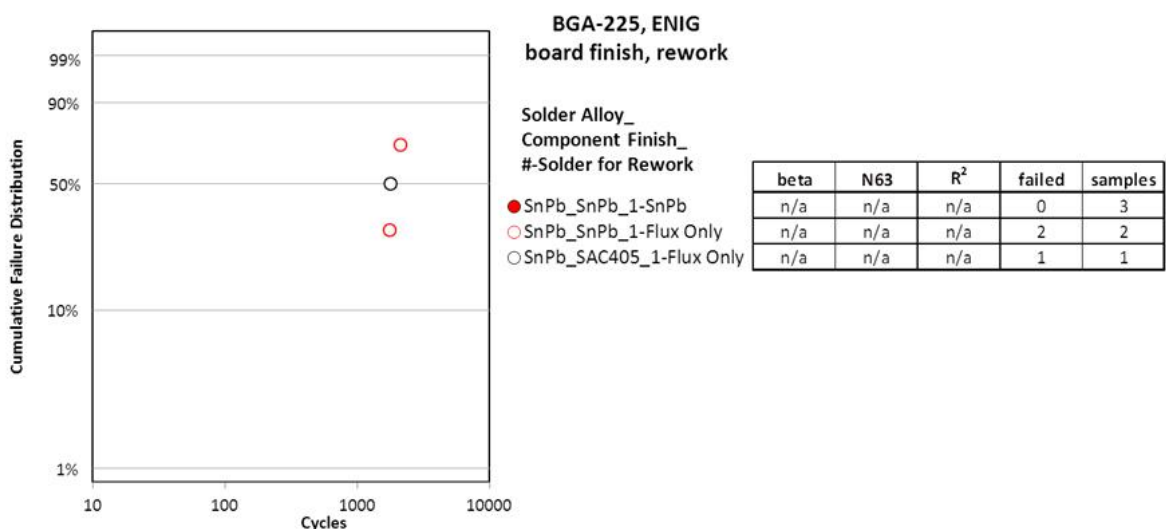


Figure 147 - Reworked PBGA-225 Weibull Plot for ENIG PWB Finish

5.4.2.4.2 Physical Failure Analysis

Metallographic cross-sectional analysis was conducted on the PBGA-225 components to document the solder joint failure location, crack morphology and solder joint microstructure. A significant amount of physical failure analysis was conducted on the PBGA-225 rework test vehicles. General physical failure observations of the failed PBGA-225 components were:

- The cracks in the solder joints initiated at the solder joint/component pad interface. The crack formation and location are in agreement with industry knowledge of PBGA failure modes(6), (7).

- The solder joint geometries and wetting angles were acceptable and met industry workmanship criteria. There were a number of instances where the voids were observed in the solder joints but their presence was not detrimental to the solder joint integrity.
- The manufactured test vehicle solder joint microstructures were homogenous with no segregation regions and the solder ball alloy (i.e. SnPb or SAC405) dominated the microstructure as it provided the largest material contribution to the solder joint formation. Some instances of large intermetallic compound (IMC) phases were observed but they typically have minimal interaction with the crack failure path.
- The reworked test vehicle solder joint microstructures had a number of mixed metallurgy cases where the solder joint was not homogenous. These solder joints tended to fail at the solder joint/test vehicle pad interface with lead (Pb) segregated in the crack interface. This failure mode previously documented in the JCAA/JGPP testing program (8).

Figure 148 thru Figure 157 illustrate the typical PBGA-225 solder joint failures observed.

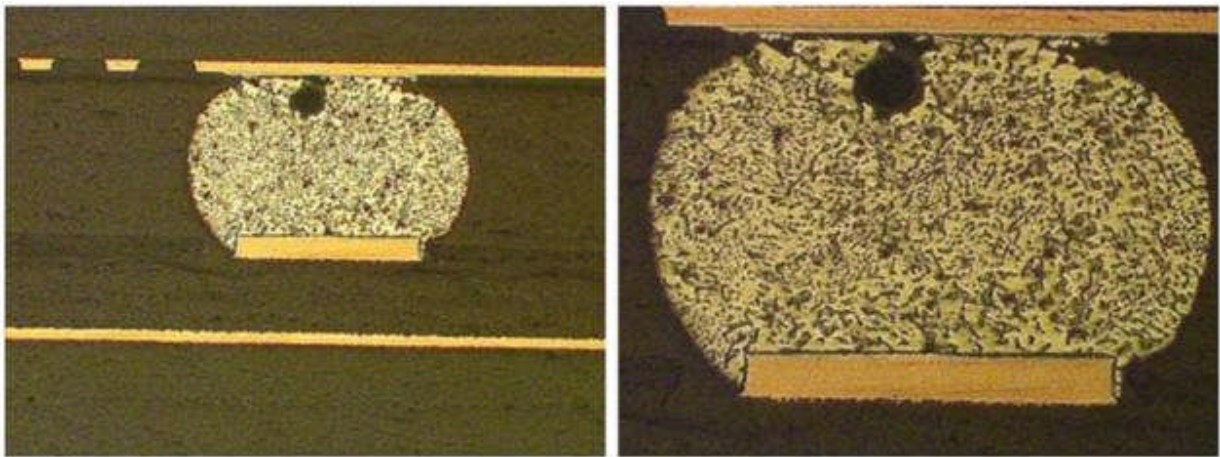


Figure 148 - PBGA-225 Solder Joints, Board 8, Component U5, SnPb/SnPb, Failed @ 2431 Cycles

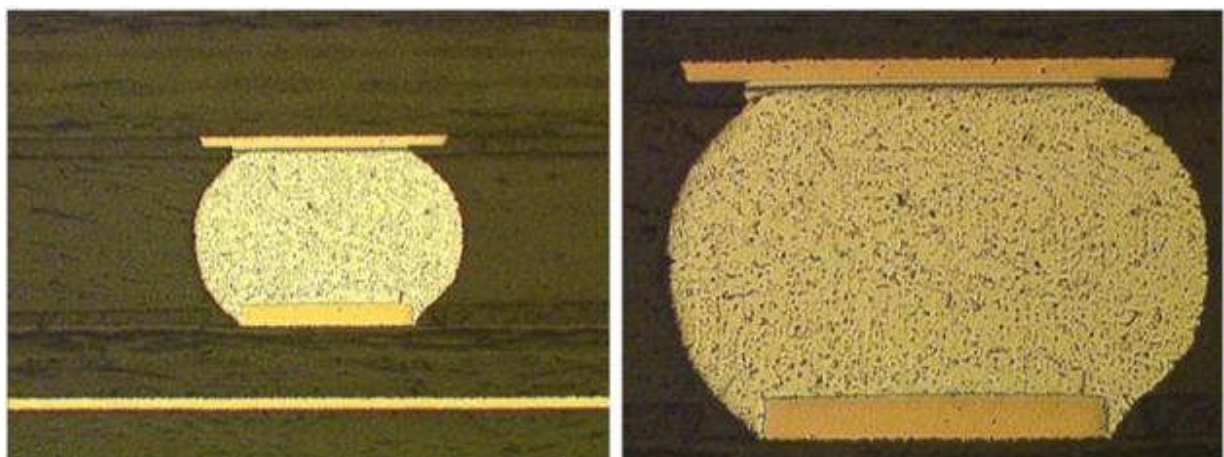


Figure 149 - PBGA-225 Solder Joints, Board 127, Component U5, SnPb/SAC405, DNF

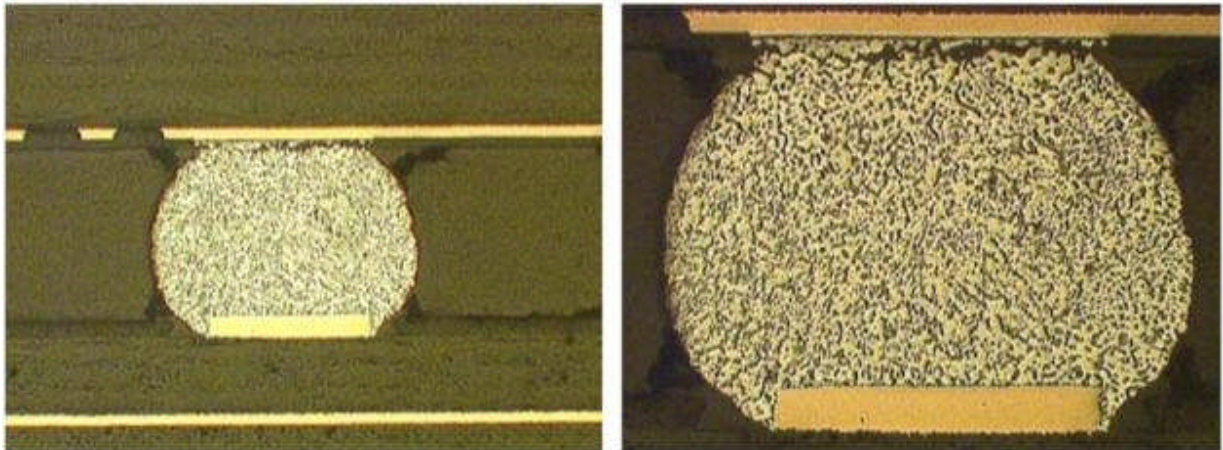


Figure 150 - PBGA-225 Solder Joints, Board 168, Component U5, SAC305/SnPb, Failed @ 1926 Cycles

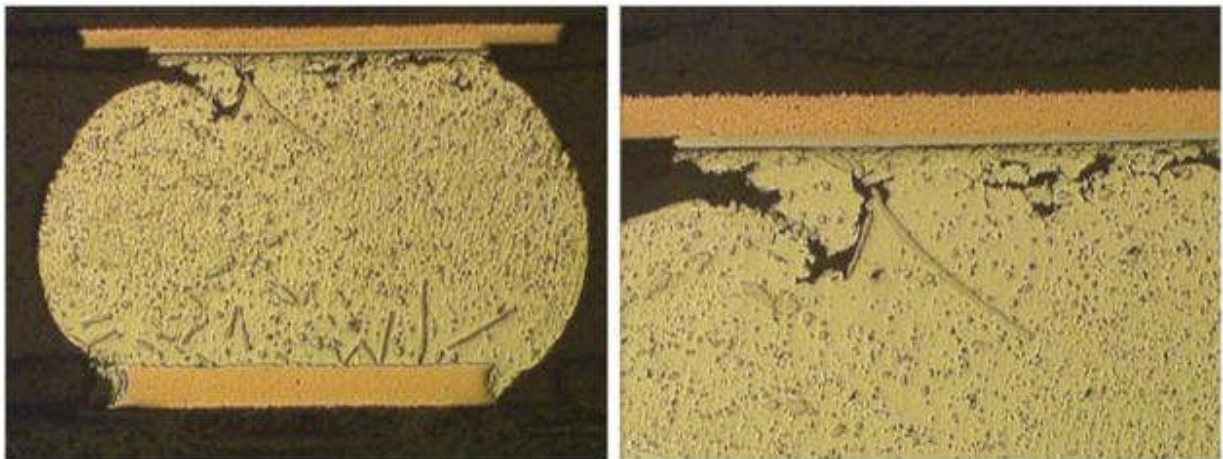


Figure 151 - PBGA-225 Solder Joints, Board 49, Component U6, SAC305/SAC405, Failed @ 2763 Cycles

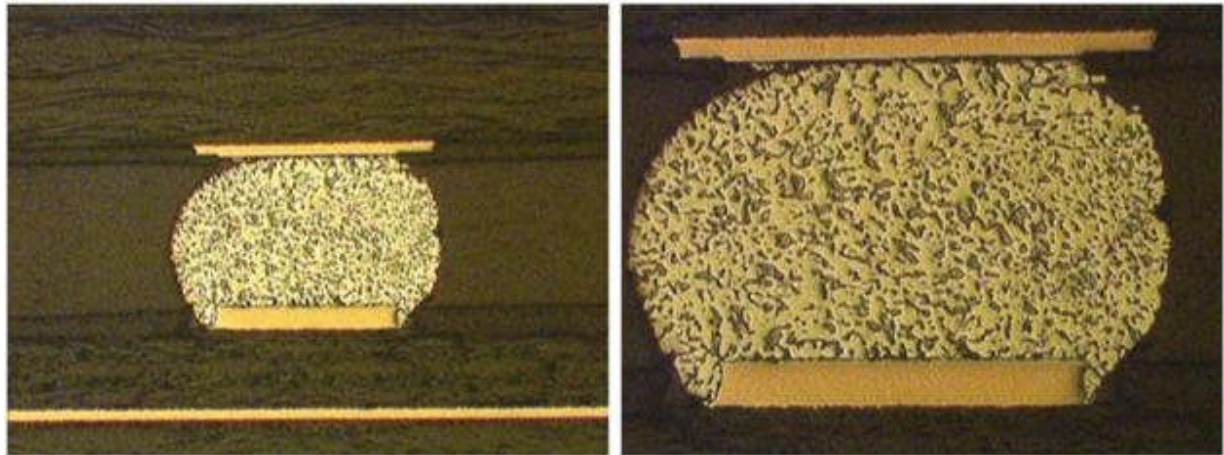


Figure 152 - PBGA-225 Solder Joints, Board 106, Component U55, SN100C/SnPb, Failed @ 1064 Cycles

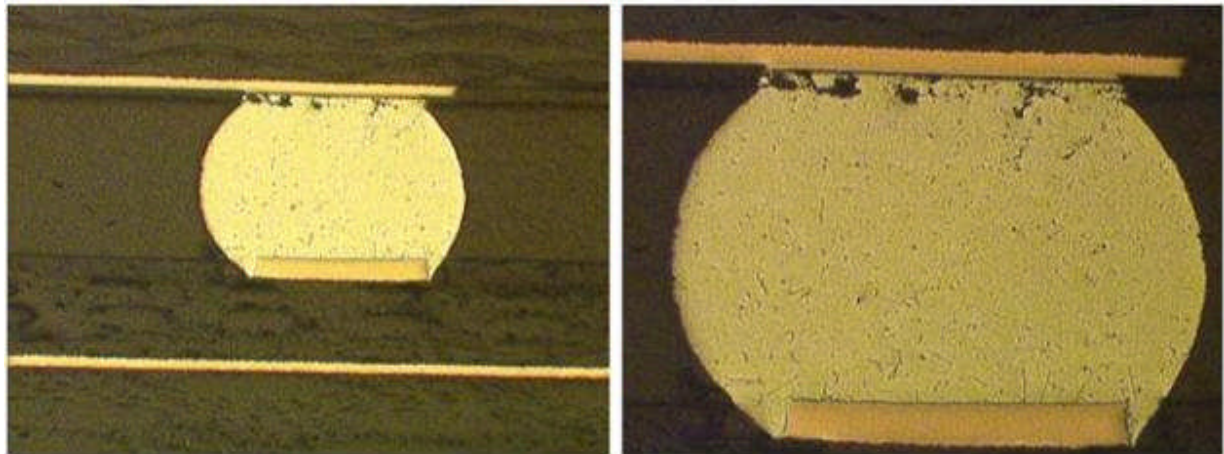


Figure 153 - PBGA-225 Solder Joints, Board 104, Component U21, SN100C/SAC405, Failed @ 3812 Cycles

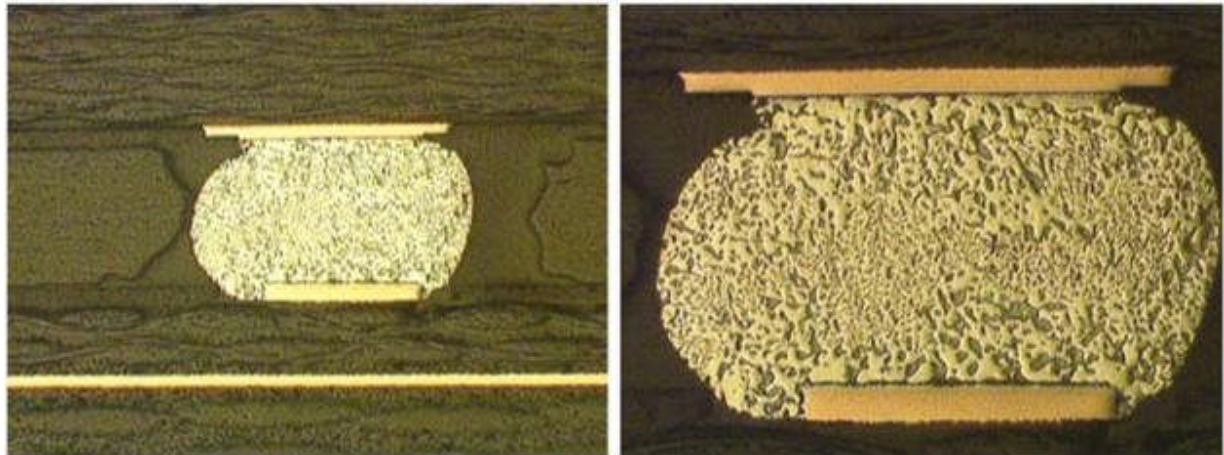


Figure 154 - Reworked PBGA-225 Solder Joints, Board 127, Component U56, Initially SnPb/SnPb, 1 rework Flux Only/SnPb, Failed @ 2349 Cycles

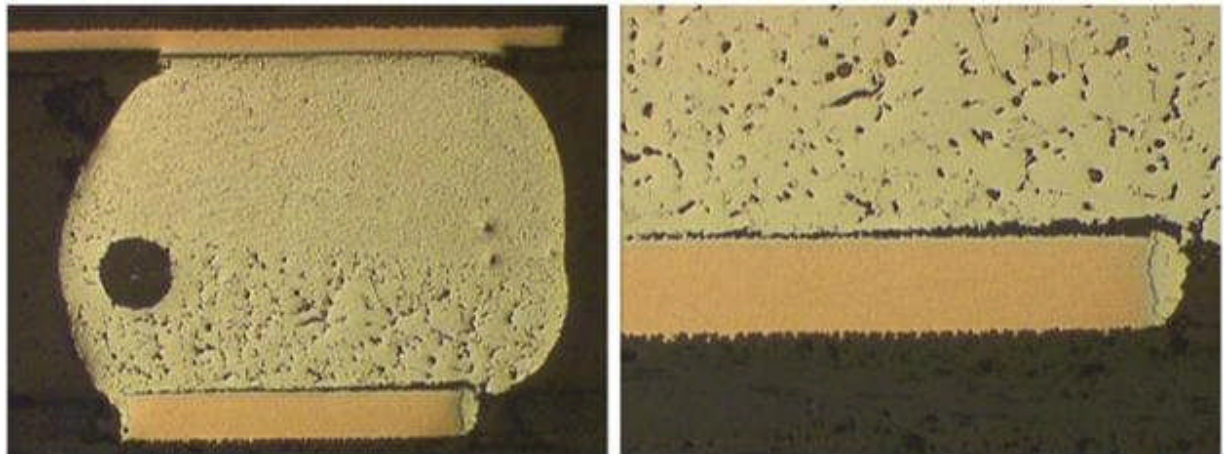


Figure 155 - Reworked PBGA-225 Solder Joints, Board 124, Component U6, Initially SnPb/SnPb, 1 rework SnPb/SAC405, Failed @ 2137 Cycles

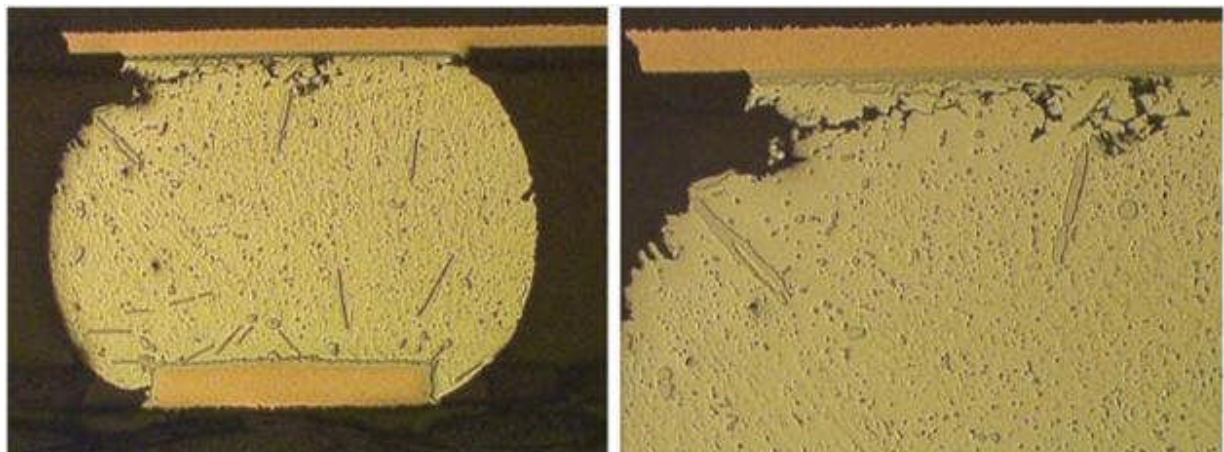


Figure 156 - Reworked PBGA-225 Solder Joints, Board 127, Component U56, Initially SAC305/SAC405, 1 rework Flux Only/SAC405, Failed @ 2349 Cycles

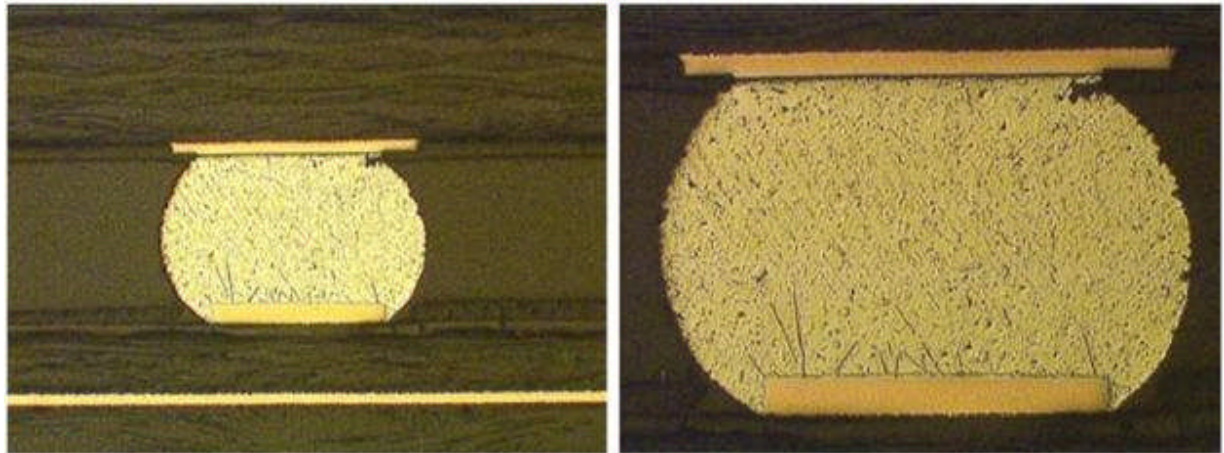


Figure 157 - Reworked PBGA-225 Solder Joints, Board 164, Component U18, Initially SAC305/SAC405, 1 rework SnPb/SAC405, DNF

5.4.2.5 Chip Scale Package (CSP-100) Results

5.4.2.5.1 Statistical Analysis

The CSP-100 components had accumulated 68% population failure after the completion of 4068 thermal cycles. CSP-100 components had six different combinations (SAC/SAC105, SAC/SnPb, SN100C/SAC105, SN100C/SnPb, SnPb/SAC105, SnPb/SnPb) tested. The solder alloy / component finish combinations were statistically indistinguishable from each other thus no best performing combination was identified. There were a few early failures but overall the results populations were well behaved. The SnPb/SAC105 combination did not have sufficient failures to calculate a valid N63 metric although the lack of failures is a good indication of its thermal cycle solder joint integrity robustness. The small number of solder joint failures for the ENIG test vehicles was very small and therefore no conclusions were made.

The reworked CSP-100 components had accumulated 37% population failure after the completion of 4068 thermal cycles. The reworked CSP-100 component results were very successful with few failures being recorded. One clear result was the impact of using the flux only procedure in comparison to the solder paste procedure. Similar to the reworked BGA flux only procedure, the CSP-100 components reworked with the flux only procedure were not as robust to thermal cycling as the solder paste procedure. It is hypothesized that the smaller solderball diameter of the CSP-100 exacerbates any coplanarity differences in the component solderball array impacting solder joint integrity.

The Weibull plots in Figure 158 through Figure 161 summarize the CSP-100 thermal cycle test results.

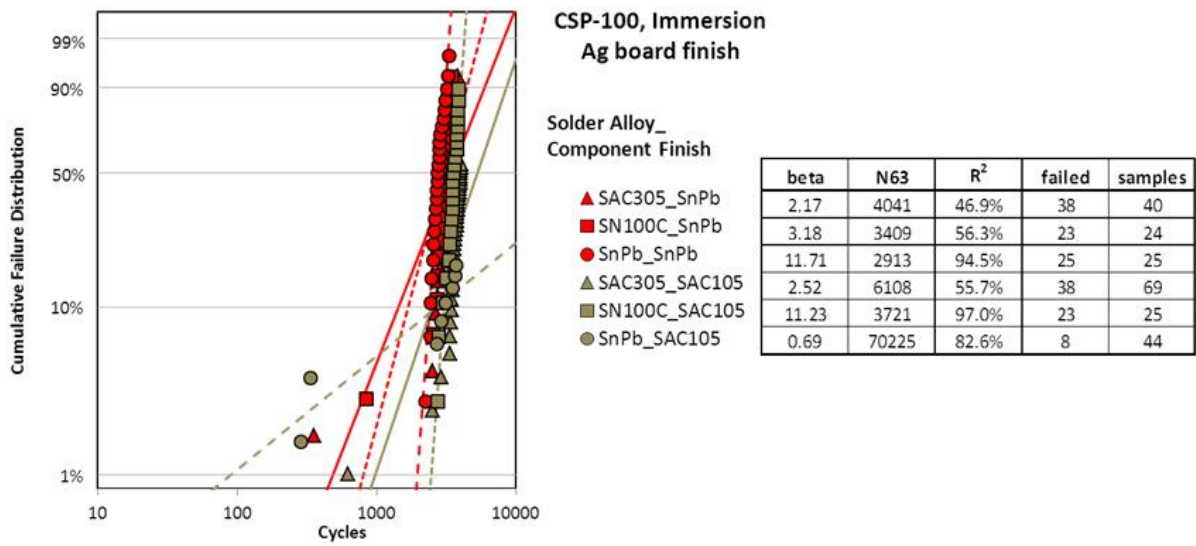


Figure 158 - CSP-100 Weibull Plot for Immersion Silver PWB Finish

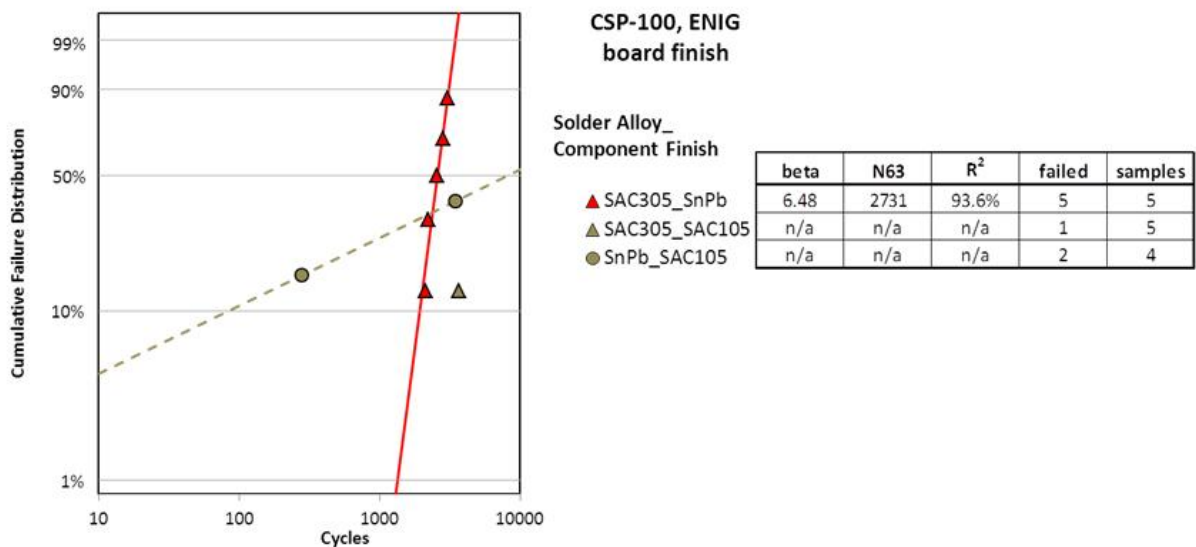


Figure 159 - CSP-100 Weibull Plot for ENIG PWB Finish

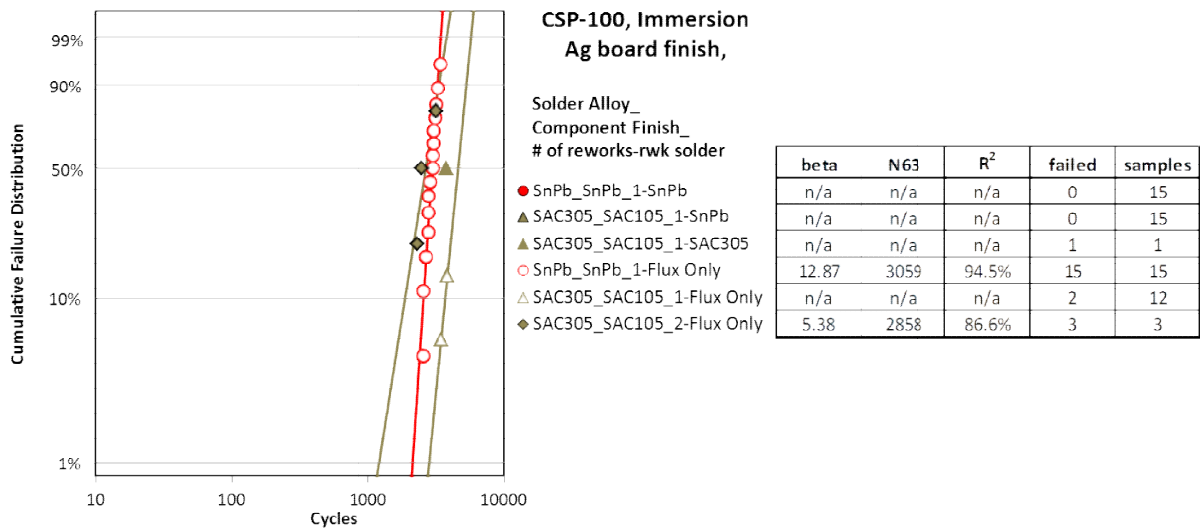


Figure 160 - Reworked CSP-100 Weibull Plot for Immersion Silver PWB Finish

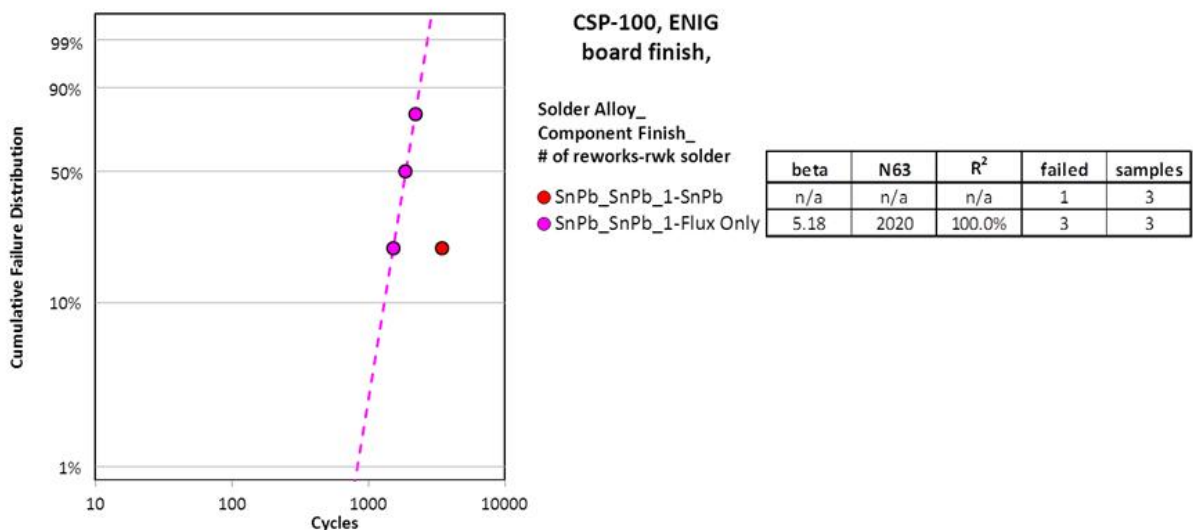


Figure 161 - Reworked CSP-100 Weibull Plot for ENIG PWB Finish

5.4.2.5.2 Physical Failure Analysis

Metallographic cross-sectional analysis was conducted on the CSP-100 components to document the solder joint failure location, crack morphology and solder joint microstructure. A significant amount of physical failure analysis was conducted on the CSP-100 rework test vehicles. General physical failure observations of the failed CSP-100 components were:

- The cracks in the solder joints were observed to have to failure modes: (1) initiation at the solder joint/component pad interface; (2) significant solder ball deformation with cracks at either solder joint component pad or solder joint/test vehicle pad interface.

- The solder joint geometries and wetting angles were acceptable and met industry workmanship criteria. There were a number of instances where the voids were observed in the solder joints but their presence was not detrimental to the solder joint integrity
- The manufactured test vehicle solder joint microstructures were homogenous with no segregation regions and the solder ball alloy (i.e. SnPb or SAC405) dominated the microstructure as it provided the largest material contribution to the solder joint formation. All of the CSP-100 solder microstructures had significant shear deformation with grain coarsening observed.
- The reworked test vehicle solder joint microstructures did not appear to be different than the as-manufactured solder joint microstructures.

Figure 162 thru Figure 171 illustrate the typical PBGA-225 solder joint failures observed.

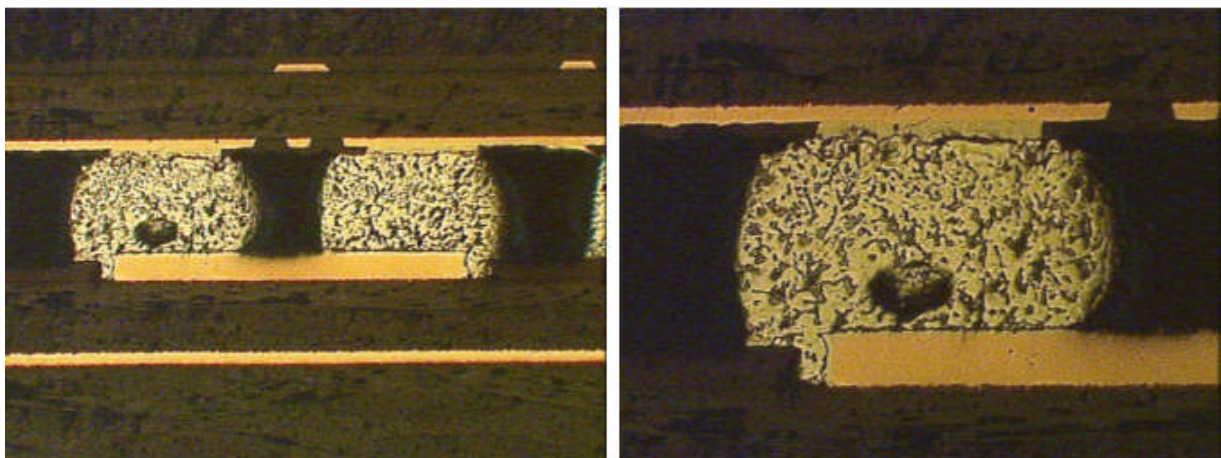


Figure 162 - CSP-100 Solder Joints, Board 7, Component U37, SnPb/SnPb, Failed @ 2837 Cycles

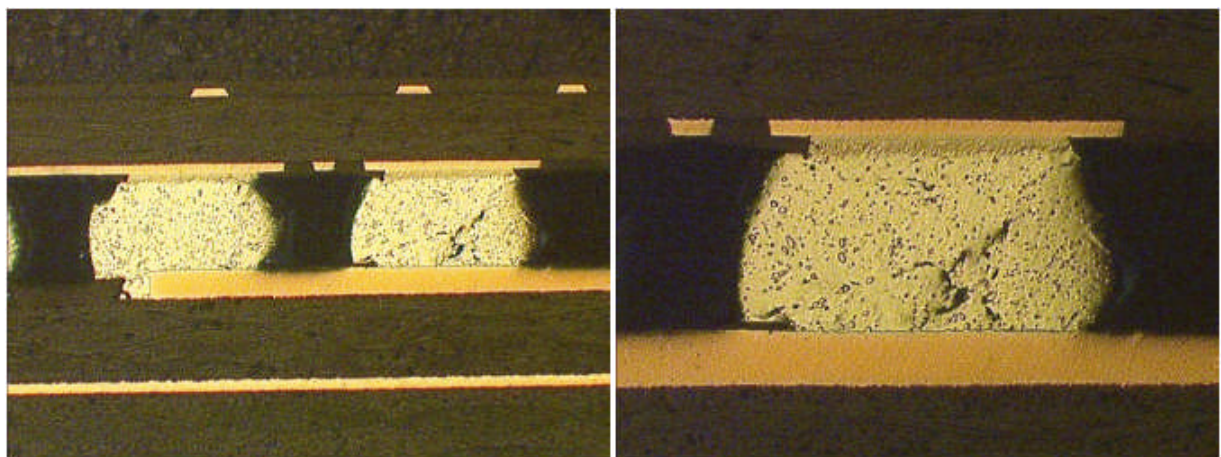


Figure 163 - CSP-100 Solder Joints, Board 124, Component U32, SnPb/SAC105, Failed @ 287 Cycles

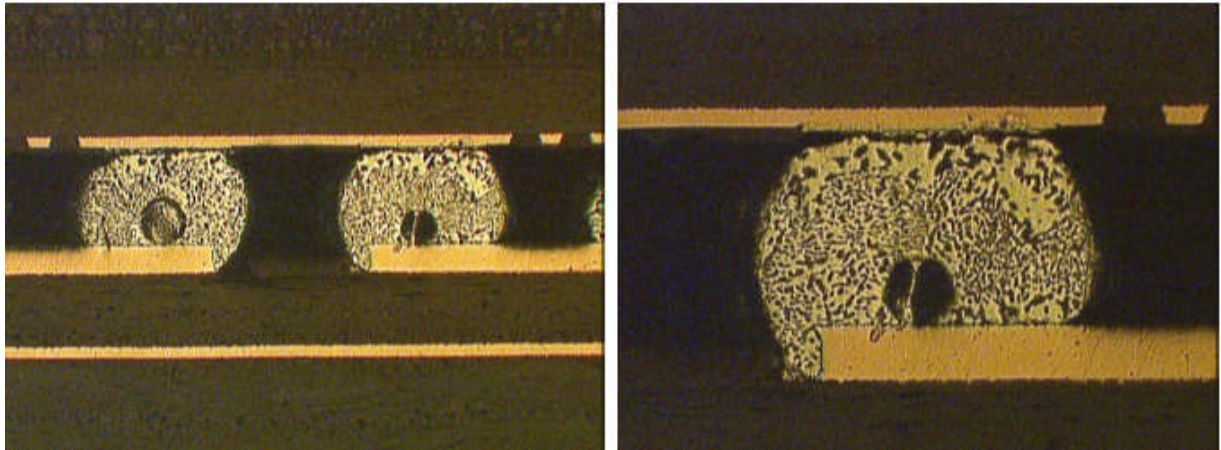


Figure 164 - CSP-100 Solder Joints, Board 166, Component U32, SAC305/SnPb, Failed @ 3417 Cycles

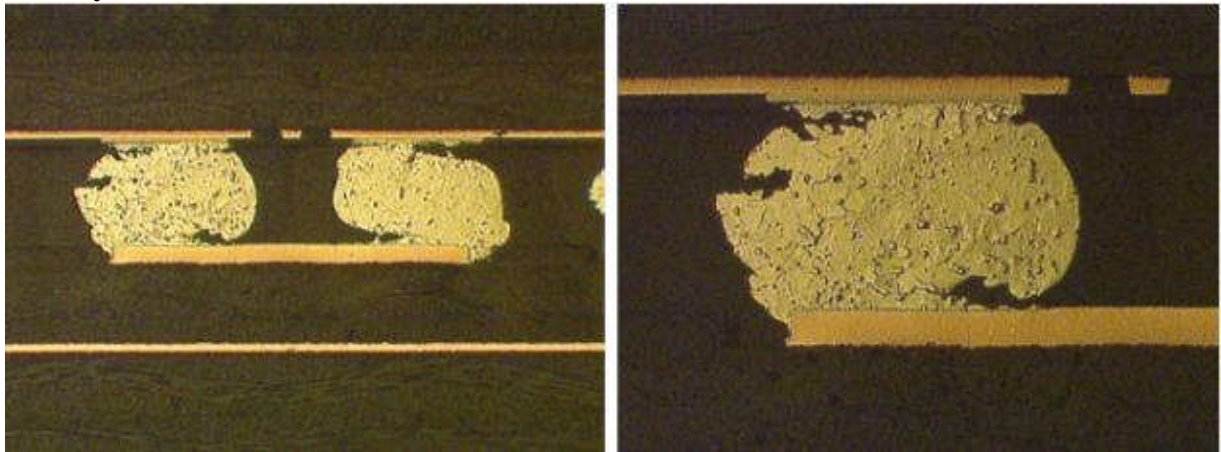


Figure 165 - CSP-100 Solder Joints, Board 49, Component U60, SAC305/SAC105, Failed @ 3908 Cycles

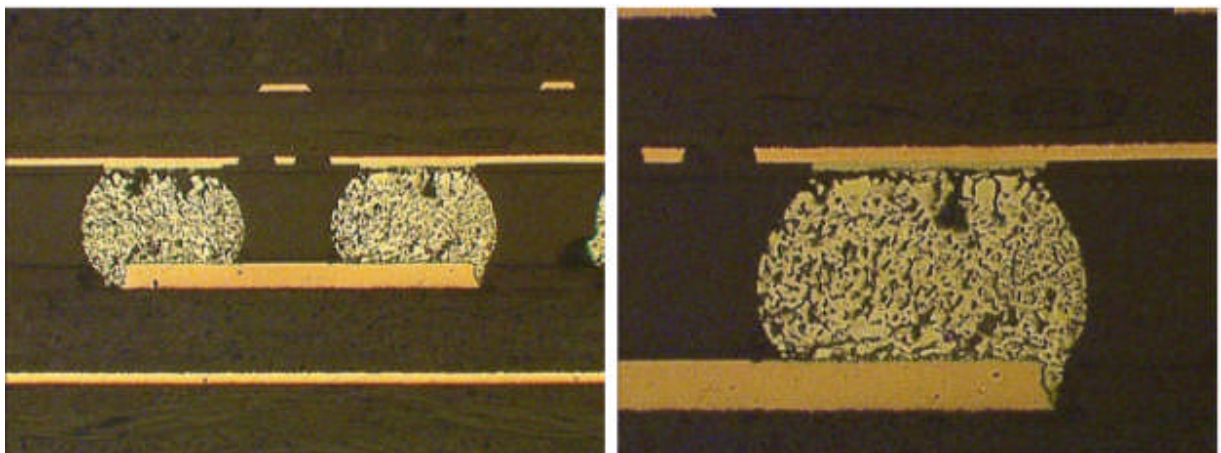


Figure 166 - CSP-100 Solder Joints, Board 103, Component U33, SN100C/SnPb, Failed @ 2932 Cycles

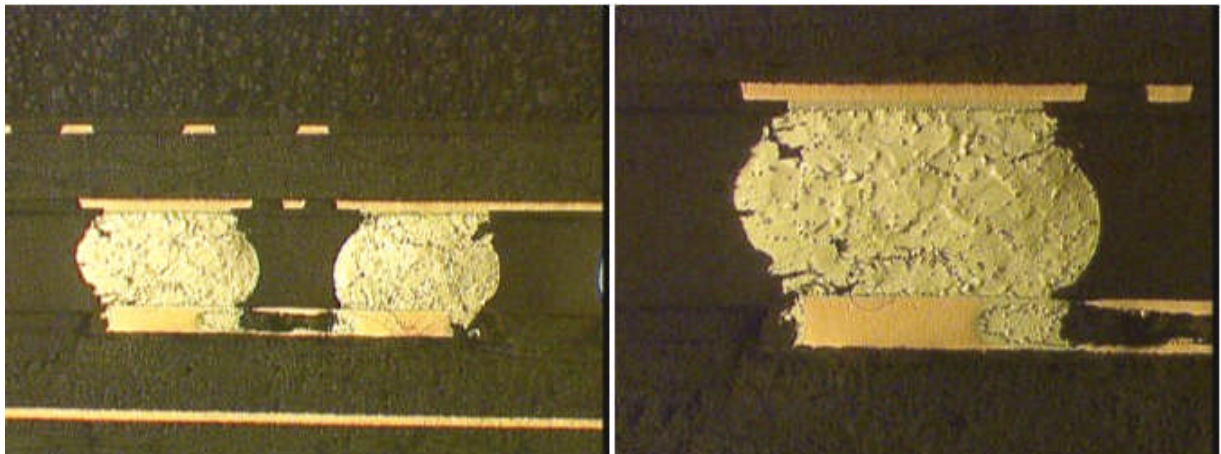


Figure 167 - CSP-100 Solder Joints, Board 106, Component U36, SN100C/SAC105, Failed @ 3908 Cycles

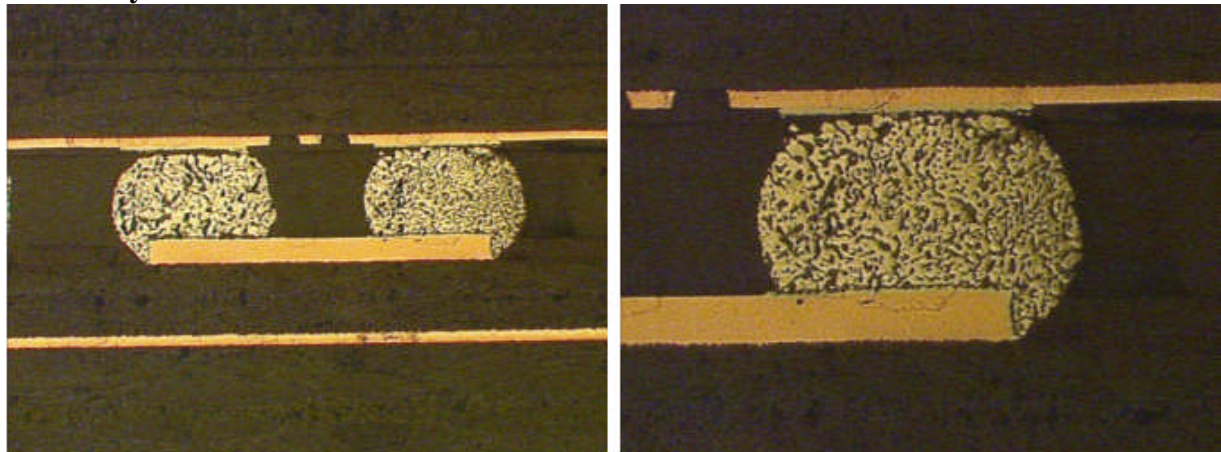


Figure 168 - Reworked CSP-100 Solder Joints, Board 128, Component U19, Initially SnPb/SnPb, 1 rework Flux Only/SnPb, Failed @ 3012 Cycles

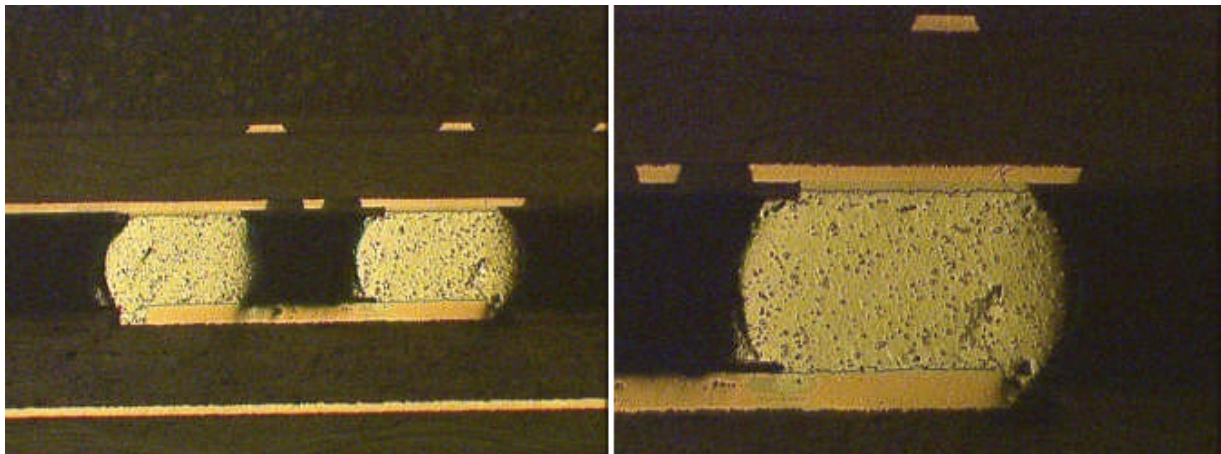


Figure 169 - Reworked CSP-100 Solder Joints, Board 126, Component U60, Initially SnPb/SnPb, 1 rework SnPb/SAC105, DNF

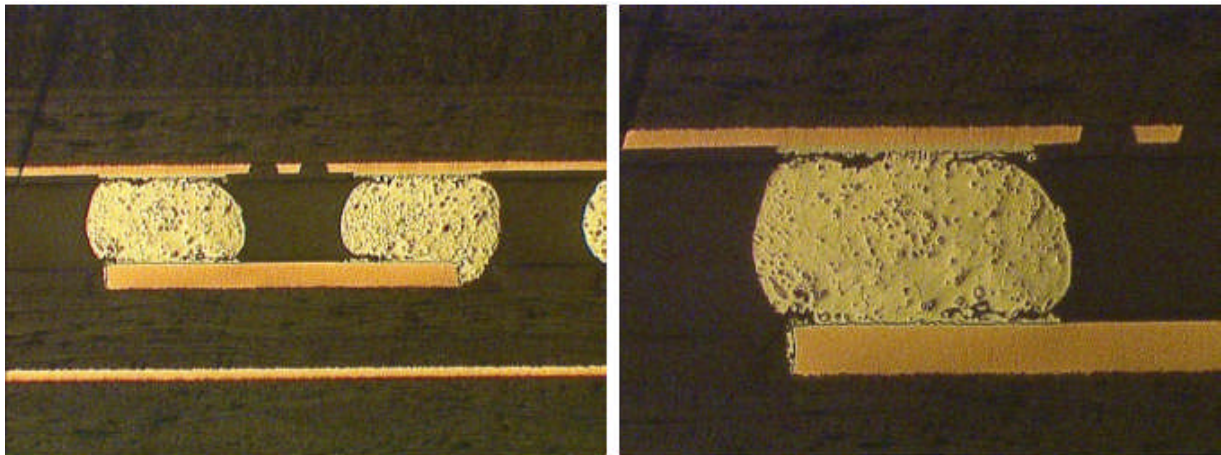


Figure 170 - Reworked CSP-100 Solder Joints, Board 168, Component U19, Initially SAC305/SAC105, 1 rework Flux Only/SAC105, DNF

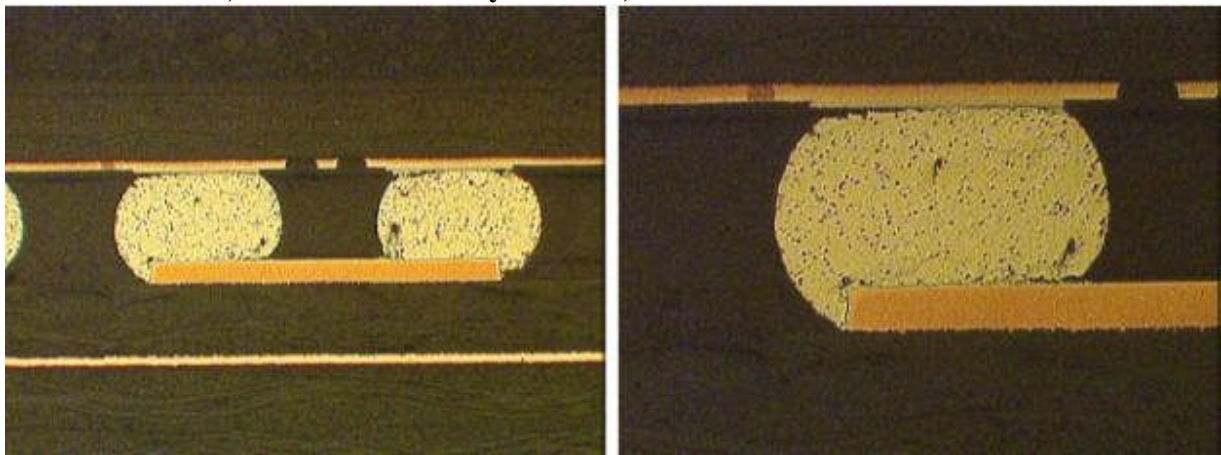


Figure 171 - Reworked CSP-100 Solder Joints, Board 164, Component U33, Initially SAC305/SAC105, 1 rework SnPb/SAC105, DNF

5.4.2.6 Thin Small Outline Package (TSOP-50) Results

5.4.2.6.1 Statistical Analysis

The TSOP-50 components had accumulated 99% population failure after the completion of 4068 thermal cycles. TSOP-50 components had nine different combinations (SAC/SnPb, SAC/SnBi, SAC/Sn, SN100C/SnPb, SN100C/SnBi, SN100C/Sn, SnPb/SnBi, SnPb/Sn, SnPb/SnPb) tested. This result is not surprising as TSOP components which use an Alloy 42 lead material are known to have solder joint integrity issues in High Performance electronics applications (9). The solder alloy/component finish combinations were statistically indistinguishable from each other thus no best performing combination was identified. The results populations were very well behaved. The small number of solder joint failures for the ENIG test vehicles was very small and therefore no conclusions were made.

The reworked TSOP-50 components had accumulated 100% population failure after the completion of 4068 thermal cycles. The results show that no preferred alloy/component finish combination could be selected from the data as the combination populations were statistically indistinguishable from each other for both the 1 Rework and 2 Rework cases.

The Weibull plots in Figure 172 through Figure 175 summarize the TSOP-50 thermal cycle test results.

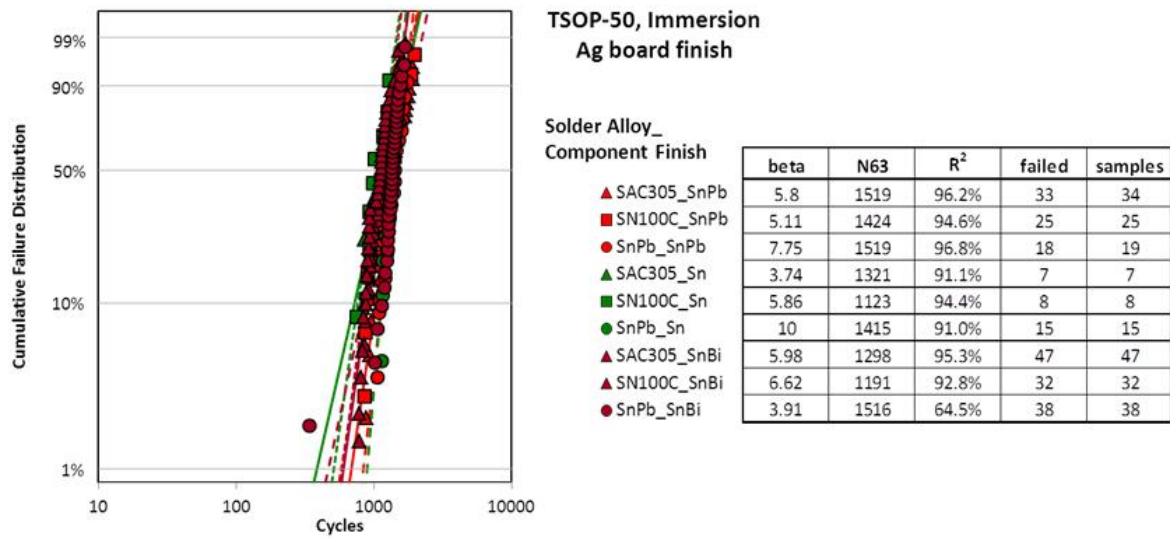


Figure 172 - TSOP-50 Weibull Plot for Immersion Silver PWB Finish

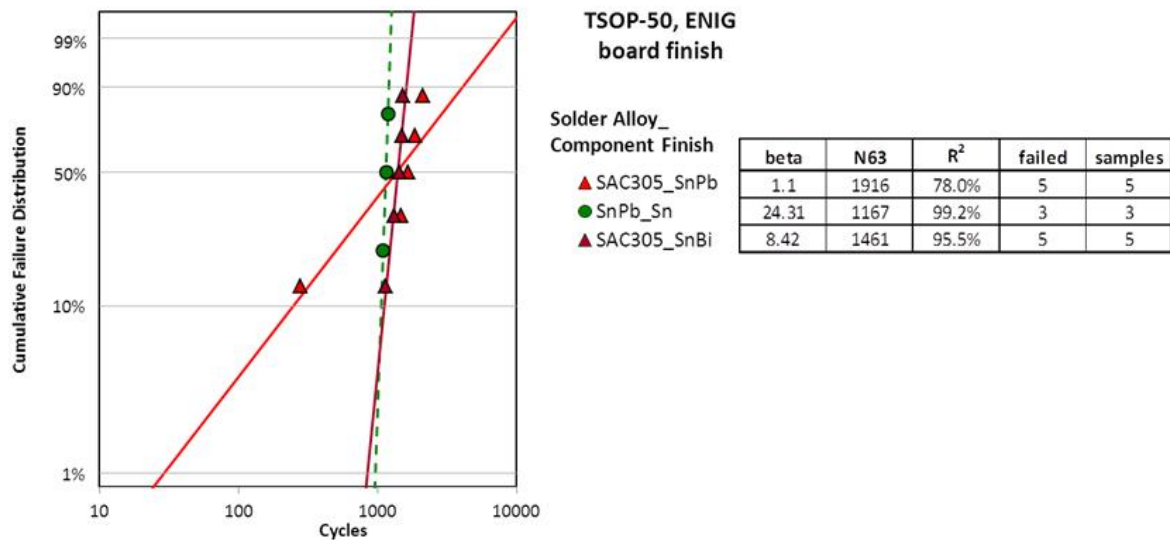


Figure 173 - TSOP-50 Weibull Plot for ENIG PWB Finish

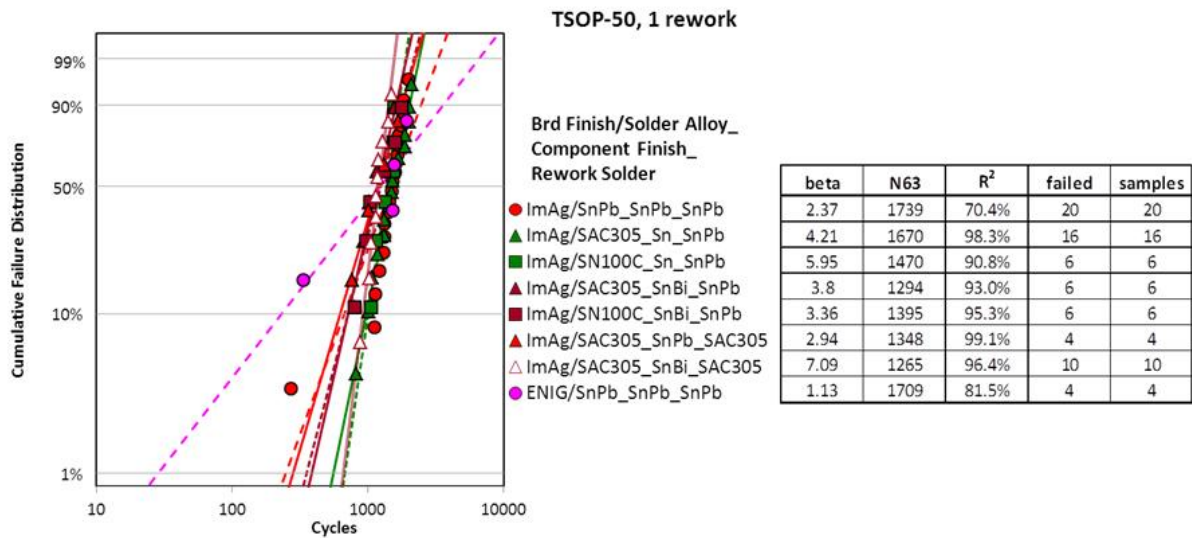


Figure 174 - TSOP-50 Rework Weibull Plot for 1 Rework

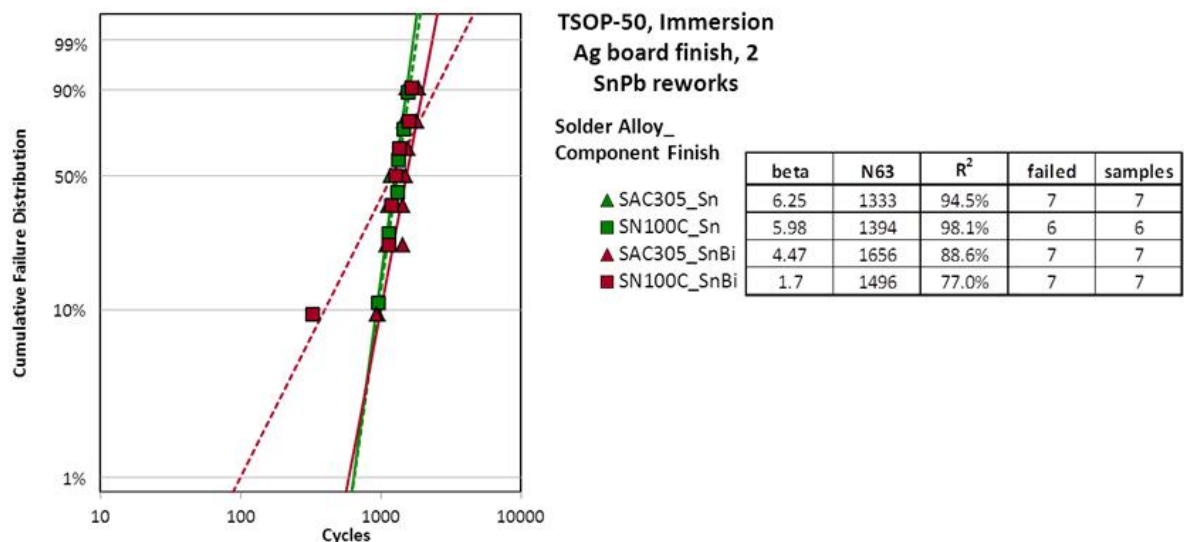


Figure 175 - TSOP-50 Rework Weibull Plot for 2 Rework

5.4.2.6.2 Physical Failure Analysis

Metallographic cross-sectional analysis was conducted on the TSOP-50 components to document the solder joint failure location, crack morphology and solder joint microstructure. General physical failure observations of the failed TSOP-50 components were:

- The cracks in the solder joints initiated in the heel fillet region and traversed under the foot towards the lead toe. The crack formation and location are in agreement with industry knowledge of Alloy 42 TSOP failure modes (9).

- The solder joint geometries and wetting angles were acceptable and met industry workmanship criteria (IPC J-STD-001D “Requirements for Soldered Electrical and Electronic Assemblies”, end-product Class 3 “High Performance Electronics Products”). There were a number of instances where the solder did flow into the upper lead bend region. In most cases this condition is acceptable per industry standards. However several solder joints, primarily reworked cases, were observed with excessive solder in the upper lead bend which violated industry standards. Rockwell Collins has conducted internal studies demonstrating that solder material located between the component lead and the component body does not cause solder joint integrity issues for plastic bodied components (10).
- The solder joint microstructures were reasonably homogenous with no segregation regions observed in the mixed metallurgy cases.

Figure 176 thru Figure 185 illustrate the typical TSOP-50 solder joint failures observed.

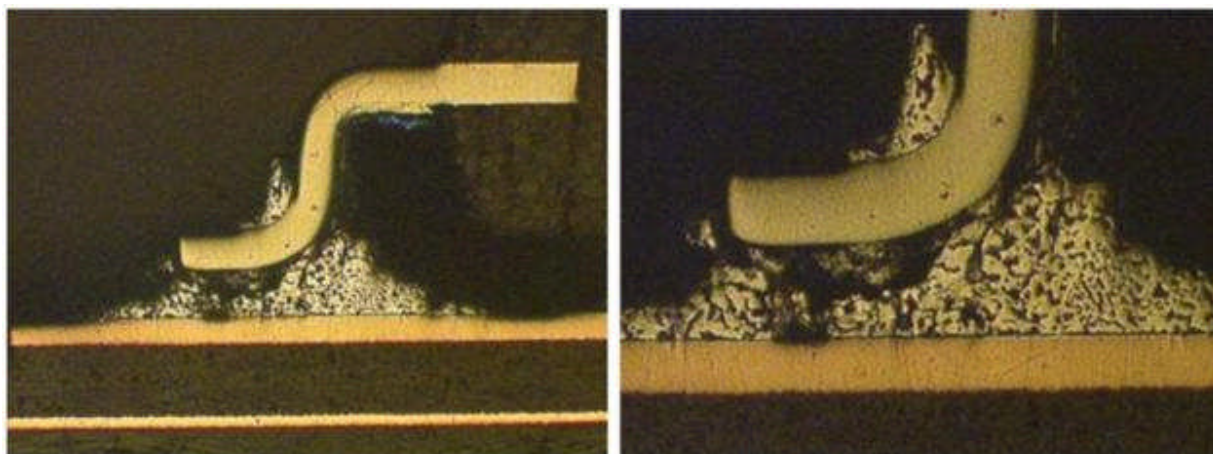


Figure 176 - TSOP-50 Solder Joints, Board 8, Component U40, SnPb/SnPb, Failed @ 1252 Cycles

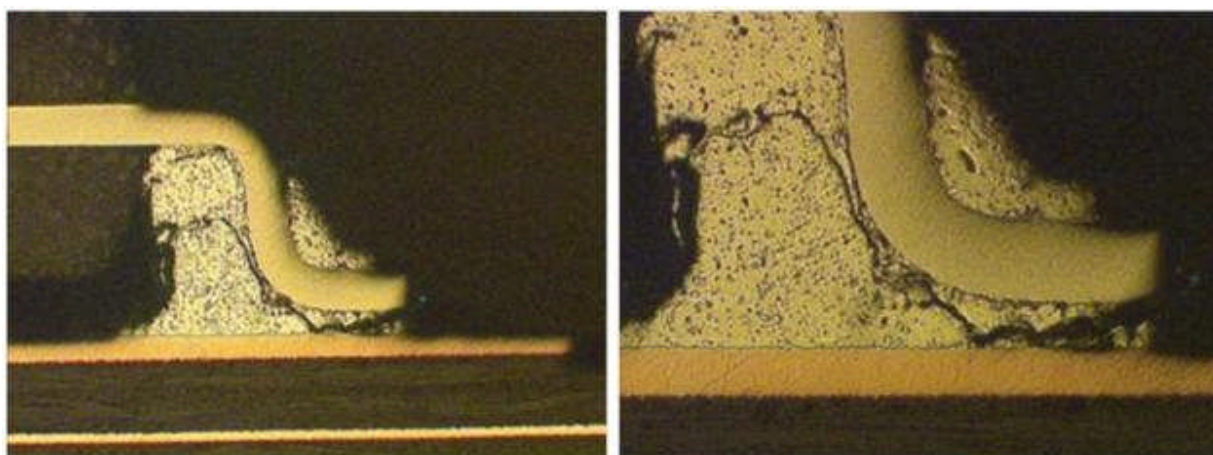


Figure 177 - TSOP-50 Solder Joints, Board 44, Component U25, SAC305/SnPb, Failed @ 1787 Cycles

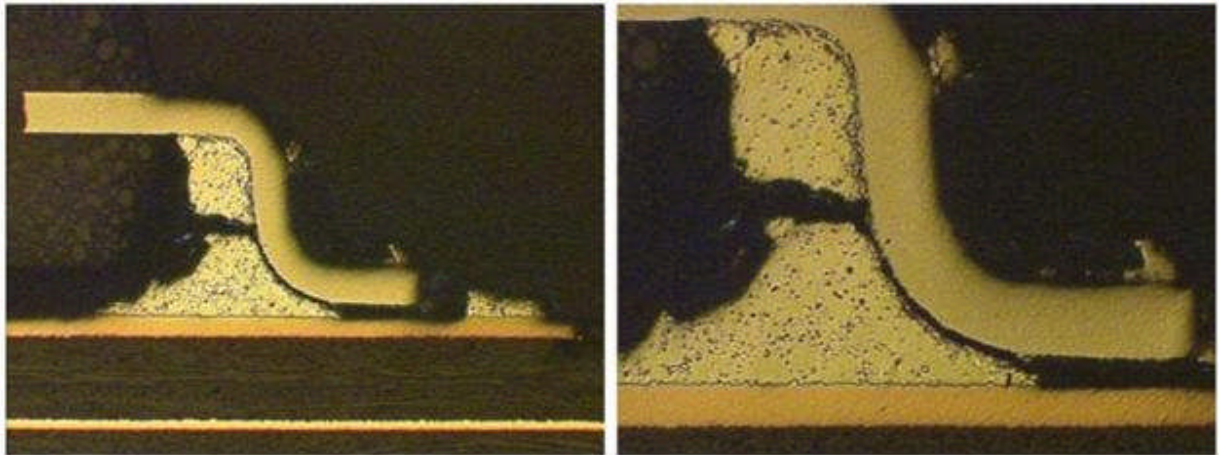


Figure 178 - TSOP-50 Solder Joints, Board 103, Component U39, SN100CSnPb, Failed @ 851 Cycles

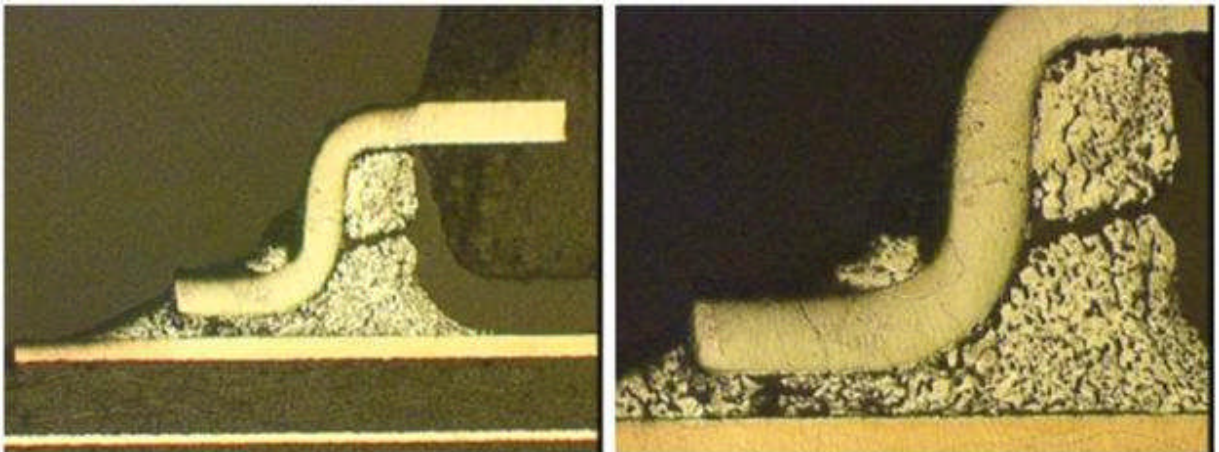


Figure 179 - TSOP-50 Solder Joints, Board 8, Component U29, SnPb/SnBi, Failed @ 1424 Cycles

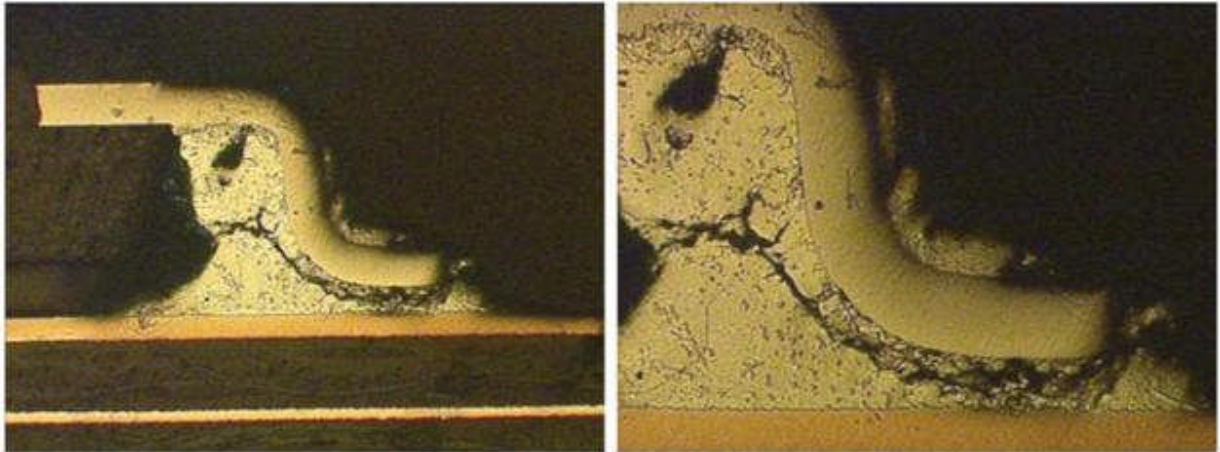


Figure 180 - TSOP-50 Solder Joints, Board 166, Component U39, SAC305/SnBi, Failed @ 1594 Cycles

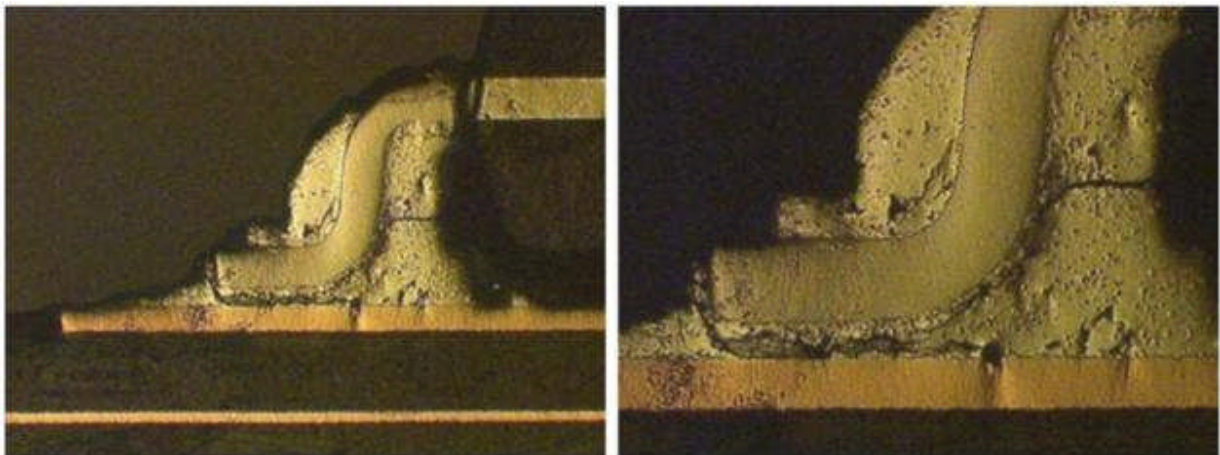


Figure 181 - TSOP-50 Solder Joints, Board 102, Component U34, SN100C/SnBi, Failed @ 1985 Cycles

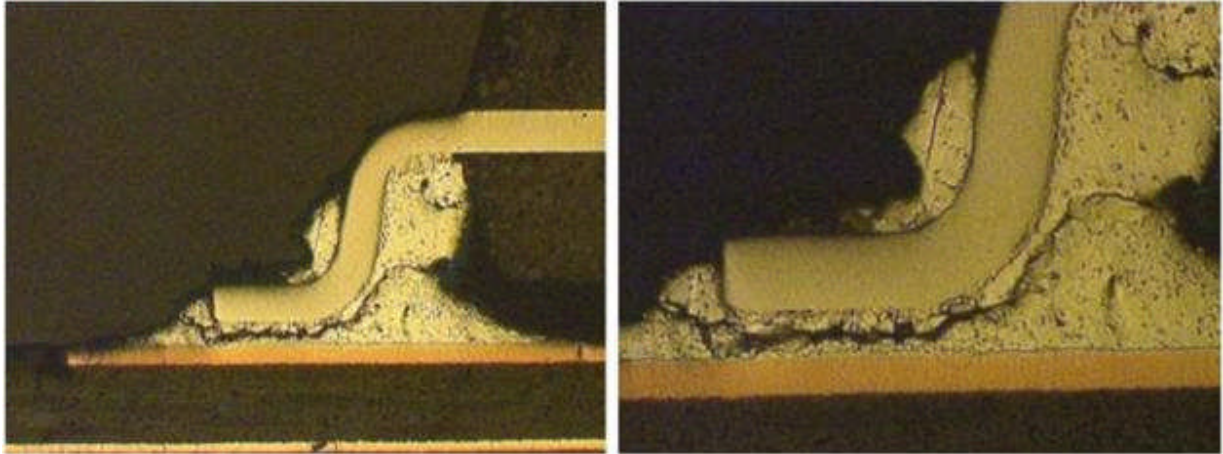


Figure 182 - TSOP-50 Solder Joints, Board 107, Component U61, SN100C/Sn, Failed @ 1258 Cycles

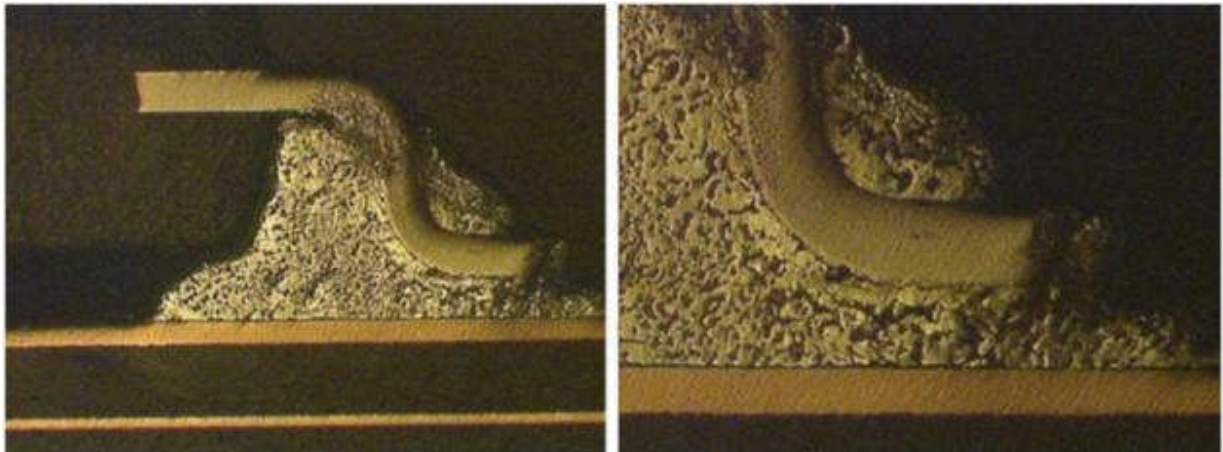


Figure 183 - Reworked TSOP-50 Solder Joints, Board 127, Component U12, Initially SnPb/SnPb, 1 rework SnPb/SnPb, Failed @ 1443 Cycles

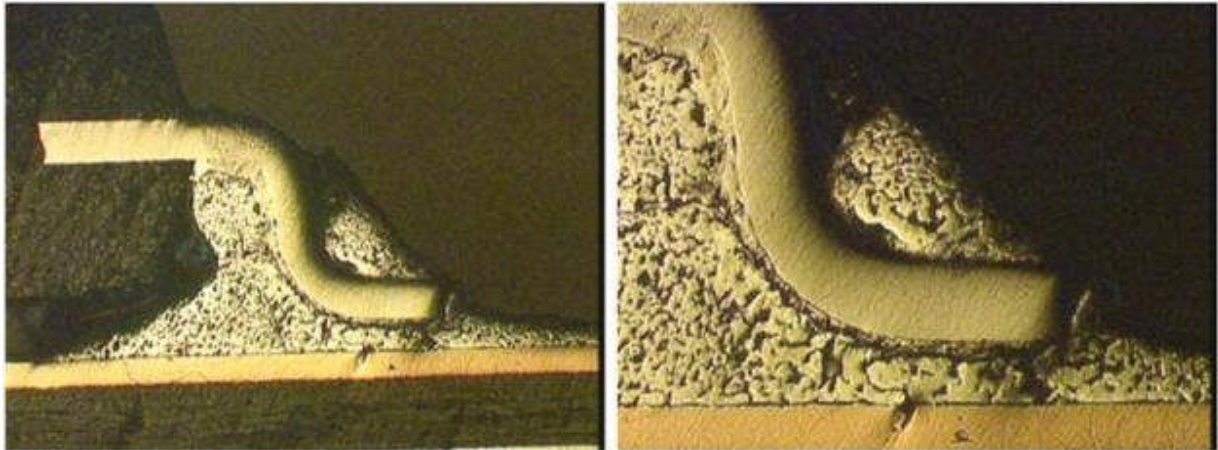


Figure 184 - Reworked TSOP-50 Solder Joints, Board 47, Component U24, Initially SAC305/SnBi, 2 rework SnPb/SnBi, Failed @ 1810 Cycles

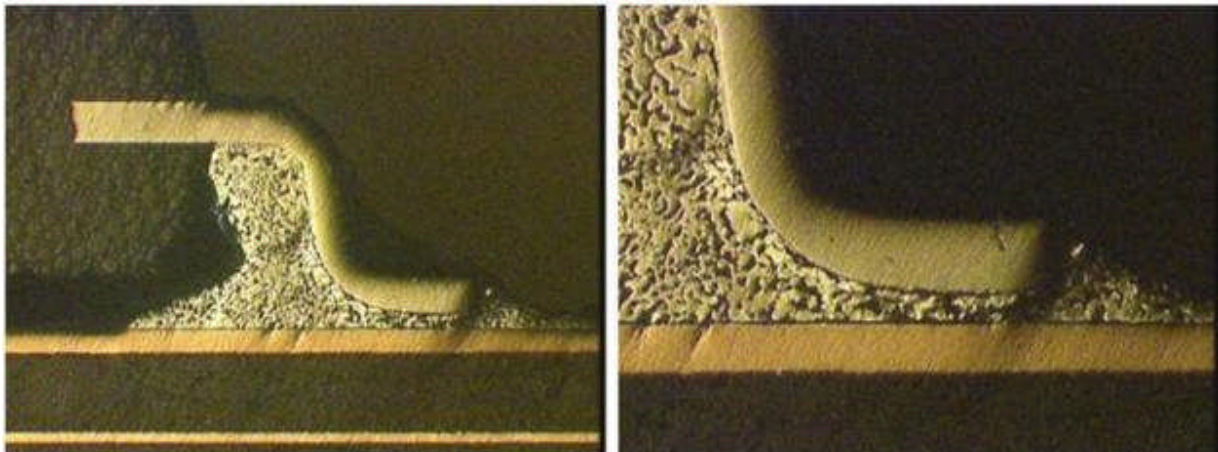


Figure 185 - Reworked TSOP-50 Solder Joints, Board 47, Component U29, Initially SAC305/Sn, 1 rework SnPb/Sn, Failed @ 1010 Cycles

5.4.2.7 Dual In-Line Package (PDIP-20) Results

5.4.2.7.1 Statistical Analysis

The PDIP-20 components had accumulated 38% population failure after the completion of 4068 thermal cycles. The solder joint failure behavior of the PDIP-20 components was a surprise to the consortium team as the PDIP-20 failure rate documented in the JCAA/JGPP investigation results was only 8% after 4743 total thermal cycles. Physical failure analysis of the failed PDIP-20 components revealed a test vehicle fabrication error as the root cause of the dramatically different failure rates. In-depth statistical analyses of test vehicles that contained and did not contain the fabrication defect reveal a significant difference in the results (see Table 32). Plotting of the PDIP-20 components by assembly lot designation conducted by Aaron Pedigo, NSWC Crane, is shown in Figure 186 and Figure 187. The plotted data is in agreement with Table 32 data and illustrates how assembly lots F, G, and I were compromised by the fabrication defect.

Table 32 - Comparison of Test Vehicles With and Without Fabrication Defect: *Note - one failure at 1 cycle excluded from data analysis

PDIP-20 Test Combination			Test vehicles with fab defect			Test vehicles without fab defect		
<i>board finish</i>	<i>solder</i>	<i>component finish</i>	<i># samples</i>	<i>failure rate</i>	<i>first failure</i>	<i># samples</i>	<i>failure rate</i>	<i>first failure</i>
Immersion Ag	SAC305	NiPdAu	0	n/a	n/a	5	20%	1322
		Sn	0	n/a	n/a	5	20%	1593
	SN100C	NiPdAu	17	65%	1037	6	24%	1565
		Sn	46	96%	1024	36	8%	2454
	SnPb	NiPdAu	3	0%	n/a	32	0%	n/a
		Sn	3	100%	2858	31	55%	1010*
ENIG	SN100C	NiPdAu	7	43%	2090	0	n/a	n/a
		Sn	1	100%	2044	0	n/a	n/a
	SnPb	NiPdAu	0	n/a	n/a	3	0%	n/a
		Sn	0	n/a	n/a	3	0%	n/a

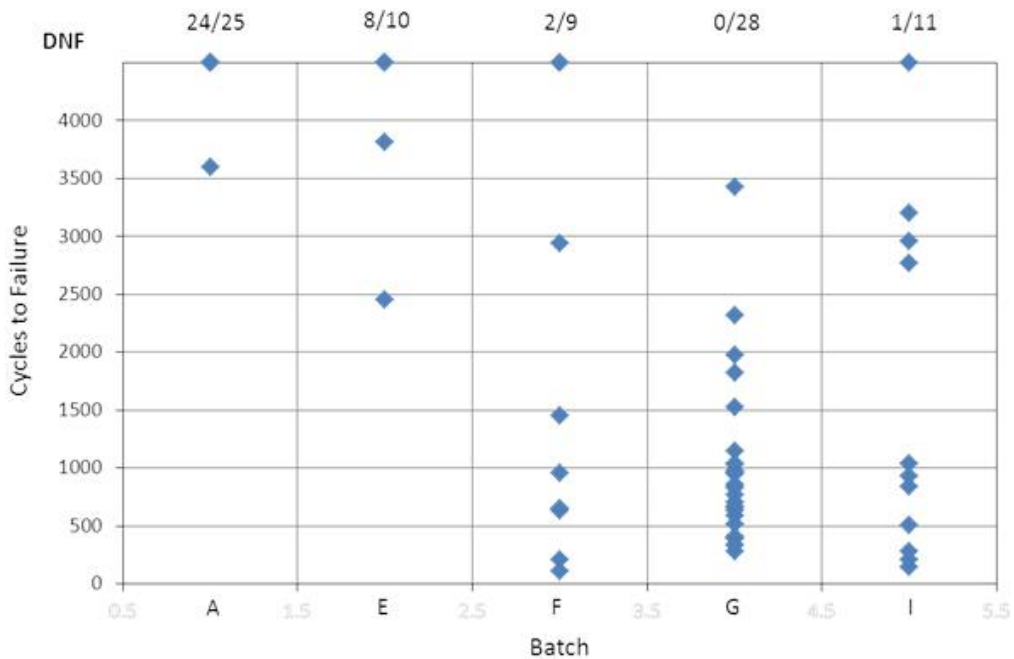


Figure 186 - Cycles to failure for as-manufactured Sn finished PDIP's soldered with SN100C as a function of production batch showing a faster rate of failure for batches F, G, and I.

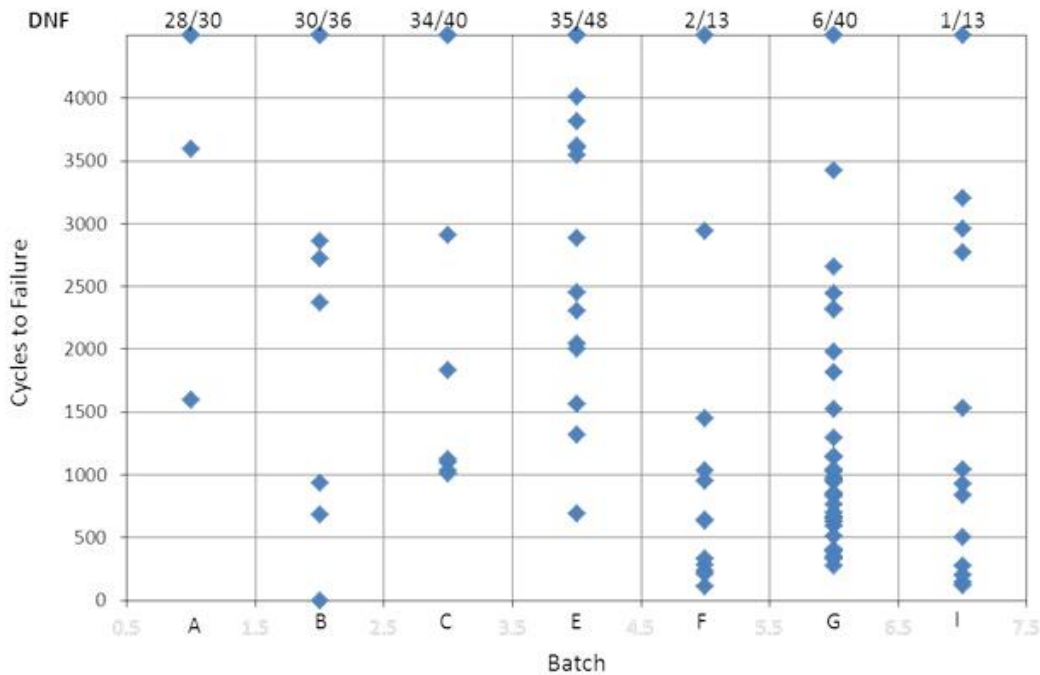


Figure 187 - Cycles to failure agglomerated for all as-manufactured PDIP's as a function of production batch showing a faster rate of failure for batches F, G, and I.

The fabrication defect, which will be thoroughly described in the next section, was found on some of the test vehicles. However, post test electrical continuity testing showed that the defect only influenced the results for the PDIP-20 components, which were the only Plated-Through-Hole (PTH) components in the test. It is believed that the thermal expansion of the PDIP-20 leads within the plated through holes generated z-axis stress that cracked the traces at the defect. The other surface mount components did not produce these out-of-plane stresses and therefore did not encounter these same false failures due to broken circuit traces at the defect. PDIP-20 components had six different combinations (SN100C/Sn, SN100C/NiPdAu, SnPb/NiPdAu, SnPb/Sn, SAC305/NiPdAu, SAC305/Sn) tested. The SN100C/NiPdAu and SnPb/Sn combinations had similar thermal cycle performance results that were slightly better than the other combinations. The remaining combinations – SAC305/NiPdAu, SnPb/NiPdAu, and SAC305/Sn – had insufficient failures to produce valid Weibull characteristics. The number of solder joint failures for the ENIG test vehicles was very small and therefore no conclusions were made.

The reworked PDIP-20 components had accumulated 56% population failure after the completion of 4068 thermal cycles. The non- mixed metallurgy alloy/component finish combinations exhibited better thermal cycle performances than mixed metallurgy combination. The reworked PDIP-20 components with mixed metallurgy combinations showed the same thermal cycle results trends as the mixed metallurgy PBGA-225 alloy/component finish combinations despite being two completely different component technologies (Plated-Through-

Hole versus Surface Mount), demonstrating that a mixed metallurgy situations tend to have more degraded solder joint integrity.

The Weibull plots in Figure 188 through Figure 190 summarize the TSOP-50 thermal cycle test results.

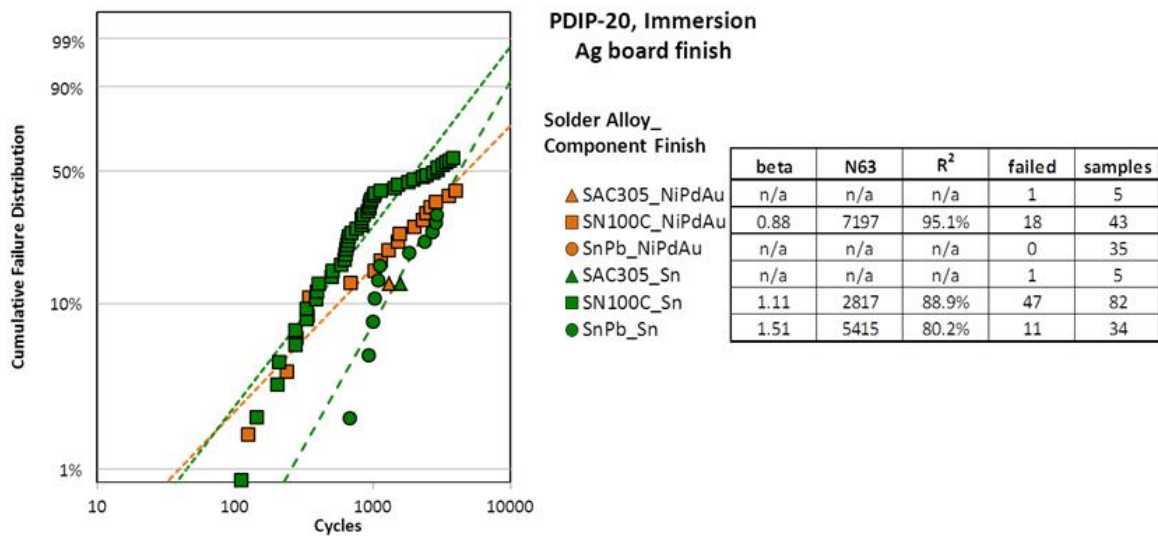


Figure 188 - PDIP-20 Weibull Plot for Immersion Silver PWB Finish

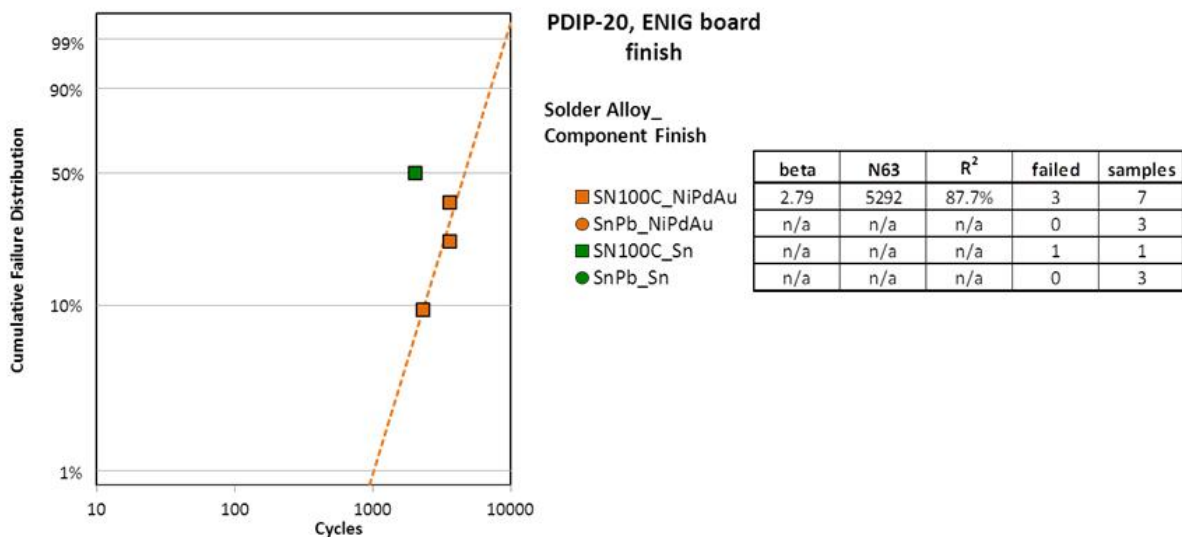


Figure 189 - PDIP-20 Weibull Plot for ENIG PWB Finish

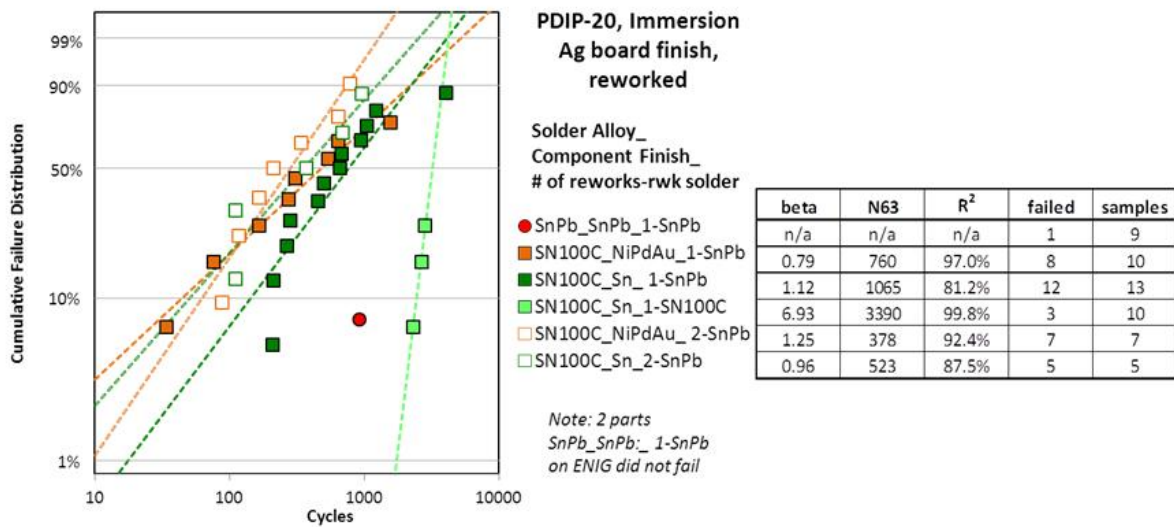


Figure 190 - Reworked PDIP-20 Weibull Plot

5.4.2.7.2 Physical Failure Analysis

Metallographic cross-sectional analysis was conducted on the PDIP-20 components to document the solder joint failure location, crack morphology and solder joint microstructure. One of the issues observed during the NASA DoD testing program was the significant solder joint integrity difference in the PDIP-20 components in comparison with the JCCA/JGGP testing program results. Failure analysis reviewed a fabrication defect in the test vehicle associated with the surface traces for the PDIP-20 components. Poor cleaning/entrapment of fabrication chemistry resulted in the removal of copper beneath the soldermask. Figure 191 and Figure 192 shows a cross-sectional view of the fabrication defect in the test vehicle at the PDIP-20 locations. Fabrication chemistry was trapped under the soldermask edge along the PDIP-20 pads resulting in a reduction of the copper trace thickness.

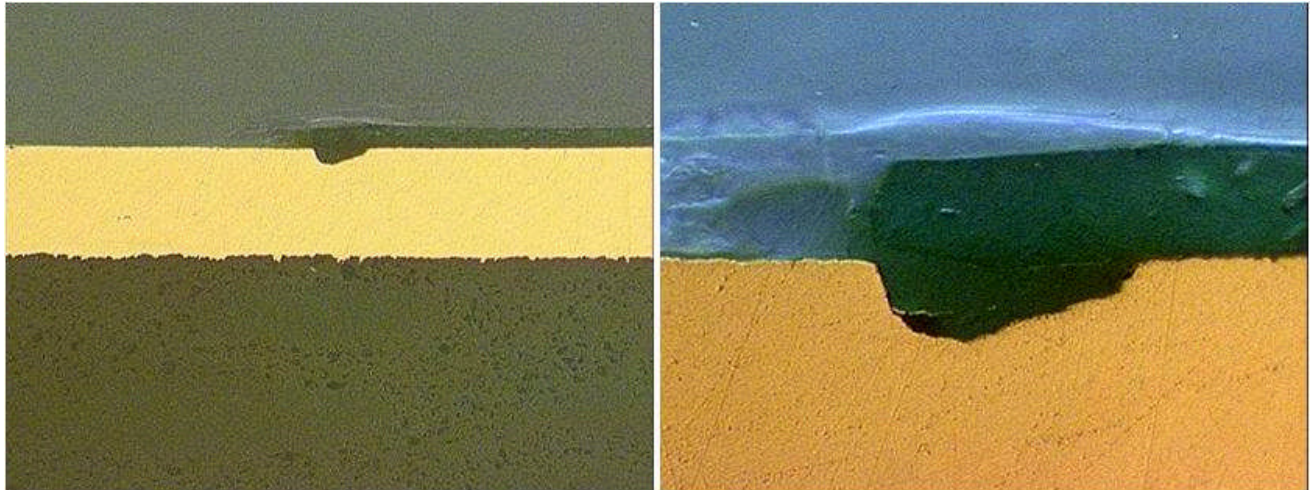


Figure 191 - Cross-sectional Views of the Fabrication Defect in the Test Vehicle at the PDIP-20 Locations (Left – Macro View, Right – Magnified View)

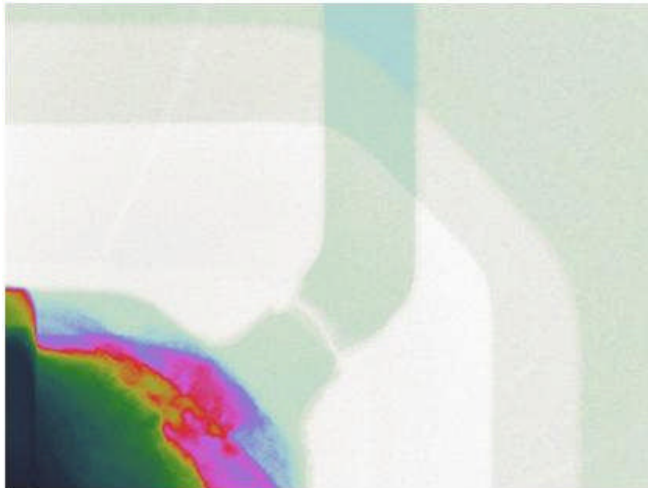


Figure 192 - Color X-ray Image of PDIP-20 Thermal Cycling Induced Cracked Trace

This “necked down” region of the trace cracked during thermal cycling. In addition, the lead-free solder alloys had additional trace integrity degradation due to their copper dissolution characteristics. Figure 193 illustrates the resulting trace cracks due to thermal cycle testing of a PDIP-20 component.

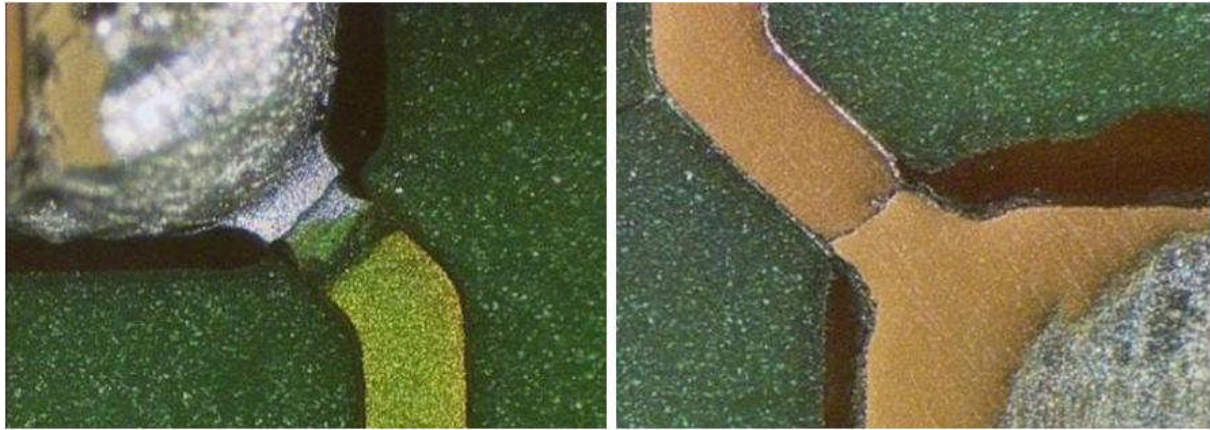


Figure 193 - PDIP-20 Thermal Cycling Induced Cracked Trace at Fabrication Defect Location

Other general physical failure observations of the failed PDIP-20 components in addition to the test vehicle fabrication issue were:

- The cracks in the solder joints initiated in the heel fillet region and traversed under the foot towards the lead toe. The crack formation and location are in agreement with industry knowledge of PDIP failure modes (11).
- The solder joint geometries and wetting angles were acceptable and met industry workmanship criteria. There were a number of instances where the solder did flow into the upper lead bend region which is acceptable per industry standards.
- The solder joint microstructures were reasonably homogenous with no segregation regions observed in the mixed metallurgy cases.

Figure 194 through Figure 196 illustrate the typical TSOP-50 solder joint failures. Note that the “failed cycle” value is when the copper trace broke and not a failure of the solder joint in these figures.

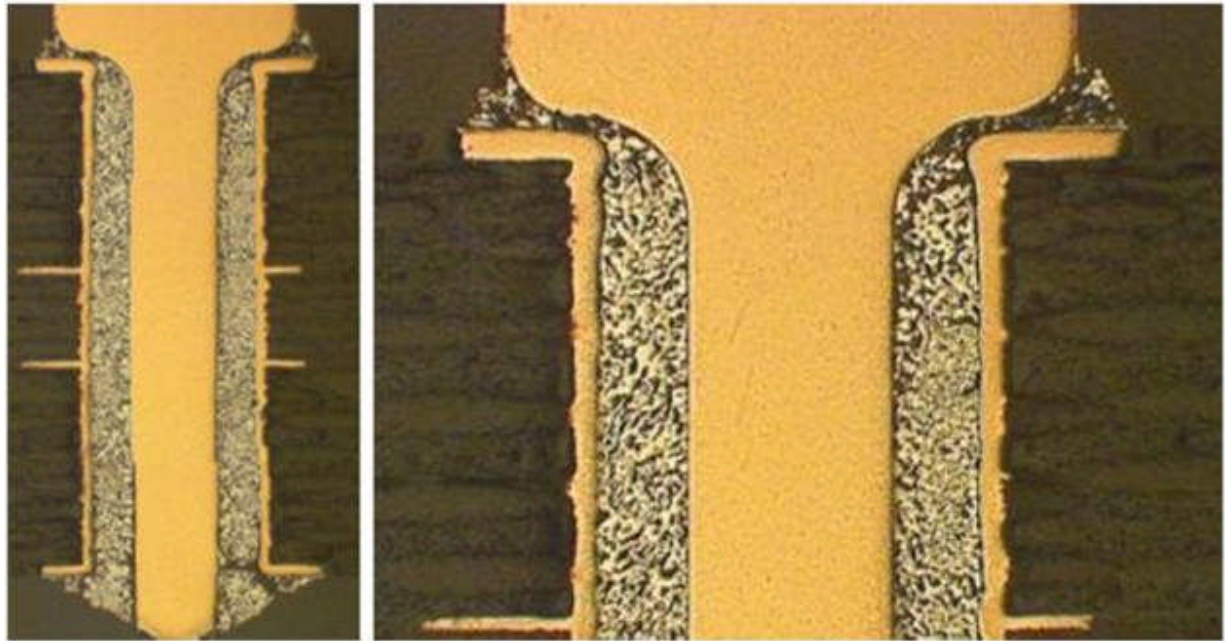


Figure 194 - PDIP-20 Solder Joints, Board 124, Component U23, SnPb/NiPdAu, DNF

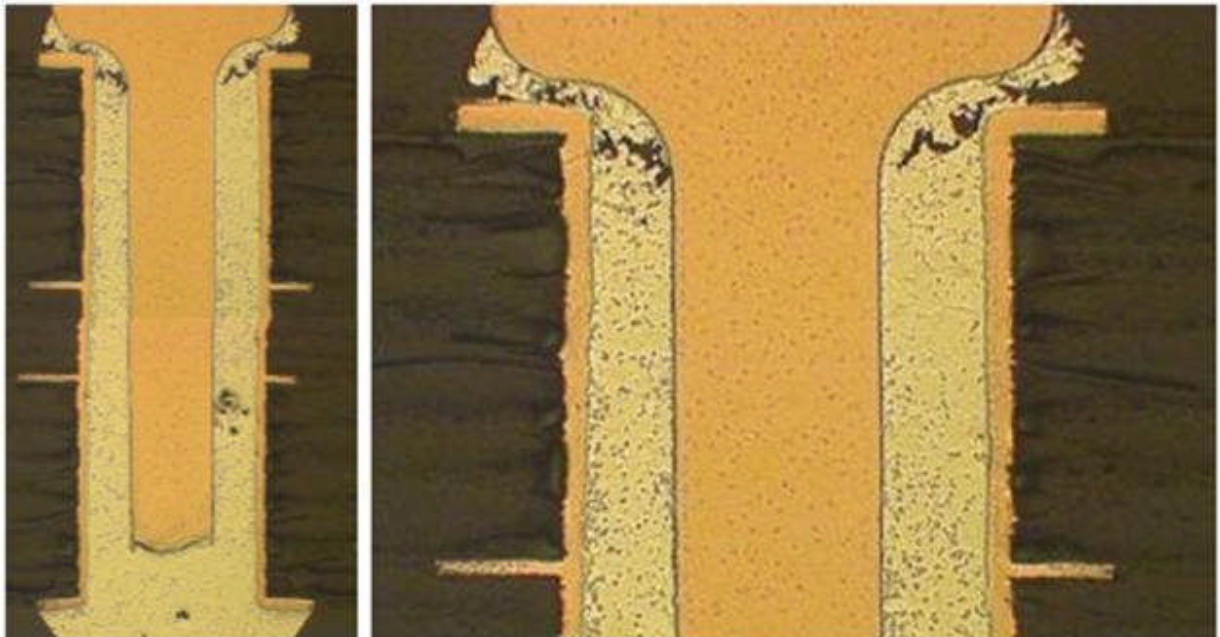


Figure 195 - PDIP-20 Solder Joints, Board 43, Component U8, SN100C/NiPdAu, DNF

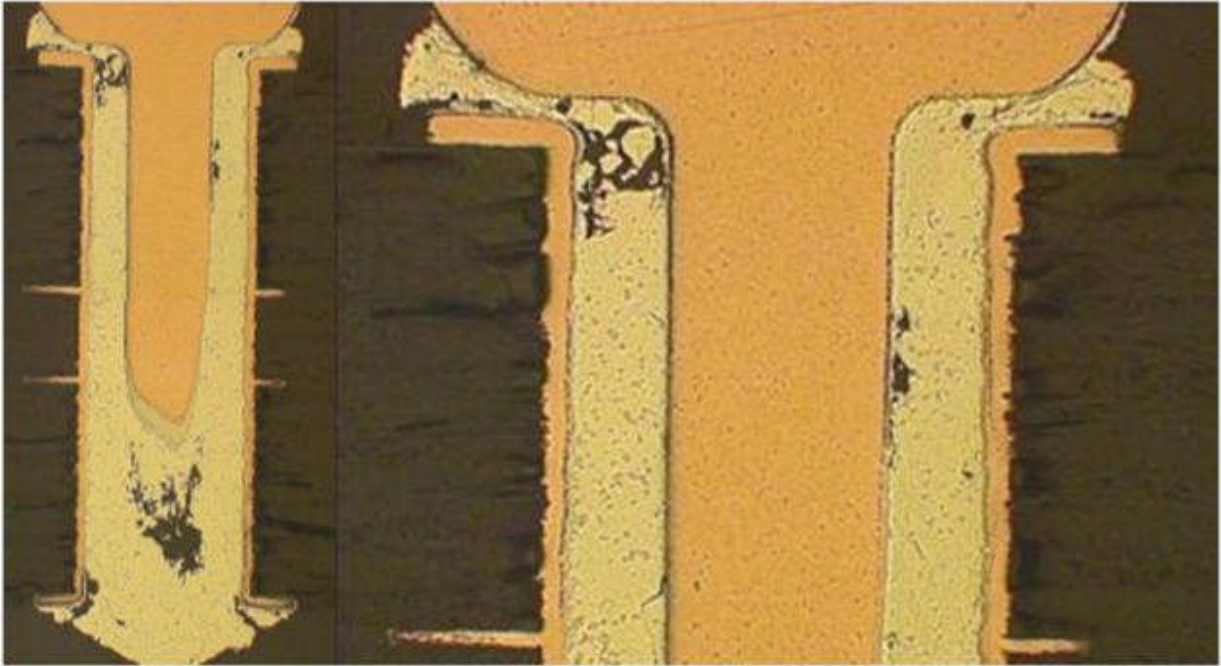


Figure 196 - PDIP-20 Solder Joints, Board 168, Component U49, SN100C/Sn, DNF

5.4.3 NSWC Crane Test Vehicle Thermal Cycle -55°C to 125°C Results Summary

A summary of the number of samples per chemistry and rework condition and the percent of components that failed during test is shown in Table 33. This table is limited to the reworks performed on the Crane test vehicles.

Table 33 - Number of samples and percent failures per Crane rework condition thermally cycled between -55°C and 125°C. All test vehicles had an immersion Ag finish

	As-Manufactured		Rework		Number of Samples			Percent Failure		
	Finish	Solder	Finish	Solder	Original	Rework 1	Rework 2	Original	Rework 1	Rework 2
CLCC	SAC305	SAC305	SAC305	SnPb	48	13	9	98	85	100
	SAC305	SN100C	SAC305	SnPb	48	9	8	92	100	100
QFN	Sn	SAC305	Method 1		25	7	6	8	0	0
	Sn	SAC305	Method 2		25	7	--	8	14	--
	Sn	SN100C	Method 1		25	6	7	12	33	0
	Sn	SN100C	Method 2		25	7	--	12	14	--
PDIP	Sn	SN100C	Sn	SnPb	83	9	6	56	100	100
	NiPdAu	SN100C	Sn	SnPb	43	5	5	42	80	100
	NiPdAu	SN100C	NiPdAu	SnPb	43	6	2	42	83	100
TQFP	Sn	SAC305	Sn	SnPb	47	9	9	100	100	89
	Sn	SN100C	Sn	SnPb	47	9	9	100	89	78
TSOP	Sn	SAC305	Sn	SnPb	7	16	7	100	100	100
	Sn	SN100C	Sn	SnPb	8	6	6	100	100	100
	SnBi	SAC305	SnBi	SnPb	41	6	7	100	100	100
	SnBi	SN100C	SnBi	SnPb	32	6	7	100	100	100

The average thermal cycles to failure are shown in Table 34. A student t-test was used to compare the cycles to failure for the as-manufactured components to the cycles to failure for the 1st and 2nd reworked components, as well as the 1st reworked to the 2nd reworked components. Differences were considered statistically significant at the 95% confidence level for a p-value less than 0.05. Statistical significance indicates that the differences between thermal cycles to failure for two groups are distinguishable. Otherwise, there is not enough evidence to reject the hypothesis that the means are the same. All calculations were performed by assigning a value of 4069 cycles to components that did not fail to avoid skewing the data towards earlier failure times except for QFN's. There were too few QFN failures to calculate a representative average cycles to failure. Components that failed on the first thermal cycle were not used in any calculations.

Table 34 - As-manufactured (O), 1st rework (1), and 2nd rework (2) thermal cycles to failure and p-values for reworked CLCC's, PDIP's, TQFP's, and TSOP's. A p-value of <0.05 is considered statistically significant. All test vehicles had an immersion Ag finish

	As-Manufactured		Rework		Average			p-values		
	Finish	Solder	Finish	Solder	Original	1st Rework	2nd Rework	(O→1)	(O→2)	(1→2)
CLCC	SAC305	SAC305	SAC305	SnPb	894	1312	1041	0.2817	0.5493	0.5254
	SAC305	SN100C	SAC305	SnPb	1088	997	1095	0.6369	0.9777	0.7124
PDIP	Sn	SN100C	Sn	SnPb	2398	550	403	<0.0001	<0.0001	0.4476
	NiPdAu	SN100C	Sn	SnPb	3027	1168	385	0.0609	<0.0001	0.4069
	NiPdAu	SN100C	NiPdAu	SnPb	3027	1185	214	0.0751	<0.0001	0.2817
TQFP	Sn	SAC305	Sn	SnPb	1630	2677	2705	0.0012	0.0013	0.9309
	Sn	SN100C	Sn	SnPb	1634	2436	2697	0.0259	0.0064	0.5387
TSOP	Sn	SAC305	Sn	SnPb	1191	1519	1244	0.0546	0.7257	0.039
	Sn	SN100C	Sn	SnPb	1044	1367	1298	0.0166	0.0441	0.5967
	SnBi	SAC305	SnBi	SnPb	1204	1169	1508	0.7987	0.0387	0.07593
	SnBi	SN100C	SnBi	SnPb	1111	1250	1224	0.4185	0.5301	0.9101

5.4.3.1 Rework of CLCC-20 Components

A box and whisker plot comparing the cycles to failure for SAC305 finished CLCC's soldered with SAC305 and reworked with SAC305 finished CLCC's soldered with eutectic SnPb solder is shown Figure 197. A box and whisker plot comparing the cycles to failure for SAC305 finished CLCC's soldered with SN100C and reworked with SAC305 finished CLCC's soldered with eutectic SnPb solder is shown Figure 198.

Both rework scenarios resulted in reworked CLCC's with thermal cycles to failure comparable to the as-manufactured CLCC's. The p-values, shown in Table 34, were all greater than 0.05 and the percentages of components that failed during testing, shown in Table 33, were all within expected variation.

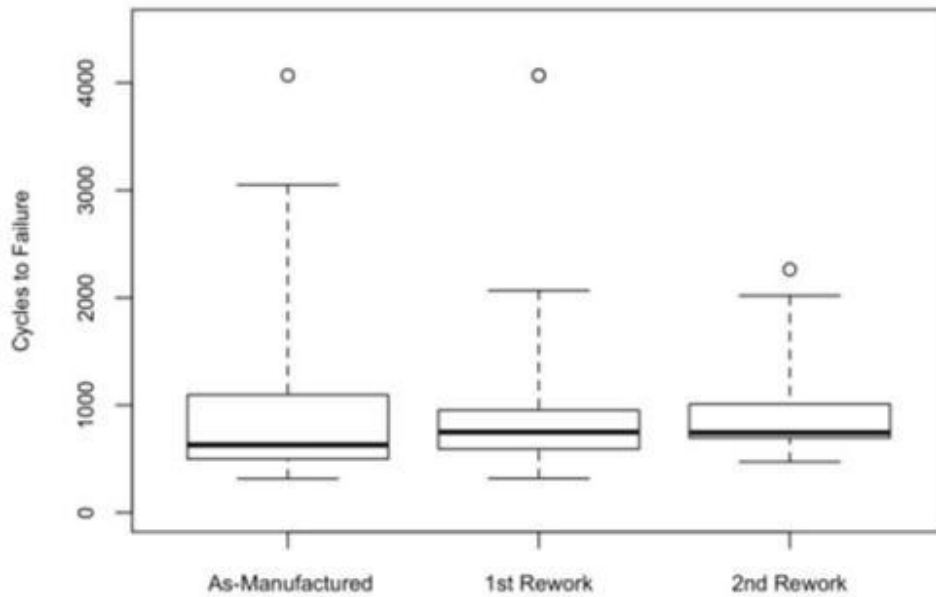


Figure 197 - Box and whisker plot comparing thermal cycles to failure for SAC305 finished CLCC's originally soldered with SAC305 and reworked 1 or 2 times with SAC305 finished CLCC's soldered with eutectic SnPb. No differences in cycles to failure were considered statistically significant.

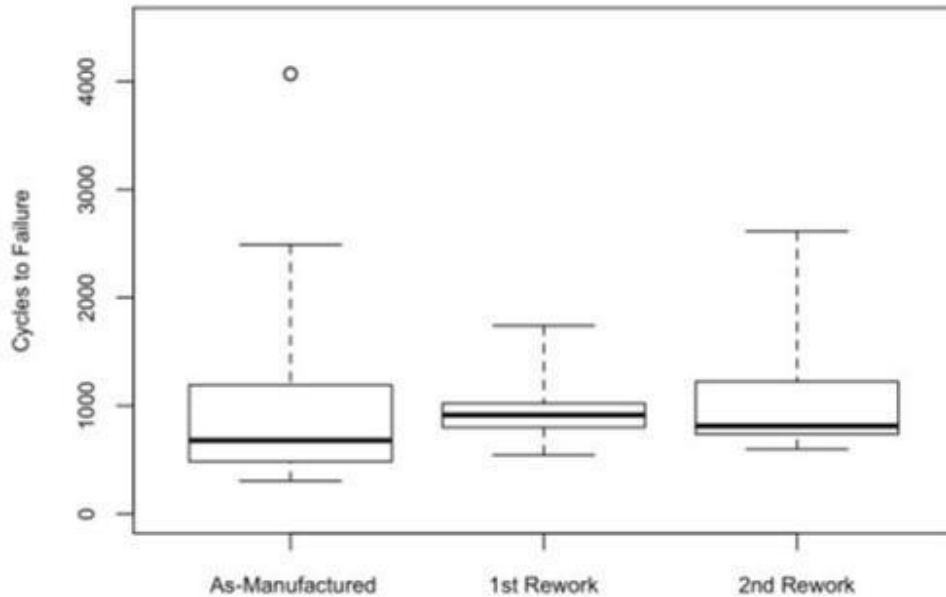


Figure 198 - Box and whisker plot comparing thermal cycles to failure for SAC305 finished CLCC's originally soldered with SN100C and reworked 1 or 2 times with SAC305 finished CLCC's soldered with eutectic SnPb. No differences in cycles to failure were considered statistically significant.

5.4.3.2 Rework of QFN's

The low percentage of failures for all QFN's, regardless of chemistry, number of reworks, or rework method, make it difficult to determine the influence of any of these factors. No analyses of variance was performed, nor were box and whisker plots created due to the small number of failures. No more than 2 samples failed per any rework group (consisting of 6 to 7 QFN's), and no more than 3 samples failed for any as-manufactured group (consisting of 25 QFN's). However, within the scope of this testing, reworking QFN's did not negatively affect the reliability during thermal cycling testing.

5.4.3.3 Rework of PDIP's

A box and whisker plot comparing the cycles to failure for Sn finished PDIP's soldered with SN100C and reworked with Sn finished PDIP's soldered with eutectic SnPb solder is shown Figure 199. Box and whisker plots comparing the cycles to failure for NiPdAu finished PDIP's soldered with SN100C and reworked with Sn finished PDIP's soldered with eutectic SnPb solder or NiPdAu finished PDIP's soldered with eutectic SnPb solder are shown respectively in Figure 200 and Figure 201.

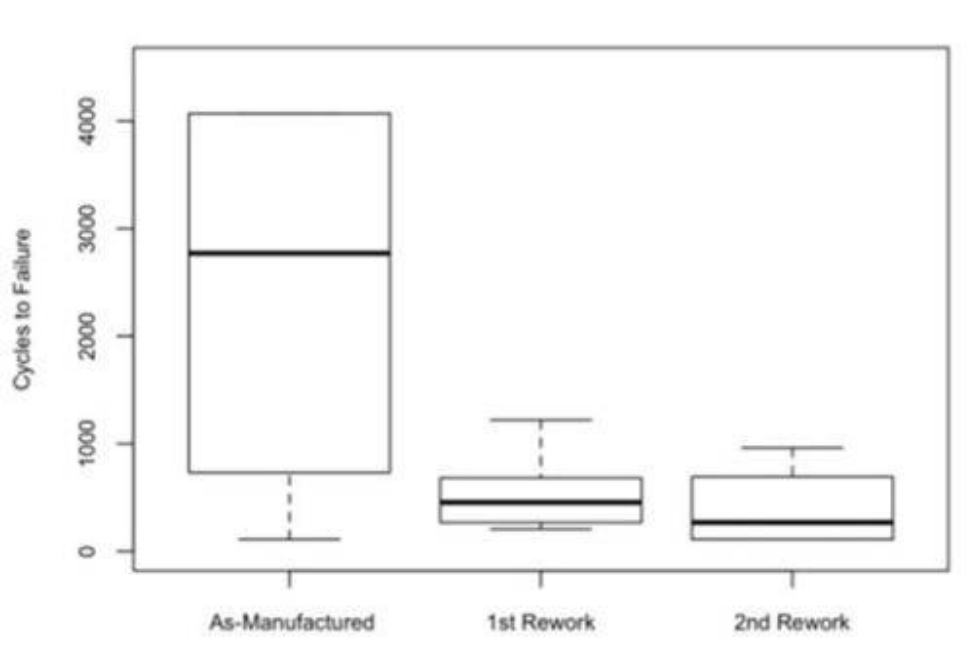


Figure 199 - Box and whisker plot comparing thermal cycles to failure for Sn finished PDIP's originally soldered with SN100C and reworked 1 or 2 times with Sn finished PDIP's soldered with eutectic SnPb. The decrease in cycles to failure for both reworks was considered statistically significant.

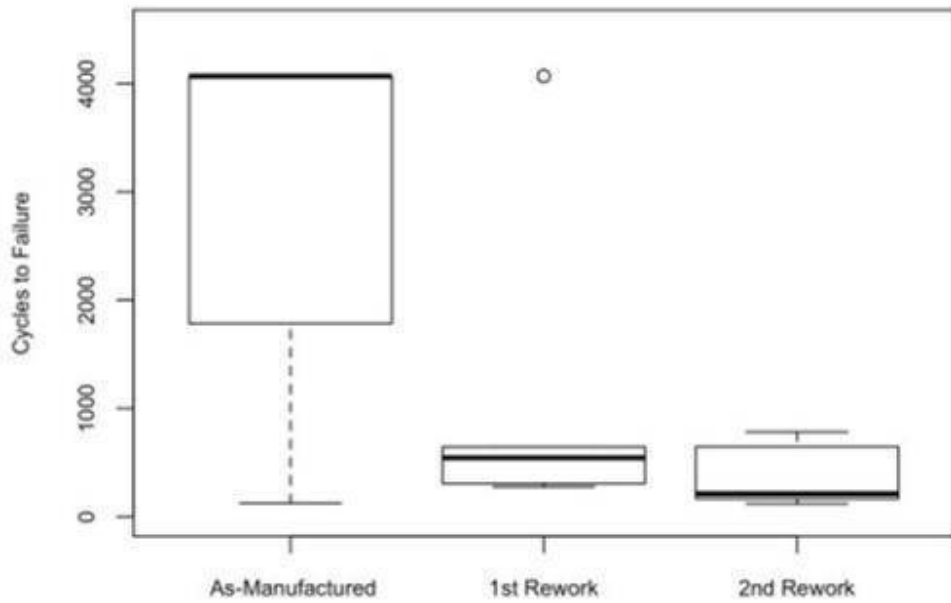


Figure 200 - Box and whisker plot comparing thermal cycles to failure for NiPdAu finished PDIP's originally soldered with SN100C and reworked 1 or 2 times with Sn finished PDIP's soldered with eutectic SnPb. The decrease in cycles to failure for the second rework was considered statistically significant.

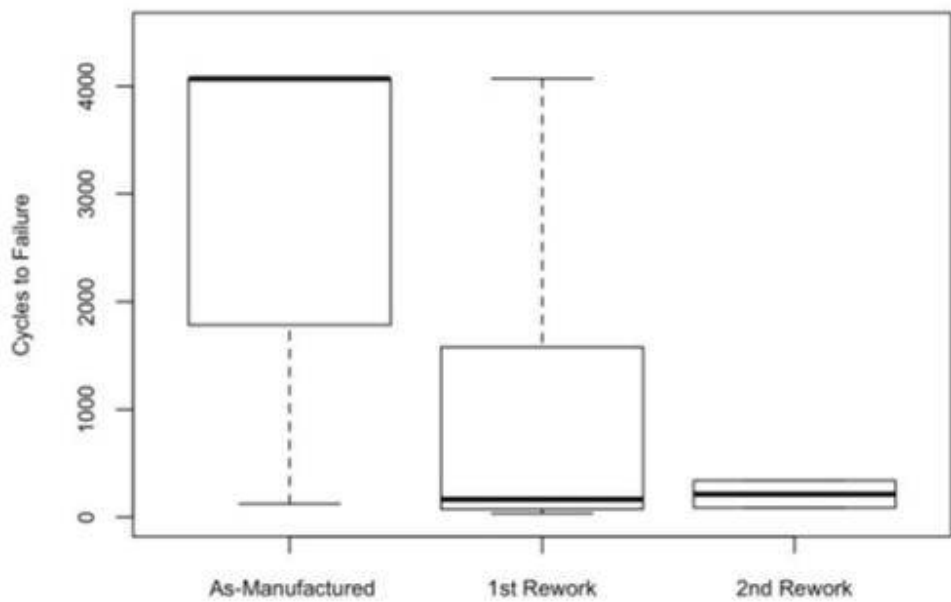


Figure 201 - Box and whisker plot comparing thermal cycles to failure for NiPdAu finished PDIP's originally soldered with SN100C and reworked 1 or 2 times with NiPdAu finished PDIP's soldered with eutectic SnPb. The decrease in cycles to failure for the second rework was considered statistically significant.

All reworked PDIP's came from batches F and I. As previously discussed in section 3.1, a production issue resulted in PDIP's from both of these batches and batch G being less reliable than PDIP's from batches A, B, C, and E. The increased rate of failure is illustrated in Figure 202 and Figure 203 and shown in Table 35. This production issue convolutes the meaning of both the percent of components that failed during testing, shown in Table 33 and the p-values, shown in Table 34.

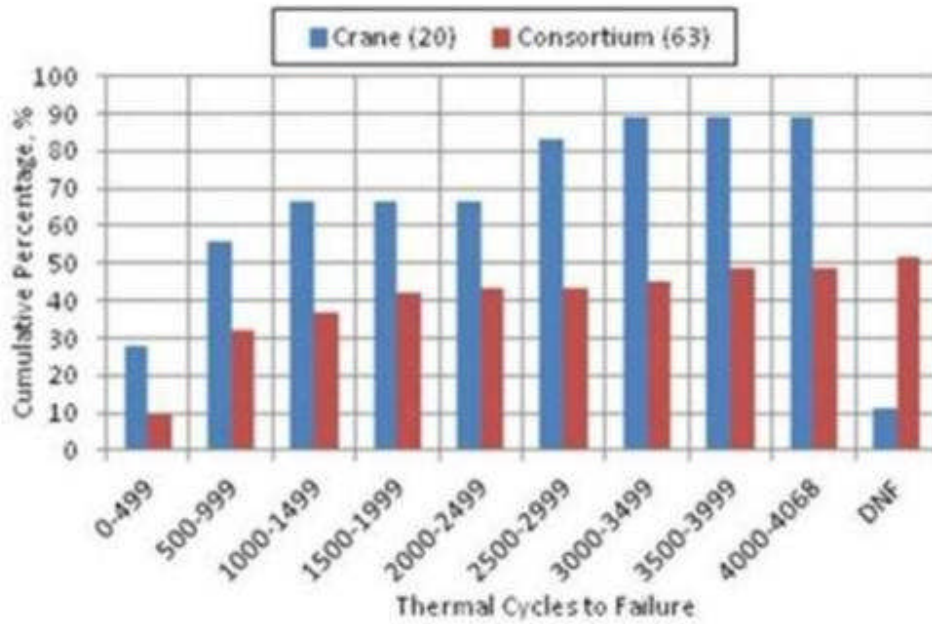


Figure 202 - Cumulative Percentage of failures for as-manufactured Sn finished PDIP's soldered with SN100C showing a faster rate of failure and higher overall rate of failure for PDIP's on Crane test vehicles vs. other test vehicles in the consortium. There were 20 Crane specific PDIPs vs. 63 general to the consortium.



Figure 203 - Cumulative Percentage of failures for as-manufactured NiPdAu finished PDIP's soldered with SN100C showing a faster rate of failure and higher overall rate of failure for PDIP's on Crane test vehicles vs. other test vehicles in the consortium. There were 6 Crane specific PDIPs vs. 37 general to the consortium.

Table 35 - Failure percentage for all PDIP's from a specific batch. The percentage of PDIP's reworked and the percentage of PDIP's that were reworked and failed are also listed.

Batch	Boards	Finish(es)	Solder(s)	Reworked Components [%]	Total Failures [%]	Reworked and Failed [%]
A	164, 165, 166, 167, 168	Immersion Ag	SAC305, SN100C	25.0	12.5	7.5
B	124, 125, 126, 127, 128, 155	Immersion Ag, ENIG	SnPb	25.0	16.7	4.2
C	5, 6, 7, 8, 9	Immersion Ag	SnPb	0.0	15.0	0.0
E	41, 42, 43, 44, 45	Immersion Ag, ENIG	SAC305, SN100c	0.0	27.1	0.0
F	46, 47, 48, 49	Immersion Ag	SN100C	59.4	90.6	56.3
G	102, 103, 104, 105, 106	Immersion Ag	SN100C	0.0	85.0	0.0
I	107, 108, 109, 110	Immersion Ag	SN100C	59.4	90.6	53.1

The statistical test used in this case, analysis of variance, assumes that the sample subgroups will have roughly similar variances, a property that is called homoscedasticity. Unfortunately, for the PDIPs, this is clearly not the case due to the production error for batches F,G, and I. Therefore the p-value, though it does show a significant difference between the subgroups, may not be as accurate as we might want. We can probably conclude that the results did actually differ by examining the graph and observing that the average time to failure after one or two rework cycles was far lower than as received, when within subgroup variation is taken into consideration; the boxes do not overlap.

A repeat analysis of the PDIP cycles to failure was performed, only considering PDIP's from batches F, G, and I. All differences that were previously statistically significant were still determined to be statistically significant. However, the average cycles to failure for Sn finished PDIP's soldered with SN100C decreased from 2398 cycles to 1228 cycles; the average cycles to failure for NiPdAu finished PDIP's soldered with SN100C decreased from 3027 cycles to 2120 cycles. An example of the change in the box and whisker plot for Sn finished PDIP's soldered with SN100C is shown in Figure 204; and example of the change in the box and whisker plot for NiPdAu finished PDIP's soldered with SN100C is shown in Figure 205.

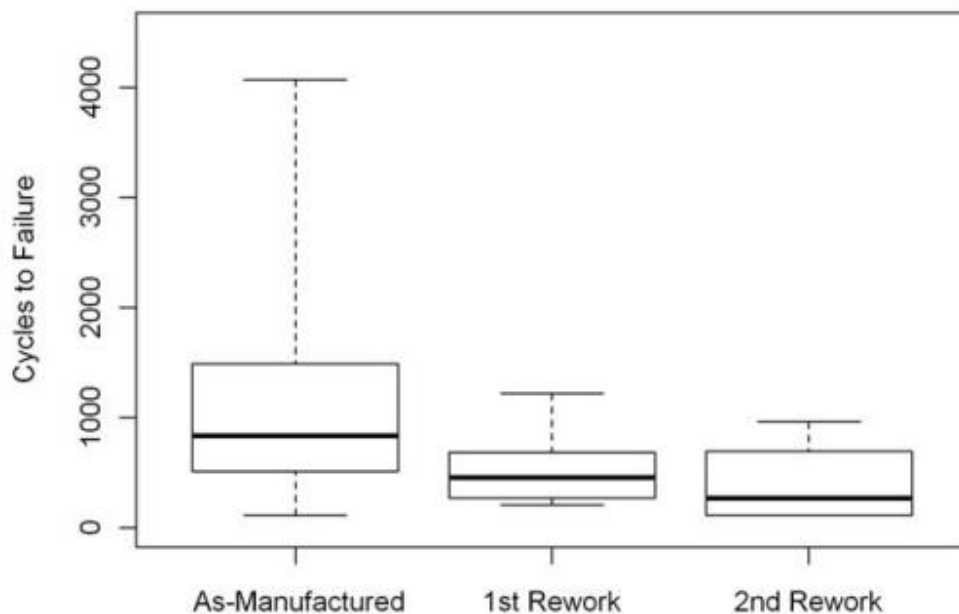


Figure 204 - Recreated box and whisker plot comparing thermal cycles to failure for Sn finished PDIP's originally soldered with SN100C and reworked 1 or 2 times with Sn finished PDIP's soldered with eutectic SnPb showing the effect of only considering times to failure from batches F, G, and I.

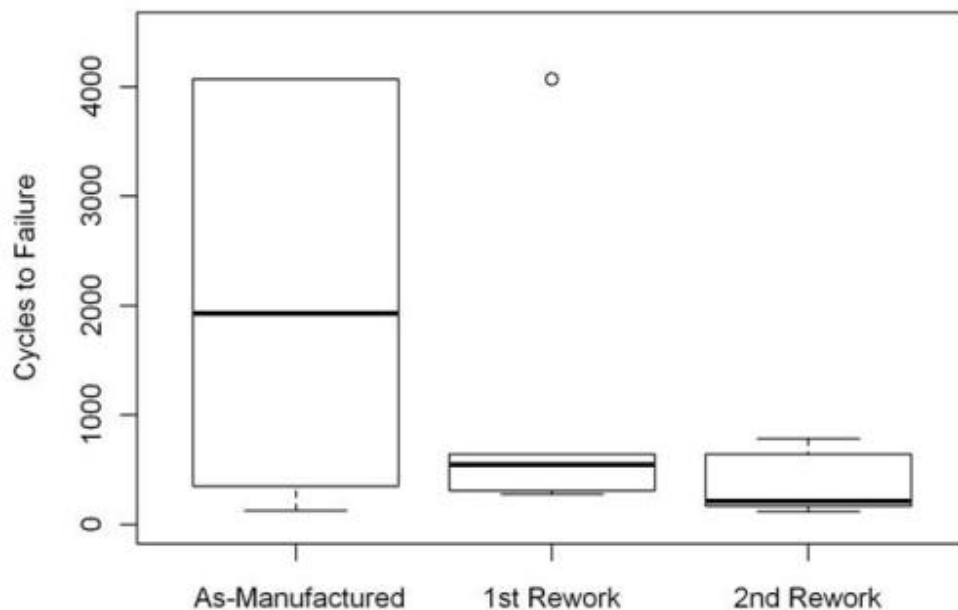


Figure 205 - Recreated box and whisker plot comparing thermal cycles to failure for NiPdAu finished PDIP's originally soldered with SN100C and reworked 1 or 2 times with Sn finished PDIP's soldered with eutectic SnPb showing the effect of only considering times to failure from batches F, G, and I.

Overall, it is difficult to determine the true effect of reworking PDIP's on the thermal cycles to failure. There is a significant decrease in cycles to failure for reworked PDIP's compared to the as-manufactured PDIP's. However, a production issue affecting reworked PDIPS's convoluted the results. Further testing is required to determine the effect of rework on PDIP's.

5.4.3.4 Rework of TQFP's

A box and whisker plot comparing the cycles to failure for Sn finished TQFP's soldered with SAC305 and reworked with Sn finished TQFP's soldered with eutectic SnPb solder is shown Figure 206; A box and whisker plot comparing the cycles to failure for Sn finished TQFP's soldered with SN100C and reworked with Sn finished TQFP's soldered with eutectic SnPb solder is shown Figure 207.

Both rework scenarios resulted in reworked TQFP's with a statistically significant increase in thermal cycles to failure comparable to the as-manufactured TQFP's. Reworking Sn finished TQFP's originally soldered with SAC305 resulted in an increase in cycles to failure from 1630 cycles to 2677 cycles after one rework and 2705 cycles after two reworks; reworking Sn finished TQFP's originally soldered with SN100C resulted in an increase in cycles to failure from 1634 cycles to 2436 cycles after one rework and 2697 cycles after two reworks. The p-values, shown in Table 34, were all less than 0.05. The percentages of components that failed during testing, shown in Table 33, were all within expected variation.

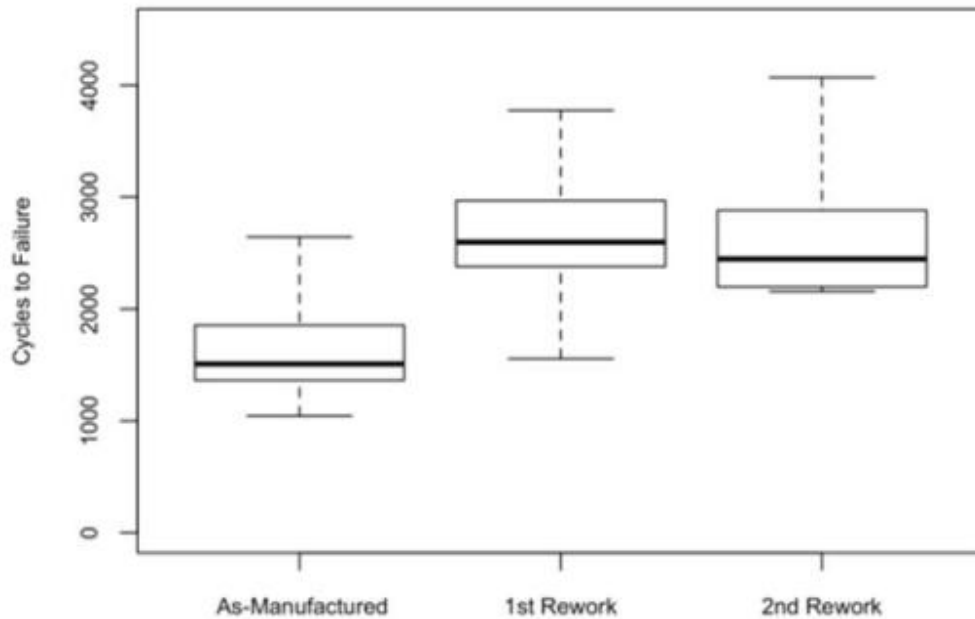


Figure 206 - Box and whisker plot comparing thermal cycles to failure for Sn finished TQFP's originally soldered with SAC305 and reworked 1 or 2 times with Sn finished TQFP's soldered with eutectic SnPb. The increase in cycles to failure for both reworks was considered statistically significant.

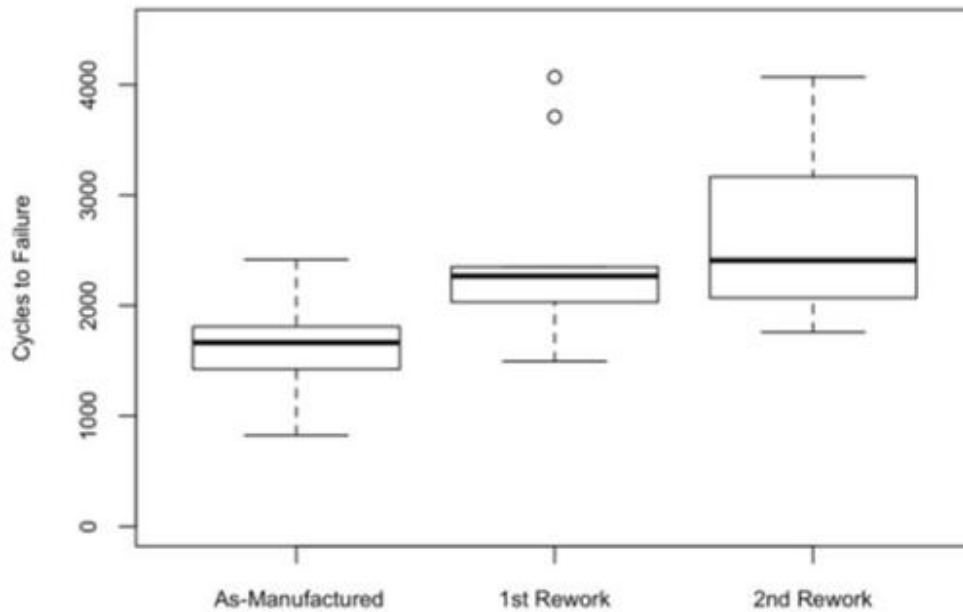


Figure 207 - Box and whisker plot comparing thermal cycles to failure for Sn finished TQFP's originally soldered with SN100C and reworked 1 or 2 times with Sn finished TQFP's soldered with eutectic SnPb. The increase in cycles to failure for both reworks was considered statistically significant.

TQFP's soldered with eutectic SnPb. The increase in cycles to failure for both reworks was considered statistically significant.

5.4.3.5 Reworked TSOP's

A box and whisker plot comparing the cycles to failure for Sn finished TSOP's soldered with SAC305 and reworked with Sn finished TSOP's soldered with eutectic SnPb solder is shown Figure 208; A box and whisker plot comparing the cycles to failure for Sn finished TSOP's soldered with SN100C and reworked with Sn finished TQFP's soldered with eutectic SnPb solder is shown Figure 209. A box and whisker plot comparing the cycles to failure for SnBi finished TSOP's soldered with SAC305 and reworked with SnBi finished TSOP's soldered with eutectic SnPb solder is shown Figure 210; A box and whisker plot comparing the cycles to failure for SnBi finished TSOP's soldered with SN100C and reworked with SnBi finished TQFP's soldered with eutectic SnPb solder is shown Figure 211.

The rework scenarios resulted in reworked TSOP's that were either equivalently or more reliable during thermal cycling testing when compared to the as-manufactured TSOP's. Reworked Sn finished TSOP's originally soldered with SN100C, increasing from 1044 cycles to 1367 cycles after the first rework and 1298 after the second rework. Reworked SnBi finished TSOP's, originally soldered with SAC305, increased from 1204 cycles to 1508 cycles after the second rework. All other differences between the as-manufactured and reworked cycles to failure were not considered statistically significant. There was a statistically significant decrease in cycles to failure between the first and second rework of Sn finished TSOP's originally soldered with SAC305, but this trend was not observed for any other TSOP chemistry, nor was it observed for any other component type.

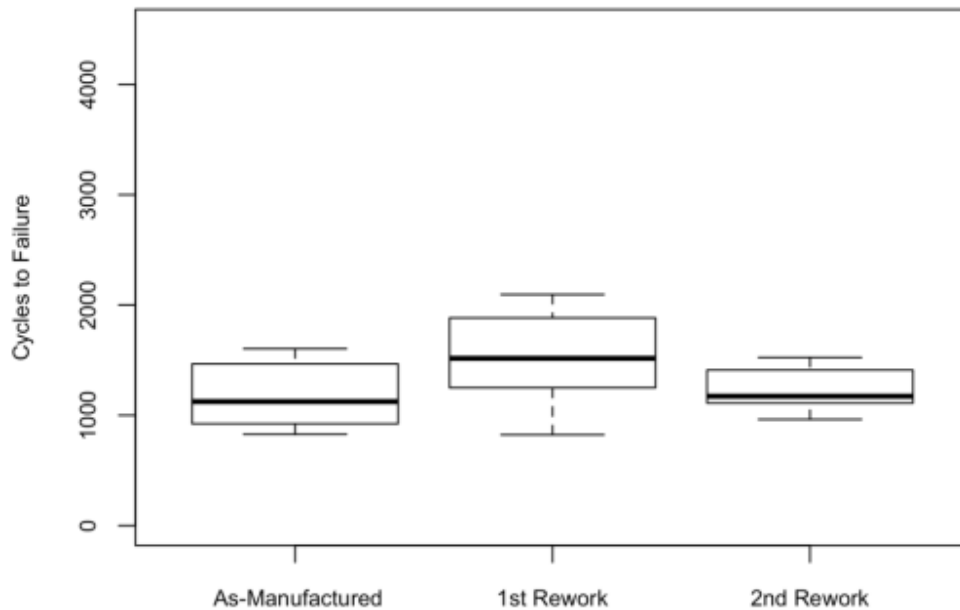


Figure 208 - Box and whisker plot comparing thermal cycles to failure for Sn finished TSOP's originally soldered with SAC305 and reworked 1 or 2 times with Sn finished TSOP's soldered with eutectic SnPb. No differences in cycles to failure between the as-manufactured and reworked conditions were considered statistically significant, but the decrease in cycles to failure between the 1st and 2nd rework was considered significant.

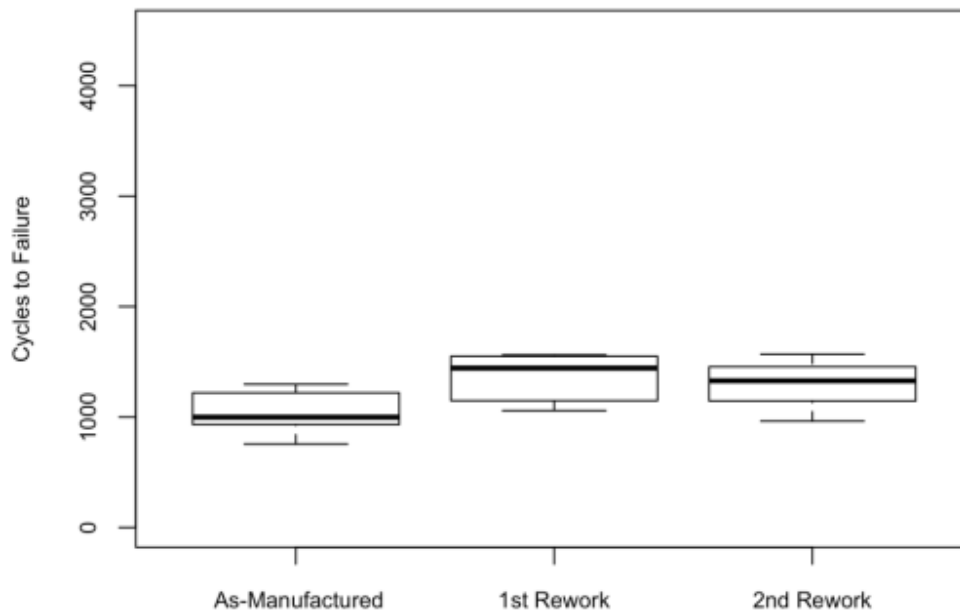


Figure 209 - Box and whisker plot comparing thermal cycles to failure for Sn finished TSOP's originally soldered with SN100C and reworked 1 or 2 times with Sn finished

TSOP's soldered with eutectic SnPb. The increase in cycles to failure for both reworks was considered statistically significant.

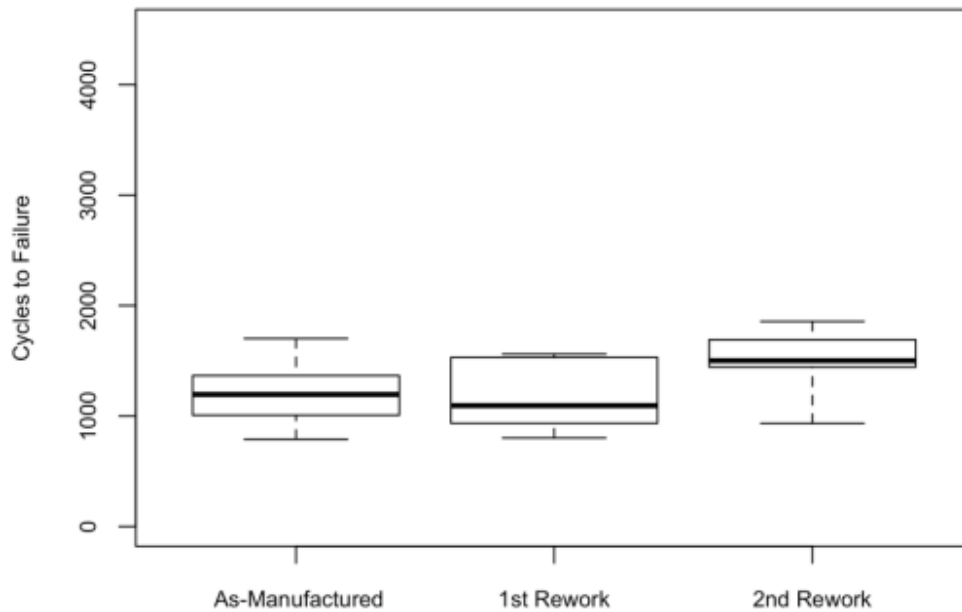


Figure 210 - Box and whisker plot comparing thermal cycles to failure for SnBi finished TSOP's originally soldered with SAC305 and reworked 1 or 2 times with SnBi finished TSOP's soldered with eutectic SnPb. Only the increase in cycles to failure for the 2nd rework was considered statistically significant.

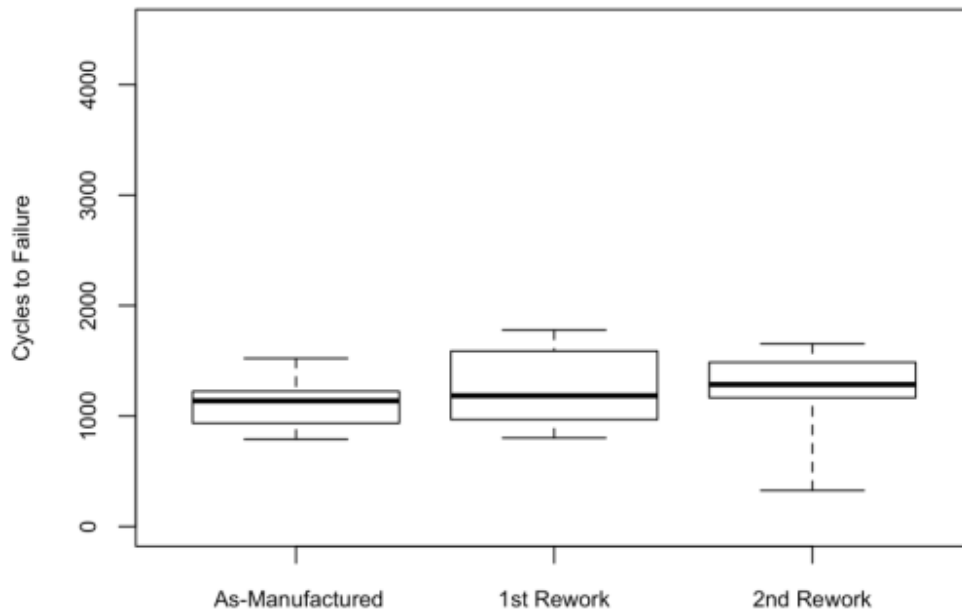


Figure 211 - Box and whisker plot comparing thermal cycles to failure for SnBi finished TSOP's originally soldered with SN100C and reworked 1 or 2 times with SnBi finished TSOP's soldered with eutectic SnPb. No differences in cycles to failure between the as-manufactured and reworked conditions were considered statistically significant.

5.4.4 Thermal Cycle -55°C to +125°C Testing Summary Tables

Table 38, Table 39, Table 41, and Table 42 provide a qualitative comparative summary of the relative performance of the Pb-free solder alloys based on N1, N10 and N63 Weibull failure numbers. Table 38 and Table 39 are for “Manufactured” test vehicles and Table 41 and Table 42 for “Rework” test vehicles. Please note, for Table 41 and Table 42 the data for SnPb/SnPb Manufactured test vehicles was used as the baseline for the relative solder performance, rework test vehicles. All comparisons are based on a two-parameter Weibull analysis of the data.

Baseline SnPb data and other solder alloy/component finish data which is within 5% of the baseline is denoted with a 0. Single symbols, – or +, denote data that is 5% to 20% above (+) or below (-) the baseline. Double symbols, -- or ++, denote data that is more than 20% above (++) or below (--) the baseline. Green cells denote performance better than the SnPb baseline. Yellow cells denote performance worse than the SnPb baseline. Red cells denote data that is grossly worse than the SnPb baseline. Numerical values can be found in the “Weibull Numbers” Tables. Data that is not available or where there were not enough failures to rank the solders is denoted with a NF. Some solder alloy/component finish combinations were not on the thermal cycle test vehicles which is denoted by an NA.

Table 36 - N1/N10/N63 Solder Performance for -55C to +125 C Thermal Cycle Testing

Solder Performance				
Component	Solder/Finish	1st Failure	N10	N63
BGA-225	SnPb/SnPb	2041 (25 samples)	2089	2536
	SnPb/SAC405	443 (44 samples)	1027	4649
	SAC305/SnPb	166 (45 samples)	644	2132
	SAC305/SAC405	2509 (65 samples)	2706	3367
	SN100C/SnPb	216 (25 samples)	286	1393
	SN100C/SAC405	308 (65 samples)	1849	4982
	SAC305/SnPb (ENIG)	111 (5 samples)	NF	4086
	SAC305/SAC405 (ENIG)	2819 (5 samples)	NF	4291
	SnPb/SAC405 (ENIG)	3676 (4 samples)	NF	NF
CSP-100	SnPb/SnPb	2248 (25 samples)	2404	2913
	SnPb/SAC105	287 (44 samples)	2692	70225
	SAC305/SnPb	355 (40 samples)	1433	4041
	SAC305/SAC105	626 (69 samples)	2501	6108
	SN100C/SnPb	851 (24 samples)	1680	3409
	SN100C/SAC105	2769 (25 samples)	3045	3721
	SAC305/SnPb (ENIG)	2123 (5 samples)	1930	2731
	SAC305/SAC105 (ENIG)	3661 (5 samples)	NF	NF
	SnPb/SAC105 (ENIG)	280 (4 samples)	NF	NF
CLCC-20	SnPb/SnPb	482 (20 samples)	536	1954
	SnPb/SAC305	341 (75 samples)	320	1060
	SAC305/SnPb	124 (70 samples)	256	1148
	SAC305/SAC305	315 (47 samples)	319	952
	SN100C/SnPb	369 (25 samples)	244	1014
	SN100C/SAC305	304 (48 samples)	320	1015
	SAC305/SnPb (ENIG)	501 (5 samples)	250	1468
	SAC305/SAC305 (ENIG)	426 (5 samples)	262	836
	SnPb/SAC305 (ENIG)	390 (10 samples)	229	805
PDIP-20	SnPb/SnPb	NA	NA	NA
	SnPb/Sn	682 (34 samples)	1220	5415
	SnPb/NiPdAu	DNF (35 samples)	NF	NF
	SAC305/SnPb	NA	NA	NA
	SAC305/Sn	1593 (5 samples)	NF	NF
	SAC305/ NiPdAu	1322 (5 samples)	NF	NF
	SN100C/SnPb	NA	NA	NA
	SN100C/Sn	111 (82 samples)	371	2817
	SN100C/ NiPdAu	124 (43 samples)	558	7197
	SN100C/NiPdAu (ENIG)	2309 (7 samples)	NF	NF
	SnPb/NiPdAu (ENIG)	DNF (3 samples)	NF	NF
	SN100C/Sn (ENIG)	2044 (1 sample)	NF	NF
SnPb/Sn (ENIG)	DNF (3 samples)	NF	NF	

Note - NF = Insufficient Failures to generate Weibull N10 and N63 Values

Note - NA = Solder Alloy/Component Finish Combination Not On Thermal Cycle Test Vehicles

Table 37 - N1/N10/N63 Solder Performance for -55C to +125 C Thermal Cycle Testing

Solder Performance				
Component	Solder/Finish	1st Failure	N10	N63
QFN-20	SnPb/SnPb	NA	NA	NA
	SnPb/Sn	DNF (50 samples)	NF	NF
	SAC305/SnPb	NA	NA	NA
	SAC305/Sn	1480 (25 samples)	NF	NF
	SN100C/SnPb	NA	NA	NA
	SN100C/Sn	2671 (25 samples)	NF	NF
	SAC305/SnPb (ENIG)	1916 (25 samples)	NF	NF
	SAC305/ Sn (ENIG)	DNF (5 samples)	NF	NF
	SnPb/ Sn (ENIG)	DNF (5 samples)	NF	NF
TQFP-144	SnPb/ SnPb	1985 (44 samples)	2257	2901
	SnPb/ Sn	1322 (28 samples)	2044	3003
	SnPb/ SAC305	NA	NA	NA
	SnPb/ NiPdAu	1169 (25 samples)	1470	2333
	SAC305/ SnPb	2291 (27 samples)	2679	3582
	SAC305/ Sn	1043 (47 samples)	1146	1774
	SAC305/ SAC305	NA	NA	NA
	SAC305/ NiPdAu	351 (25 samples)	1227	4315
	SN100C/ SnPb	1676 (25 samples)	1768	2637
	SN100C/ Sn	826 (47 samples)	1225	1756
	SN100C/ SAC305	NA	NA	NA
	SN100C/ NiPdAu	NA	NA	NA
	SAC305/Sn (ENIG)	1981 (5 samples)	1772	3219
	SAC305/SnPb (ENIG)	3827 (4 samples)	NF	NF
	SnPb/SnPb (ENIG)	2226 (5 samples)	2108	2531
SnPb/NiPdAu (ENIG)	1307 (5 samples)	1138	2057	
TSOP-50	SnPb/SnPb	1060 (19 samples)	1136	1519
	SnPb/Sn	1141 (15 samples)	1130	1415
	SnPb/SnBi	343 (38 samples)	853	1516
	SAC305/SnPb	884 (34 samples)	1031	1519
	SAC305/Sn	828 (7 samples)	724	1321
	SAC305/SnBi	789 (47 samples)	891	1298
	SN100C/SnPb	863 (25 samples)	917	1424
	SN100C/Sn	755 (8 samples)	765	1123
	SN100C/SnBi	790 (32 samples)	848	1191
	SAC305/SnPb (ENIG)	281 (5 samples)	248	1916
	SnPb/Sn (ENIG)	1097 (3 samples)	NF	NF
	SAC305/SnBi (ENIG)	1141 (5 samples)	1118	1461

Note - NF = Insufficient Failures to generate Weibull N10 and N63 Values

Note - NA = Solder Alloy/Component Finish Combination Not On Thermal Cycle Test Vehicles

Table 38 - Solder Performance Comparison for -55C to +125 C Thermal Cycle Testing

Solder Performance				
Component	Solder/Finish	1st Failure	N10	N63
BGA-225	SnPb/SnPb	0	0	0
	SnPb/SAC405	---	---	++
	SAC305/SnPb	---	---	---
	SAC305/SAC405	++	++	++
	SN100C/SnPb	---	---	---
	SN100C/SAC405	---	-	++
	SAC305/SnPb (ENIG)	---	NF	++
	SAC305/SAC405 (ENIG)	++	NF	++
	SnPb/SAC405 (ENIG)	++	NF	NF
CSP-100	SnPb/SnPb	0	0	0
	SnPb/SAC105	---	+	++
	SAC305/SnPb	---	---	++
	SAC305/SAC105	---	+	++
	SN100C/SnPb	---	---	++
	SN100C/SAC105	++	++	++
	SAC305/SnPb (ENIG)	-	-	-
	SAC305/SAC105 (ENIG)	++	NF	NF
SnPb/SAC105 (ENIG)	---	NF	NF	
CLCC-20	SnPb/SnPb	0	0	0
	SnPb/SAC305	---	---	---
	SAC305/SnPb	---	---	---
	SAC305/SAC305	---	---	---
	SN100C/SnPb	---	---	---
	SN100C/SAC305	---	---	---
	SAC305/SnPb (ENIG)	+	---	---
	SAC305/SAC305 (ENIG)	-	---	---
SnPb/SAC305 (ENIG)	-	---	---	
PDIP-20	SnPb/SnPb	NA	NA	NA
	SnPb/Sn	0	0	0
	SnPb/NiPdAu	DNF	NF	NF
	SAC305/SnPb	NA	NA	NA
	SAC305/Sn	++	NF	NF
	SAC305/ NiPdAu	++	NF	NF
	SN100C/SnPb	NA	NA	NA
	SN100C/Sn	---	---	---
	SN100C/ NiPdAu	---	---	++
	SN100C/NiPdAu (ENIG)	++	NF	NF
	SnPb/NiPdAu (ENIG)	DNF	NF	NF
	SN100C/Sn (ENIG)	++	NF	NF
SnPb/Sn (ENIG)	DNF	NF	NF	

Table 39 - N1/N10/N63 Solder Performance for -55C to +125 C Thermal Cycle Testing

Solder Performance				
Component	Solder/Finish	1st Failure	N10	N63
QFN-20	SnPb/SnPb	NA	NA	NA
	SnPb/Sn	0	NF	NF
	SAC305/SnPb	NA	NA	NA
	SAC305/Sn	■	NF	NF
	SN100C/SnPb	NA	NA	NA
	SN100C/Sn	■	NF	NF
	SAC305/SnPb (ENIG)	■	NF	NF
	SAC305/ Sn (ENIG)	DNF	NF	NF
TQFP-144	SnPb/ SnPb	0	0	0
	SnPb/ Sn	■	■	■
	SnPb/ SAC305	NA	NA	NA
	SnPb/ NiPdAu	■	■	■
	SAC305/ SnPb	+	+	++
	SAC305/ Sn	■	■	■
	SAC305/ SAC305	NA	NA	NA
	SAC305/ NiPdAu	■	■	++
	SN100C/ SnPb	■	■	■
	SN100C/ Sn	■	■	■
	SN100C/ SAC305	NA	NA	NA
	SN100C/ NiPdAu	NA	NA	NA
	SAC305/Sn (ENIG)	0	■	■
	SAC305/SnPb (ENIG)	++	NF	NF
	SnPb/SnPb (ENIG)	+	■	■
SnPb/NiPdAu (ENIG)	■	■	■	
TSOP-50	SnPb/SnPb	0	0	0
	SnPb/Sn	+	■	■
	SnPb/SnBi	■	■	0
	SAC305/SnPb	■	■	0
	SAC305/Sn	■	■	■
	SAC305/SnBi	■	■	■
	SN100C/SnPb	■	■	■
	SN100C/Sn	■	■	■
	SN100C/SnBi	■	■	■
	SAC305/SnPb (ENIG)	■	■	++
	SnPb/Sn (ENIG)	+	NF	NF
	SAC305/SnBi (ENIG)	+	0	■

Table 40 - N1/N10/N63 Solder Rework Performance for -55C to +125 C Thermal Cycle Testing

"NF" Solder Performance				
Component	Solder/Finish/Rework	1st Failure	N10	N63
BGA-225	SnPb/SnPb/SnPb	813 (15 samples)	853	2737
	SAC305/SAC405/SnPb	2138 (15 samples)	NF	7237
	SnPb/SnPb/Flux Only	2144 (10 samples)	2110	2512
	SAC305/SAC405/Flux Only	983 (15 samples)	1710	4118
	SnPb/SAC405/Flux Only	1907 (5 samples)	1779	2604
	SnPb/SnPb/SnPb (ENIG)	DNF (3 samples)	NF	NF
	SnPb/SnPb/Flux Only (ENIG)	1760 (2 samples)	NF	NF
	SnPb/SAC405/Flux Only (ENIG)	1794 (1 samples)	NF	NF
CSP-100	SnPb/SnPb/SnPb	DNF (15 samples)	NF	NF
	SAC305/SAC105/SnPb	DNF (15 samples)	NF	NF
	SAC305/SAC105/SAC305	3795 (1 samples)	NF	NF
	SnPb/SnPb/Flux Only	2550 (15 samples)	2568	3059
	SAC305/SAC105/Flux Only	3458 (12 samples)	NF	NF
	SAC305/SAC105/Flux Only (2)	2299 (3 samples)	NF	2858
	SnPb/SnPb/1-SnPb	3488 (3 samples)	NF	NF
	SnPb/SnPb/Flux Only	1525 (3 samples)	NF	2020
PDIP-20	SnPb/SnPb/SnPb	928 (9 samples)	NF	NF
	SN100C/NiPdAu/SnPb	34 (10 samples)	44	760
	SN100C/Sn/SnPb	209 (13 samples)	143	1065
	SN100C/Sn/SN100C	2304 (10 samples)	NF	3390
	SN100C/NiPdAu/ SnPb (2)	88 (7 samples)	62	378
	SN100C/Sn/SnPb (2)	111 (5 samples)	50	523
TSOP-50	SnPb/SnPb/SnPb	272 (20 samples)	673	1739
	SAC305/Sn/SnPb	824 (16 samples)	979	1670
	SN100C/Sn/SnPb	1058 (6 samples)	1007	1470
	SAC305/SnBi/SnPb	801 (6 samples)	716	1294
	SN100C/SnBi/SnPb	801 (6 samples)	714	1395
	SAC305/SnPb/SAC305	765 (4 samples)	NF	1348
	SAC305/SnBi/SAC305	879 (10 samples)	921	1265
	SAC305/Sn/ SnPb (2)	963 (7 samples)	930	1333
	SN100C/Sn/ SnPb (2)	963 (6 samples)	957	1394
	SAC305/SnBi/ SnPb (2)	933 (7 samples)	1001	1656
	SN100C/SnBi/ SnPb (2)	326 (7 samples)	398	1496
	SnPb/SnPb/SnPb (ENIG)	336 (4 samples)	NF	1709
QFN	SAC305/Sn/SnPb	DNF (7 samples)	NF	NF
	SN100C/Sn/ SnPb	277 (6 samples)	NF	NF
	SAC305/Sn/SnPb (2)	DNF (6 samples)	NF	NF
	SN100C/ Sn/ SnPb (2)	DNF (7 samples)	NF	NF
	SAC305/ Sn/StencilQuik	3660 (7 samples)	NF	NF
	SN100C/Sn/StencilQuik	3547 (7 samples)	NF	NF
CLCC	SAC305/SAC305/ SnPb	319 (12 samples)	324	1122
	SN100C/SAC305/ SnPb	545 (9 samples)	539	1120
	SAC305/SAC305/SAC305	735 (1 samples)	NF	NF
	SAC305/SAC305/ SnPb (2)	473 (9 samples)	354	1195
	SN100C/SAC305/ SnPb (2)	600 (8 samples)	411	1265

Note - NF = Insufficient Failures to generate Weibull N10 and N63 Values

Table 41 - Solder Rework Performance Comparison for -55C to +125 C Thermal Cycle Testing

"NF" Solder Performance				
Component	Solder/Finish/Rework	1st Failure	N10	N63
BGA-225	SnPb/SnPb/SnPb	0	0	0
	SAC305/SAC405/SnPb	++	NF	++
	SnPb/SnPb/Flux Only	++	++	-
	SAC305/SAC405/Flux Only	++	++	++
	SnPb/SAC405/Flux Only	++	++	-
	SnPb/SnPb/SnPb (ENIG)	DNF	NF	NF
	SnPb/SnPb/Flux Only (ENIG)	++	NF	NF
	SnPb/SAC405/Flux Only (ENIG)	++	NF	NF
CSP-100	SnPb/SnPb/SnPb	DNF	NF	NF
	SAC305/SAC105/SnPb	DNF	NF	NF
	SAC305/SAC105/SAC305	-	NF	NF
	SnPb/SnPb/Flux Only	-	+	+
	SAC305/SAC105/Flux Only	-	NF	NF
	SAC305/SAC105/Flux Only (2)	-	NF	+
	SnPb/SnPb/1-SnPb	-	NF	NF
	SnPb/SnPb/Flux Only	-	NF	+
PDIP-20	SnPb/SnPb/SnPb	0	NF	NF
	SN100C/NiPdAu/SnPb	-	-	-
	SN100C/Sn/SnPb	-	-	-
	SN100C/Sn/SN100C	++	NF	-
	SN100C/NiPdAu/ SnPb (2)	-	-	-
	SN100C/Sn/SnPb (2)	-	-	-
TSOP-50	SnPb/SnPb/SnPb	0	0	0
	SAC305/Sn/SnPb	++	++	-
	SN100C/Sn/SnPb	++	++	-
	SAC305/SnBi/SnPb	++	+	-
	SN100C/SnBi/SnPb	++	+	-
	SAC305/SnPb/SAC305	++	NF	-
	SAC305/SnBi/SAC305	++	++	-
	SAC305/Sn/ SnPb (2)	++	++	-
	SN100C/Sn/ SnPb (2)	++	++	-
	SAC305/SnBi/ SnPb (2)	++	++	-
	SN100C/SnBi/ SnPb (2)	+	-	-
	SnPb/SnPb/SnPb (ENIG)	+	NF	-

Table 42 - Solder Rework Performance Comparison for -55C to +125 C Thermal Cycle Testing

"NF" Solder Performance				
Component	Solder/Finish/Rework	1st Failure	N10	N63
QFN	SAC305/Sn/SnPb	DNF	NF	NF
	SN100C/Sn/ SnPb	-	NF	NF
	SAC305/Sn/SnPb (2)	DNF	NF	NF
	SN100C/ Sn/ SnPb (2)	DNF	NF	NF
	SAC305/ Sn/StencilQuik	-	NF	NF
	SN100C/Sn/StencilQuik	-	NF	NF
CLCC	SAC305/SAC305/ SnPb	0	0	0
	SN100C/SAC305/ SnPb	++	++	0
	SAC305/SAC305/SAC305	++	NF	NF
	SAC305/SAC305/ SnPb (2)	++	+	+
	SN100C/SAC305/ SnPb (2)	++	++	++

5.4.5 Thermal Cycle -55°C to +125°C Testing Results Discussion

The main “take aways” from the thermal cycle testing project are:

- The CLCC-20 and the TSOP-50 components functioned as designed within the DOE matrix. Both component types are known failure issues in High Performance electronic products and both are considered “high stress” solder joint integrity situations. The investigation test data shows that the SnPb outperformed both Lead-free solder alloys in agreement with the JCAA/JGPP program results(8) and conventional industry published data (1).
- The rework portion of the DOE matrix was severely scrutinized prior to execution in an effort to minimize test result variation due to the rework processes/procedures. The “flux only” procedures which are widely used industry area array rework/repair procedures were problematic for the lead-free BGA and CSP DOE parameter segments. The poor performance of several of the rework/repair alloy/component finish combinations may be a maturity issue or a process refinement issue but it is clear that additional rework trials and process refinement are necessary in this area of lead-free solder processes.
- The physical failure analysis of the CSP-100 components revealed severe solder joint deformation. The SnPb solder alloy joints had readily apparent regions of grain coarsening and the Lead-free solder alloys had significant “spider web cracking” and joint deformation – both indications that the use of CSP-100 components in high performance electronic products, regardless of solder alloy selection, needs to be conducted with due diligence.
- The PDIP-20 thermal cycle results were confounded by the test vehicle fabrication error. This is an unfortunate portion of the test program but demonstrates that components with industry established solder joint integrity reputations can fall victim to other failure mechanisms. An analysis/comparison of the PDIP-20 components thermal cycle performance versus published industry data (11) reveals that the solder joint integrity performance would be similar to the JCAA/JGPP test program results if the test vehicle fabrication confounded components could be eliminated from the data set. The NASA DoD 38% PDIP failure rate is more of a measure of the fabrication error than an increase of the JCAA/JGPP 8% PDIP failure rate.

- The QFN-20 component was a new component style for the consortium as it was not included in the JCAA/JGPP test program. The QFN-20 component had the best overall thermal cycle solder joint integrity of all the component styles tested. The results demonstrate that the QFN style component can find application in a number of High Performance electronic product use environments. It should be noted that the QFN-20 components used in the thermal cycle testing contained a metallized thermal pad that was soldered to the test vehicles that has a significant influence on the thermal cycle solder joint integrity in comparison to QFN components without metallized thermal pads.
- There were no surprises in the PBGA-225 thermal cycle test results. The test results demonstrated that mixed metallurgy situations are non-optimal. An all SnPb or all Lead-free solder alloy/component finish combination had a more consistent, predictable final solder joint integrity result compared to a mixed alloy solder joint configuration. The impact of mixed metallurgy solder joints and the influence of reflow profiles on producing uniform solder joint microstructures have been shown in other industry investigations (6).

5.5 Thermal Cycle -20°C to +80°C Test

5.5.1 Thermal Cycle -20°C to +80°C Test Method

This test determines a test specimen's resistance to degradation from thermal cycling. The limits identified in thermal cycle testing were used to compare performance differences in the Pb-free test alloys and mixed solder joints vs. the baseline standard SnPb (63/37) alloy.

Perform this test in accordance with IPC-SM-785 (*Guidelines for Accelerated Reliability Testing of Surface Mount Solder Attachments*) and the following procedure.

- Continuously monitor the electrical continuity of the solder joints during the test. It is desirable to continue thermal cycling until 63% of each component type fails.

Table 43 - Thermal Cycling Test Methodology; -20°C to +80°C

Parameters	<ul style="list-style-type: none"> ▪ -20°C to +80°C ▪ 5 to 10°C/minute ramp ▪ 30 minute high temperature dwell ▪ 10 minute low temperature dwell 		
Number of Test Vehicles Required			
Mfg. SnPb = 5		Mfg. LF = 5	
Rwk. SnPb = 5	Rwk. SnPb {ENIG} = 1	Rwk. LF = 5	
Trials per Specimen		1	

5.5.2 Thermal Cycle -20°C to +80°C Testing Results Summary

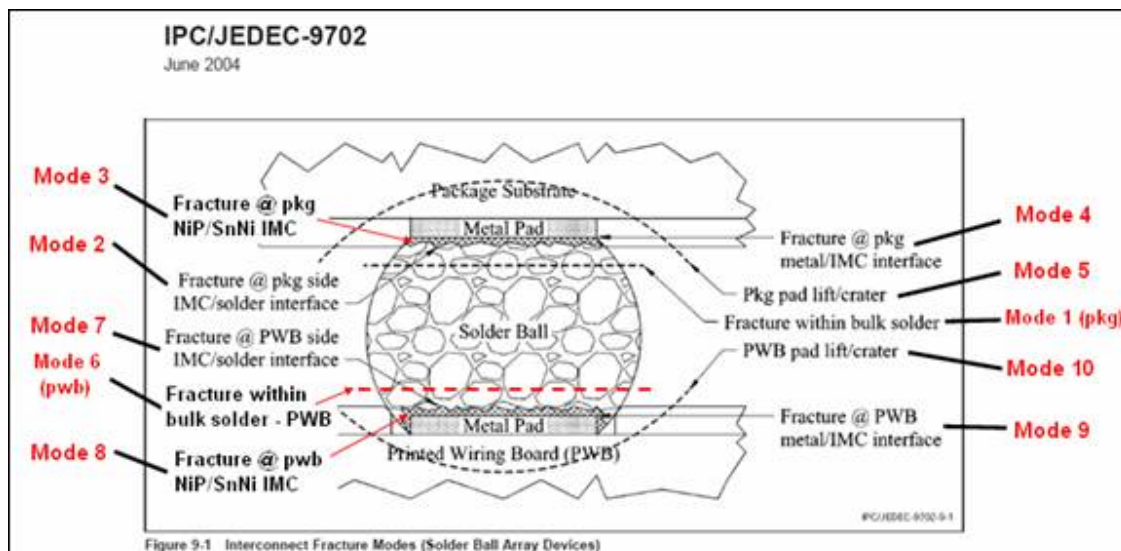
At the time this report was written, Thermal Cycle -20°C to +80°C testing was ongoing. Thermal Cycle -20°C to +80°C data and testing analysis contained in this document were obtained from in-progress test results (NASA/DoD Lead-Free Electronics Project: -20°C TO +80°C Thermal Cycle Test, Thomas A. Woodrow, Ph.D., Boeing Research & Technology).

Once testing is complete, a final Thermal Cycle -20°C to +80°C test report will be drafted and placed onto the NASA TEERM website (<http://teerm.nasa.gov>).

5.6 Drop Testing

5.6.1 Drop Test Method

This test determines the resistance of board level interconnects to board strain induced by dynamic bending as a result of drop testing. Boards tested using this method typically fail either as interfacial fractures in the solder joint (most common with ENIG) or as pad cratering in the component substrate and/or board laminate (Figure 212). These failure modes commonly occur during manufacturing, electrical testing (especially in-circuit test), card handling and field installation. The root cause of these types of failures are typically a combination of excessive applied strain due to process issues and/or weak interconnects due to process issues and/or the quality of incoming components and/or boards.



NOTE: SEM/EDX is required to distinguish between Failure Modes 2 & 3 as well as between Modes 7 & 8.

Figure 212 - Interconnect Fracture Modes (Solder Ball Array Device) IPC 9702

This board-level drop test is based on the JEDEC Standard JESD22-B110A known as Subassembly Mechanical Shock as well as insight gained by Celestica after performing numerous drop tests.

The drop test process can identify design, process, and raw material related problems in a much shorter time frame than other development tests. For this project, the drop test determines the operation and strain endurance limits of the solder alloys and interconnects by subjecting the test vehicles to accelerated environments. The limits identified in drop testing were used to compare performance differences in the Pb-free test alloys and mixed solder joints vs. the baseline standard SnPb (63/37) alloy. The primary accelerated environments are strain and strain rate.

Table 44 - NASA-DoD Lead-Free Electronics Test Vehicle Drop Test Methodology

Parameters	<ul style="list-style-type: none"> ▪ Shock testing conducted in the -Z direction ▪ 500G pk input, 2ms pulse duration ▪ Test vehicles dropped until all monitored components fail or 10 drops have been completed 	
Number of Test Vehicles Required		
Mfg. SnPb = 5		Mfg. LF = 5
Rwk. SnPb = 5	Rwk. SnPb {ENIG} = 1	Rwk. LF = 5
Trials per Specimen	A maximum of 10 drops	

Table 45 - NSWC Crane Test Vehicle Drop Test Methodology

Parameters	<ul style="list-style-type: none"> ▪ Shock testing conducted in the -Z direction ▪ 340G pk input, 2ms pulse duration for test vehicles 80, 82, 87 for first 10 drops <ul style="list-style-type: none"> ○ Following the initial 10 drops, only BGA components had failed. In an attempt to generate additional failure data, the consortium decided to increase the testing to 500G pk input for 10 additional drops. For the remaining 6 test vehicles, all drops were conducted at the 500G pk input. ▪ 500G pk input, 2ms pulse duration for test vehicles 60, 81, 82, 84, 85, and 86 ▪ Test vehicles dropped until all monitored components fail or 20 drops have been completed 	
Number of Test Vehicles Required		
Mfg. LF then Rwk. SnPb = 9 test vehicles		
Trials per Specimen	A maximum of 20 drops	

5.6.2 NASA-DoD Test Vehicle Drop Testing Results Summary

The complete test report, “Drop Testing Report for NASA; TOL0702030”, can be found on the NASA TEERM website (<http://teerm.nasa.gov>).

Although there were duplicates of each component type on the test vehicle, every component experienced a unique strain/strain rate condition due to its particular location on the board. As a result each sample depicts a unique data point and these cannot be easily lumped together. Due to the limited number of samples, the absence of physical failure analysis (at this time) and the lack of electrical opens, excluding the BGAs, it is not possible to draw any firm conclusions as to the significance of the electrical failure data.

It is likely that a great deal of the electrically-functional parts on these drop tested boards have hidden mechanical failures. Any future physical failure analysis should include dye and pry mapping of the majority of the components from a sample of the boards. The results of the dye and pry analysis could then be used to determine which of the remaining parts/boards should be targeted for cross-sectional analysis and possibly scanning electron microscopy to characterize the damage.

The only component type to show a significant number of electrical failures during this test were the plastic ball grid array (PBGA) components. The PBGA component electrical failures mostly occurred at or near the corner joints. Twenty-eight out of the 176 PBGA components survived all 10 drops. The surviving parts were located near the outer edge of the board where the strain was found to be minimal. On average, most reworked parts failed after a fewer number of drops than compared to non-reworked PBGA components. There was no significant difference in the number of drops until failure between PBGA components reworked 1 time versus 2 times, versus 3 times. SnPb and SAC305 PBGA components on immersion Ag boards had similar failure rates, possibly due to the predominance of pad cratering. PBGA components reflowed on ENIG boards typically failed after fewer drops than those on immersion Ag boards.

There were no electrical failures for the chip-array ball grid array (CSP-100), quad flat no leads (QFN) or thin small outline package (TSOP) components during the 10 drops. Future physical failure analysis however may reveal hidden mechanical damage which could be a reliability concern. Only three of the 60 ceramic leadless chip carrier (CLCC) components showed electrical fails (all failed during the 4th drop). The physical failure mechanism of these outliers is unknown at this time. One of the thin quad flat pack (TQFP) components showed an electrical fail during drop 3. Note, however, that this part was marked as a “touch-up” by the assembly team.

5.6.3 NASA-DoD Test Vehicle Drop Test Failure Analysis

After the drop testing was completed, several boards were selected for destructive failure analysis. Both dye-and-pry and cross sectioning were performed, each of which was designed to determine the location, mode and mechanism of the failure. The samples selected for dye-and-pry were examined using an optical microscope after the parts were pried from the board and the results were further mapped. The cross sectioned samples were examined using optical and scanning electron microscopy (SEM) as well as analyzed by energy dispersive x-ray (EDX). The focus was to compare the quality of the solder joints of components that were reworked once using SnPb solder (therefore consisting of a mixed metallurgy of Pb and Pb-free solder), those that were reworked twice using SnPb solder (consisting of leaded solder), and those which were not reworked at all- therefore Pb-free. Table 46 shows which components were selected by Celestica for failure analysis.

Table 46 - Components that Celestica Performed Failure Analysis On

Test Vehicle	Component	Solder	Rework	Finish	Location	Failure Cycle	Cross Section	Dye and Pry	Selection Criteria	Failure Mode
144	LF	SnPb	N/A	ImAg	U4	1	+		Electrical failure row Q	#4 - Ni/IMC brittle
25	SnPb	SnPb	SnPb	ImAg	U4	5	+		Electrical failure row A	#10 – Pad Cratering
27	SnPb	SnPb	N/A	ImAg	U5	3	+		Electrical failure row Q	No failure confirmed
29	SnPb	SnPb	N/A	ImAg	U6	3		+	Electrical failure row A and row Q	All failure are Pad Cratering
26	SnPb	SnPb	N/A	ImAg	U56	No failure	+		Comparison	Pad Cratering
77	LF	LF	N/A	ImAg	U4	5	+		Electrical failure row A	#10 – Pad Cratering
187	SnPb	LF	N/A	ImAg	U4	2	+		Electrical failure row Q	#2 – IMC/Solder #10 – Pad Cratering
92	LF	LF	N/A	ImAg	U5	3	+		Electrical failure row A	#10 – Pad Cratering
59	LF	LF	N/A	ImAg	U6	3		+	Electrical failure row Q	All failure are Pad Cratering
58	LF	LF	N/A	ImAg	U56	No failure	+		Comparison	No failure
159	LF	SnPb	N/A	ENIG	U4	2	+		Electrical failure row A, row B and row 15	#8 – NiP/IMC brittle
159	LF	SnPb	N/A	ENIG	U44	2	+		Electrical failure row A and row Q	#8 – NiP/IMC brittle
159	SnPb	LF	SnPb	ENIG	U6	2	+		Electrical failure row A and row 15	#8 – NiP/IMC brittle
159	SnPb	SnPb	SnPb	ENIG	U56	4	+		Electrical failure row A and row B	#8 – NiP/IMC brittle #10 – Pad Cratering

The main focus of the NASA drop test failure analysis was the 225 I/O plastic BGAs. This was because the vast majority of electrical failures on the test vehicle were these larger PBGAs. All CSPs electrically passed drop testing. For the PBGAs there was a wide range in number of drops until failure: 40% failed electrically within less than 6 drops and 99% failed electrically by 20 drops. Less than 1% of non-BGA components electrically failed after 20 drops. Pad cratering was the predominant failure mode for all samples destructively analyzed. Dye-and-pry and cross-sections of failed joints are shown below; Figure 213 and Figure 214.

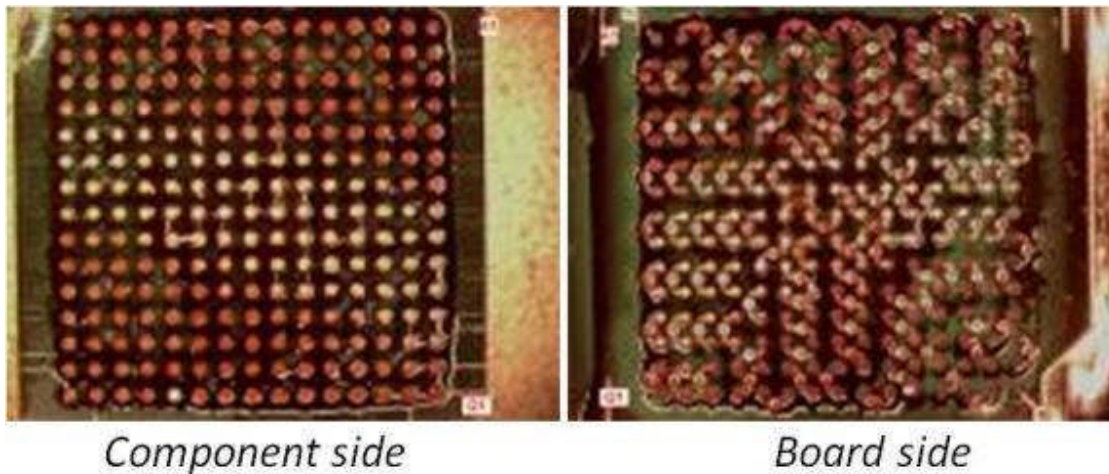


Figure 213 - Typical Pad Cratering seen on BGA225 after Dye-and-Pry

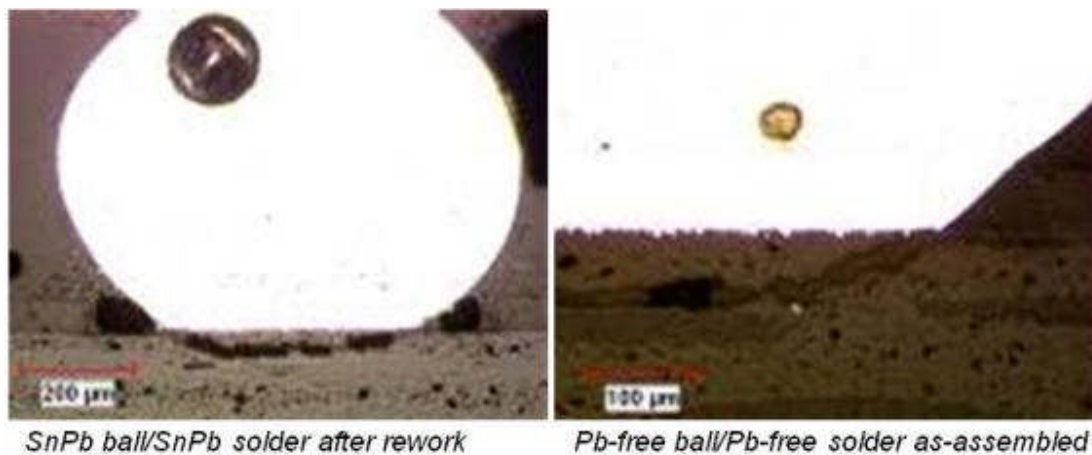


Figure 214 - Typical Pad Cratering seen on BGA225 after cross-section

An additional mechanism that caused electrical failure in mixed solder joints was crack propagation through a low melting $\text{Sn}+\text{Pb}+\text{Ag}_3\text{Sn}$ ternary and/or $\text{Sn}+\text{Pb}+\text{Ag}_3\text{Sn} + \text{Cu}_6\text{Sn}_5$ quaternary eutectic accumulation layer at the board or component interface depending on sample history. In as-assembled condition the crack grew between the intermetallic layer and the bulk solder at the board side and after rework the more susceptible location was the interface between the intermetallic layer and the bulk solder at the component side; Figure 215. For the ENIG finished boards the predominant failure modes were brittle intermetallic cracking on both board and component sides.

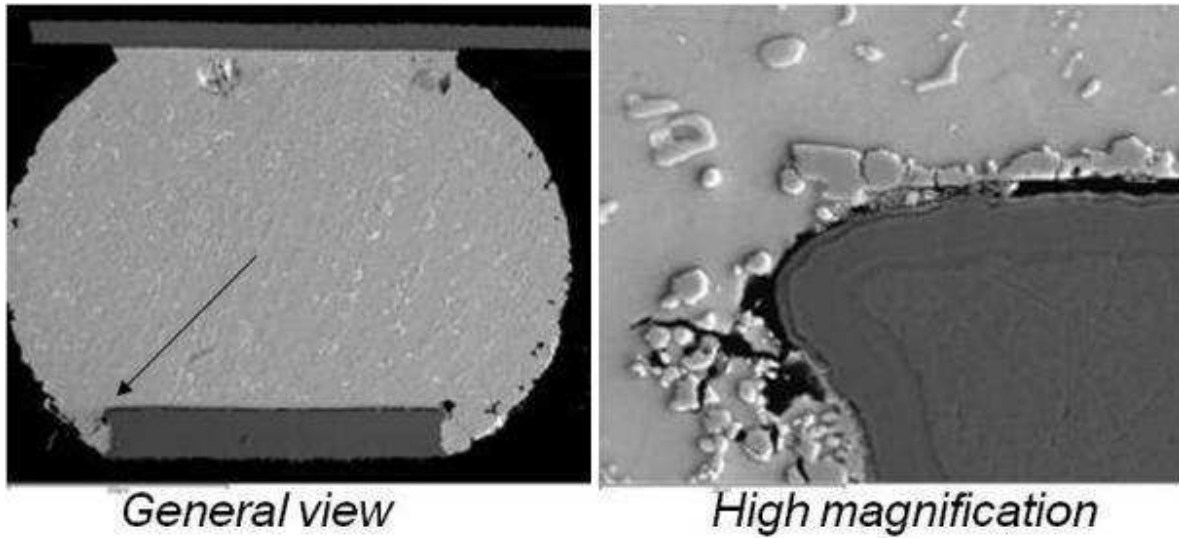


Figure 215 - SEM of Brittle Intermetallic Failure on BGA225

One of the cards tested, which had no electrically failing leaded parts, was chosen for dye & pry of all 63 parts in order to map the mechanical damage. Figure 216 summarizes the mechanical failure (red overlay) of one board after 20 drops at 500G. In-situ electrical data on BGAs showed that some PBGAs failed after as little as 5 drops – this implies that mechanical failure may have occurred after even fewer drops. Interesting to note that the board was held by posts in the 4 corners and as such the strain is not symmetrical across the card.

Mechanical Failures

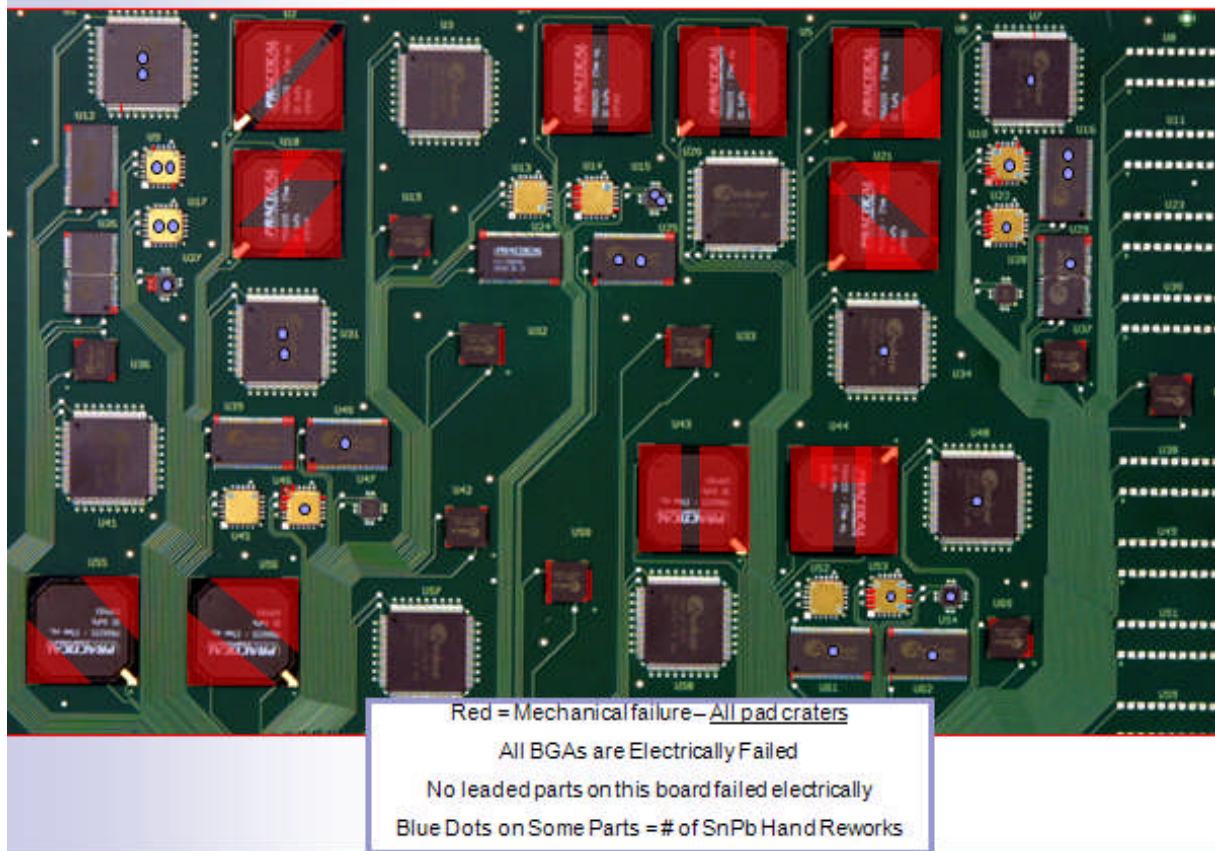


Figure 216 – Mechanical Failure Mapping

5.6.4 NSWC Crane Test Vehicle Drop Testing Results Summary

The complete test report, “Drop Testing Report for Crane; TOL0801002”, can be found on the NASA TEERM website (<http://teerm.nasa.gov>).

Although there were duplicates of each component type on the test vehicle, every component experienced a unique strain/strain rate condition due to its particular location on the board. As a result each sample depicts a unique data point and these cannot be easily lumped together.

After drop testing only three of the leaded components had electrical failures:

- SN 85, TQFP 144, U57; reworked once
- SN 85, PDIP-20, U8; reworked once
- SN 84, CLCC-20, U14; not reworked

One of the quad flat no leads (QFN-20) components had an electrical failure after drop testing:

- SN 86, QFN-20, U15; reworked twice

99 percent (89 out of 90) of the plastic ball grid array (PBGA) components had an electrical failure following drop testing. All of the Pb-free PBGAs (non-reworked) electrically failed by 20 drops at 500G.

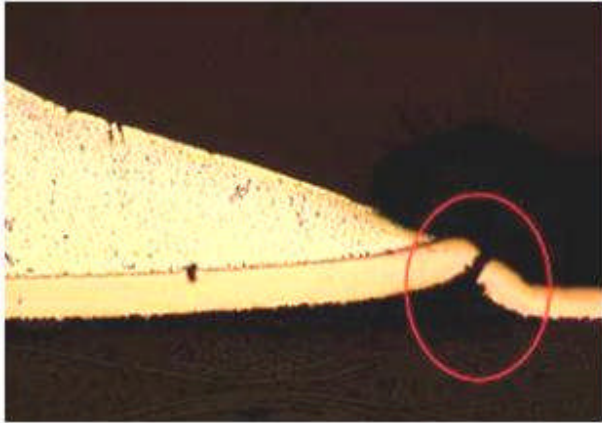
Twenty-three leaded components from various cards were selected for failure analysis and subjected to dye & pry testing. None of the components selected for dye & pry testing had electrical failures. Ten out of the 23 components that were selected for dye & pry testing showed signs of mechanical fracture. All except 2 mechanical fractures inspected were in the laminate under the pad; pad cratering. Only two out of the 23 components showed signs of solder joint fractures. Based on the 23 components selected for dye & pry, there is no correlation between the number of reworks and the amount of mechanical damage. This selection of components shows no difference in drop test performance between SnPb and Pb-free solder.

Fifteen components were also selected for cross-sectioning, three of which were electrical failures after drop testing {SN 85, TQFP 144, U57; reworked once, SN 85, PDIP-20, U8; reworked once, SN 84, CLCC-20, U14; not reworked}. Five out of the 15 cross-sectioned joints were found to have some level of mechanical damage, or pad cratering. For two of the electrically failing parts the root cause of the electrical failure was a trace break due to pad cratering. The other part failed due to solder fatigue fracture. The remaining 2 samples had pad cratering which did not sever the copper trace.

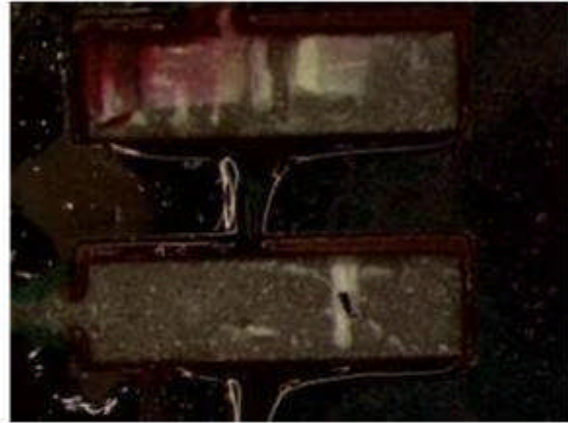
5.6.5 NSWC Crane Test Vehicle Drop Test Failure Analysis

After the drop testing was complete, several boards were selected for destructive failure analysis. Both dye-and-pry and cross sectioning were performed, each of which was designed to determine the location, mode and mechanism of the failure. The samples selected for dye-and-pry were examined using an optical microscope after the parts were pried from the board and the results were further mapped. The cross sectioned samples were examined using optical and scanning electron microscopy (SEM) as well as analyzed by energy dispersive x-ray (EDX). The focus was to compare the quality of the solder joints of components that were reworked once using SnPb solder (therefore consisting of a mixed metallurgy of Pb and Pb-free solder), those that were reworked twice using SnPb solder (consisting of leaded solder), and those which were not reworked at all- therefore Pb-free. Only non-BGA components are described in detail in this project.

Pad cratering was the predominant failure mechanism in all components, as observed through both dye-and-pry and cross sectioning; Figure 217. In two cases the pad cratering was significant enough to break the trace and cause an electrical failure. However in most cases the trace remained intact and therefore no electrical failure was detected.



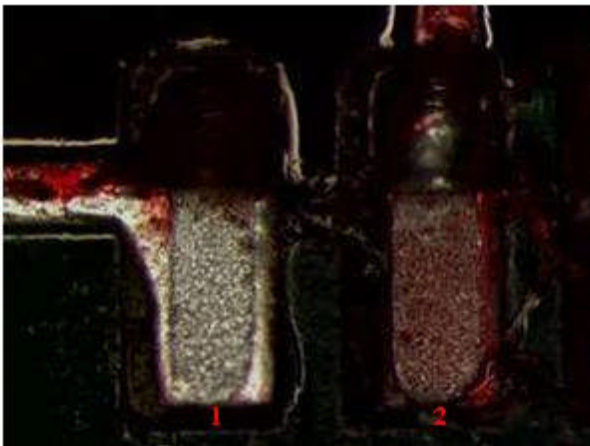
Cross-sectioning



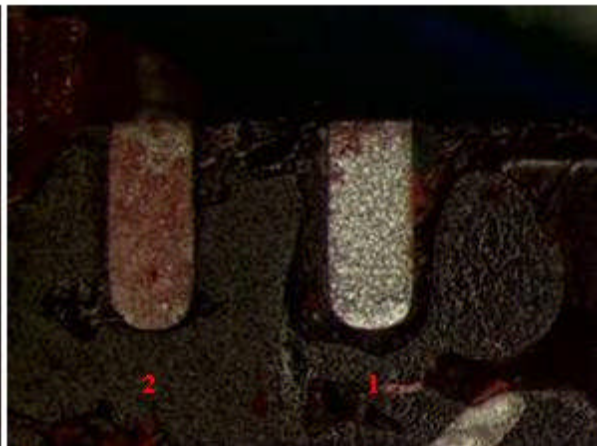
Dye and pry

Figure 217 - Pad Cratering seen on CLCC-20

A small number of the analyzed solder joints had signs of solder fracture; however only in one case did this lead to an electrical failure; Figure 218. This indicates that, for the most part, the solder fractures did not penetrate through the entire solder joint.



Board side



Component side

Figure 218 - Dye and Pry of a QFN-20 showing dye penetration through the bulk solder

Pad cratering occurred in all package types (CLCC-20, QFN-20, TQFP-144, TSOP-50) but was less prevalent in the TQFP-144 in which pad cratering was observed on only one out of nine dye-and-pry samples. This is likely due to the structure of the part which has compliant copper leads on all four sides, ensuring efficient stress distribution. However, in one part, the interconnect failure was through the bulk solder in a fatigue failure mode; Figure 219.



Figure 219 – Fatigue Failure of TQFP-144 with 1x Rework as seen through cross sectioning

6 Assembly Observations

Each testing location was asked to provide observations and conclusions for the test vehicles that they tested and analyzed.

6.1 Combined Environments Test Vehicles – Raytheon

Raytheon, located in McKinney, Texas, conducted the combined environments testing for the NASA-DoD Lead-Free Electronics Project as well as the JCAA/JGPP Lead-Free Solder Project. The following assembly observations were made based on post test analysis, data review and statistical analysis.

- Based on the results of the combined environments testing, component type had the greatest effect on solder joint reliability performance. When considering design, the plated-through-hole components, such as PDIP-20, prove to be more reliable than surface mount technology components. Of the surface mount technology, TQFP-144 and QFN-20 components performed the best while the BGA-225 components performed the worst.
- Solder alloy had a secondary effect on solder joint reliability. In general, tin-lead finished components soldered with tin-lead solder paste were the most reliable. In general, tin-silver copper soldered components were less reliable than the tin-lead soldered controls. The lower reliability of the tin-silver-copper (SAC305) solder joints does not necessarily rule out the use of tin silver copper solder alloy on military electronics. In several cases, tin-silver-copper 305 solder performed statistically as good as or equal to the baseline tin-lead solder.
- The effect of tin-lead contamination on Pb-free BGA-225 components degrades early life performance of tin-copper (SN100C) solder paste. It can also degrade early life performance of tin-silver-copper (SAC305) solder paste. Although, the effect of tin-lead contamination on Pb-free BGA-225 components soldered with tin-silver-copper (SAC305) solder paste was less than the effect on tin-lead contamination on tin-copper solder. Factory controls to eliminate tin-lead contamination will improve performance of Pb-free technology.
- During analysis of the data, there were several instances of early life failures that were traced back to components that were adjacent to areas of the board that had been through rework. Please note that failures failing within the first 10 cycles of testing were excluded from the data analysis and Weibull charts.
- Overall, the results of the 2009 NASA-DoD Lead-Free Electronics Project are comparable to the results of the 2005 JCAA/JG-PP Lead-Free Solder Project study, with the exception of the CSP components.

6.2 Combined Environments Test Vehicles – COM DEV International

COM DEV International, located in Cambridge, Ontario, Canada, provided extensive failure analysis work on the combined environments test vehicles from the NASA-DoD Lead-Free Electronics Project. The following assembly observations were made based on a review of the failure analysis findings.

TQFP Components:

- Solder mask cracking found on test vehicle 21, TQFP components U34 (Figure 220) and U57 (Figure 221).
- Coplanarity issue causing open contacts on test vehicle 21, TQFP components U34 (Figure 222) and U57 (Figure 223).

- Coarsening of solder structure and cracks specific to long exposure to combined stress environment.

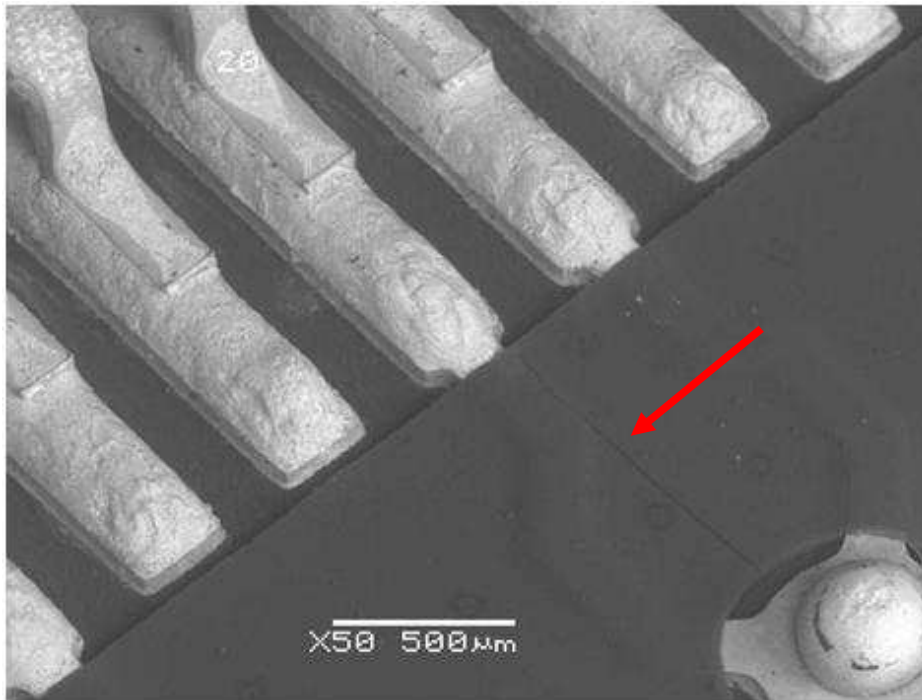


Figure 220 - U34 TQFP, SEM Image, Solder Mask Crack near Lead 20 (X50)

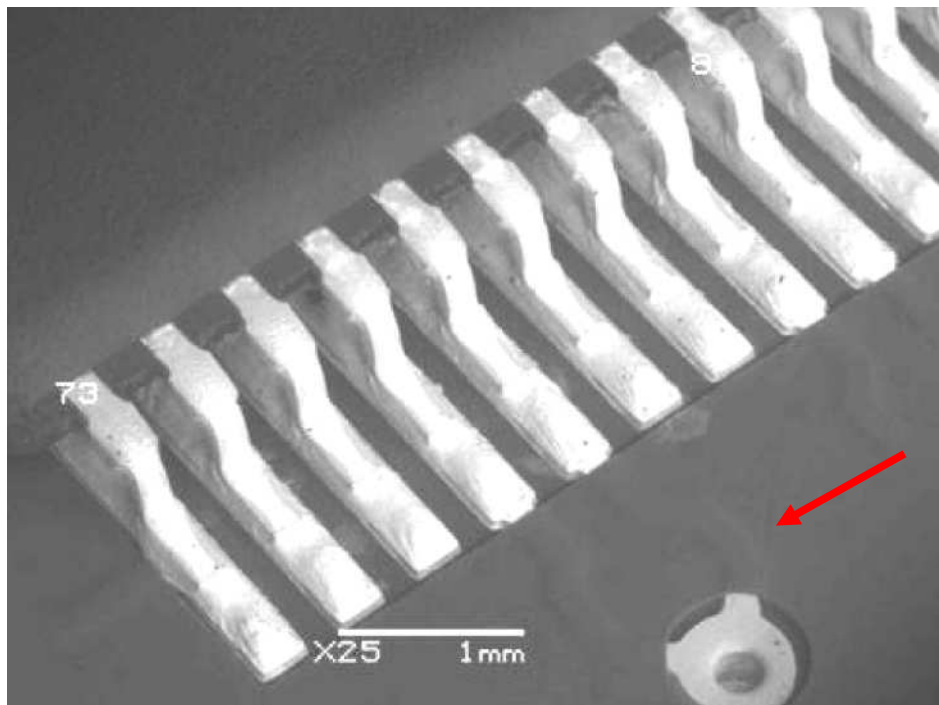


Figure 221 - U57 TQFP, SEM Image, Solder Mask Crack near Leads 73-81 (X25)

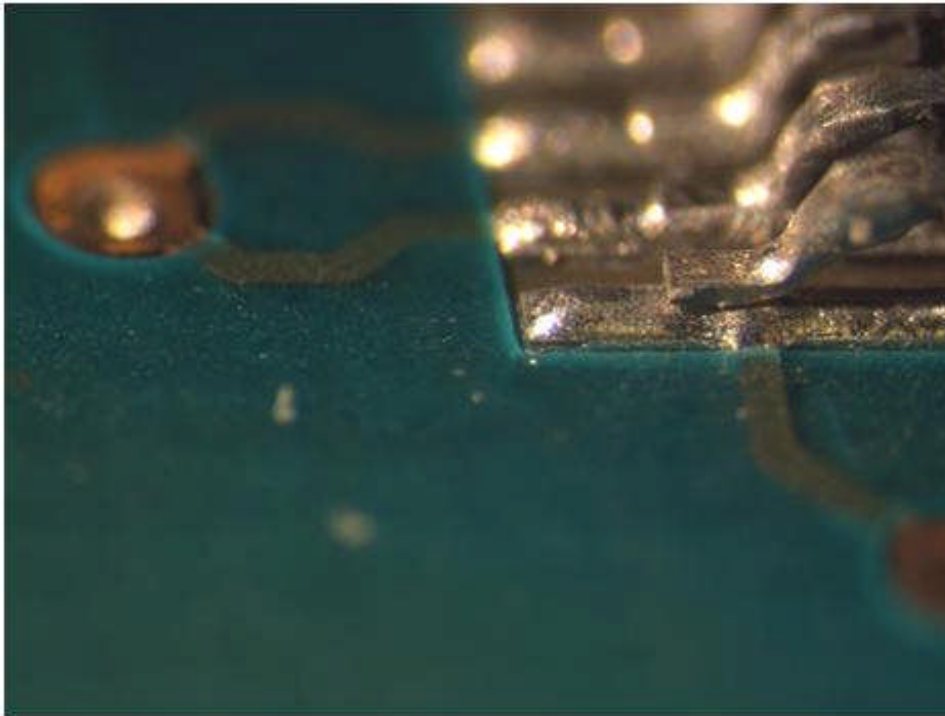


Figure 222 - U34 TQFP, Lead 72 marked (X49); Open due to Non Coplanarity

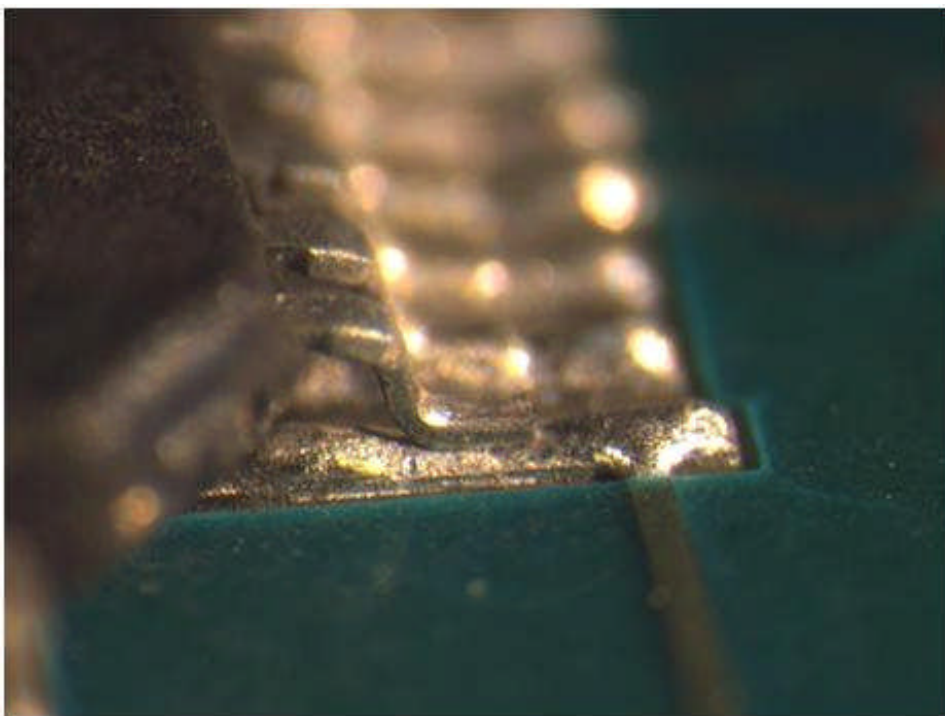


Figure 223 - U57 TQFP, No Solder Contact to Lead 1 (X49); Open due to Non Coplanarity

TSOP Components:

- Solder mask cracking found on test vehicle 119, TSOP component U39 (Figure 224).
- Solder mask cracking found on test vehicle 181, TSOP component U25 (Figure 225).
- Voids in solder joints, test vehicle 119, TSOP component U39 (Figure 226)
- Solder in the upper bend area of test vehicle 119, TSOP component U39 (Figure 227) and test vehicle 181, TSOP component U25 (Figure 228).
- Presence of Pb phase in the vicinity and along the cracks on both parts; test vehicle 119, TSOP component U39 and test vehicle 181, TSOP component U25.

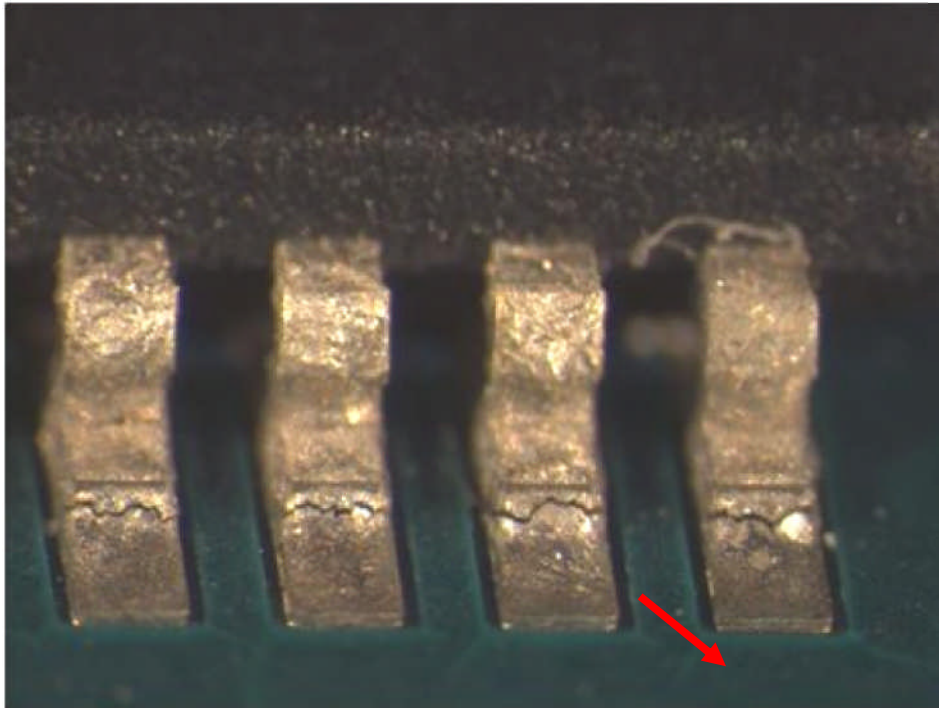


Figure 224 – U39 TSOP, Cracks in Solder Joints and Solder Mask (X49)

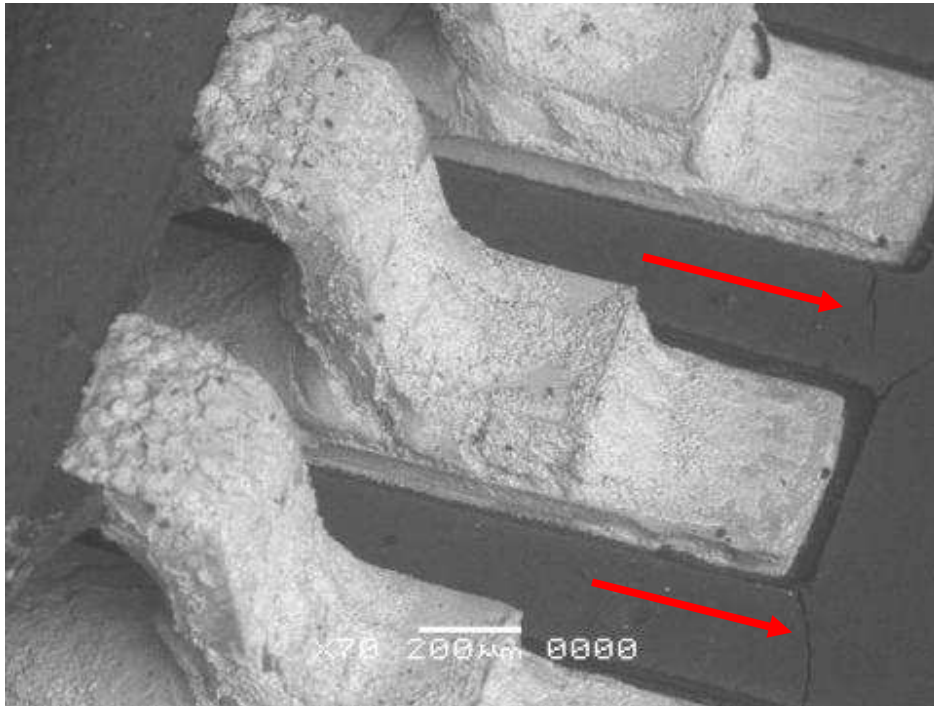


Figure 225 - U25 TSOP, SEM Image, Lead 2 in Center, Lead 1 Left (X70)

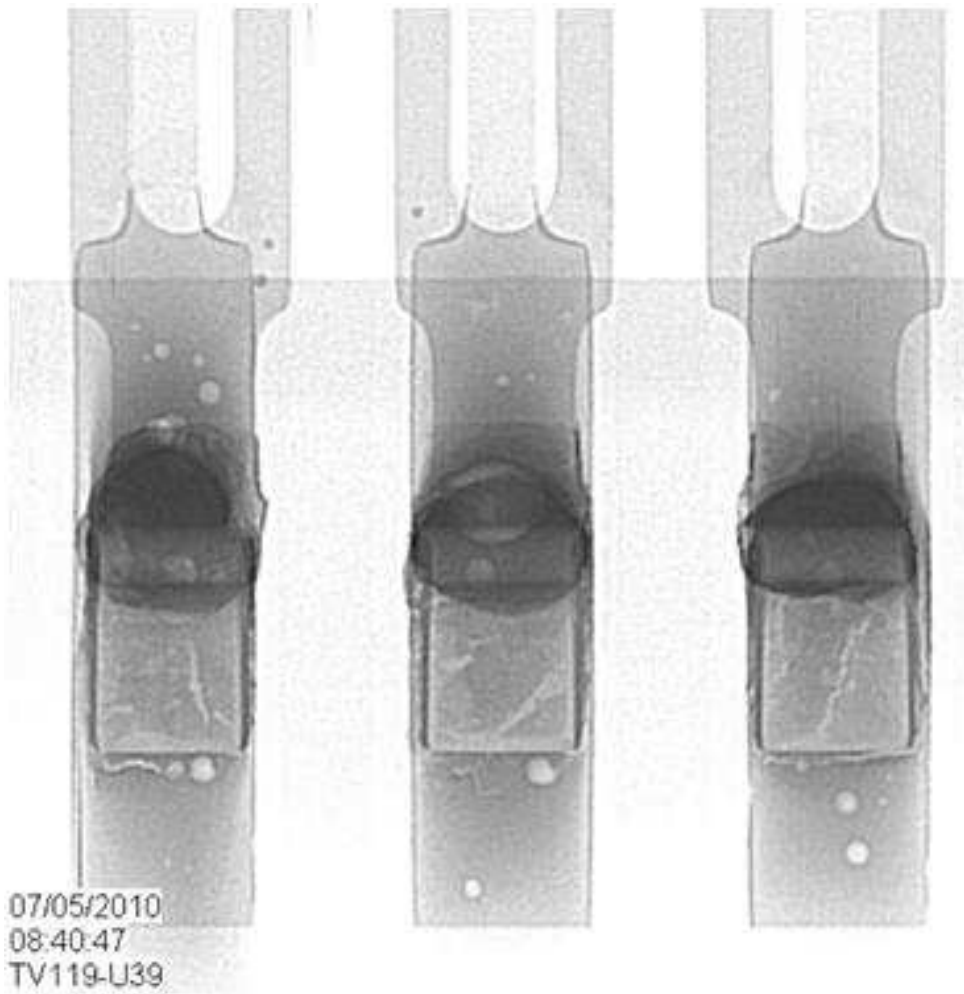


Figure 226 - U39 TSOP, X-ray Image, Leads 1-3, Voids in Solder Joints

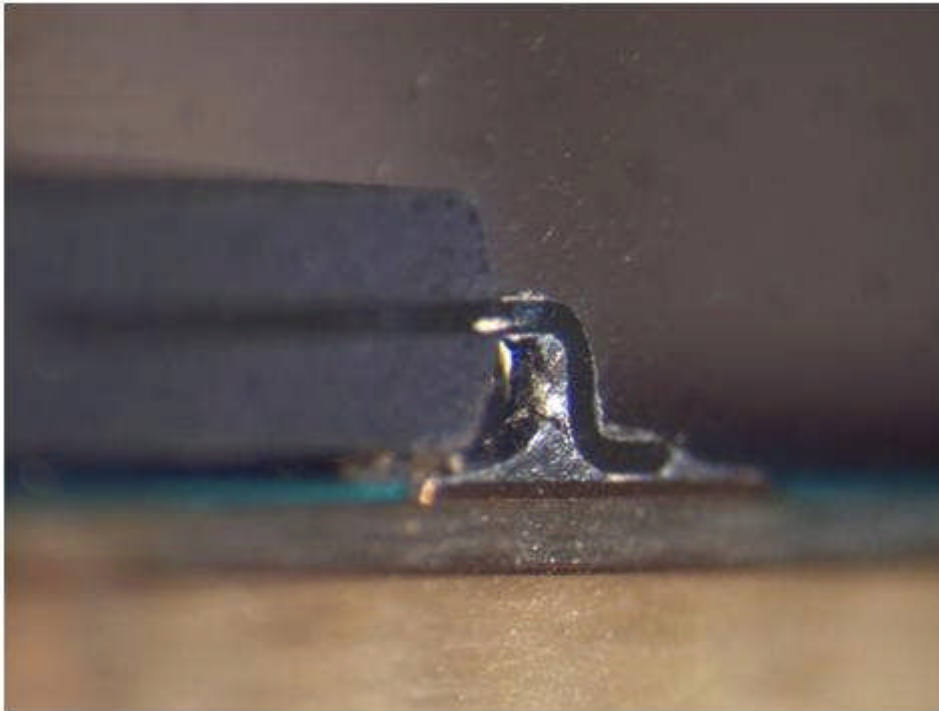


Figure 227 – U39 TSOP, Cross Sectional View of Lead 1, Solder (X49)

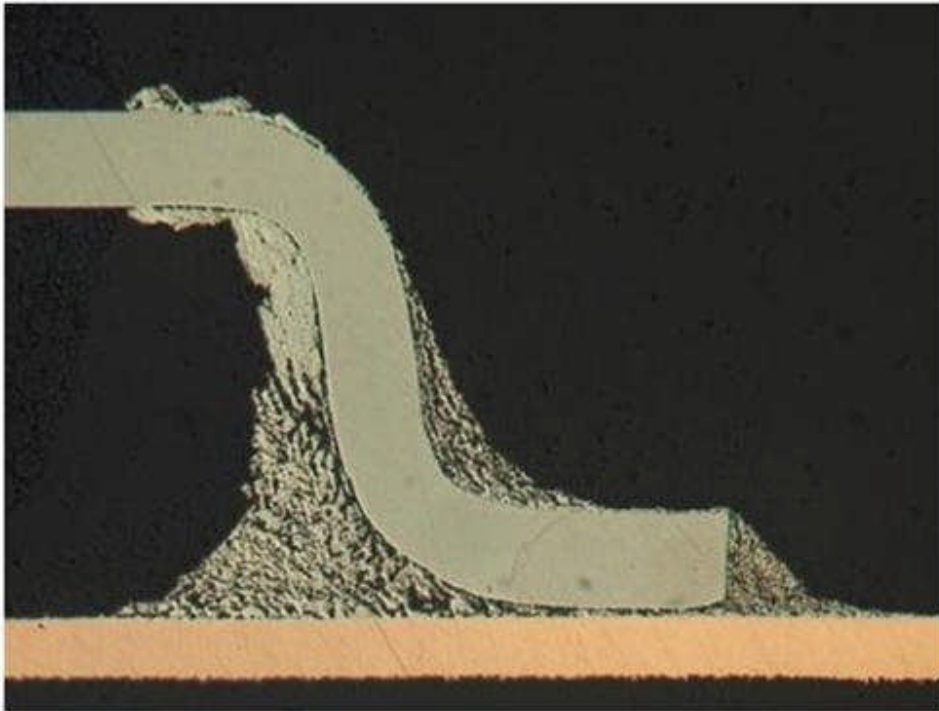


Figure 228 – U25 TSOP, Cross Sectional View of Lead 2, Solder (X136)

CSP Component:

- Solder mask cracking found on test vehicle 119, CSP component U36 (Figure 229).
- Cracks developed at SnCu phase, PCB interface; test vehicle 119, CSP component U36 (Figure 230).
- Cracks developed at Sn rich phase adjacent to Ni barrier; test vehicle 119, CSP component U36 (Figure 231).

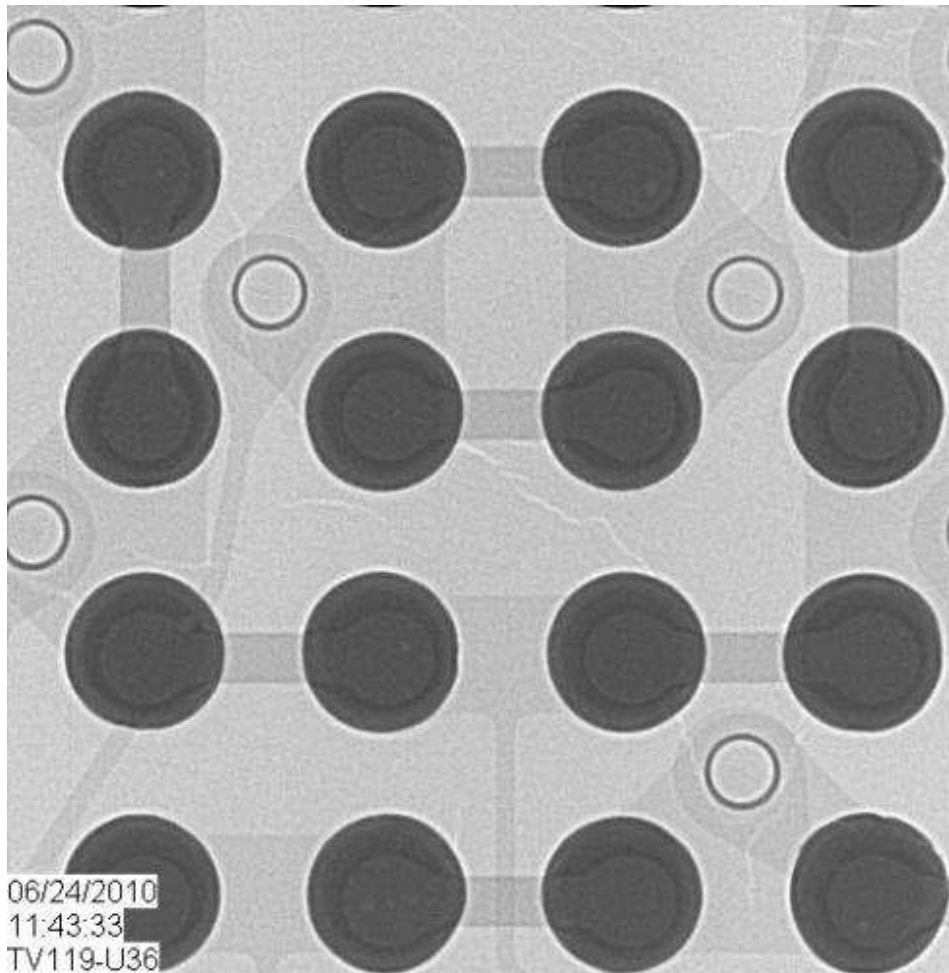


Figure 229 - U36 CSP, X-ray Image, Center Region, Solder Mask Cracks

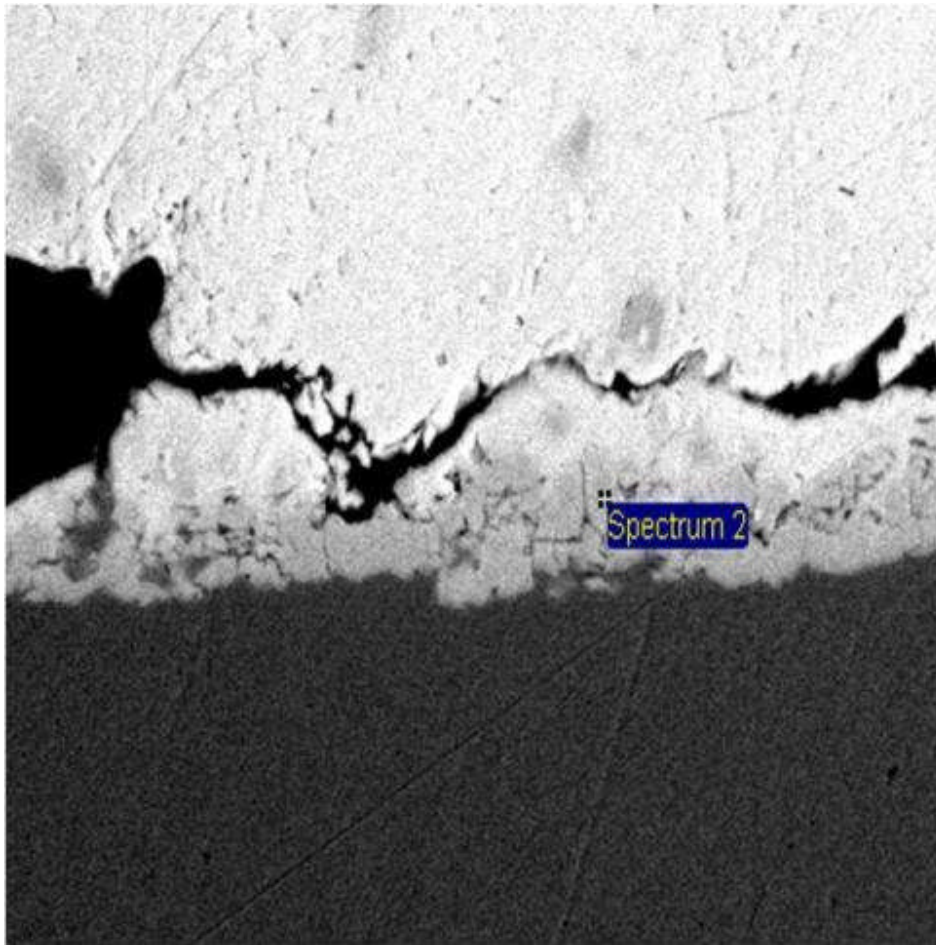


Figure 230 – U36 CSP, Solder Ball A10, PCB Side, Cracks Developed at SnCu Phase

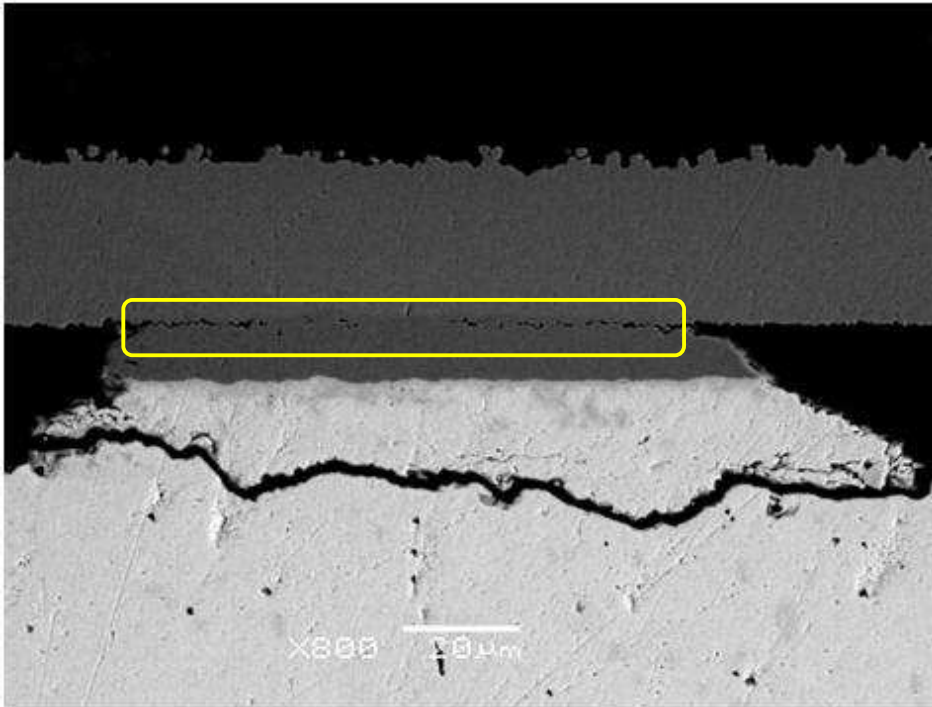


Figure 231 - U36 CSP, SEM image of Ball A2, Component Side (X800)

CLCC Component:

- Solder mask cracking found on test vehicle 142, CLCC component U13 (Figure 232).
- Cracks developed through Sn phase; test vehicle 142, CLCC component U13 (Figure 233).
- Voids in solder joints; test vehicle 142, CLCC component U13 (Figure 234).

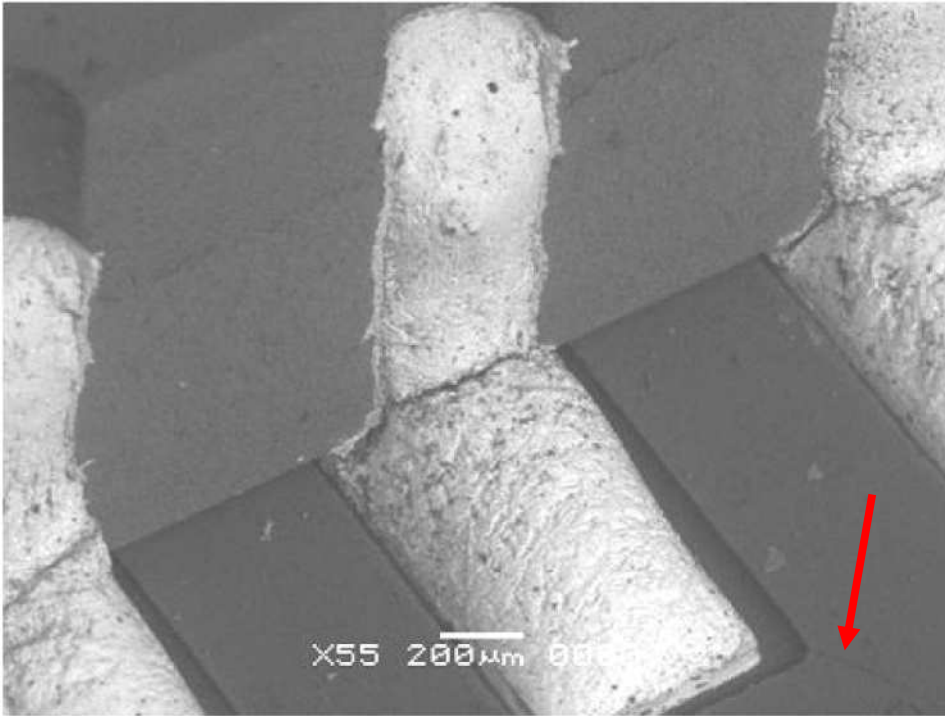


Figure 232 – U13 CLCC, SEM Image, Lead 8, Solder Crack and Solder Mask Crack (X55)

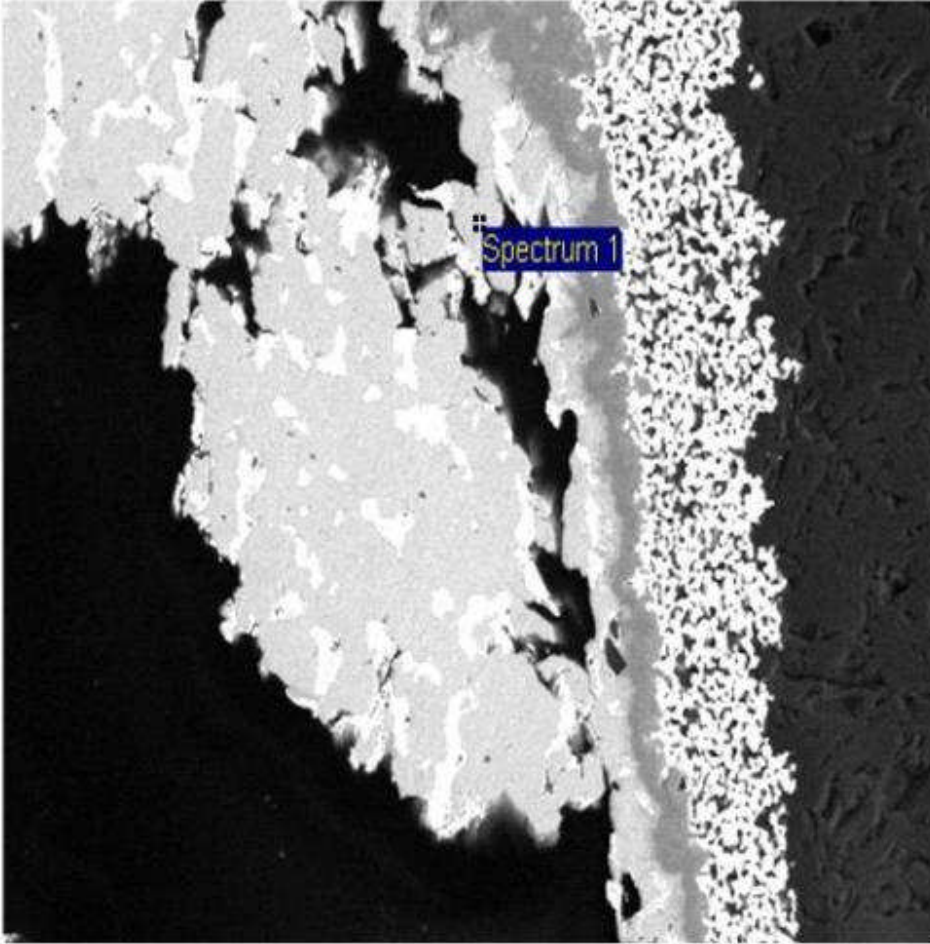


Figure 233 – U13 CLCC, Cracks Developed Through Sn Phase, Lead 20

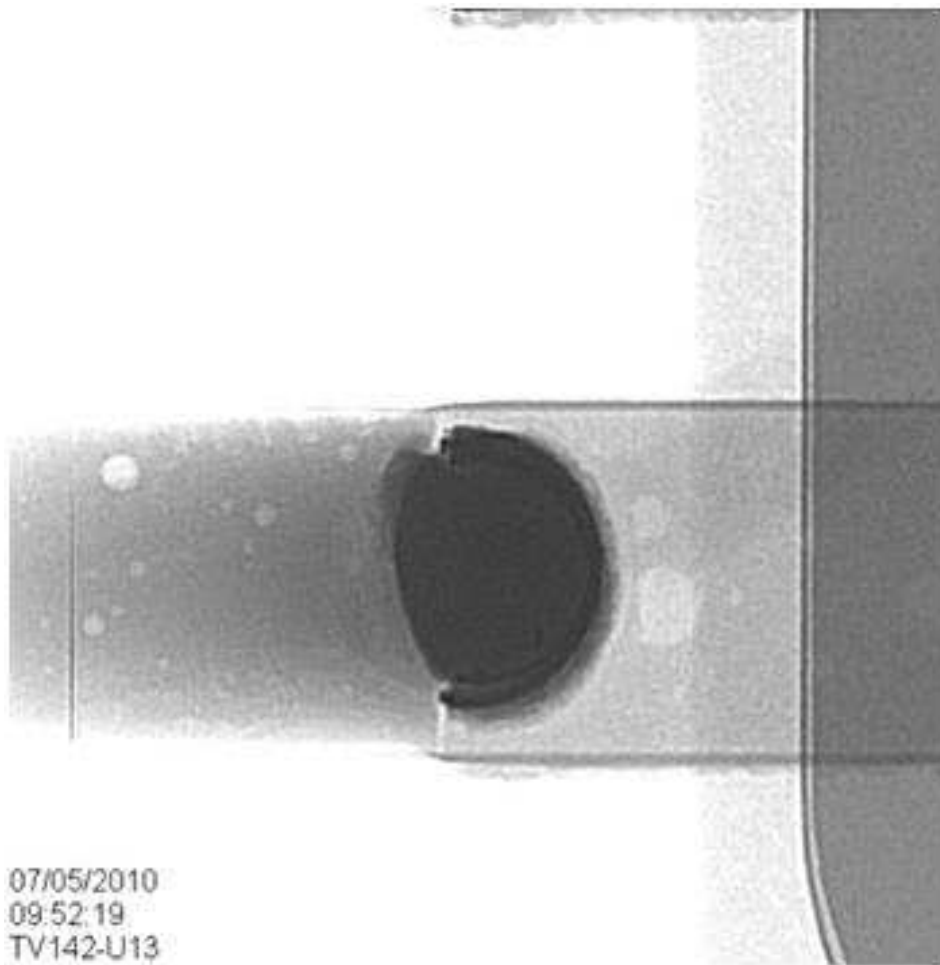


Figure 234 - U13 CCLC, X-ray Image, Voiding, Lead 20

BGA Component:

- Test vehicle 181, BGA component U56; cracks developed at SnCu phase starting in some cases at voids. IMC identified on solder ball to component and on solder joint to PCB. Ag rich phase solidification (plates) identified on solder balls (Figure 235).
- Test vehicle 181, BGA component U56; voids in solder joints (Figure 236).
- Test vehicle 181, BGA component U56; insufficient solder due to solder mask misprint (Figure 237).

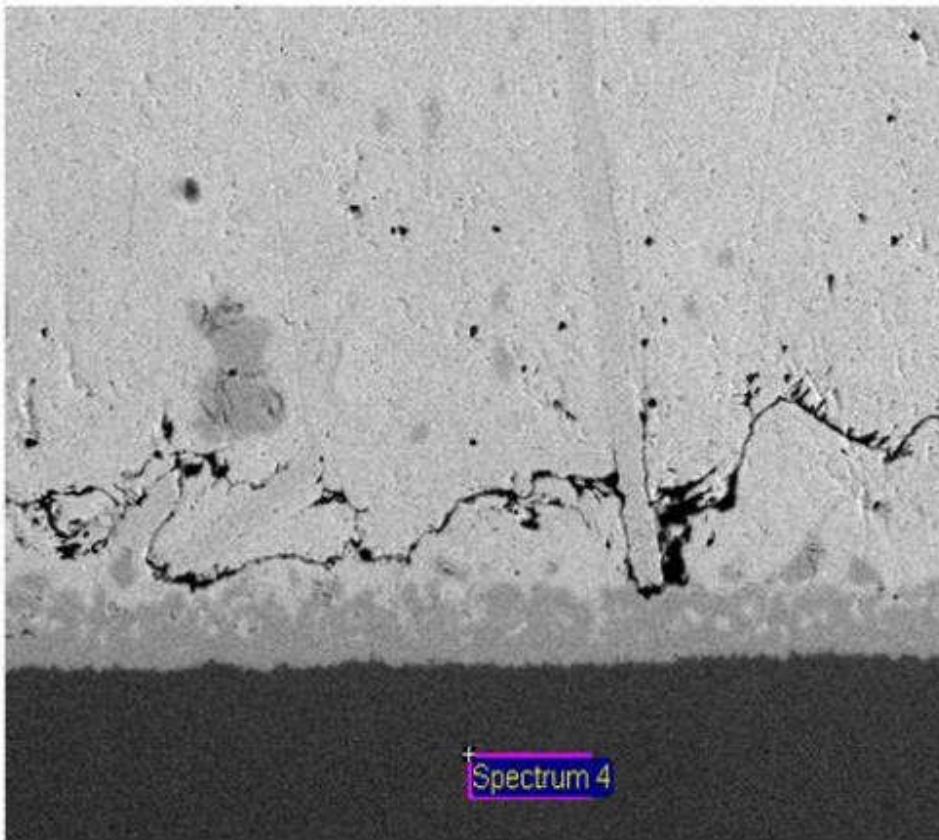


Figure 235 – U56 BGA, Solder Ball A15, Cracks Developed at SnCu Phase

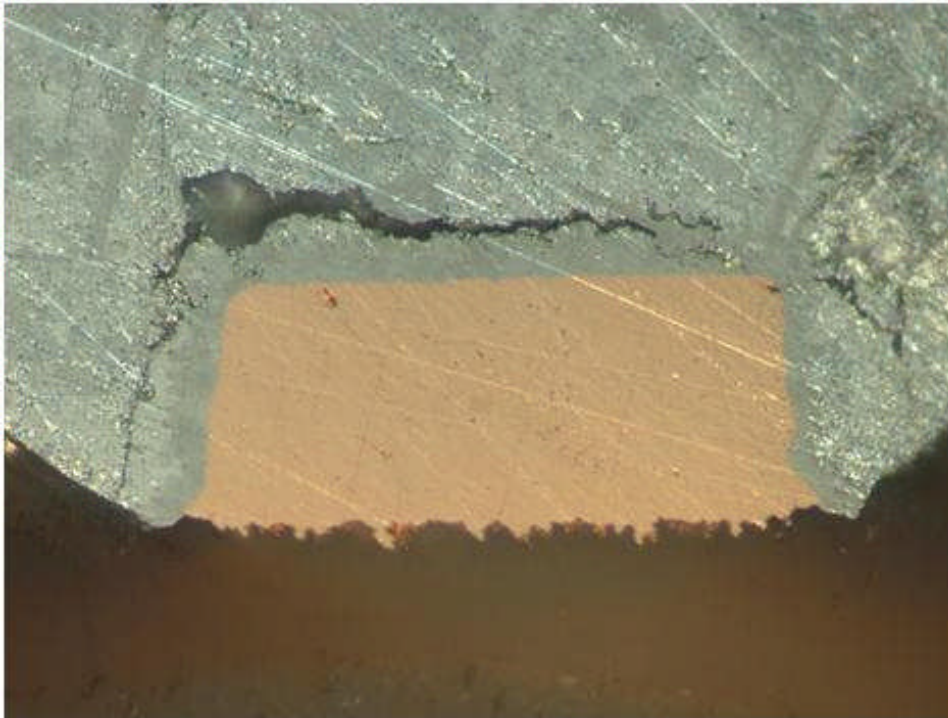


Figure 236 – U56 BGA, Cross Sectional View of Solder Ball A9, Void in Solder Joint (X682)

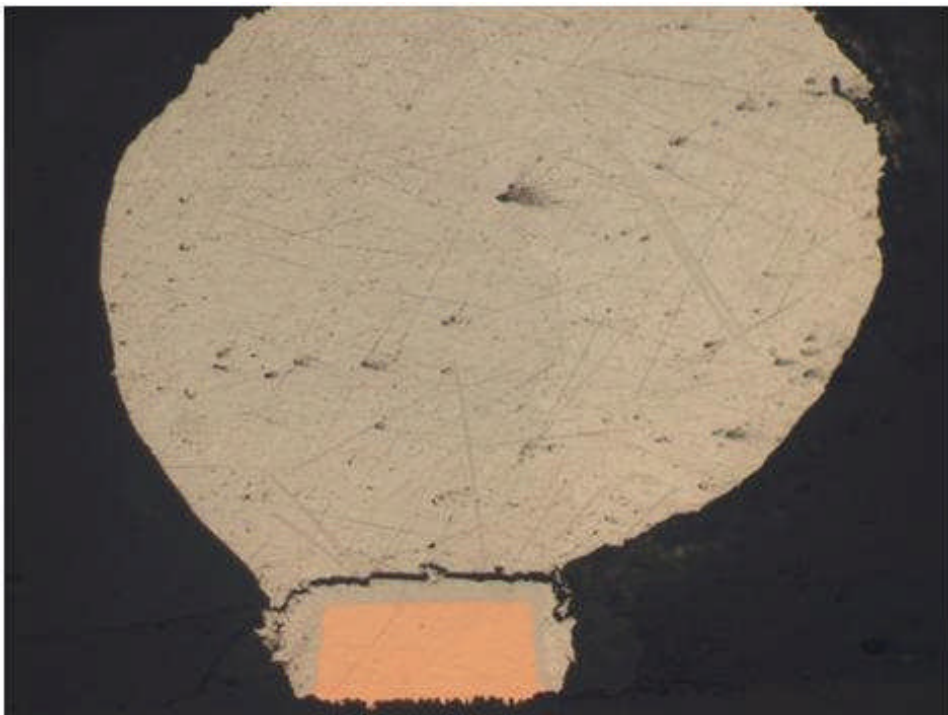


Figure 237 – U56 BGA, Cross Sectional View of Solder Ball A7, Crack on the Solder Joint at PCB Trace Interface

6.3 Combined Environments Test Vehicles – Lockheed Martin

Lockheed Martin located in Ocala, Florida, provided failure analysis work on the combined environments test vehicles from the NASA-DoD Lead-Free Electronics Project. The following assembly observations were made based on a review of the failure analysis findings.

Test vehicle 183 (lead-free rework) assembled using SAC305 for reflow soldering and SN100C for wave soldering. The component analyzed was component U41 (TQFP-144) with a SAC305 component finish obtained by tinning. This particular component was not reworked. This component was of interest since it failed at cycle 1. It was determined that the failure mode was an unsoldered lead from the original manufacturing process (Figure 238 and Figure 239).

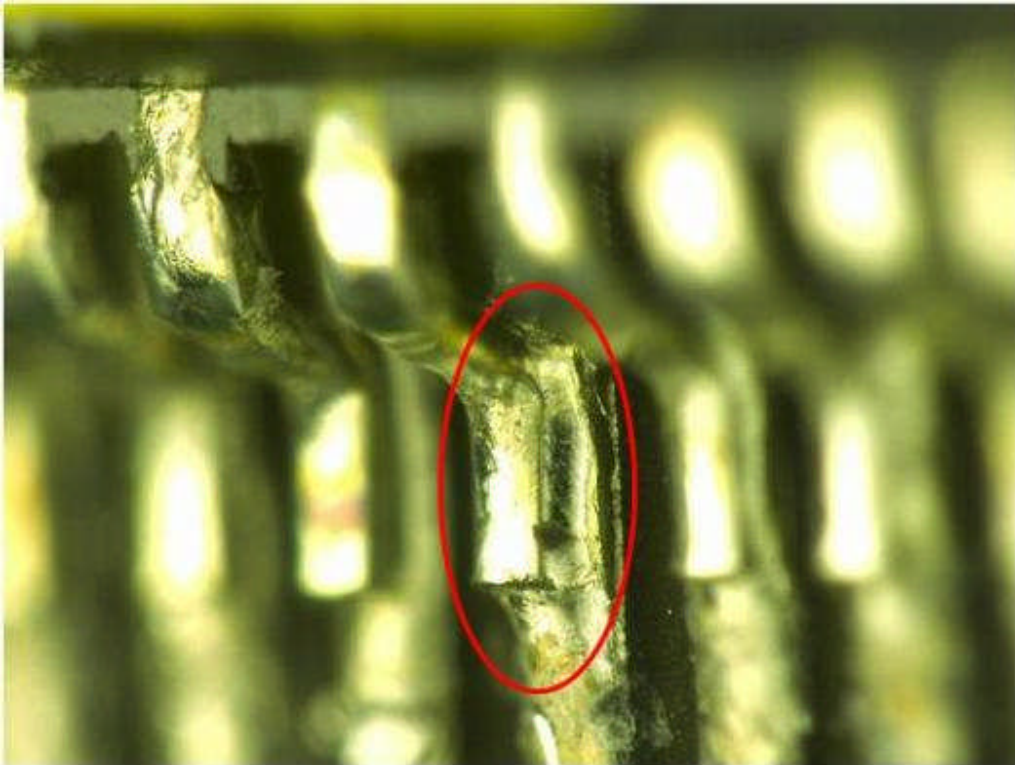


Figure 238 - Test Vehicle 183, Component U41 (TQFP-144); Unsoldered Lead from the Original Manufacturing Process

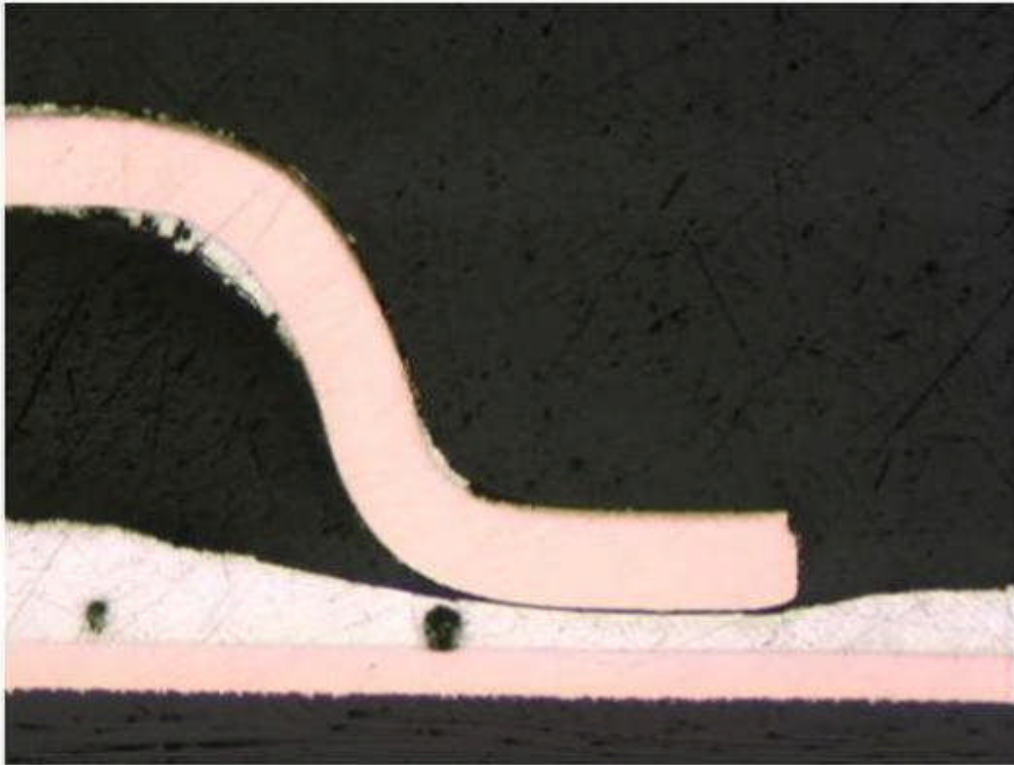


Figure 239 - Test Vehicle 183, Component U41 (TQFP-144); Unsoldered Lead from the Original Manufacturing Process

It was observed, with some surprise, that the SAC solder alloy did not wet to itself. It was concluded that coplanarity and proximity of the lead to the pad is more critical than in SnPb processing. It was observed that even on the “good” solder joint example cross section, the solder behind the lead at the heel was very irregular (Figure 240).

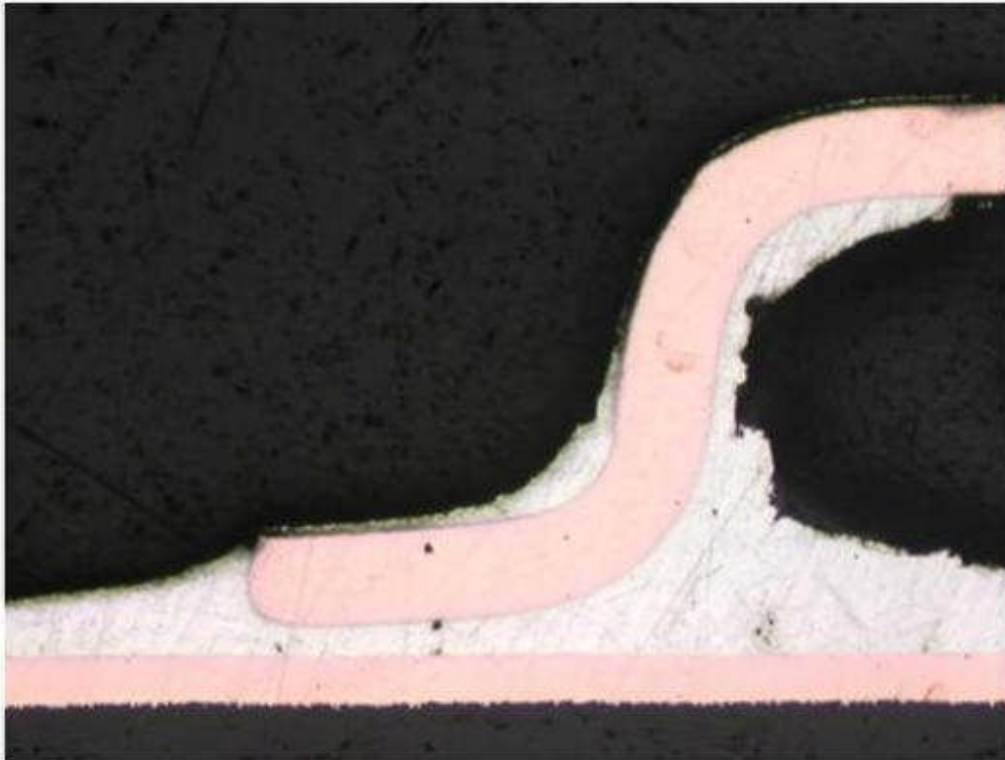


Figure 240 - Test Vehicle 183, Component U41 (TQFP-144); Solder Behind the Lead at the Heel is Irregular

Test vehicle 117 (lead-free manufactured) assembled using SN100C for reflow and wave soldering. The component analyzed was component U4 (BGA-225) with SnPb solder balls. This component was not reworked. This component failed at 20 cycles, it was determined that the failure mode was typical thermal cycle fatigue cracks both at the part and at the board (Figure 241 and Figure 242).

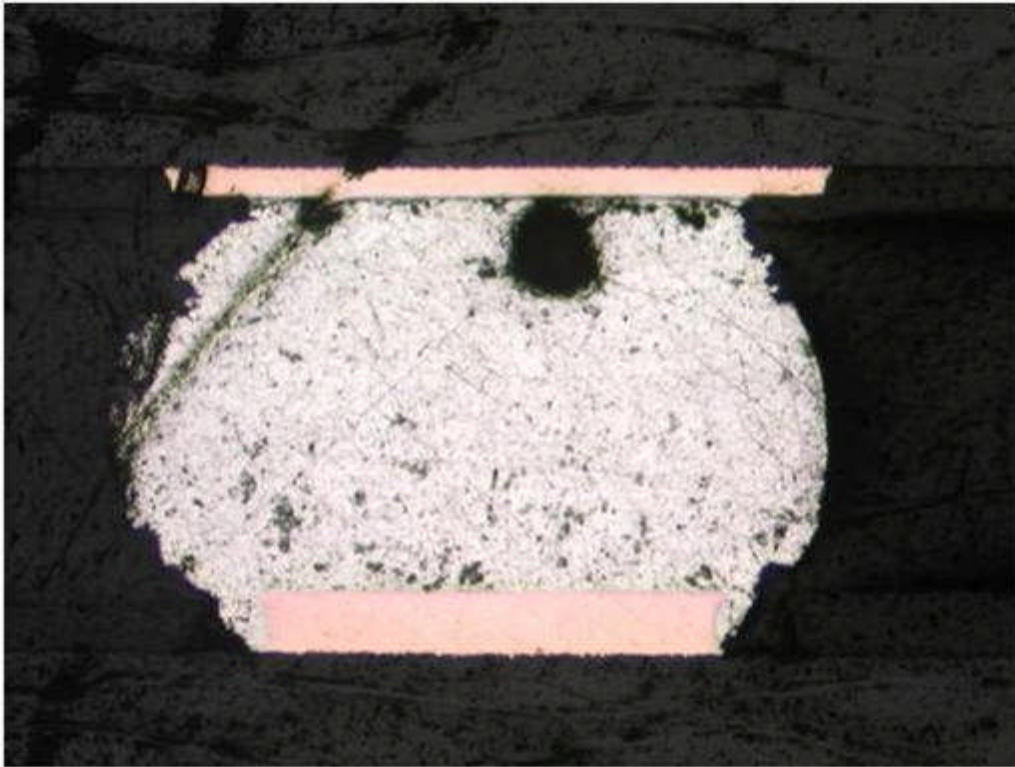


Figure 241 - Test vehicle 117, Component U4 (BGA-225); Crack at the Component Pad

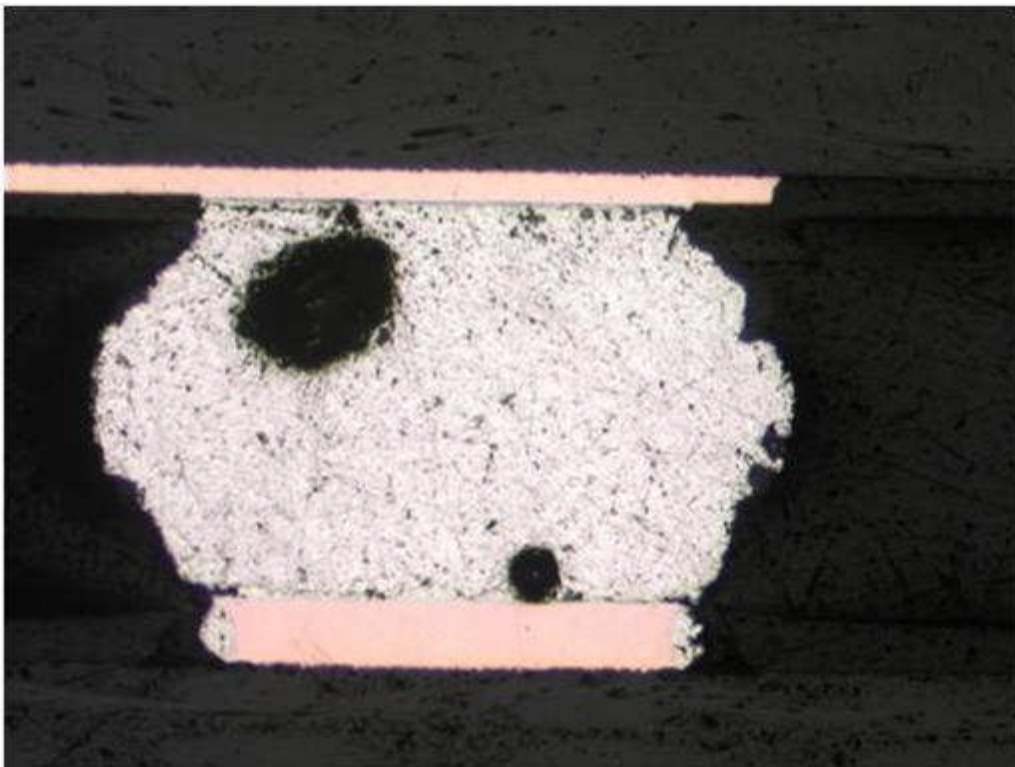


Figure 242 - Test vehicle 117, Component U4 (BGA-225); Crack at the PWB Pad

No cracked joints were observed under the die. Mixing of the solder appeared adequate and the cracks did not relate to any unmixed areas. There were some large voids observed, but they were not related to the failures.

Test vehicle 140 (SnPb rework) assembled using SnPb for reflow and wave soldering. The component analyzed was component U11 (PDIP-20) with a SnPb component finish. This component was reworked. The new component finish was Sn and the rework solder alloy was SnPb. This component failed at 398 cycles. The reworked part showed lifted pad (Figure 243) and a partial crack (Figure 244) but no obvious failure mechanisms.

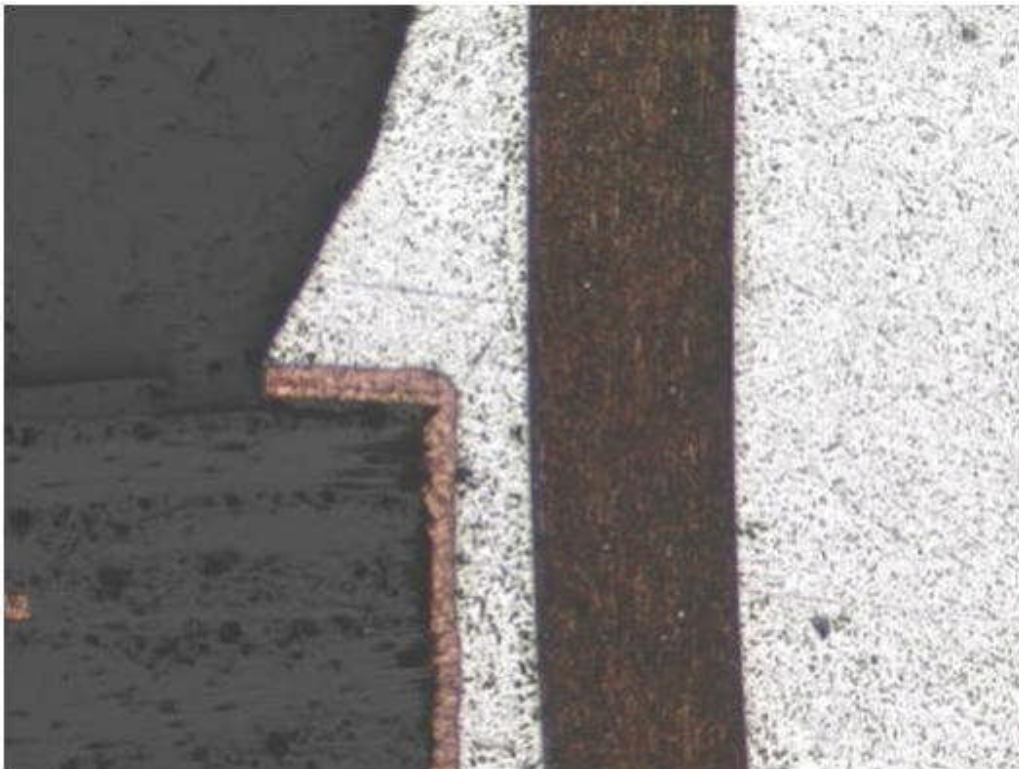


Figure 243 - Test Vehicle 140, Component U11 (PDIP-20); Lifted Pad

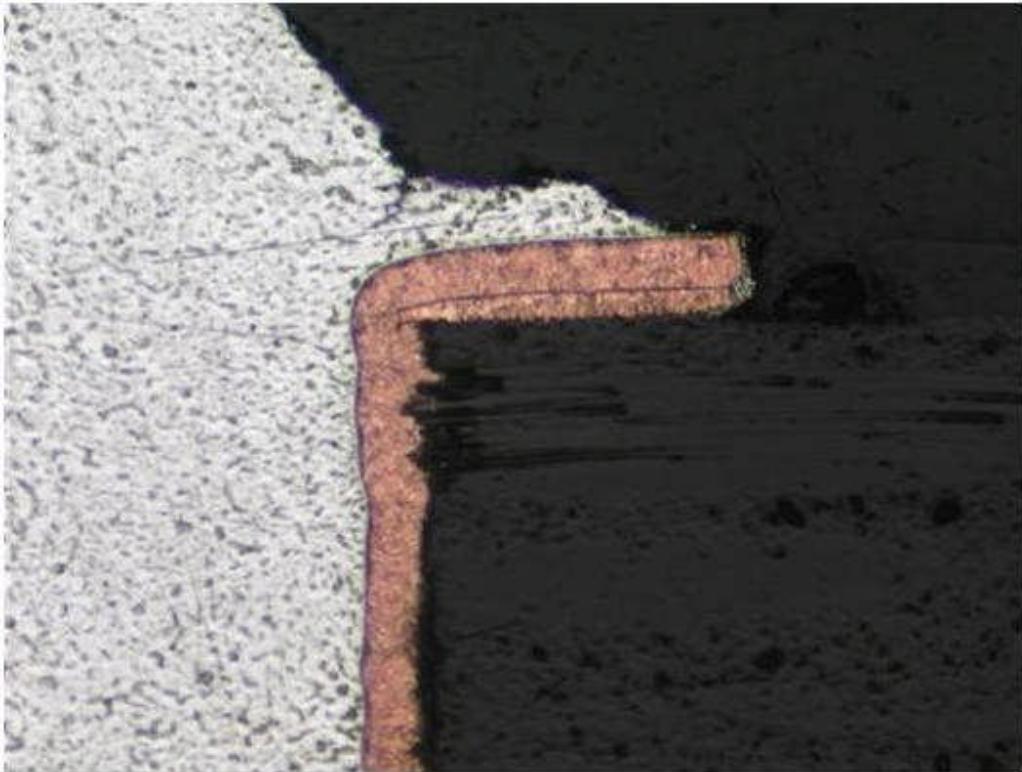


Figure 244 - Test Vehicle 140, Component U11 (PDIP-20); Partial Crack

An exact failure mode was not found. Since this is a SnPb PDIP reworked using SnPb solder, the analysis contained in Section 9 does not seem to fit this particular situation.

7 Copper Dissolution Testing

7.1 SAC305 & SN100C Copper Dissolution Testing

7.1.1 Introduction

Copper dissolution is a concern for products making the conversion to lead-free solder alloys. In these alloys, the reaction of the tin/copper is much faster than that of tin-lead solders/copper, which increases the degradation of the plated copper connections. Since no copper dissolution testing was conducted during Phase 1 (JCAA/JGPP Lead-Free Solder Project) testing, which focused on the reliability of solder joints, Phase 2 (NASA-DoD Lead-Free Electronics Project) included testing to validate copper dissolution measurements report by the commercial electronics industry. Copper dissolution is of particular concern if components are to be reworked, which is much more commonly used on high-reliability electronics than in consumer electronics. Reworking product that has lead-free solder joints may impact the repair depot operations as the copper dissolution may remove over half of the Plated-Through-Hole (PTH) copper in a single rework cycle. Multiple rework cycles may not be acceptable for lead-free products due to copper dissolution impact.

7.1.2 Test Vehicle

The test vehicle used for the copper dissolution testing was a modified Interconnect Stress Test (IST) PTH reliability coupon. Four plated-through-hole, dual in-line package (PTH DIP) patterns and two surface mount technology quad flat pack (SMT QFP) patterns were added to the IST coupon design for the copper dissolution testing. Figure 245 illustrates the copper dissolution test coupon used in the testing efforts.

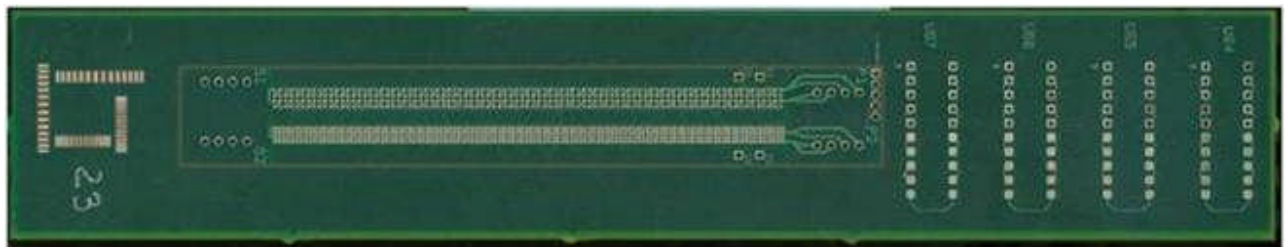


Figure 245 – NASA-DoD Lead-Free Electronics Project, Copper Dissolution Test Coupon

The test coupon, which was approximately 2" x 9" and 0.092" thick, was fabricated with an IPC-4101/26 laminate (Isola 370 HR) with a 170°C T_g minimum material. The coupon surface finish was immersion silver (MacDermid Sterling 0.2-0.4 microns). Two PTH sizes were used: 0.036" and 0.015" finished diameter.

7.1.3 Test Machine & Solder Alloy

An Air-Vac PCBRM12 Solder Fountain mini-pot wave machine was used for this test. A FWL-1248 nozzle was used for the SMT QFP footprint and a FWL-2448 nozzle was used for PTH DIP footprint. Both nozzles were a rectangular fountain type nozzle that completely covered the SMT QFP footprint and covered three PDIP component footprints. Two solder alloys were used:

SAC305 (supplied by AIM^[1]) and SN100C (Nihon Superior) with one at each of the two test facilities included in this study. Table 47 lists the solder alloy test information.

Table 47 - Solder Alloy Test Information

Solder Alloy	Wave Pot Temperature	Test Facility
SAC305	260°C	Celestica
SN100C	270°C	Rockwell Collins

The wave height and contact area were validated using a quartz glass plate. Thermocouples were used to record temperature profiles for each of the timed exposures, which were conducted in an air environment. Figure 246 illustrate the wave solder setup.



Figure 246 - Wave Solder Equipment Setup

7.1.4 Experimental setup

A fixture was fabricated to support the test vehicle for the exposures. This provided a stable platform for repeating the cycles and minimizing any setup variability. Each exposure was thermal profiled using embedded thermocouples located at the PTH base, mid-point, and top

locations. The machine/fixture and the thermocouple setup are shown in Figure 247 and Figure 248. The solder flow rates were held constant across the various exposures.

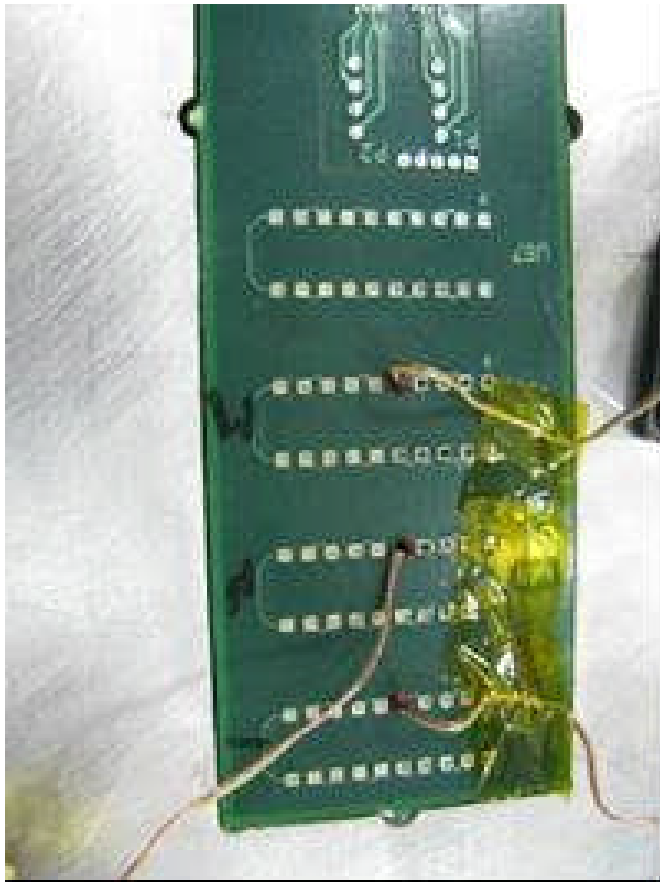


Figure 247 - Thermocouple Placement



Figure 248 - Wave Solder Equipment with Test Coupon

A total of 32 test vehicles per alloy were subjected to various exposure times and number of cycles. In the SAC305 testing, one location of the test vehicle (PTH DIP U67) was taped off with Kapton tape to preserve the copper baseline data for that serial number card. In the SN100C testing, the baseline copper thickness was determined by measuring the thickness of copper under those samples that had Electroless Nickel Immersion Gold (ENIG) surface finish. The test matrix is listed in Table 48 and Table 49.

Table 48 - Test Coupon Exposure Parameters; Celestica

Coupon ID	PTH Contact Time	# PTH cycles	Total PTH Exposure	SMT Contact time all in one cycle
190	80	3	240	120
191	80	3	240	120
170	35	2	70	40
171	35	2	70	40
172	35	2	70	40
173	35	2	70	40
174	35	2	70	40
175	35	3	105	50
176	35	3	105	50
177	35	3	105	50
178	35	3	105	50
179	35	3	105	50
180	40	2	80	15
181	40	2	80	15
182	40	2	80	15
183	40	2	80	15
184	40	2	80	15
185	40	3	120	20
186	40	3	120	20
187	40	3	120	20
188	40	3	120	20
189	40	3	120	20
165	40	1	40	10
166	40	1	40	10
167	40	1	40	10
168	40	1	40	10
169	40	1	40	10
41	40	4	160	25
42	40	4	160	25
43	40	4	160	25
44	40	4	160	25
45	40	4	160	25

Table 49 - Test Coupon Exposure Parameters; Rockwell Collins

Coupon ID	Through Hole Wave Exposure (s)	Surface Mount Wave Exposure (s)
35	240+Baseline (14)	120
39	240+Baseline (14)	120
50	160+Baseline(14)	50
51	160+Baseline(14)	50
52	160+Baseline(14)	50
53	160+Baseline(14)	50
54	160+Baseline(14)	50
69	120+Baseline(14)	40
70	120+Baseline(14)	40
71	120+Baseline(14)	40
72	120+Baseline(14)	40
73	120+Baseline(14)	40
98	105+Baseline(14)	25
99	105+Baseline(14)	25
100	105+Baseline(14)	25
101	105+Baseline(14)	25
102	105+Baseline(14)	25
103	80+Baseline(14)	20
104	80+Baseline(14)	20
105	80+Baseline(14)	20
106	80+Baseline(14)	20
107	80+Baseline(14)	20
110	70+Baseline(14)	15
111	70+Baseline(14)	15
112	70+Baseline(14)	15
113	70+Baseline(14)	15
114	70+Baseline(14)	15
115	40+Baseline(14)	10
116	40+Baseline(14)	10
117	40+Baseline(14)	10
118	40+Baseline(14)	10
119	40+Baseline(14)	10

The exposure times selected in developing the test matrix were selected based on the goal of testing 3 rework cycles with a typical cycle of 40 seconds. A test point at 160 seconds was included to include a possible 4th rework cycle. There are many variables that can affect the outcome of the rework process. A number of the most significant of these, including pot temperature, contact time, alloy type, were investigated in this evaluation. Other process variables, such as the mini-pot flow rate, nozzle type, preheat temperature; product internal copper thermal load, component type, and operator technique are potential sources for variance in the rework process that should be included in a complete evaluation of the rework processes.

7.1.5 Copper Dissolution Measurements

The Celestica test coupon copper dissolution data (for SAC305) were measured using cross-sectioning per the following details:

- Measurements were taken at 3 locations on the test coupons.
- The “A” measurements were taken on the SMT QFP pattern.
- The “B” measurements were taken in the 10 hole PTH DIP pattern of those holes that were not exposed (Masked with Kapton Tape) to the mini-pot wave solder (U67=baseline copper measurement time zero).
- The “C” measurements were taken at the 10 hole pattern of the PTH DIP for each of the 10 holes and the averages and variation recorded by group 1-5 and 6-10 in addition to the individual measurements.

The Rockwell Collins test coupon copper dissolution data (for SN100C) were likewise measured using cross-sectioning per the following details:

- PTH DIP measurements were taken at 10 locations for each plated-through-hole: the top plated-through-hole knee, $\frac{1}{4}$ of PTH thickness, $\frac{1}{2}$ of PTH thickness, $\frac{3}{4}$ of PTH thickness, bottom plated-through-hole knee. Ten plated-through-holes were measured on each test coupon. These measurements are the same as those for the Celestica/SAC305 data with the addition of a measurement at the top plated-through-hole knee.
- SMT QFP measurements were taken at 6 locations for each test footprint: 3 pads exposed to the wave soldering process and 3 pads not exposed to the wave soldering process as a control. All measurements were taken at the center of the pad.

Figure 249 and Figure 250 illustrates PTH DIP and SMT QFP cross-sections with the copper dissolution measurement locations and values.

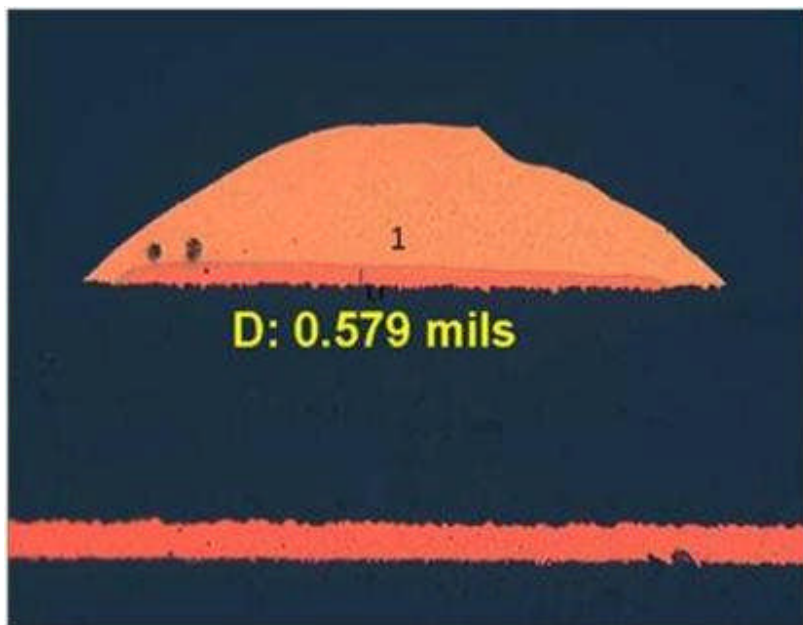


Figure 249 - Rockwell Collins Dissolution Measurement Locations; SMT QFP

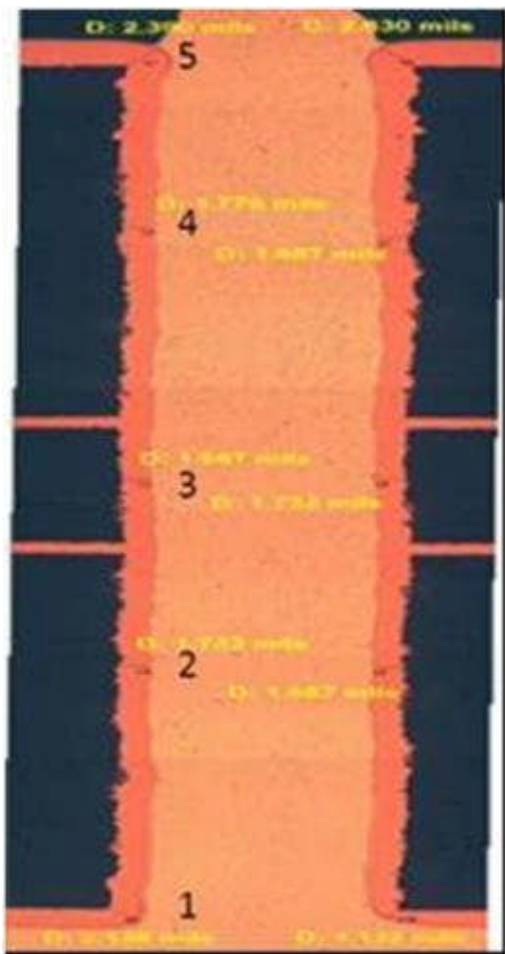


Figure 250 - Rockwell Collins Dissolution Measurement Locations; PTH DIP with Measurement Location Designators Shown

7.1.6 Results

The SN100C solder alloy copper dissolution test results are plotted in Figure 251 and Figure 252. The PTH DIP test coupons with the 0.036" holes exhibit a linear dissolution of copper as the wave solder exposure time increases. The PTH DIP test coupons with the 0.015" holes exhibit minimal-to-no copper dissolution even with longer wave solder exposure times. This is considered to be due to the reduced wetting and capillary action in the smaller hole, which was insufficient to allow consistent flow of molten solder up and down the barrel with these alloys. This is not a surprise as the volume of alloy exposure to the copper interface is much greater for the larger hole. Other industry reports show similar results for larger PTH holes. This issue is exacerbated by Design for Manufacturing (DFM) rules for lead-free alloys, which require a larger hole to permit proper hole fill for PTH solder joints (12). The plated-through-hole knees for both hole sizes exhibited completed copper dissolution for wave solder exposure times that exceeded ~70 seconds.

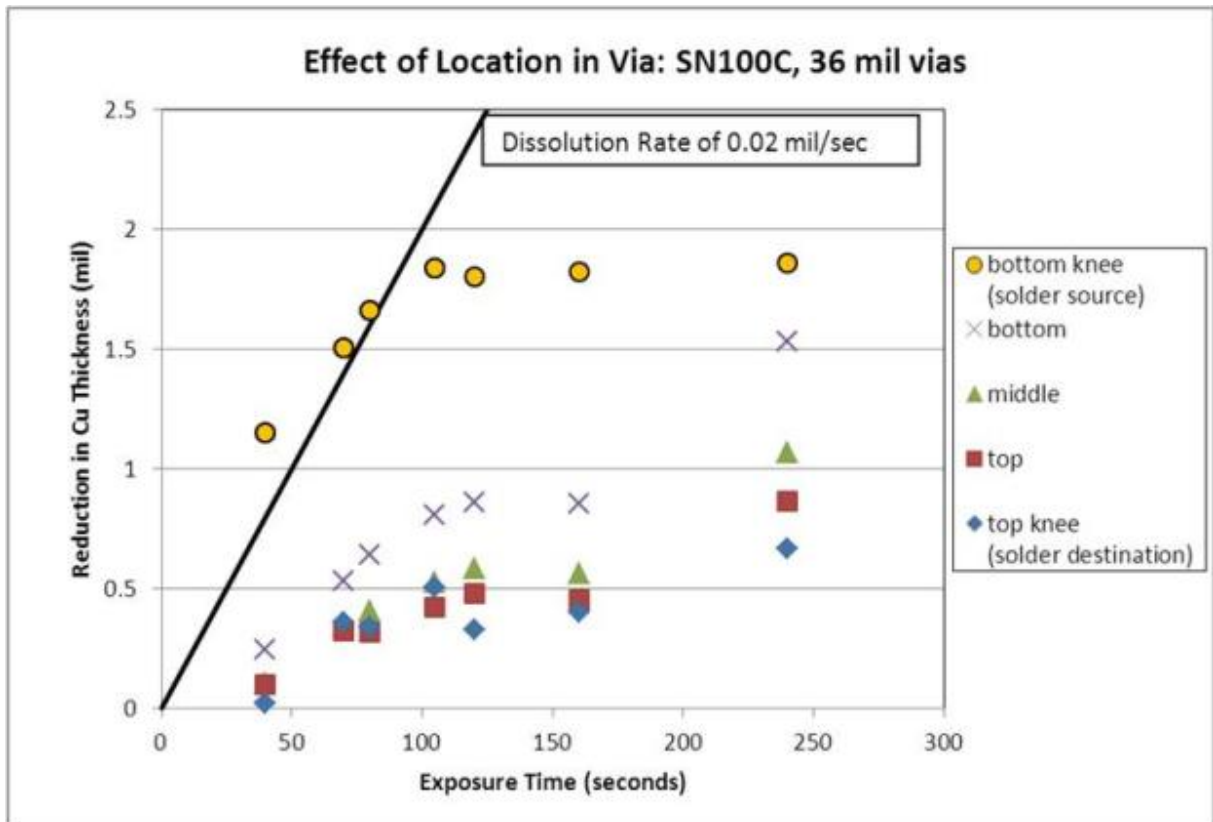


Figure 251 - SN100C Copper Dissolution Results; 0.036" PTH

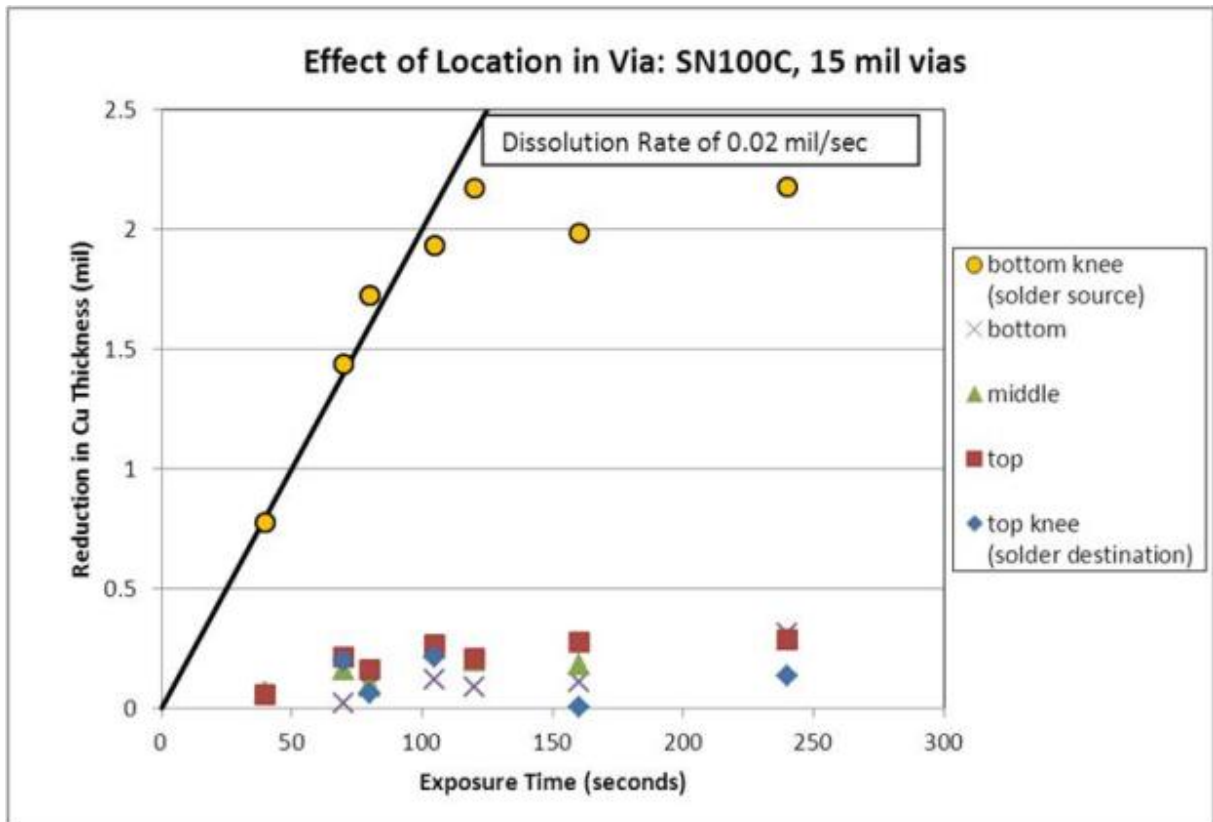


Figure 252 - SN100C Copper Dissolution Results; 0.015" PTH

Figure 253 shows a trace that is disconnected from the PTH barrel and therefore represents a board defect resulting from excessive copper dissolution. DfX rules could redirect the location of these signal connections within the barrel towards the upper layers to minimize the risk of an interconnection failure in the product. Figure 254 illustrates a 0.036" PTH that was subjected to a total of 240 seconds of wave solder exposure. The PTH copper has been completely dissolved in the wave soldering process to nearly 30% of the plated-through-hole copper height.



Figure 253 - Damage example – PTH trace disconnected from PTH barrel

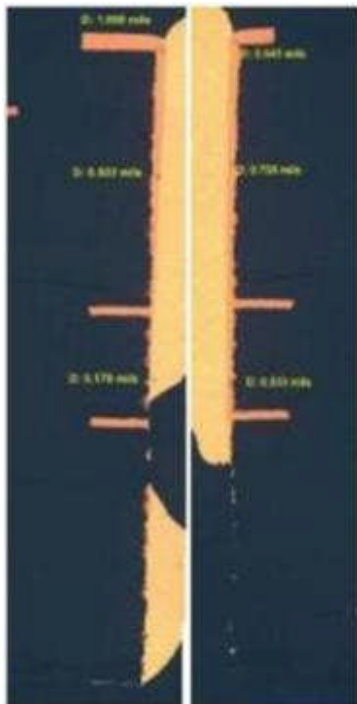


Figure 254 - SN100C Cross-section of 0.036" PTH with 240 Seconds Exposure

As expected, the height of the plated through via also plays a role in the copper dissolution issue. Increasing the exposure time to the molten solder wave causes greater plated through via copper dissolution. Figure 255 illustrates how copper dissolution rates vary as a function of plated via measurement location along the length of the via. The bottom knee location had complete copper dissolution after approximately 100 seconds but the top knee location suffered only a reduction

of 0.6 mils of copper after 240 seconds. This copper dissolution impact is important as product designers can make their designs inherently less vulnerable to the effects of copper dissolution by placing critical signal layers further from the printed wiring board lower half locations. Note that the dissolution rates shown in Figure 255 are specific to that particular via diameter and alloy. As will be shown in the subsequent sections of these reports, the smaller vias and other solder alloy showed significantly different rates of copper dissolution.

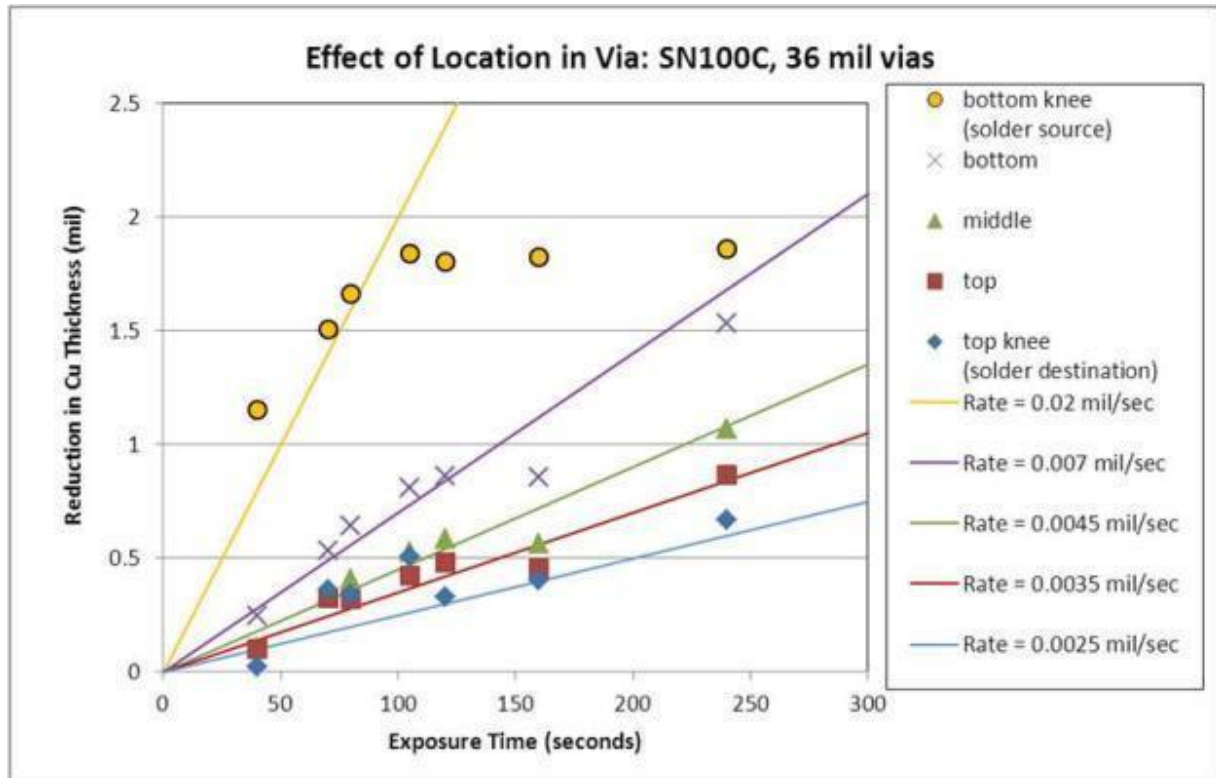


Figure 255 - Copper Dissolution for SN100C Alloy Illustrating Impact of Location on Via Height

The dissolution rate of copper is a function of the specific solder alloy, via geometry, temperature and contact time during the PTH rework using a conventional mini-pot wave rework machine. Previous studies (13) (14) have shown that preheat temperature has an influence on dissolution. These studies indicated that using a higher preheat temperature helped to reduce the degree of Cu dissolution as it shortened the molten exposure time of the process, but not to a significant degree. For this study, the process temperatures were kept constant and the samples all started from room temperature.

Figure 256 illustrates the differences in copper dissolution rates for the SAC305 and SN100C alloys for the SMT QFP pad feature. The results shown in Figure 256 are in good agreement with the industry literature, with the SAC305 solder alloy having a higher copper dissolution rate than the SN100C solder alloy.

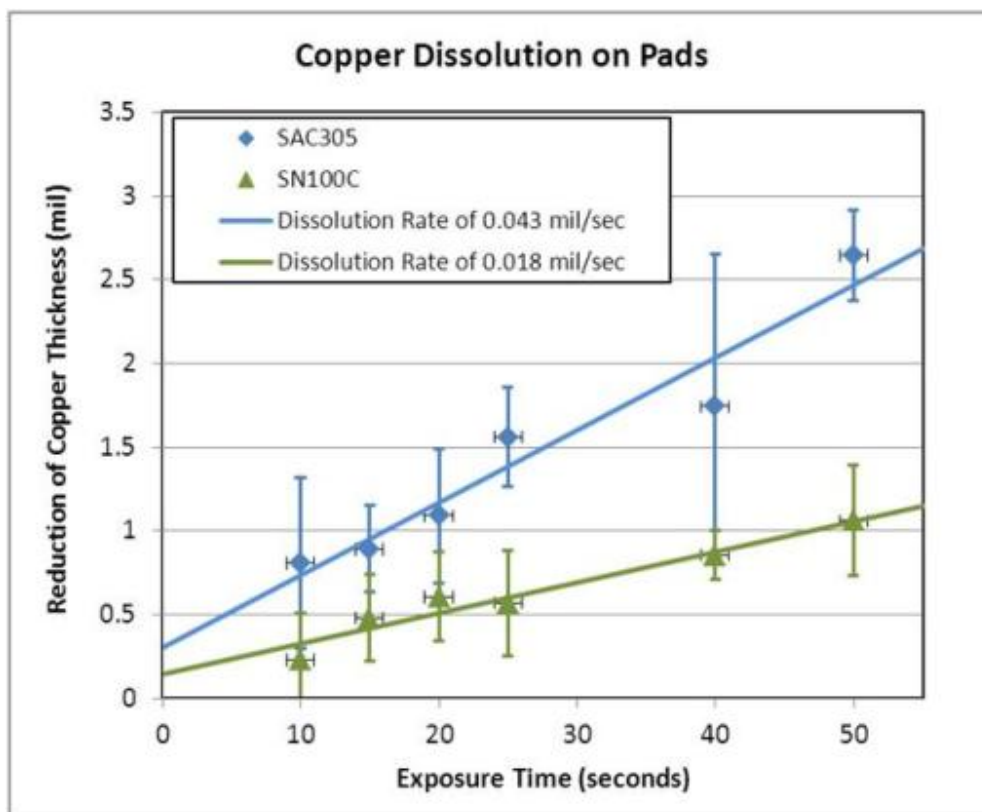


Figure 256 - SAC305 and SN100C Copper Dissolution Results for SMT QFP

Figure 257 illustrates the differences in copper dissolution rates for the SAC305 and SN100C alloys for the PTH DIP via feature. This figure shows the rates of copper dissolution of the midpoint of the 36 mil and 15 mil vias for both types of solder alloys tested. Similarly to the SMT QFP pad results, the SAC305 solder alloy has a higher copper dissolution rate than the SN100C solder alloy for the 36 mil via size. The influence of the plated through via feature is illustrated in Figure 257 as the copper dissolution rates for the SAC305 and SN100C alloys are very similar for the 15 mil via size. The geometry of the 15 mil via reduces the molten solder contact exposure, which reduces the effective copper dissolution rates. This influence of the plated through via size can be potentially be used as a design advantage for copper dissolution concerns dependent upon necessary via functionality. For lead-free alloys, it has been shown that larger hole to pin ratios are required (12). This larger hole requirement to enhance the via fill and resulting solder joint is inversely related to the copper dissolution interaction. Design considerations for lead-free products must take into account and balance the risks between copper dissolution and PTH solder hole fill.

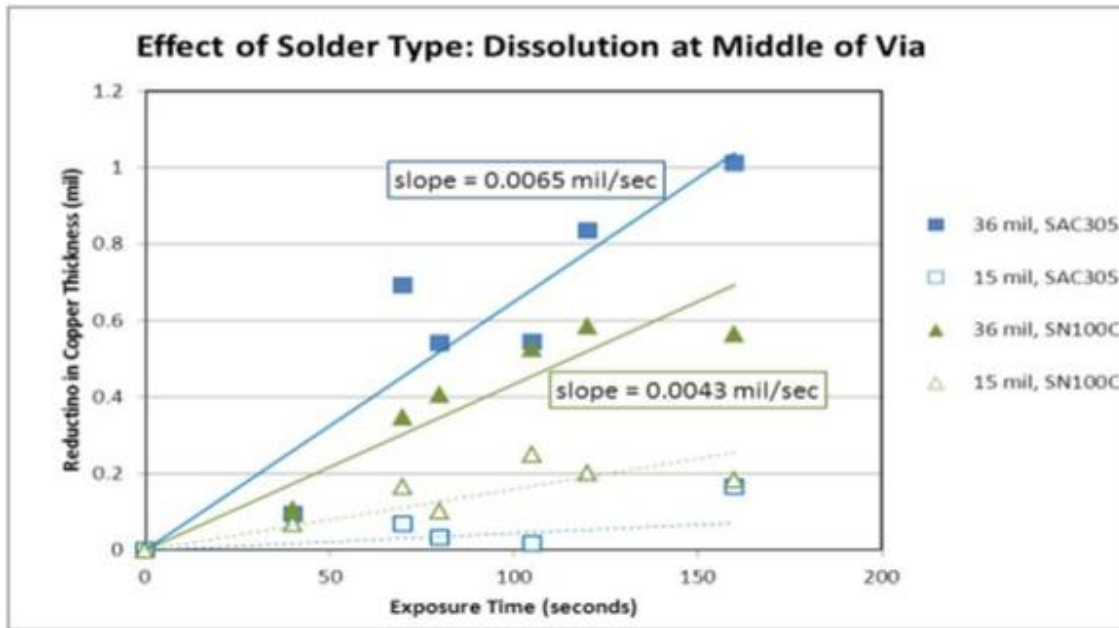


Figure 257 - SAC305 and SN100C Copper Dissolution Results for PTH DIP at Middle Via Measurement Location

Figure 258 illustrates the slight differences in the average copper dissolution rates between the 36 mil and 15 mil via sizes for both solders that were evaluated. The error bars on this figure represent one standard deviation of the data.

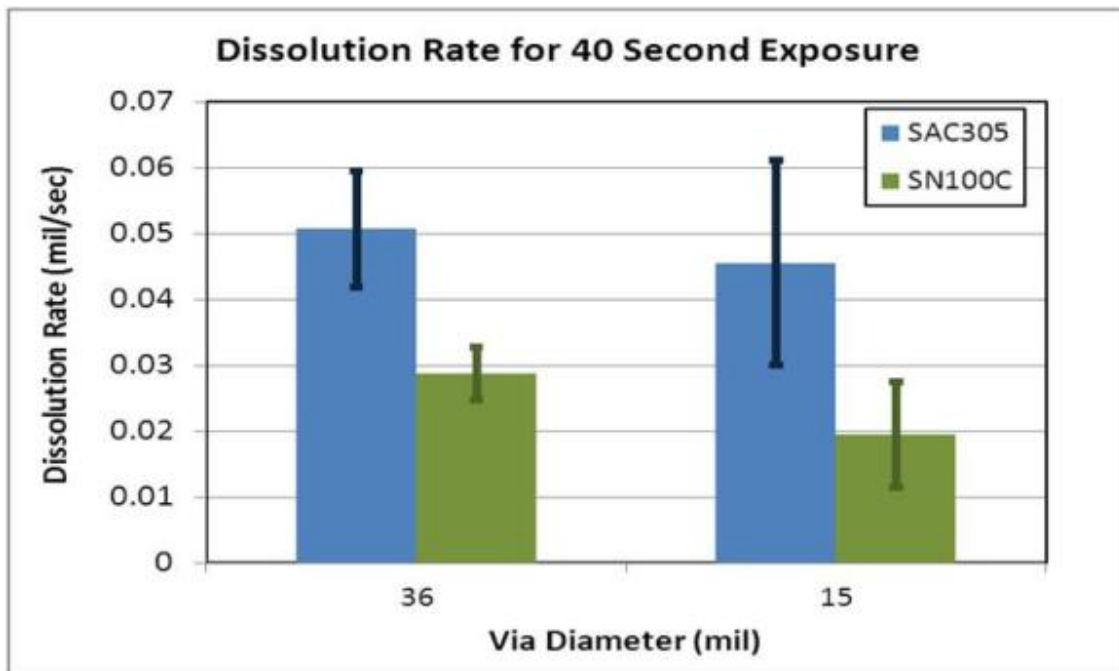


Figure 258 - SAC305 and SN100C Copper Dissolution Rate Comparison for 40 Second Exposure

Since the dissolution of a plated through via knee is not readily detectible using typical assembly product stress screening, strict assembly process control limits are necessary to yield acceptable product reliability. Figure 259 shows soldering process windows for the SAC305 and SN100C solder alloys for two classes of electronic products. The dissolution rates used to define the process window values correlate to the test results plotted in Figure 258. The minimum copper plating thickness required for Class 3 products is 1 mil and for Class 2 products is 0.5 mils.

Based on the investigation data, the Figure 259 graph shows that the acceptable process window, i.e. cumulative wave solder exposure time is:

- ~77 seconds for SN100C and ~35 seconds for SAC305 in Class 3 products
- ~100 seconds for SN100C and ~44 seconds for SAC305 in Class 2 products

The selection of a particular lead-free soldering alloy significantly impacts the allowable assembly process window. Some product designs that had adequate process windows using tin/lead solder would be impossible to process using some lead-free solder alloys, since the time required to remove and replace a component would result in copper plating thickness falling below the required Class 2 or 3 minimum values.

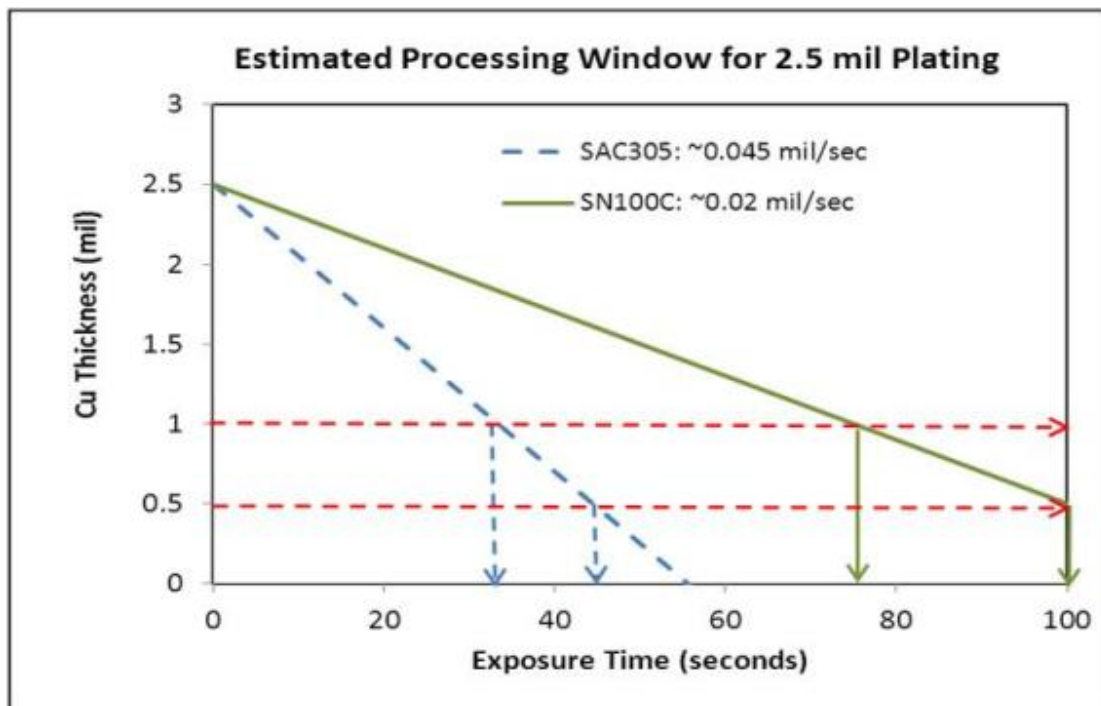


Figure 259 - Mini Wave Soldering Processing Window Estimation

Figure 251, Figure 252, and Figure 255 showed that copper is preferentially dissolved from the bottom of the hole towards the top. This is a result of the bottom side heating up first as it is exposed to the mini-wave rework pot. Thus the copper at the bottom of the via has a longer exposure to the copper dissolution reaction during a typical rework cycle. The impact to the

PWB is that the bottom side catch pad (annular ring) and the knee of the PTH barrel will be the first to be impacted by the dissolution reaction. Traces that connect at the surface of the catch pad (annular ring) will experience greater dissolution, which may result in a broken connection by ring void at the PTH knee. This is a key visual indicator of copper dissolution and only x-ray can provide more detail on the internal PTH barrel condition.

The profile in Figure 260 shows how the hole typically heats up during the mini-pot wave rework cycle/exposure. This data shows that it requires 25 to 30 seconds for the top of the hole to reach the melting point.

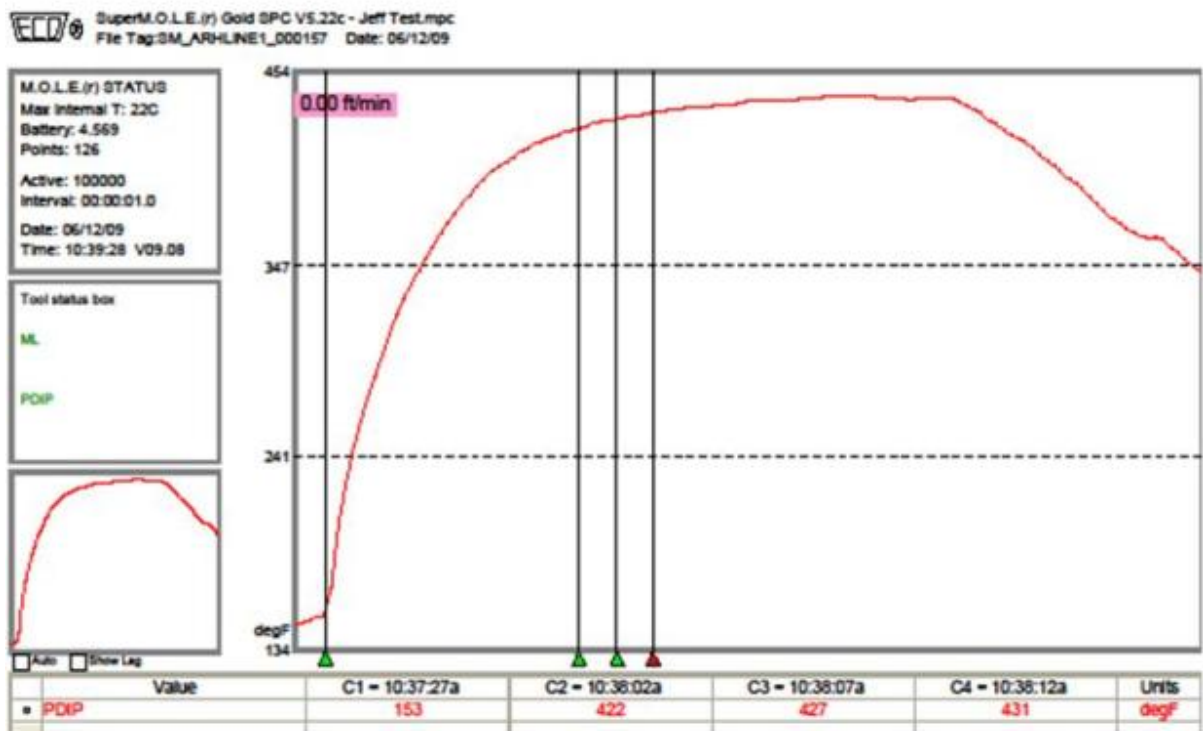


Figure 260 - Rework Temperature Profile

7.1.7 Data and discussion for SMT pattern

The surface mount pads were also exposed to the mini-pot wave fountain to identify any drastic difference in copper dissolution between foil copper and plated copper. Normally, this exposure would not be part of a rework operation. Figure 261 shows the cross-section orientation for a SAC305 test coupon.

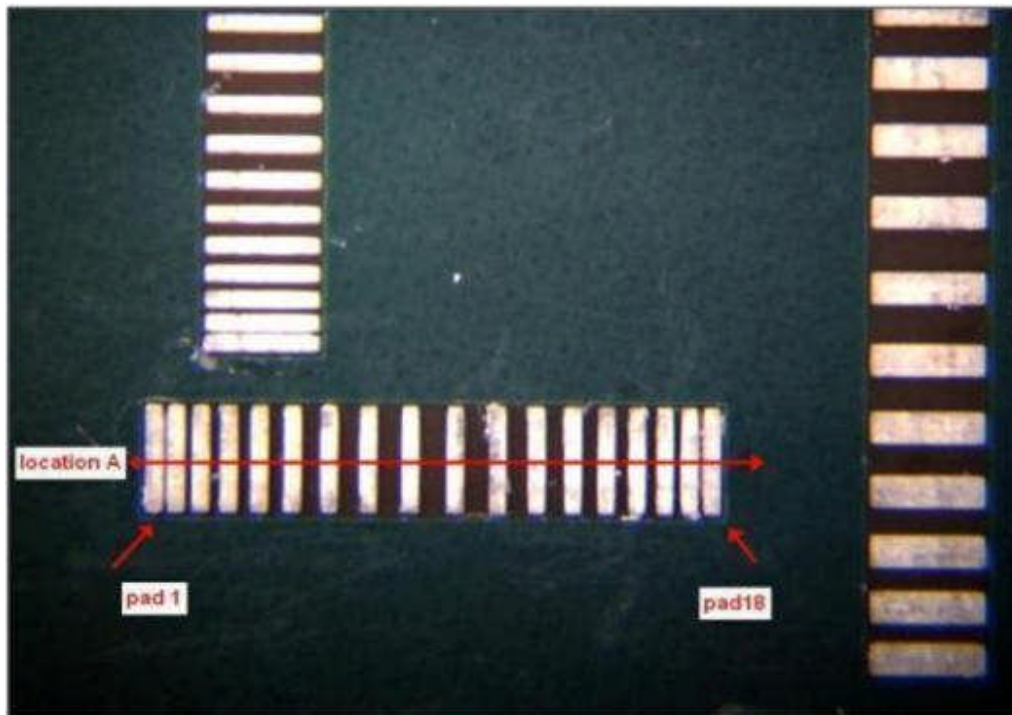


Figure 261 - Celestica Location A Cross-section Location and Pad Number

Figure 262 shows the sequence of pad foil copper dissolution over a period of time. The slope, i.e. the copper dissolution rate, was found to be approximately 0.04 mils/second. This is very similar to the rate of copper dissolution determined at the knee of the DIP PTH for SAC305.



Figure 262 - Sequence of Pad Copper Dissolution by Exposure Time

Figure 263 shows an example of the copper dissolution variance within a specific exposure time. The dynamic nature of the molten wave as it interacts with the plated through via or surface mount pad results in variation of remaining copper plating thickness, despite using tightly controlled test parameters and procedures. It should be noted that the copper dissolution rate for the SMT pads is not much different that of the PTH. This indicates that foil copper dissolves at nearly the same rate as the plated PTH copper.



Sample A185, pad 9, 200x

Sample A186, pad 9, 200x

Sample A187, pad 9, 200x

Figure 263 - Illustration of Copper Dissolution Rate Variance for A Specific Exposure Time

Figure 264 illustrates a temperature profile that shows the SMT QFP pads reaching reflow temperature within 5 seconds. The copper is exposed to molten alloy from the moment of contact, so the effect of the copper dissolution reaction is more damaging than in a plated PTH barrel. Typically, the surface mount pads would start with a lower copper thickness than those of a PTH barrel on the same circuit card assembly (depending on whether it is pattern plated or panel plated) so those features would be more severely impacted if they were in the vicinity of a PTH connection that is exposed to the rework process.

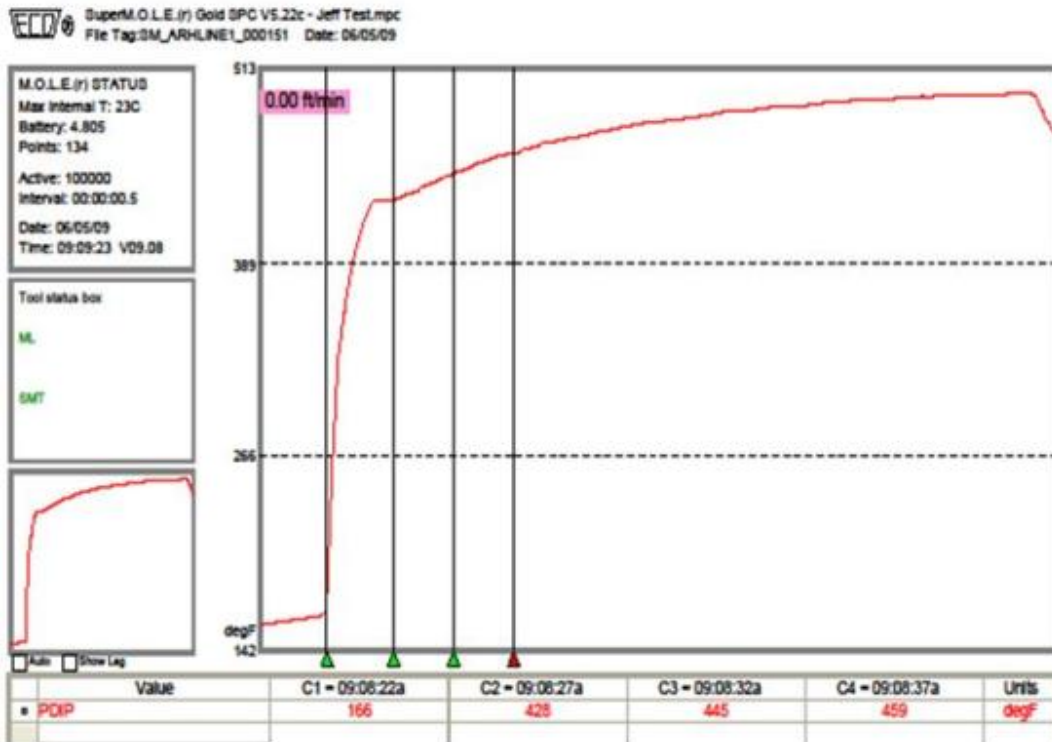


Figure 264 - SMT QFP Pad Thermal Profile

7.1.8 Inspection Criteria – Visual Indicators of Copper Dissolution

Visual inspection confirmed that the PTH catch pad and the knee of the PTH solder joint were the most susceptible locations for copper dissolution. The rate of copper dissolution is greater at this surface as compared to the inner barrel wall. Fillets at the knee may indicate a discontinuity at the location and may be a visual indicator for possible partial void/disconnection location. These visual indicators, illustrated in Figure 265 can be used by the operator to determine if there is an out-of-control process.

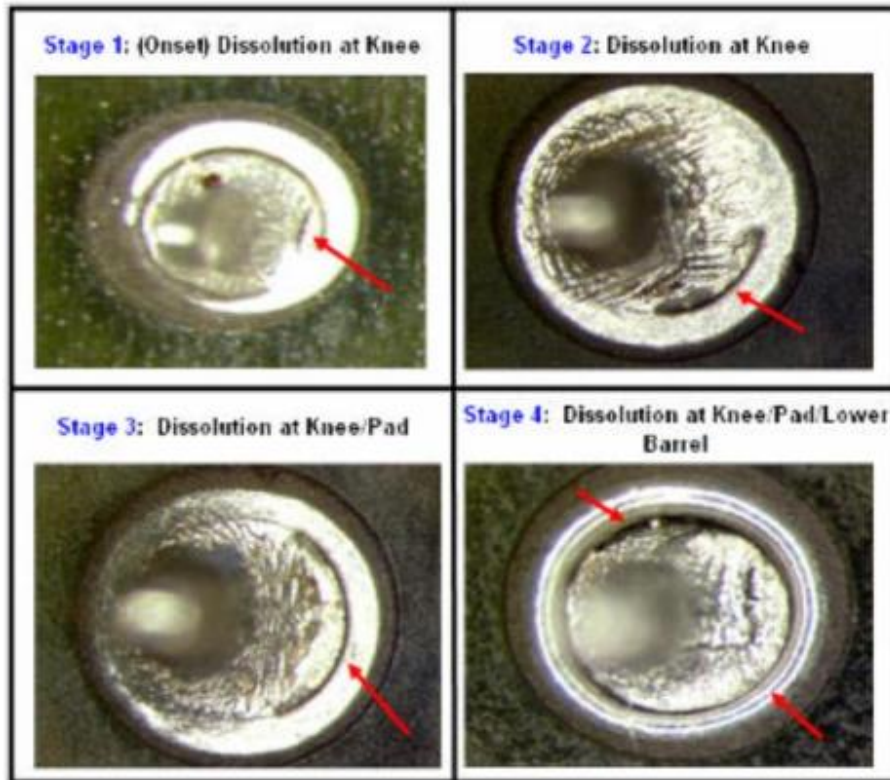


Figure 265 - Visual Indicators of Copper Dissolution(13): Knee- Pad- Barrel for Location of Copper Reduction Sequence

7.1.9 Kinetics of Copper Dissolution

Celestica and Rockwell Collins have conducted past investigations to understand copper dissolution in a lead-free soldering process (12) (15). The dissolution of copper by a tin/lead solder alloy is not a “new” topic and is fairly well documented. The following information details the basics of copper dissolution. The copper dissolution process itself can be considered a result of the following mechanisms (16):

- (1) Departure of atoms of the solid surface and
- (2) Diffusion into the molten solder

Diffusion controlled processes result in a uniform attack while interface controlled reactions may be recognized by preferential etching of grain boundaries. In this study, smooth

copper/intermetallic interface without any sign of grain boundary attack was detected. The mechanisms occur in series and the slowest one determines the overall kinetics of the process. The most general dissolution rate equation is shown below (17):

$$C = C_s (1 - \exp^{-K(A/V)t}),$$

Where C is the solute concentration at time t, K is the solution rate constant and V is the volume of liquid. This equation can be applied for diffusion controlled or interface controlled processes. The solution rate constant K is D/d for the case of diffusion control, where D is the diffusion coefficient in liquid and d is the thickness of the effective concentration boundary layer. In general, the boundary layer thickness is less than 0.1mm. This boundary layer is a layer of liquid existing immediately adjacent to the solid copper interface/intermetallic layer (Figure 266). The copper concentration gradient exists within this layer. During the diffusion controlled process, the liquid boundary layer that is formed during the solder fountain rework is an important feature of copper dissolution.

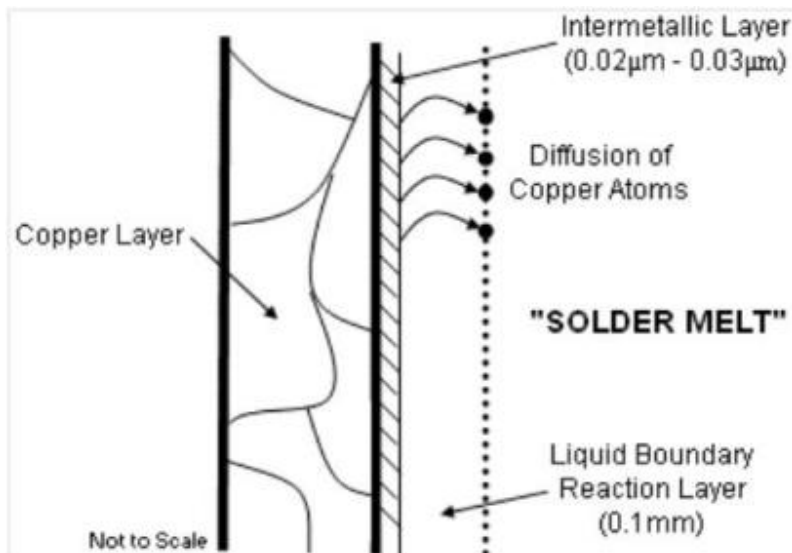


Figure 266 - Departure and Diffusion of Copper Atoms into Solder Melt (Kinetics of Copper Dissolution)

7.1.10 Sn-Pb and Sn-Ag-Copper and Sn-Copper Based Alloys

It has been recognized that it is the Sn component of most solders that reacts with the copper substrate (18). In the case of Sn-Pb solders, only the tin components react, since copper is nearly insoluble in liquid lead at soldering temperatures and forms no intermetallic compounds with it. Therefore, Sn-rich solders dissolve more copper than eutectic Sn-Pb solder. With increasing copper concentration in the solder, the rate of dissolution decreases because of the concentration gradient reduction. Thus, solders with 0.7% copper remove less copper from the plating layer than solders with 0.5% copper. The thickness of this liquid diffusion boundary layer is a function of the physical properties, the velocity of the solution and the diffusion coefficient. The

dissolution rate increases with increasing peripheral velocity, which is relevant to the fountain rework situation (19) (14).

7.1.11 Copper Dissolution Impact on Assembly Practices

The impact of solder alloy copper dissolution on assembly procedures and practices is significant. The process window for the removal and repair of a Pb-free plated-through-hole components is significantly smaller than the process window used for tin/lead solder alloys. A complicating factor is that a copper dissolution defect is not readily detectible by visual or functional test protocols. The solder filled plated-through-hole has an acceptable functional response due to the solder providing signal continuity. However, the reality of the situation is that once the solder cracks, the lack of copper plating results in the loss of electrical continuity. The following sections detail several aspects of copper dissolution on assembly procedures/practices:

- The plated-through-hole component rework/repair procedure
Traditional tin/lead solder alloy provided a very large rework/repair process window with little concern for copper dissolution of the copper plating and more emphasis was placed on potential printed wiring board laminate defects such as delamination or component damage due to total heat exposure duration. The impact of using either the SAC305 or SN100C solder alloys is that the maximum exposure time to a dynamic solder wave is approximately 25 seconds. This time constraint can be especially problematic for heavy copper /thermally loaded printed wiring assemblies by severely limiting the exposure time and allowable additional exposures. The use of alternative component removal methodologies such as hot air and/or rework attachment using a selective solder process should be considered as possible substitutive process methodologies for the removal of components to minimize the impact of copper dissolution.
- The use of alternative printed wiring board surface finishes
The characteristics of some printed wiring assemblies, such as the number of copper layers and/or how the plated-through-holes are connected, may make lead-free solder alloy rework/repair unachievable. Consideration of, and risk analysis for, the use of alternative printed wiring board surface finish such as electroless nickel/immersion gold (ENIG) that are plated directly on copper with no intermediary plating layer such as nickel may be necessary. Figure 267 and Figure 268 illustrates the difference between two surface finishes. ENIG nickel plating on the left hand side show that the nickel plating protects 0.0015” of copper plating from copper dissolution even after 60 seconds exposure in a SAC305 flowing solder pot. The immersion tin surface finish shown on the right hand side allowed nearly completed dissolution of the copper plating at the knee of the plated-through-hole for the same 60 second exposure time.



Figure 267 - Impact of PWB Surface Finish on Copper Dissolution; ENIG

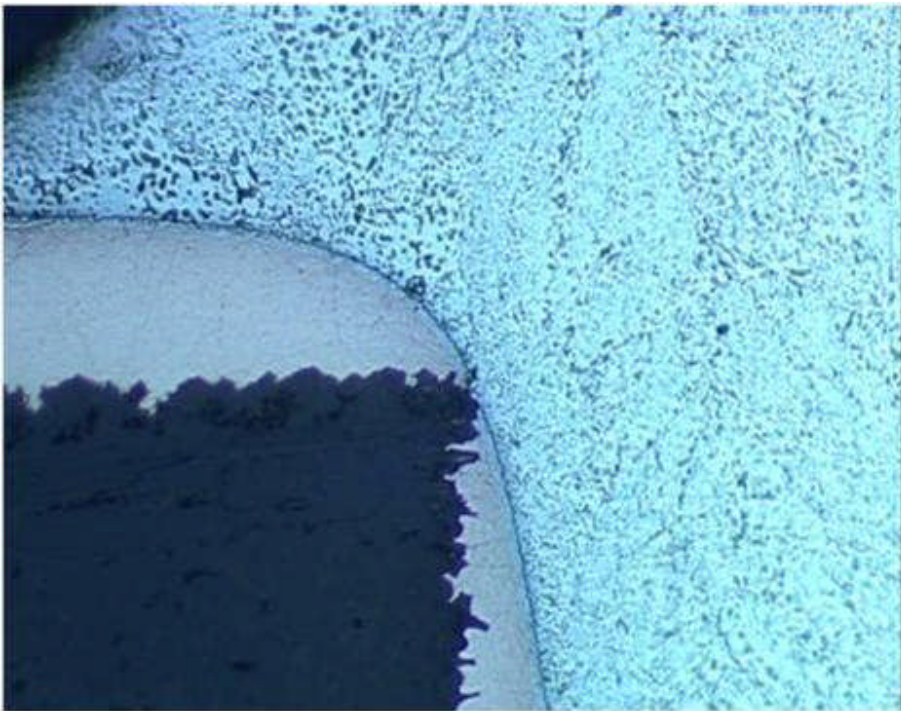


Figure 268 - Impact of PWB Surface Finish on Copper Dissolution; Immersion Tin

7.1.12 Conclusions/Summary

A number of issues related to copper dissolution should be addressed for products to making the transition to lead-free assembly. These include:

- The amount of initial copper plated in the PTH hole may need to be increased to establish a greater margin of safety. The current requirement for 1 mil copper plating minimum may need to be increased to as high as 2.0 mils to provide this margin.
- A resultant minimum copper thickness after rework process may need to be specified and validation methods to ensure compliance would need to be established.
- Alloy selection for rework may be different than for primary attach depending on the expected number of rework cycle requirements for the given product lifetime. Some initial studies have indicated that mixing various Pb-free alloys will not degrade solder joint quality or solder joint reliability (20).
- Copper dissolution rates vary somewhat with the PTH diameter. This study included only two hole sizes: 0.036” and 0.015”. The smaller hole may have impact on material flow up and down the PTH barrel, which affects the copper dissolution rate. Product design consideration may require some additional testing to validate product parameters and associated process requirements (12).
- Rework locations need to be identified by reference designator.
- Control and recording of rework exposure time may also be required to ensure the connection will meet lifetime requirements of the product.
- Tighter controls on solder pot contaminant levels and maintenance of pot composition may be required to reduce variance of the copper dissolution effect during rework operations.
- Consideration for larger component sizes with regard to nozzle design and alloy flow during the rework procedure may be necessary (19).

8 Thermal Aging Discussion

The project consortia members reviewed intermetallic calculations generated by Rockwell Collins and compared the calculations to data sets from the Center for Advanced Vehicle Electronics (CAVE) at Auburn University, the National Physics Laboratory (NPL), the National Institute of Standards and Technology (NIST), and the Center for Advanced Life Cycle Engineering (CALCE) at University of Maryland. The thermal aging procedure was selected to establish a common, standard starting point such that all test vehicles were relatively equal in terms of solder joint microstructure, printed wiring board stress state, surface finish oxidation condition, and intermetallic phase formation/thickness. The project consortia members desired to have the test vehicles begin the various testing procedures with a common starting state point in an effort to eliminate potential assembly differences which could possibly inadvertently/unintentionally influence the testing results. The thermal aging procedure is not necessarily, nor intended to be, representative of the various burn-in, bake-out, or other environmental stress screening (ESS) procedures that are used to evaluate electronics hardware quality/functionality. Additionally, it should be noted that the thermal aging procedure being used by the NASA-DoD LFE Project consortia is not meant to be representative of operational field life. A wide range of ESS procedures and operational field expectations exist in the high performance electronics industry, from telecom applications to space applications, thus an industry consensus "standard" thermal aging procedure that fits all electronics users is not available.

Industry published data (21) has shown that there are metallurgical reactions that occur in lead-free solder alloys can be influenced by thermal excursions. Smetana et al documented that Ag_3Sn particle coarsening (growth or ripening) was evident after the 240 hour preconditioning excursion. It is industry knowledge that micro-structural evolution is considered to be the precursor to re-crystallization, creep, crack initiation, and fatigue crack propagation to failure. The project consortia members consider the utilization of thermal age preconditioning as a necessary protocol in a lead-free solder joint integrity test program.

Test vehicle Batches B, F and I were exposed to extended thermal aging, 4 days, instead of 24 hours.

9 Joint Test Report Summary

9.1 Joint Test Report Data Comparison

The SnPb and Pb-free solder joint integrity results can be dependent on the type of testing that the test vehicles were subjected to. An example of this dependence is that the -20°C to +80°C thermal cycle test results can be different than the -55°C to +125°C thermal cycle results as each test creates a different level of stress on the component solder joints. High performance electronic products are subjected to numerous product use conditions so it is not recommended that a single test data set be used for understanding solder joint integrity and Pb-free solder alloy performance. A data comparison of thermal cycle test results and combined environment test results is shown in Table 50 for the BGA-225 and TQFP-144 component types. It is recommended that similar comparisons be considered when evaluating the solder joint integrity results.

Table 50 – N63 Solder Performance Comparison

N63 Solder Performance Comparison				
Component	Solder/Finish	Combined	Thermal Cycle	Thermal Cycle
		Environments Test	-55 / +125°C	-20 / +80°C
BGA-225	SnPb/SnPb	757	2536	6953
	SnPb/SAC405	148	4649	6302
	SAC305/SnPb	539	2132	901
	SAC305/SAC405	638	3367	DNF @ 12,000 Cycles
TQFP-144	SnPb/SnPb	DNF	2901	9503
	SnPb/Sn	757	3003	9032
	SAC305/SnPb	DNF	3582	DNF @ 12,000 Cycles
	SAC305/Sn	629	1744	DNF @ 12,000 Cycles

NOTE - Data in the table is for as-manufactured only

9.2 Joint Test Report Conclusions

The following statements summarize the data and findings contained within this document.

1. SnPb/SnPb or Pb-free/Pb-free systems are more reliable than mixed metallurgy.
2. Mixed metallurgy solder joints containing a higher percentage of SnPb are more reliable than solder joints that contain a higher percentage of Pb-free solders.
3. Rework using SnPb resulted in a solder joint as reliable as the as-manufactured solder joints.
 - a. For some of the tests, reworked BGA-225 and CSP-100 components were not as robust as the as-manufactured.
 - b. Despite rigid rework procedures, there were issues with successfully reworking the Pb-free BGA-225 components, primarily with the flux only option.
 - c. The reliability of reworked BGA-225 components degrades under a vibration environment.
4. QFN-20 components with the thermal die pad soldered to the board were the most reliable components under this test program.
5. CLCC-20 and TSOP-50 components performed poorly, as they did during the JCAA/JGPP Lead-Free Solder Project.
6. Laminate selection is an important factor in lead-free solder assembly integrity, as evidence by pad cratering defects.
7. Traditional fabrication defects such as the documented PDIP-20 trace cracks influenced results regardless of solder alloy.
8. The effects of copper dissolution must be taken into consideration for any lead-free solder assembly processes.
9. Tin whiskers were observed on Sn finished Alloy 42 TSOP-50 components, in non-soldered areas, subjected to thermal cycle testing -55 to +125°C. No tin whiskers were observed on the TQFP-144 Sn or SAC305 finished components. No tin whiskers were observed on the PDIP-20 Sn finished components.
10. For this project there was no significant difference in solder joint reliability between the two board finishes (ImAg and ENIG) tested.
11. Under high-stress mechanical and thermal conditions, SnPb generally outperforms Pb-free. For low stress conditions, Pb-free generally outperforms SnPb. One exception to this trend is the mechanical shock test results. These results are similar to the JCAA/JGPP Lead-Free Solder Project results.
12. The results of this study suggest that for some component types and environments, Pb-free solders are as reliable as the currently used eutectic SnPb solder. This study also demonstrates that with other component types and environments, the Pb-free solders fail before the SnPb control.

10 Recommendations

1. The lower reliability of the Pb-free solder joints does not rule out the use of Pb-free solder alloys on aerospace and defense electronics.
2. Qualification testing is recommended for high performance systems utilizing lead-free solder joints.
3. Models supported by empirical data may be acceptable for some applications. Validation of models should be conducted using actual field data.
4. Printed wiring board laminate testing must be conducted to ensure the materials can withstand the effects of lead-free processing.
5. Mix metallurgy solder processes must be thoroughly characterized, tested, and controlled when used in high performance systems.
6. Lead-free and/or mixed metallurgy rework processes must be thoroughly characterized, tested, and controlled when used in high performance systems.
7. The results of this study should be used with other industry data as part of a comprehensive data set when considering Pb-free solder process implementation.
8. Conduct extensive failure analysis to account for multiple failure mechanisms. Investigate and define the probable solder alloys composition characteristics (phase) affects on the root cause of the failures.
9. Perform testing to include underfill materials and other printed wiring board laminates, board surface finishes, component configurations, and lead-free alloys.
10. System-level demonstration/validation of Pb-free solders on functional Class 3 aerospace and defense electronic systems must be conducted to validate Pb-free assemblies in an operational environment.

11 Phase III

The JCAA/JGPP Lead-Free Solder Project and NASA-DoD Lead-Free Electronics Project greatly increased the electronics industry understanding of Pb-free solder interconnect reliability under harsh environments testing. However, data gaps still remain. In an effort to fill some of the data gaps that remain, a Phase III effort is being proposed to look at new/different laminate materials and Pb-free solder alloys. In an effort to reduce cost, the Phase III effort could use the same test vehicle design and components as the NASA-DoD Lead-Free Electronics Project. In maintaining the same test vehicle configuration and component selection, reliability assessments of new generation solder alloys, board materials and surface finishes will be comparable across all Phases of the project; JCAA/JGPP Lead-Free Solder Project, NASA-DoD Lead-Free Electronics Project and the proposed Phase III effort.

11.1 Overview

The NASA-DoD Lead-Free Electronics Project confirmed that pad cratering is one of the dominant failure modes that occur in various board level reliability tests, especially under dynamic loading. Pad Cratering is a latent defect that may occur during assembly, rework, and post assembly handling and testing. Pad cratering cannot be identified during back-end-of-line in-circuit test (ICT) or functional circuit test (FCT) protocols and poses a high reliability risk under mechanical and thermo-mechanical loading.

Pb-free solder joints are stiffer than tin-lead (SnPb) solder joints, in addition, Pb-free compatible PCB dielectric materials (High Tg board materials) used with mainstream Pb-free solders (SAC305) cannot withstand higher processing temperatures and are more brittle than FR4 laminate used with SnPb solder. These two factors, coupled with the higher peak reflow temperatures used for Pb-free assemblies, could transfer more strain to the PCB dielectric structure, causing a failure in the resin system.

One potential solution would be to select Pb-free solders with lower process temperatures. A 10°C reduction in process temperature would allow for the use of dicy-cured FR4 laminate, potentially preventing pad cratering failures. The reduced process temperature would also reduce the risk of damaging temperature sensitive components such as aluminum capacitors, fuses, and light-emitting diodes (LEDs).

In continuing the NASA-DoD Lead-Free Electronics Project, Phase III, it is being proposed that solder alloys with a process temperature in the range of 220°C to 226°C be evaluated for solder joint reliability. Several ternary tin-silver-bismuth (SnAgBi) and quaternary tin-silver-copper-bismuth (SnAgCuBi) Pb-free solder alloys have shown great mechanical and thermo-mechanical reliability in previously completed projects {National Center for Manufacturing Sciences (NCMS) and JCAA/JGPP Lead-Free Solder Project} and new studies {GJP Lead-Free Avionics and Celestica}. Some of these Pb-free alloys have melting temperatures comparable to SnPb, allowing for the use of SnPb processing temperatures for Pb-free assemblies.

Alloys containing bismuth (Bi) have not been widely utilized due to the formation of a low melting ternary tin-lead-bismuth (SnPbBi) alloy when SnAgCu Bi solder joints are contaminated with Pb from SnPb component finishes. With the increased use of lead-free solder alloys and components finishes, SnPb component finishes are becoming obsolete reducing the risk of Pb contaminating Bi containing solder alloys. In addition, using Bi containing solder alloys may reduce the propensity of tin whisker growth.

The Phase III effort may also evaluate new board materials which have been shown to be more stable when exposed to mechanical and thermo-mechanical stresses and less prone to pad cratering. Alternative surface finishes should also be evaluated; Electroless Nickel Electroless Palladium Immersion Gold (ENEPIG) is one option that shows a lot of promise and could be evaluated in a Phase III effort.

12 System-Level Demonstration

With all of the work completed to date in evaluating Pb-free, there still remains a major gap; system-level demonstration/validation of promising Pb-free solders on functional Class 3 aerospace and defense electronic systems. This will also help validate entire Pb-free assemblies in an operational environment.

12.1 Flight Test Pb-free Solders

12.1.1 Objective

Pb-free solder interconnects must be extensively tested to ensure their structural and electrical reliability will meet the rigors of military and aerospace applications. This proposal would test aircraft line replaceable units (LRU) assembled with Pb-free interconnects, one area of research that is severely lagging. Testing will be comprised of laboratory testing that meets or exceeds military and aerospace specifications. The data gathered will help design engineers with the monumental task of designing Pb-free electronic assemblies that must meet military and aerospace design criteria.

This project will answer if functioning aircraft line replaceable units (LRU) built using Pb-free solder alloys are as reliable, both structurally and electrically, as electronic assemblies built using the SnPb baseline. If feasible, this effort would evaluate two different Pb-free alloys. In using two different Pb-free solder alloys, it can be determined if one alloy performs better under thermal stress while another alloy performs better under mechanical stress. This is important since it may not be possible to have a single drop-in replacement for SnPb. Design engineers may have to select solder alloys based on the weapons systems end use and known environmental stresses.

Understanding how the rework of functioning aircraft line replaceable units (LRU) assembled with Pb-free will affect the structural and electrical reliability will be covered in this project. If military hardware is to be assembled using Pb-free materials, it is assumed that these assemblies will be reworked as failures occur during the life-cycle of the product. Data has been collected

from the rework of non-functioning electronic assemblies, but not only has this data been limited, it may not be directly transferable to functional assemblies. Additional data is needed to better understand how rework procedures affect functioning military hardware.

12.1.2 Concept

Aircraft line replaceable units (LRU) will be built using Pb-free circuit board finishes, solder, and component finishes. To date, there is no consensus for selecting the best Pb-free circuit board finishes, solder, or component finishes. The following versions of the aircraft line replaceable units (LRU) will be built:

1. Tin-lead (SnPb) baseline, as currently manufactured
2. Pb-free version A, the circuit board surface finish and bulk solder alloy will be selected by the project stakeholders (immersion silver and SAC305 potentially). Component finishes will be Pb-free, dictated by the component supplier.
3. Pb-free version B, the circuit board surface finish and bulk solder alloy will be selected by the project stakeholders (ENEPIG and SN100C potentially). Component finishes will be Pb-free, and dictated by the component supplier.

The test assets in an aircraft environment would be exposed to a combination of harsh environments including, vibration, mechanical shock, thermal cycling and altitude changes that cannot be individually isolated.

This effort proposes that 3 circuit cards be placed in each of 4 different zones on the aircraft. This could vary by aircraft type. For this proposal, an F-15 was used as an example. The zones are forward fuselage, cockpit, engine bay, and center fuselage. The intent of the two fuselage locations is to ensure one is placed near the gun.



Figure 269 - F-15 Test Zones; Forward Fuselage, Cockpit, and Engine Bay



Figure 270 - F-15 Test Zones; Center Fuselage

12.2 Field Test Pb-Free Solders in Harsh Environments

12.2.1 Objective

Numerous laboratory studies, past, present and planned, are attempting to better understand how Pb-free will affect the reliability of electronics exposed to the harsh operating conditions of military applications. However, there is a lack of data from actual field testing electronics containing Pb-free components or that have been assembled using only Pb-free components and solder alloys. Pb-free solder interconnects must be extensively tested to ensure their structural and electrical reliability will meet the rigors of military and aerospace applications. This proposal would test Pb-free assemblies on a ground based military vehicle platform expected to operate in harsh environments.

The intent of this effort is to;

- Obtain reliability data from electronics assemblies operating in harsh military environments for comparison to laboratory test data
- Capture lessons learned regarding safe conditions and durations for the use of Pb-free technology in military hardware

12.2.2 Concept

The following is a generic scenario that could be used across a multitude of military platforms, the harsher the operating environment the better. An ideal scenario would be to have a military vehicle (tank, Humvee, troop-carrier, light tactical vehicle, other) involved in training or proving ground operations.

Field testing implementation approach;

1. Build circuit cards for use in stakeholder approved applications (radio, control box, navigational system, other). If an application cannot be found with three matching circuit cards, multiple end-use products could be built to cover the three build scenarios. The circuit cards will be divided into the following categories;
 - a. Tin-lead (SnPb) baseline, as currently manufactured
 - b. Pb-free, the circuit board surface finish and bulk solder alloy will be selected by the project stakeholders (immersion silver and SAC305 potentially). Component finishes will be Pb-free, and dictated by the component supplier
 - c. Mixed technology, a SnPb board with Pb-free parts using SnPb solder, component finishes will be Pb-free, and dictated by the component supplier
2. Install the circuit cards or end-use products onto a military vehicle which will be subjected to harsh conditions (vibration, mechanical shock, temperature cycling) as part of normal training or proving ground operations.
3. Track the circuit cards or end-use products for a duration agreed upon by the project stakeholders (12, 18, 24 months) recording all failures and maintenance activities.
4. Once the circuit cards or end-use products have been in service for the pre-determined duration, a full examination will be completed including visual inspection, continuity testing, x-ray analysis and micro-section analysis.
5. As funding allows, additional circuits or end-use products could be built and subjected to laboratory testing, vibration, mechanical shock and thermal cycle with vibration.

12.3 Electronic assemblies designed for operation in harsh aerospace environments {Lead-free Technology Experiment in a Space Environment (LTESE)} II

12.3.1 Objective

The single Pb-free experiment that has flown in space, LTESE, was exposed to the harsh environments of space for approximately 18 months and none of the Pb-free or mixed solder joints under test failed. The only degradation seen was the formation of tin whiskers on some tin plated electronic parts. Tin whiskers are a known potential for failure in Pb-free systems and the following commercial (non-NASA) satellites have reportedly suffered on-orbit failures of their satellite control processors (SCP) where the suspected root cause was tin whisker induced short circuits where the whiskers grew on pure tin plated electromagnetic relays. Each satellite was designed with a primary and one redundant SCP. Failure of both primary and redundant SCPs results in a complete loss of the satellite's primary mission.

Table 51 - On-Orbit Commercial (non-NASA) Satellite Failures(22)

		Date When SCP Failure Occurred -- Suspected Root Cause = Tin Whisker Induced Short Circuit	
Satellite Name	Launch Date	First Satellite Control Processor Failure	Redundant Satellite Control Processor Failure
Complete Losses -- Both Primary and Redundant SCPs failed			
GALAXY VII [PanAmSat]	27 October 1992	13 June 1998	22 November 2000
GALAXY IV [PanAmSat]	24 June 1993	(not caused by 'tin whiskers')	19 May 1998
SOLIDARIDAD 1 [SatMex]	19 November 1993	28 April 1999	27 August 2000
GALAXY IIIIR [PanAmSat]	15 December 1995	21 April 2001	15 January 2006
Partial Losses- Only 1 of 2 Redundant SCPs failed			
OPTUS B1	13 August 1992	21 May 2005	Still Operational
DBS-1 [DirecTV]	17 December 1993	4 July 1998	Still Operational
PAS-4 [PanAmSat]	3 August 1995	3rd quarter 1998	Still Operational
DirecTV 3 (DirecTV)	9 June 1995	4 May 2002	Still Operational

The objective of this experiment is to evaluate, in space, several promising techniques believed to prevent the formation of tin whiskers rather than only mitigate the risk of tin whisker failures.

12.3.2 Concept

The first element of the experiment will be to prepare a sample known to grow tin whiskers rapidly (Figure 271) and expose it to the temperatures, radiation, ultra violet and atomic oxygen environments of space and compare the results with “terrestrial” data, such as how fast whiskers grow on the uncoated side and verifying the minimum Ni thickness to block whiskers. The experiment would be to compare what has been seen on Earth to a chosen space environment.

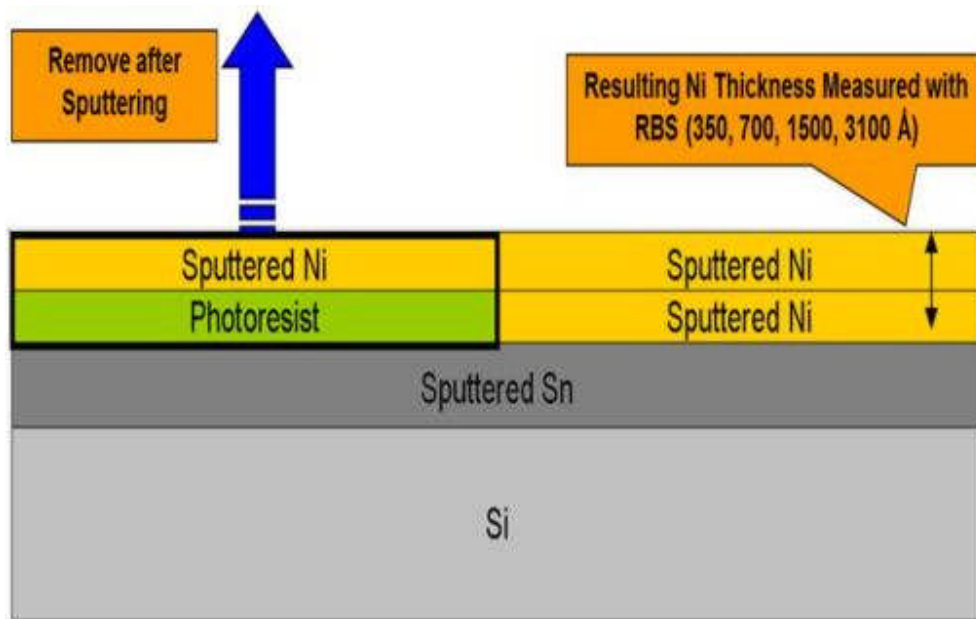


Figure 271 - Cross-sectional View of Ni Cap Test Coupons for ISS Whisker Experiments

The second element of the experiment is to build some small printed circuit assemblies and have them subjected to electroless plating baths to build up nanometer thick coatings of nickel, palladium and gold to establish that the plating process is fast and does not adversely affect the function of the assemblies, and to show that each of these platings will prevent the formation of tin whiskers during long exposures to the space environments.

The experiment is totally passive and would reside outside the Space Station for some extended period of time then be returned to earth for analysis.

13 Bibliography

1. **Lau, J. and Pao, Y.** *Solder Joint Reliability of BGA, CSP, Flip Chip, and Fine Pitch SMT Assemblies.* s.l. : McGraw Hill, 1996. ISBN 0-07-036648-9.
2. **Wild, R.** Some Factors Affecting Leadless Chip Carrier Solder Joint Fatigue Life II. *Some Factors Affecting LeCircuit World, Volume 14, No. 4.* 1988, pp. 29-41.
3. **Burke, M. and Pearson, R.** *Solder Alloy Development for Electronic Chip Carriers.* s.l. : AFWAL-TR-88-4215, 1988.
4. *Temperature cycling Performance of a Quad Flat No Lead (QFN) Package Assembled with Multiple Pb-free Solders.* **Coyle, R., et al.** 2011. SMTAI Conference Proceedings, Paper AAT1.2.
5. *Quad Flat No Lead (QFN) Package Processing in High Thermal Mass Assembly.* **J. Songnanluck, et al.** 2010. SMTAI Conference Proceedings, Paper AAT4.1.
6. *Microstructure, Defects and Reliability of Mixed Pb-free/SnPb Assemblies.* **P. Snugovsky, et al.** 2008. TMS Proceedings, V1: Materials Processing and Properties. pp. 631-642.
7. *Solder Joint Reliability of Pb-free Sn-Ag-Cu Ball Grid Array (BGA) Components in Sn-Pb Assembly Process.* **R. Kinyanjui, et al.** 2008. APEX Proceedings.
8. NASA TEERM. *NASA Technology Evaluation for Environmental Risk Mitigation (TEERM) Principal Center.* [Online] <http://teerm.nasa.gov>.
9. **Viswanadham, P. and Singh, P.** *Failure Modes and Mechanisms in Electronic Packages.* s.l. : Chapman & Hall, ISBN 0-412-10591-8.
10. **D. Hillman, et al.** *Component Integrity and Product Integrity Investigation for Wide Bodied Dual Inline Package (DIP).* s.l. : Rockwell Collins Internal Working Paper WP07-2003, 2003.
11. *Evaluation of Tin Copper (SnCu) Modified Lead-free Solder Alloys for Wave Solder Processes.* **D. Hillman, et al.** 2011. International Conference on Soldering and Reliability (ICSR) Conference Proceedings.
12. *Selective Wave Soldering DoE to Develop DFM Guidelines for Pb & Pb-free Assemblies.* **M. Boulos, C. Hamilton, M. Moreno, et al.** s.l. : SMTA International, 2008 .
13. *A Study of Copper Dissolution during Pb- free PTH Rework.* **Hamilton, C.** s.l. : International Conference on Lead-free Soldering (CMAP), 2006.
14. *HAVE HIGH COPPER DISSOLUTION RATES OF SAC305/405 ALLOYS FORCED A CHANGE IN THE LEAD FREE ALLOY USED DURING PTH PROCESSES?* **C.Hamilton, Celestica, P. Snugovsky, M. Kelly.** s.l. : C.Hamilton, Celestica, P. Snugovsky, M. Kelly "HAVE HIGH COPPER DISSOLUTION RATES OF SAC305/405 SMTA Pan-Pac, C.Hamilton, Celestica, P. Snugovsky, M. Kelly "HAVE HIGH COPPER DISSOLUTION RATES OF SAC305/405 ALLOYS FORCE 2007.
15. **D. Hillman, M. Hamand.** *Copper Dissolution Impact with Lead-Free Solder Alloys.* s.l. : Rockwell Collins Internal Report, 2008.
16. *The Isothermal Corrosion ($\alpha + \beta$) Ni-Sn Alloys in Pure Liquid Sn Component.* **N.J. Hoffman, I. Minkoff.** s.l. : American Society for Metals and the Metallurgical Society of AIME, 1969.
17. *Dissolution of Solid Copper Cylinder in Molten Tin-Lead Alloys under Dynamic Conditions.* **Y. Shoji, S. Uchida, T. Ariga.** s.l. : Proceedings of American Society for Metals and the Metallurgical Society of AIME, 1982.

18. *Experiments on Interaction of Liquid Tin with Solid Copper*. **L. Snugovsky, M.A. Ruggerio, D.D. Perovic, J.W. Rutter**. s.l. : Journal of Materials Science and Technology, July 2003, Vol. 19., 2003, Vol. 19.
19. **C.Hamilton**. *Laminar Flow-well*. s.l. : Celestica, 2006.
20. **Seelig, K.** Pb-Free Solder Assembly for Mixed Technology Boards. *Circuits Assembly*. 2006.
21. *Variations in Thermal Cycling Response of Pb-free Solder due to Isothermal Preconditioning*. **J. Smetana, et al.** s.l. : SMTAI Conference Proceedings, paper LF4.2, 2011.
22. NASA NEPP. *NASA Whisker Failures*. [Online]
<http://nepp.nasa.gov/whisker/failures/index.htm>.
23. **Seelig, K.** Pb-Free Solder Assembly for Mixed Technology Boards. *Circuits Assembly*. 2006.